The biosynthesis of natural products: the characterisation and manipulation of AtrA, an evolutionarily conserved transcription factor

Ayat Hani Al-Tarawni

Submitted in accordance with the requirements for the degree of

Doctor of Philosophy

The University of Leeds

School of Molecular and Cellular Biology

Faculty of Biological Sciences

August 2019

The candidate confirms that the work submitted is her own and that appropriate credit has been given where reference has been made to the work of others.

This copy has been supplied on the understanding that it is copyright material and that no quotation from the thesis may be published without proper acknowledgement.

Acknowledgments

First of all, I would like to express the deepest appreciation and gratitude to my supervisor Prof. Kenneth McDowall for his continues advice, patience, understanding and tremendous efforts. He have been always guiding me throughout the work in this thesis. Without his suggestions, encouragement and help this thesis would have not been completed or written. One simply could not wish for a better supervisor.

I would like to thank Dr Ryan Seipke for his valuable advices and suggestions, and Dr Chris Randall for his helpful comments on the first chapter of this thesis. .

I would like to extend a special thanks to my colleagues Kiran and Fayez for their help, support and scientific conversations. I would also like to thank all the members of O'Neill and Seipke groups.

My sincere thanks go to Mutah University for the financial support of my PhD study.

I would like to express my heartfelt appreciation to my friend Sanaa for her constant encouragements and support. Special thanks go to Dr Ayad Hasan for his support and fruitful discussions during PhD.

Finally, massive thanks go to my family for helping me in all of my pursuits and encouraging me to follow my dreams. I am especially grateful to my parents. I know that you believe in me and you always want the best for me.

Abstract

The current need for new antibiotics clinically is well documented. A variety of approaches are being taken to meet this need including the renewed mining of *Streptomyces* natural products using methodologies that provide greater depth and target antibiotic-resistant pathogens. One key area is the development of culture conditions that induce the production of a wider range of *Streptomyces* natural products. This “secondary” metabolism is known to be regulated by numerous transduction systems but for many, if not most, the actual regulatory signal has yet to be identified. The identification of the signals for transduction systems may allow the development of media or growth conditions that extend the range of *Streptomyces* natural products identifiable by laboratory-based screens. The greatest benefit is likely to be derived from the manipulation of transduction systems that are evolutionarily conserved and have regulons covering multiple *Streptomyces* natural products. Previous work identified that the production of actinorhodin by *S. coelicolor*, a well-established model for understanding the regulation of secondary metabolism is regulated by AtrA, (SCO4118) a member of the TetR family of one-component, signal transducers. Moreover, AtrA has subsequently been shown to be evolutionarily conserved and regulate the production of secondary metabolites in several species beyond *S. coelicolor*. The first part of this thesis identifies by a combination of bioinformatics, chromatin immunoprecipitation and transcriptomics that the regulon of AtrA in *S. coelicolor* is broad and AtrA regulation extends to secondary metabolism beyond the production of actinorhodin. The mutagenesis of a selection of the members of the AtrA regulon of *S. coelicolor* is also described. The second part describes the investigation of the signal transduced by *S. coelicolor* AtrA, which encompassed an analysis of actinorhodin. This work made the unexpected finding that *S. coelicolor* produces non-specific inhibitors of DNA: protein interactions. It is speculated that such inhibitions may provide an undescribed mechanism for quelling general transcription as part of the developmental cycle of streptomycetes.

List of Contents

List of Figures

List of Tables

List of Abbreviations

ACT	actinorhodin
ATP	adenosine triphosphate
antiSMASH	Antibiotics & Secondary Metabolite Analysis Shell
APS	base pair
BGC	biosynthetic gene cluster
BSA	bovine serum albumin
CDA	calcium-dependent antibiotic
ChIP	chromatin immunoprecipitation
CLSI	Clinical and Laboratory Standards Institute
CFU	colony forming unit
CPK	cryptic polyketide antibiotic
^{o}C	degree Celsius
DNA	deoxyribonucleic acid
DE	differential expression
DMSO	dimethylsulfoxide
DTT	dithiothreitol
EMSA	electrophoretic mobility shift assay
EDTA	ethylenediaminetetraacetic acid
FAM	fluorescein amidite
g	gram(s)
g	gravity
HPLC	high pressure liquid chromatography
h	hour(s)
IMAC	immobilized metal-affinity chromatography
iChip	isolation chips
IPTG	isopropyl-βs-D-thiogalactopyranoside
kbp	kilo base pair
kDa	kilodalton
kg	kilogram (10^3 g)
LMWS	low-molecular-weight substances
LB	Luria Bertani medium
m / z	M stands for mass and Z stands for charge number of ions
MSF	Mannitol soya flour medium

MeOH	methanol
MRSA	methicillin-resistant Staphylococcus aureus
µg	microgram (10-6 g)
µL	microlitre(s) (10-6 L)
µM	micromolar
mg	milligram (10-3 g)
mL	millilitre(s) (10-3 L)
mm	millimetre
mM	millimolar
min	minute(s)
MACS	Model-based Analysis of ChIP-Seq
MDR	multiple-drug resistant
TEMED	N,N,N',N'-tetramethylethylenediamine
ng	nanogram (10-9 g)
nM	nanomolar
TES	N-Tris(hydroxymethyl)methyl-2-aminoethanesulfonic acid
NMR	Nuclear magnetic resonance
NOESY	Nuclear overhauser effect spectroscopy
nt	nucleotide
ORF	open reading frame
OD	optical density
PAGE	polyacrylamide gel electrophoresis
PCR	polymerase chain reaction
psi	pounds per square inch
rpm	revolutions per minute
RNase	ribonuclease
RNA	ribonucleic acid
rRNA	ribosomal ribonucleic acid
s	second(s)
SMs	secondary metabolites
SELEX	selective enrichment of ligands by exponential enrichment
sRNA	small ribonucleic acid
SDS	sodium dodecyl sulphate
TOCSY	Total correlation spectroscopy
TSS	transcriptional start site
tRNA	transfer ribonucleic acid

Tris	Tris(hydroxymethyl)aminomethane
TBE	Tris-borate-EDTA
TE	Tris-EDTA
TGED	Tris-glycine-EDTA
TGEK	Tris-glycine-EDTA-potassium chloride
TSA	tryptone soya agar medium
TSB	tryptone soya broth medium
UV	ultra violet
RED	undecylprodigiosin antibiotic
UCSC	University of California, Santa Cruz
V	volts
v/v	volume (ml) per volume (ml)
w/v	weight (g) per volume (ml)
WHO	World Health Organization

Chapter 1 Introduction

1.1 The history and impact of *Streptomyces* in relation to antibiotic discovery

The majority of antibiotics in clinical and veterinary use today have been derived from soil bacteria in particularly members of the *Streptomyces* genus (Table 1.1). The remaining antibiotics are derived from other species of bacteria, a few fungi and synthetic chemistry (for reviews, see (Davies & Davies, 2010, Lewis, 2013). The demand for new antibiotics is high as their use has led inevitably to the emergence of multi-drug resistant strains (Lewis, 2013, Clardy et al., 2006, Yoneyama and Katsumata, 2006, Alanis, 2005). Moreover, new antibiotics are not being developed at a rate sufficient to replace those lost to resistance. Consequently, there is a growing shortfall in the successful treatment of bacterial infections as antibiotic reach the end of their lifespan. Currently, each year in the US, at least 2 million people become infected with bacteria resistant to antibiotics and of these individuals, at least 23,000 die as a direct result of their infections (Centers for Disease Control and Prevention, 2013). Genome sequencing has revealed that all *Streptomyces* encode a large arsenal of bioactive, secondary metabolites, only a fraction of which are produced under normal laboratory conditions (for reviews, see (van Wezel & McDowall, 2011, Zhu *et al.*, 2014). Thus, the *Streptomyces* and other microorganisms could prove to be a valuable source of new antibiotics through further screening, but this is likely to be highly dependent on effective and efficient strategies for 'awakening' otherwise 'sleeping' clusters of secondary metabolites (Hopwood, 2006).

Streptomyces sp.	**Antibiotic**	***Streptomyces sp.***	**Antibiotic**
S. garyphalus	Cycloserine	*S. erythraea*	Erythromycin
S. orientalis	Vancomycin	S. venezuelae	Chloramphenicol
S. fradiae	Neomycin, Actinomycin, Fosfomycin, Dekamycin	*S. aureofaciens*	Chlortetracycline, Dimethylchlor, tetracycline
S. nodosus	Amphotericin B	*S. ambofaciens*	Spiramycin
S. noursei	Nistatin	*S. avermitilis*	Avermectin
S. mediterranei	Rifamycin	*S. alboniger*	Puromycin
S. griseus	Streptomycin	*S. niveus*	Novobicin
S. kanamyceticus	Kanamycin	*S. platensis*	Platensimycin
S. tenebrarius	Tobramycin	*S. roseosporus*	Daptomycin
S. spectabilis	Spectinomycin	*S. ribosidificus*	Ribostamycin
S. viridifaciens	Tetracycline	*S. garyphalus*	Cycloserine
S. lincolnensis	Lincomycin, Clindamycin	*S. vinaceus*	Viomycin
S. rimosus	Oxytetracycline	*S. lclavuligerus*	Cephalosporin

Table 1.1. Antibiotics produced by *Streptomyces* species. Modified from (Hasani *et a*l., 2014).

1.1.1 Infectious disease in the pre-antibiotic era

Although the ancient civilizations used natural substances with some antimicrobial activity for many years in the pre-antibiotic era, their activity was very limited. Thus, the spread of infectious bacteria could be very rapid (Ashkenazi, 2013). Prior to the beginning of the 20th century, infectious diseases had high morbidity and mortality rates worldwide, e.g. smallpox, cholera, diphtheria, pneumonia, typhoid fever, plague, tuberculosis, typhus and syphilis (Adedeji, 2016) and the treatment of these diseases was mostly based on patient isolation (Ashkenazi, 2013). Medical or surgical intervention increased the risks of severe infection by, for example, staphylococci (Finch *et al.*, 2010). Bubonic plague, caused by *Yersinia pestis*, is believed to have been responsible for the death of higher than 60% of the population of Europe during the 14th century (Spyrou *et al.*, 2018). Syphilis, the causative agent of which is *Treponema pallidum,* spread over all of Europe in the 18th and 19th centuries and it is proposed to have caused the death of numerous philosophers, painters, and musicians including Mozart (Franzen, 2008).

From the late 19th century, antiseptics were used for sterilization of the infected wounds (carbolic acid, mercury salts and boric acid). Although reducing the most common bacteria at the site of the wound, the used compounds had a toxic effect on the tissues (Fleming, 1919). In the early 20th century, mortality rates reached approximately 40% due to childhood diseases such as diphtheria, pneumonia and rheumatic fever (Armstrong *et al.*, 1999).

1.1.2 The "Golden Age'' of antibiotic discovery

The spread of infectious disease prompted more experimentation with possible treatments, many chemicals and dyes were screened for inhibitory activity. Prontosil was the first synthetic antibiotic. It was produced by combining sulphanilamide with a dye and this combination was used to treat streptococcal and other general bacterial infections in 1931 (Gould, 2016). The achievement that changed the course of medicine was the discovery of penicillin, a natural product antibiotic, by Alexander Fleming in 1928 (Fleming, 1929) .Its extraction and characterisation was done by Florey and his colleagues in 1940 (Abraham *et al.*, 1941, Gaynes, 2017). The antimicrobial effect of penicillin was determined against staphylococci and other Gram-positive pathogens and it became available for patient use in the 1940s (Gaynes, 2017).

The following two decades, antibiotic discovery progressed rapidly and new classes of antibiotics were developed, leading to a Golden Age of antibiotic discovery. The demand for new antibiotics during this phase was driven not only by the need for effective or more effective treatments for the wide range of bacteria that infect humans, but even then a

growing realisation that with use bacteria were becoming resistant, i.e. individual antibiotics had a limited lifespan in the clinic (Clatworthy *et al.*, 2007). The best source of new antibiotics was the *Streptomyces*, a genus of soil bacteria. In 1944, streptomycin and aminoglycoside antibiotics were obtained from *Streptomyces griseus* (Krause et al., 2016, Saga & Yamaguchi, 2009). Thereafter, vancomycin was eventually extracted from *Amycolatopsis orientalis* and it came into clinical use in 1958 (Levine, 2006). During this era, chloramphenicol was discovered from *Streptomyces venezuelae,* tetracycline from *Streptomyces aureofaciens* (Darken *et al.*, 1960), macrolides from various species of *Streptomyces* (Woodford, 2010) and nalidixic acid which was the first synthetic quinolone antibiotic (Saga & Yamaguchi, 2009).

1.1.3 The major classes and modes of action of antibiotics

An antibiotic is defined as a chemical compound that is able, at low concentration, to either kill other bacteria, in which case it is termed bacteriocidal or inhibit bacterial growth, in which case it is termed bacteriostatic (Walsh, 2013). Antibiotics are classified based on their chemical structure into β-lactams, macrolides, tetracyclines, quinolones, aminoglycosides, sulphonamides, glycopeptides and oxazolidinones. The β-lactam class includes penicillin, cephalosporins, monobactams and carpenems (Etebu & Arikekpar, 2016). The members of the β-lactam class are characterized by a 3-carbon and 1-nitrogen ring (β-lactam ring, Figure1.1) and they either kill or inhibit bacterial growth by inhibiting bacterial cell wall biosynthesis. They do so by interfering with the enzymes essential for the synthesis of peptidoglycan (Etebu & Arikekpar, 2016). The chemical structure of macrolide antibiotics contains 14-, 15-, or 16-membered macrocyclic lactose rings in which several sugars and/or side chains have been attached (Wang *et al.*, 2017) (Figure1.1). The mechanism of action of macrolides is inhibition of bacterial protein synthesis by binding to the bacterial 50S ribosomal subunit and blocking the formation of peptide bonds (Fyfe *et al.*, 2016). Erythromycin is probably the most well-known antibiotic in this class, which includes also Azithromycin and Clarithromycin.

Another class of antibiotics that acts on the bacterial ribosome is tetracycline, members of this class prevent the addition of amino acid to polypeptide chains during protein synthesis (Chopra & Roberts, 2001). This class includes numerous antibiotics, such as tetracycline, doxycycline, oxytetracycline and tigecycline. The members of tetracycline antibiotics have a common basic structure of four hydrocarbon rings (Etebu & Arikekpar, 2016) (Figure 1.1). The quinolones class of antibiotics includes nalidixic acid, which was first discovered, oxolinic, norfloxacin, ciprofloxacin, ofloxacin, levofloxacin, sparfloxacin and moxifloxacin (Aldred *et al.*, 2014). All of these antibiotics contain two rings called the quinolone pharmacore (Figure 1.1). They are able to interfere with bacterial gyrase or

topoisomerase IV activity, they are required for DNA replication during cell division. Ultimately, quinolones cause inhibition of bacterial growth (Aldred *et al.*, 2014, Hawkey, 2003). Regarding the aminoglycosides class, the members of this class were obtained from soil Actinomycetes and have a broad spectrum of antimicrobial activity (Krause *et al.*, 2016). They inhibit protein synthesis by binding to the 30S ribosomal subunit (Leggett, 2017). Streptomycin is a well-known example of this class. The basic chemical structure of the members of aminoglycosides is three amino sugars connected by glycosidic bonds (Mingeot-Leclercq *et al.*, 1999) (Figure1.1). The first group of antibiotics used in therapeutic medicine was sulphonamides and this class of synthetic antibiotics is still used widely to treat various diseases and infections (Etebu & Arikekpar, 2016). The common chemical structure among the member of sulphonamides is a sulphonamide group (Figure1.1). The mechanism of action of this group is blocking the metabolism of bacteria by inhibiting the enzymes needed for the synthesis of folic acid (Peterson, 2008).

Glycopeptide antibiotics (GPAs) include the natural product antibiotics, vancomycin and teicoplanin, and semi-synthetic antibiotics such as oritavancin and telavancin. The chemical structure of the members of this group of antibiotics are various and the target site of these antibiotics is the cell wall, they prevent the adding of new units to the bacterial cell wall, in addition to they are active against resistant strains of methicillin-resistant *S. aureus.* (Binda *et al.*, 2014). Lastly, the oxazolidinone class, this group includes synthetic antibiotics, such as Linezolid (Figure 1.1). The mechanism of action of this class is not yet fully understood, but it has been reported that the members of this group interfere with bacterial protein synthesis by binding to the P site of the ribosomal 50S subunit (Etebu & Arikekpar, 2016).

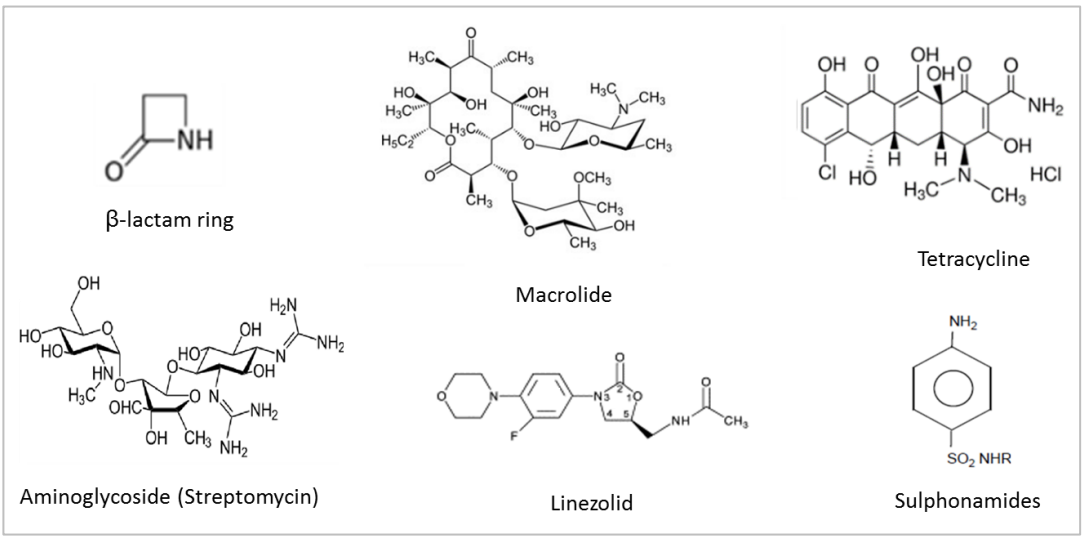

Figure 1.1. Structure of antibiotic classes. Adapted from (Etebu & Arikekpar, 2016).

As described previously, the mode of action of antibiotics against bacteria is performed by inhibiting certain vital processes of bacterial cells and metabolism. The most common targets of antibiotics are illustrated in Figure 1.2.

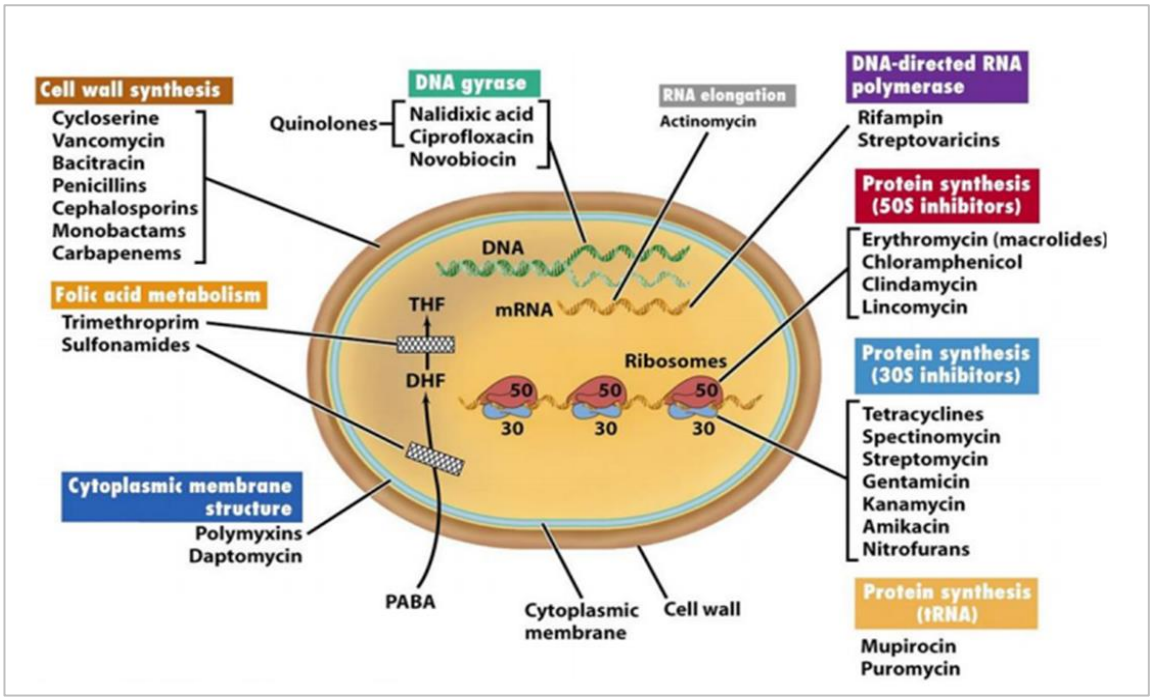

Figure 1.2. **Schematic of the cellular targets of different antibiotics**. The common antibacterial target sites of antibiotics include bacterial peptidoglycan/cell wall biosynthesis, bacterial protein synthesis, nucleic acid synthesis, folate biosynthetic pathway. Taken from (Etebu & Arikekpar, 2016).

1.1.4 The burden of "rediscovering" natural product-derived antibiotics

As mentioned earlier, the majority of antimicrobial agents in clinical use are derived from microbial sources, in particular, *Streptomyces*. Genome sequencing over the last 20 years has revealed that this genus has the genetic capacity to produce more bioactive metabolites than that detected by bioscreening. Awakening this metabolism that otherwise would likely have remained 'cryptic' may generate leads for the development of a new generation of antibiotics. The challenges that face the discovery of successful natural product antibiotics is the difficulty to find a bioactive compound with the required spectrum of activity, currently there is a greater need for antibiotics against Gram-negatives (Cars *et al.*, 2008), and a manageable level of toxicity to humans (Hughes & Karlén, 2014). As a consequence of failing these basic criteria, many leads are discarded in the early stage of the discovery process (Wright, 2017). Yet more fail to have efficacy in an animal model (Hubert *et al.*, 2017). The high failure rate contributes to the high, and some would argue almost prohibitive, costs of discovering and developing new

antimicrobial drugs. Many pharmaceutical companies started to close down their natural product research activities in 2000 (David *et al.*, 2015).

1.1.5 Methods of "derepliction"

In order to concentrate the efforts on the discovery of new natural antibiotics, dereplication strategies were introduced in the 1990s to improve the performance of screening pipelines for natural products (Hubert *et al.*, 2017). Dereplication is defined as the rapid identification of known compounds in complex mixtures such as crude extracts using analytical techniques in combination with databases detailing the properties of known compounds (Hubert *et al.*, 2017, Nielsen *et al.*, 2011). De-replication includes extraction of the crude extract followed by fractionation. The biological activities of all fractions are then screened and only the bioactive fractions are analysed to identify their chemical profiles. They are then compared with a metabolite database to identify unknown metabolites. Or after the fractionation, all the fractions are analysed to identify the unknown compounds prior to the bioactivity test (Hubert *et al.*, 2017, Tawfike *et al.*, 2013) (Figure 1.3). Briefly, the most common analytical tools used for the dereplication of natural products are based on mass spectrometry (MS), which is an accurate and sensitive method for the rapid method that provides the precise mass, elemental composition and fragmentation pattern of compounds. It is used alongside high-performance liquid chromatography (HPLC) or ultra-HPLC (Hubert *et al.*, 2017), which fractionate natural compounds at analytical scale thereby allowing the MS analysis of purified compounds (Hubert et al., 2017). HPLC is often used with a diode-array detector (DAD), which allows the continuous detection of absorbance at different wavelengths (Es'haghi, 2011). The most widely used MS-based method for analysing natural product is time-of-flight (TOF), in which the time taken for an ionised form of the compound to travel a fixed distance in a defined electric field that is used to determine the mass (Hubert *et al.*, 2017, Nielsen *et al.*, 2011). Another analytical tool is nuclear magnetic resonance (NMR), which is a spectroscopic technique used to measure magnetic fields around atomic nuclei (Halabalaki *et al.*, 2014).

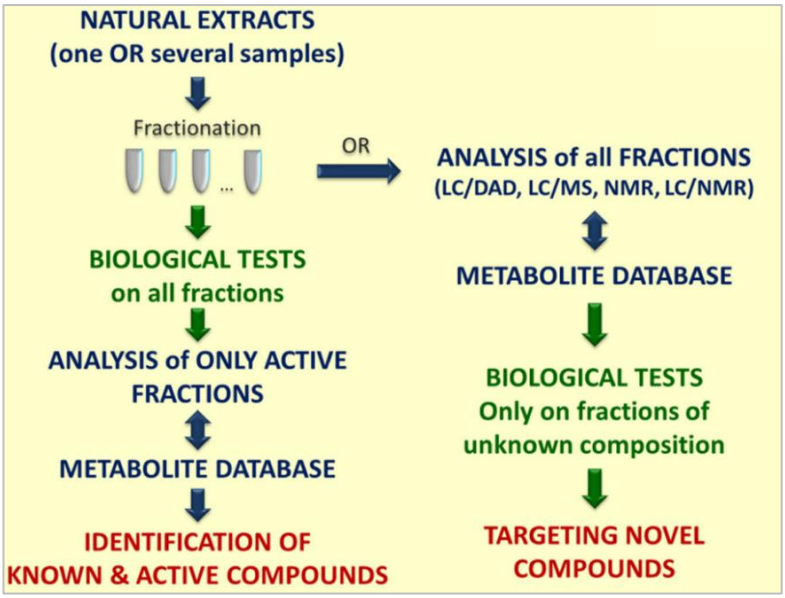

Figure 1.3. Dereplication workflow for identification a new bioactive compound(s). Taken from (Hubert et al., 2017).

1.2 Resistance mechanisms and the limited clinical lifespan of antibiotics

The spread of multidrug-resistant (MDR) bacteria (i.e. those resistance to all classes of antibiotics currently available in clinical practice) has led to untreatable infections becoming a major global healthcare problem in the 21st century (Alanis, 2005, Lewis, 2013, Munita & Arias, 2016). Improper use and over-prescription are considered to have accelerated the development of antibiotic resistance (Alanis, 2005). Bacteria may become resistant to antibiotics through spontaneous mutation (mutational adaptations) or by acquiring genes conferring resistance from other bacteria (horizontal gene transfer) often via conjugation (Munita & Arias, 2016). Bacteria resist the antibiotic using one the following mechanisms: i) modifications of the antimicrobial compound, ii) prevention of the antibiotic from reaching its target by decreasing drug uptake or activation of efflux pumps, iii) changes and/or bypass of target sites, and iv) global cell adaptive processes. Enzymatic modification of the target entails the production of an enzyme, which is able to introduce chemical changes to an antimicrobial compound resulting in impaired binding to its target. For example, aminoglycoside-modifying enzymes covalently modify the amino or hydroxyl groups of the aminoglycoside molecule (Munita & Arias, 2016) , whilst β-lactamases hydrolyse the amide bond of the β-lactam ring (Munita & Arias, 2016). Another mechanism of antibiotic resistance is reduced antibiotic influx. This is a mechanism more prevalent in Gram-negative bacteria, as the outer membrane acts as the first line of defence (Munita & Arias, 2016). The penetration of hydrophilic antibiotics

such as β-lactams, tetracyclines and some fluoroquinolones can be limited by a mutations that reduce the number of porins, which are water-filled diffusion channels, located in the outer membrane of Gram-negative bacteria (Fernández & Hancock, 2012, Munita & Arias, 2016). Bacterial strains are also able to reduce the accumulation of antibiotics within the cytoplasm by exporting them out of the cell via efflux pumps in the inner membrane. A well-known example of an efflux pump is TetA, a tetracycline-resistance determinant associated with Tn10 mobile genetic elements in *E. coli* (Fernández & Hancock, 2012, Munita & Arias, 2016). Changes in the bacterial cell wall have also been associated with resistance, e.g. one mechanisms of daptomycin resistance in *S. aureus* is associated with an increase in the overall positive charge of the cell membrane which is believed to repel this antibiotic (Miller et al., 2016, Munita & Arias, 2016).

Alteration of the target sites of an antibiotic is another common resistance mechanism, an example being methylation of the 23S rRNA component of the 50S ribosome subunit by erythromycin resistance determinants (Skinner *et al.*, 1983, Weisblum, 1995). Such a modification impairs the binding of erythromycin and several other macrolides. Targets can also be protected by ancillary proteins, examples of which are the tetracycline resistance determinants TetM and TetO. These proteins protect the ribosome by interacting with and dislodging ribosome-bound tetracycline in a GTP-dependent manner (Donhofer *et al.*, 2012, Li *et al.*, 2013). The FusB determinant mediates resistance to fusidic acid (FA) in *S. aureus* by binding to EF-G (elongation factor G) on the stalled ribosome ·EF-G·GDP·FA complex. This interaction causes dissociation of the complex, and therefore clears the ribosomal A site, which allows translation to resume (Cox *et al.*, 2012, O'Neill & Chopra, 2006). In brief, the modification of target mechanism may be due to: i) mutations in the genes encoding target sites, ii) enzymatic modification of the target, through addition or alteration of a specific chemical group, and/or iii) replacement or bypass of the target site whilst retaining the functionality of the target (Munita & Arias, 2016).

1.3 The emergence of target–orientated approaches to antibiotic discovery and the ensuing ‘Innovation Gap’

As an alternative to screening natural products, which as mentioned above is increasingly needing dereplication steps, pharmaceutical companies are increasingly exploring target-based approaches to develop new antibiotics. These target-based approaches, which are often involved *in silico* docking of small molecules to atomic structures, were being used in other areas to develop drug leads, such as inhibitors of

kinases implicated in cancer (Ferreira *et al.*, 2015). Targets for developing new antibiotics are essential, often highly conserved, genes and virulence factors, especially those that are expected to be soluble and yield high-resolution atomic structures. The former targets include aminoacyl-tRNA synthetases (aaRSs) which are essential for translation and as such are required for the viability of all bacterial strains (Randall *et al.*, 2016). The targeting of virulence factors rather than activities central to growth may not exert level of selective pressure that has yield rapid resistance to antibiotics used currently in the clinic (Heras *et al.*, 2015, Vadekeetil *et al.*, 2016). Another criteria is that the bacterial target should be absence from humans, or are at least not be high conserved (Alksne & Dunman, 2008). Although target-based approaches were expected to be effective (Alksne & Dunman, 2008, Swinney, 2013), there were several obstacles that proved to be a substantial barrier to success. Prominent amongst them were a lack of efficacy *in vivo*, with many leads failing to permeate bacteria and reach their targets or have suitable drug-like properties and pharmacokinetics (Alksne & Dunman, 2008). Synthetic inhibitors of aminoacyl tRNA synthetases with antibiotic activity have been developed, but have limited use due to the rapid acquisition of resistance (Hurdle *et al.*, 2005).

Given the above, and the profitability and the market longevity of drugs against chronic diseases not caused by bacterial infections, there has been a considerable 'Innovation Gap' in the discovery of antibiotics. Many large pharmaceutical companies left the antimicrobial discovery field and shifted their activity toward the treatment of chronic diseases that required prolonged treatment such as hypertension, diabetes and heart disease (Power, 2006, Projan, 2003, So & Shah, 2014). Consequently, the majority of antibiotics in current use were discovered between 1929 and 1962 (Coates & Hu, 2007). The years antibiotic were first used and the years resistances were first detected are shown schematically in Figure 1.4. In the period between 1960 and 2000, no new class of antibiotic was discovered and the output of antibiotic discovery was limited to introducing some derivatives from previously discovered antibiotics (Silver, 2011). From 2000 to 2010, three chemical classes of antibiotics were introduced in clinical use acid, pleuromutilins, oxazolidinones and lipopeptides, but these were first discovered in 1952, 1978 and 1987, respectively (Fischbach & Walsh, 2009, Silver, 2011).

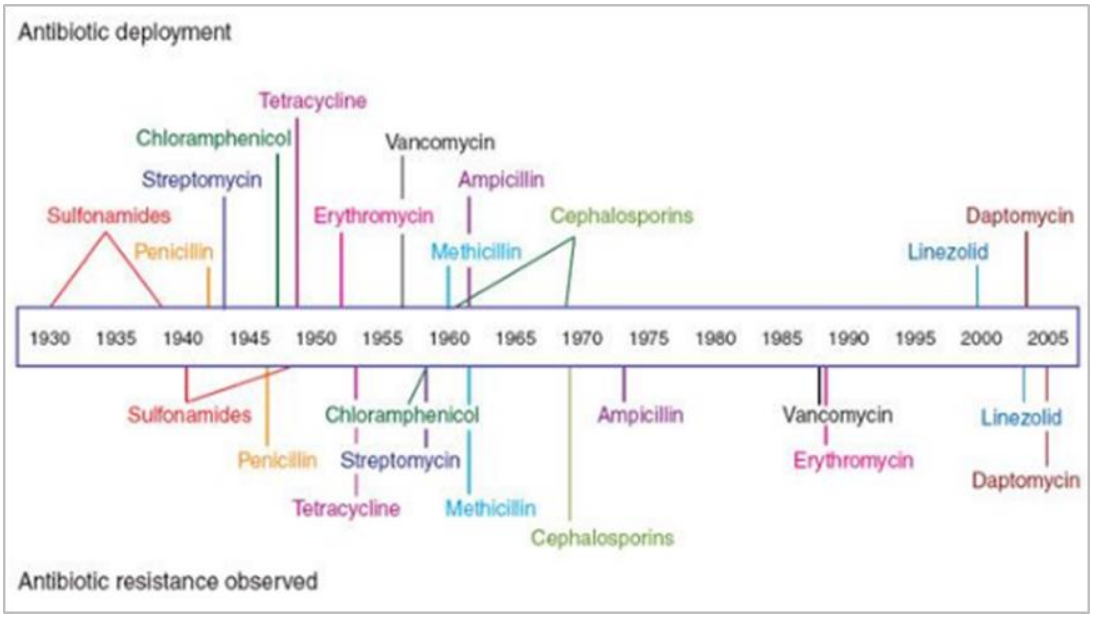

Figure 1.4. The timeline of antibiotics spread and antibiotic resistance arising. Taken from (Clatworthy et al., 2007).

1.3.1 The development of synthetic chemical libraries and high-throughput screening

Central to target-based approaches are high-throughput approaches that allow potentially tens if not hundreds of thousands of chemical compounds to be screened against particular chosen targets under given conditions. These approaches incorporate automated sample preparation, liquid sample handling, assay readout and data analysis (Carnero, 2006, Szymański *et al.*, 2012). The properties of hits are compared and contrasted within themselves and with entries in extensive databases, such as Chemical Space (Wang *et al.*, 2009b) to identify the chemical space(s) for further exploration (Carnero, 2006, Szymański *et al.*, 2012). The inclusion of the details of the synthesis of entries in databases facilitates the testing of compounds of interest in the absence of purified material being available (Marsh, 2002). The development of high-throughput approaches was accompanied by new chemistries to generate increasingly large and diverse libraries with new combinations of functional groups, libraries of compounds often very different from metabolites found in nature (Marsh, 2002). Examples of new chemistries include Biology-Oriented Synthesis (BOS) (Wetzel *et al.*, 2011) and Activity-Directed Synthesis (ADS) (Karageorgis *et al.*, 2015).

1.3.2 Synthetic inhibitors of aminoacyl tRNA- synthetases as an example

Aminoacyl tRNA–synthetases (aaRSs) have a fundamental role in protein synthesis, as they are responsible for creating aminoacyl-tRNA units through the coupling of an amino acid to tRNA containing the corresponding anticodon. These enzymes are specific for each amino acid and the cognate tRNA (Ibba & Soll, 2000). There are several classes of natural antibiotics with the ability to inhibit aminoacyl tRNA-synthetases, e.g. mupirocin (Sutherland *et al.*, 1985) and reveromycin A (Osada, 2016). However, antibiotic resistance to inhibitors of aaRSs, or at least those developed to date, has arisen rapidly. In the case of mupirocin (pseudomonic acid A), originating from *Pseudomonas fluorescens* (Sutherland et al., 1985), one study has identified resistance in around four fifth of isolates of *S. aureus* tested (Seah *et al.*, 2012) . The situation was similar for GSK'052 a novel synthetic, broad-spectrum antibacterial agent that selectively inhibits bacterial leucyl tRNA-synthetase (Gupta et al., 2016). Clearly, good pharmacokinetics and efficacious against bacteria in the lab are insufficient to ensure antibiotics are a success in the clinic (Hernandez *et al.*, 2013, Hubert *et al.*, 2017). To reduce the rate at which antibiotic resistance is acquired, an increasing number are advocating the use of the next generation of antibiotics only as combinations, each of which has a different target (Alksne & Dunman, 2008). The rationale is that properly administered it would be highly unlikely, if not impossible, for a bacteria to have spontaneous mutations that would negate the activity of multiple antibiotics.

1.4 The current burden of bacterial infections

Infectious diseases are associated with increased mortality and morbidity. It has been estimated that approximately 25% of the people who died worldwide do so as a result of a bacterial infection (Taylor *et al.*, 2001). In the US, around 23,000 deaths annually have been attributed to infection by antibiotic-resistant bacteria. The cost of bacterial infections treatment is approximately 20 billion dollars per year in the US alone (Munita & Arias, 2016). Amongst the bacteria that are considered as major threats to global health is meticillin-resistant *S. aureus* (MRSA). Currently MRSA infections cause approximately 19,000 deaths per year in the U.S (Fischbach & Walsh, 2009). MRSA is a common hospital-acquired microorganism that causes infection of the cardiovascular system, skin and soft tissue and the lower respiratory tract infarctions (Hassoun *et al.*, 2017, Klein *et al.*, 2007). Another organism of major concern is *Mycobacterium tuberculosis*, which causes serious infections in the lung (Delogu *et al.*, 2013, Ventola, 2015). The WHO (World Health Organization) reported that 170,000 people died worldwide in 2012 as a result of tuberculosis (TB) infections (Fischbach & Walsh, 2009, Gross, 2013, Ventola, 2015). The current standard treatment for TB is lengthy and incorporates expensive

drugs with often serious side effects (Fischbach & Walsh, 2009, Ventola, 2015). There are other antibacterial resistant bacteria that lead to severe infections in the healthy host but are less prevalent than above-mentioned strains, such as *E. coli* and ESKAPE pathogens group which include *Enterococcus faecium*, *Staphylococcus aureus, Klebsiella pneumoniae*, *Acinetobacter baumanni*, *Pseudomonas aeruginosa* and *Enterobacter* specie (Fischbach & Walsh, 2009, Rice, 2008).

1.5 Global and government plans to counter antimicrobial resistance

In order to combat the prevalence of antibiotic resistance, the World Health Assembly adopted in 2015 a global action plan (WHO, 2015) which recommended improving knowledge and understanding of antibiotic resistance, developing national surveillance and research systems, minimising the incidence of infections by better hygiene, effective sanitation and development of infection prevention agents (e.g. vaccines), optimising the use of antimicrobial medicines in human and animal health and increasing the investment in the development of new antibiotics, diagnostic tools and complementary therapeutics (WHO, 2015).

1.5.1.1 Vaccination and other approaches complementary to antibiotic development

Because of the difficulties facing the discovery of new classes for addressing antibiotic resistant bacteria, as described elsewhere, the efforts have been directed toward finding the alternatives of antibiotics to treat the infectious diseases as a part of the solution, such as vaccines and other health technologies (Lipsitch & Siber, 2016). The use of vaccines against common antibiotic-resistant bacteria would reduce the demand on antibiotic use by providing direct protection and minimising person to person transmission (i.e. indirect protection) (Lipsitch & Siber, 2016). Vaccines are available against tuberculosis (*M. tuberculosis*) (Bastos *et al.*, 2009), diphtheria (*Corynebacterium diphtheriae*), tetanus (*Clostridium tetani*) (Harro *et al.*, 2010), pertussis (*Bordetella pertussis*) (Decker & Edwards, 2000), some forms of severe pneumonia and meningitis (*Haemophilus influenzae* type B) (Trotter *et al.*, 2008), cholera (*Vibrio cholerae*), typhoid (*Salmonella* Typhi) (Wahdan *et al.*, 1975) and the majority of community-acquired pneumonia (*Streptococcus pneumoniae*) (Principi & Esposito, 2016). Despite the development of vaccines, antibiotics will be required in the long term to treat individuals who have not be vaccinated or are immunocompromised, become infected by a bacterial species for which there is no vaccine, or are infected by a strain that as a result of a genetic shift is not recognised by antibodies raised against a vaccine created for an ancestral strain (Tagliabue & Rappuoli, 2018). In addition to vaccines, there are other

alternatives, non-compound approaches, currently under development and it is expected that these could come to market within the next ten years (O'Neill, 2016). These include bacteriophage "phage" therapy (wild-type or engineered), which is the use of lytic bacteriophages clinically to treat bacterial infections (Czaplewski et al., 2016, O'Neill, 2016), and therapies based on the use of phage lysins, which are the enzymes of lytic phage that mediate the rupture of infected bacteria and consequently the release of progeny phage particles, and immune stimulations such as P4 peptide which is a chemically synthesised amino acid peptide (Czaplewski *et al.*, 2016, O'Neill, 2016). The current advance in human phage therapy trials is successfully targeting MDR Gram-negative bacteria such as *Acinetobacter baumannii*, *Pseudomonas aeruginosa*, and members of the *Enterobacteriaceae* (Furfaro et al., 2018*)*. However, it is unlikely that phage will replace antibiotics as their systemic use is likely to be limited because they can be expected to elicit an immune response (Pires *et al.*, 2016). A lysin (CF-301) directed to MRSA has completed phase 1 human clinical trials, demonstrating its safety, and is now entering phase 2 to test its efficacy in treating hospitalized patients with bacteraemia or endocarditis. If successful, it could be leading to the widespread development and use of acceptance of lysins as an alternative to antibiotics (Fischetti, 2018). In addition to purified components such as P4, extracts of bacteria have been reported to stimulate innate immunity and decrease the frequency of recurrent respiratory tract infections in children and chronic obstructive pulmonary disease in adults (Bangert *et al.*, 2012, Czaplewski *et al.*, 2016).

1.5.1.2 Revisiting natural products as a source of new antibiotics

Nature is a predominant source of antimicrobial compounds; natural products are at their root genetically encoded and produced by bacteria and fungi via secondary metabolic pathways (Pye *et al.*, 2017, Wright, 2014). As indicated previously, the majority of antibiotics in clinical use were obtained from a natural source, the secondary metabolism of *Streptomyces* species. The opportunity to find a novel antibiotic with drug-like properties is higher when the source is nature rather than synthetic chemistry given natural products have been selected to have some drug-like properties such as being able to enter cells. They also tend to have greater 3-dimensional structural diversity that can facilitate a greater range of contacts with their target; synthetic chemistry to date as tended to produce planar molecules (Adam Nelson, pers. comm.). Despite these advantages, there are several challenges in the natural products discovery field, as aforementioned, and no new class of antibiotic has been delivered into the clinic in over 40 years. Another important component of the dereplication process (see Section 1.1.5) is to use, during the initial screening a panel of indicator strains with resistance to multiple

antibiotics for which there is already resistance in the clinic (Cox *et al.*, 2017). Several indicators strains have been engineered and distributed by, for example, Cubist Pharmaceuticals, a US biopharmaceutical company (Baker *et al.*, 2007). Given recent developments in dereplication, it can be argued there is merit in revisiting sources that have already been screened, particular if the sources can be screened in such a way that accesses previously untapped metabolism. Genome and metagenome sequencing reveals the depth to secondary metabolism (Ziemert *et al.*, 2016).

The actinomycetes, members of the order Actinobacteria to which the *Streptomyces* genus belongs, is a major source of antibiotics in clinical use today (Wright, 2014, Wright, 2017). Whole-genome sequencing data has confirmed that each strain of *Streptomyces* is on average able to produce 20-40 secondary metabolites (Wright, 2017). Most of these compounds have not been tested and characterized yet, as they are not produced under the laboratory conditions (van der Heul *et al.*, 2018). In order to obtain new natural antimicrobial compounds, different methods are needed to activate the silent biosynthetic genes clusters (BGCs), which encoded these metabolites by, for instance, changing the growth conditions, using chemical elicitors and engineering strains to overproduce key regulatory factors (Wright, 2017).

Furthermore, genome sequencing revealed that some Gram-negative bacteria produce antibiotics that are known currently. Amongst these are myxobacteria and pseudomonads which produce myxopyronin and mupirocin, respectively. Gram-negative bacteria also have a genomic capacity to produce antibiotics, such as gramicidin which is produced by bacilli and it is still in clinical use (Wright, 2017). As for actinomycetes, genome sequencing identified that each fungal genome encoded a large number of natural product biosynthetic clusters (van der Lee & Medema, 2016, Wright, 2017), in addition to penicillin which accounts for approximately 60% of antibiotics that are used currently (Wright, 2017). Whole genome sequencing of species helps to predict the structure of a natural compound and determine whether it is known (Wright, 2017). There is an expectation that other soil bacteria other than streptomycetes will produce antimicrobial activities assuming a major role of these activities is to thwart the growth of competing organisms.

Genome mining with regard to antibiotic discovery is largely the identification of BGCs within the genome of species based on homology to known BGCs for which there the biochemical pathway, product(s) and activity might already be documented (Bachmann *et al.*, 2014, Wang *et al.*, 2013b). Genome mining is being accelerated by advances in next-generation sequencing (Bachmann *et al.*, 2014, Ward & Allenby, 2018). It is now

becoming increasingly common to sequence environmental samples without culture and purification of individual members of often diverse population (Kunin *et al.*, 2008). This is a branch of the growing field of metagenomics (Thomas *et al.*, 2012). The tools for the identification of BGCs are continuing to be developed. For example, the latest version of antiSMASH (antibiotics and secondary metabolite analysis shell) adds "detection rules" for another eight classes of secondary metabolites and predicts better the products of gene clusters encoding type II polyketide synthases (Blin *et al.*, 2019). Whilst clusters of interest can be identified more readily, a major limiting factor in their characterisation is poor expression under laboratory conditions.

1.5.2 Chemical elicitors of antibiotic production

Chemical elicitors technique has been used recently to stimulate the synthetic of the secondary metabolites that are encoded by cryptic BGCs in actinomycetes. The list of small molecule elicitors reported in the literature includes N-acetylglucosamine, sodium-butyrate, ARC2, scandium and γ-butyrolactones (Abdelmohsen *et al.*, 2015, Zhu *et al.*, 2014). N-acetylglucosamine (GlcNAc), which is a cell wall monomer, activates the production of the pigmented secondary metabolites, actinorhodin and undecylprodigiosin, in *S. coelicolor* under poor growth conditions, the mechanism of elicitation is described in Section 1.7.1.4. Sodium-butyrate, is an HDAC (histone deacetylases) inhibitor which alters the structure of chromosome resulting in change in biosynthetic gene cluster expression (Abdelmohsen *et al.*, 2015, Zhu *et al.*, 2014), it has been noticed that *S. coelicolor* showed a response to sodium-butyrate in a similar way to N-acetylglucosamine through overproduction of actinorhodin on minimal media and an opposite effect of sodium-butyrate was observed under rich growth conditions (Abdelmohsen *et al.*, 2015, Zhu *et al.*, 2014).

ARC2, defined as an antibiotic-remodelling compound, is another elicitor that activates the production of antibiotics in *S. coelicolor* (Abdelmohsen et al., 2015, Craney et al., 2012, Zhu et al., 2014). It acts as an inhibitor of fatty acid biosynthesis via inhibition of enoyl-acyl carrier protein reductase FabI which is a key enzyme responsible for the last step of fatty acid biosynthesis. Fatty acid biosynthesis (primary metabolism) and secondary metabolism compete for acyl-CoA precursor, thus ARC2 might act through the partial inhibition of FabI leading to diverting the flow of acyl-CoA towards antibiotic production (Abdelmohsen *et al.*, 2015, Zhu *et al.*, 2014). ARC2 is synthetic and was discovered by a 'checkerboard' analysis (Pillai *et al.*, 2005). This approach also identified ARC6, which appears not to have the same target as ARC2, but may inhibit the same metabolic process (Ahmed *et al.*, 2013).

Rare earth elements such as scandium also play a role in the elicitation of antibiotic production. Scandium activates the production of actinorhodin by *S. coelicolor*, actinomycin by *S. antibioticus* and streptomycin by *S. griseus* by 2 to 25-fold (Kawai *et al.*, 2007, Zhu *et al.*, 2014). It also enhanced actinorhodin production in *S. lividans* which is normally dormant in this strain (Abdelmohsen *et al.*, 2015, Kawai *et al.*, 2007, Zhu *et al.*, 2014). The exact mechanism by which this element activates some parts of secondary metabolism is unknown (Abdelmohsen *et al.*, 2015). γ-Butyrolactones showed a role in the activation and regulation of antibiotic production.This role is detailed in Section 1.7.1.3.

1.6 The biology of *Streptomyces*/Actinomycetes

The *Streptomyces* genus contains Gram-positive bacteria that are found in soils and sediments and grow via filaments that branch to produce an extensive mycelial colony (Flärdh and Buttner, 2009). It belongs to the Actinobacteria phylum. As indicated previously, bacteria of the genus *Streptomyces* have been a rich source of antibiotics, in addition to antifungals, antihelmintics and antitumor agents (Demain, 2010, Colombo et al., 2001).

1.6.1 The lifecycle and regulation of morphological development

The *Streptomyces* life cycle includes a series of morphological changes in which aerial hyphae grow up from the surface of the vegetative mycelium and eventually produce strings of spores, which are resistant to desiccation (Flärdh and Buttner, 2009). When a spore encounters suitable conditions and sufficient nutrients, it germinates to produce hyphae. The production of most, but not all secondary metabolites is triggered by the slowing growth of *Streptomyces*. The aerial hyphae are white, whereas the spores are grey. The latter is due to the production of a grey-coloured polyketide (Kelemen et al., 1998). These colour changes have made it relatively straightforward to identify mutations and conditions that affect morphological development (Chater & Horinouchi, 2003). Mutations that block the production of spores or their pigmentation are classified as white (*whi*), whilst those that block the production of aerial hyphae are classified as bald (*bld*). For a schematic of the developmental life cycle of *S. coelicolor*, see Figure 1.5.

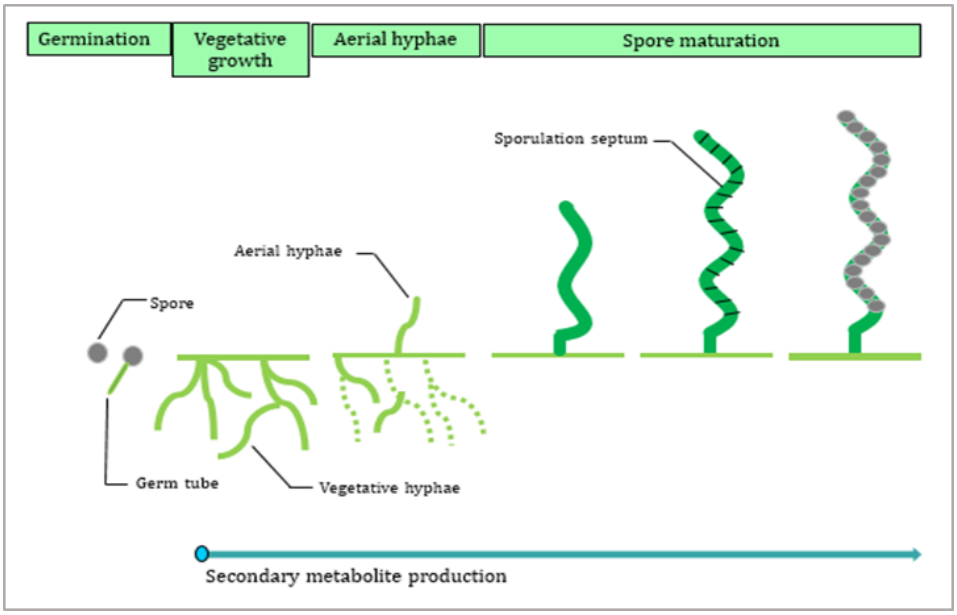

Figure 1.5. The developmental life cycle of *S. coelicolor*. A spore germinates to produce a germ tube that utilises available nutrients to produce growing branching vegetative hyphae. When nutrients become available, a programme of morphological and physiological development is triggered that results in the production of aerial hyphae and the production of a number of secondary metabolites. This programme is sustained by the lysis of the vegetative mycelium (dot lines), and the recycling of nutrients. The aerial hyphae eventually mature to produce spores and the cycle begins again. Adapted from (Flärdh & Buttner, 2009).

Formation of aerial hyphae in *Streptomyces* is controlled by *bld* (bald) genes (Figure 1.6) that form a regulatory cascade that is now relatively well characterised and is incorporated as the final step in the secretion of small surface-active peptides called SapB (Spore associated protein B) and Chaplins (coelicolor hydrophobic aerial proteins) that lower the water surface tension at the colony surface, which would otherwise serve as a physical barrier to the growth of hyphae into the air (Claessen *et al.*, 2006, Flärdh & Buttner, 2009). SapB is encoded and exported by the *ram* cluster during the vegetative phase of development, while chaplins are encoded by *chp* genes and they are organized into rodlet layers in the aerial hyphae surface by rodlins (Flärdh & Buttner, 2009). The activity of both *chp* and *ram* genes are dependent on Bld activity. The control of morphological development in the streptomycetes has been the subject of several excellent reviews (Chater & Horinouchi, 2003, Claessen *et al.*, 2006, Flärdh & Buttner, 2009).

The *bld* mutations also affect the production of secondary metabolism (Champness, 1988, Lawlor *et al.*, 1987) indicating that the underlying regulation of secondary metabolism is entwined with morphological development. The initiation of both these process also coincides with the lysis of the vegetative mycelium. The latter has been

described as form of programmed cell death that serves the purpose of releasing nutrients locally to facilitate the growth of the aerial hyphae and eventually the production of spores (Manteca & Sanchez, 2010).

The component of the *bld* cascade that links to secondary metabolism is *bldA*, which encodes the tRNA for the leucine codon UUA (Lawlor et al., 1987). This codon is not present in genes essential for vegetative growth, but in around 150 that are primarily associated with morphological development and secondary metabolism (Chater & Horinouchi, 2003). The latter include genes within the clusters for actinorhodin and prodigiosin (*actII-ORF4* and *redZ*, respectively) that regulate the transcription of the biosynthetic genes.

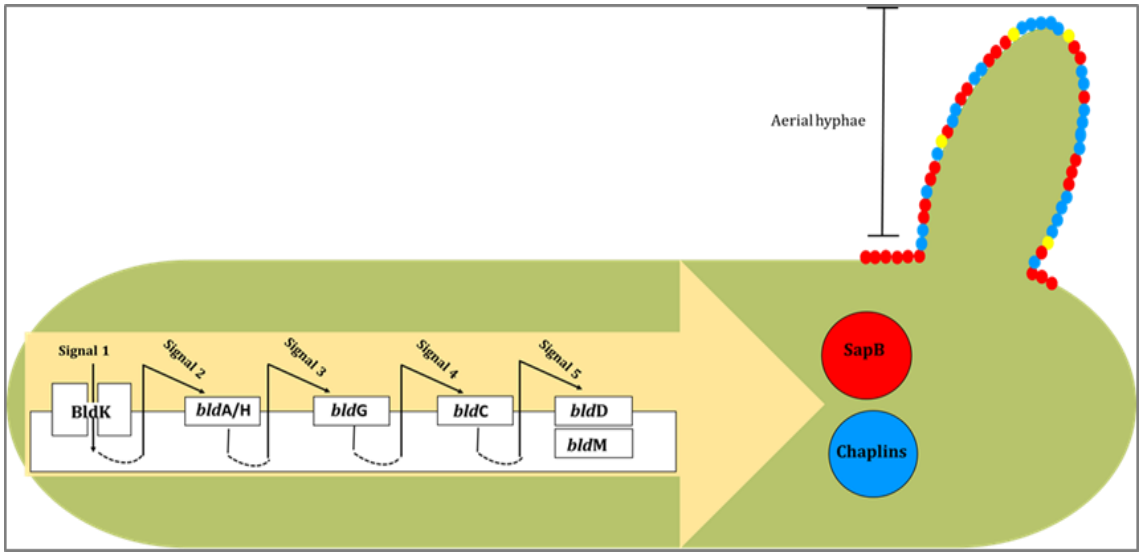

Figure 1.6. Summary of the bld cascade pathway that leads to aerial hyphae formation in *S. coelicolor*. Arrows indicate the proposed extracellular signals produced by *bld* genes, which stimulates the production of SapB and Chaplins which they act as a natural surfactant and enhance aerial hyphae growth. Chaplins are organized into rodlet layers in the aerial hyphae surface by rodlins (Flärdh and Buttner, 2009). The *bld* cascade is influenced by environmental and extracellular signals (for review, see Claassen et al., 2006). *bld* genes have a direct role in signal perception and/or signal transduction. *bldA* encodes tRNA that can translate the rare leucine codon UUA in *Streptomyces* genome. *bldD* encodes regulatory protein required for aerial hyphae formation. And BldH is an orthologue of AdpA, (see Section 1.7.1.3), in *S.coelicolor*. Whereas *bldK* encodes ATP binding cassette transporter (Den Hengst et al., 2010, Elliot et al., 2001, Flärdh & Buttner, 2009). Adapted from (Karageorgis et al., 2015, Nodwell et al., 1996).

Similar to the *bld* cascade, the characterisation of *whi* (white) mutants and the corresponding genes has led to the identification of a complex cascade that controls the septation of the aerial hyphae to produce unigenomic compartments that mature into grey-pigmented spores (Figure 1.7). *whi* mutants are classified into early (*whi A*, *B*, *H* and *I*) and late (*whi D*, *E*) genes depending on the effect of the mutation on septation

and spore maturation. Ftsz is responsible for septation, and transcription of late sporulation genes, while *whiD* and the *whiE* clusters are necessary for spore maturation and grey pigmentation, respectively. WhiG is an RNA polymerase sigma factor (sporulation-specific σWhiG factor) that directly activates the early sporulation genes *whiI* and *whiH* required for the DNA condensation septation stage (Flärdh and Buttner, 2009). In addition, *whiA* and *whiB* are also triggered by sigma factor WhiG (σ^{WhiG}). WhiB acts as an auto repressor and regulates *whiA* expression whereas WhiA acts as an auto activator and represses the transcription of *whiB*. Furthermore, *whiA* activates the expression of ParA and ParB. Both genes are essential for chromosome segregation and sporulation (Kaiser and Stoddard, 2011). Activation of the *whiE* cluster promoter depends on *sigF*, which has a role in the synthesis of the grey polyketide spore pigment (Flärdh and Buttner, 2009).The association between *bld* and *whi* genes appears through BldD which inhibits *whiG* and *whiA* before the sporulation stage (Jakimowicz et al., 2006, Elliot et al., 2001).

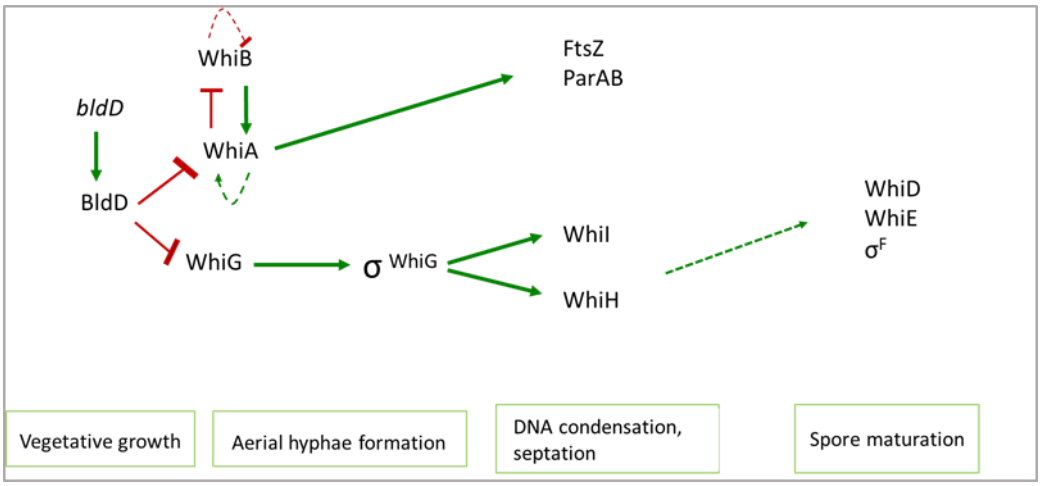

Figure 1.7. Schematic summary of key regulators require for the development of aerial hyphae into spores in *S. coelicolor*. A Green arrow indicates the activation effect, a red line ended with rectangle indicates deactivation effect. BldD is required to limit the activity of WhiG prior to sporulation. Once WhiG becomes active, σ WhiG directly activates the transcription of *whiH* and *whiI* which encode two further key sporulation transcription factors. Both WhiA and WhiB regulate the expression of each other, also WhiA is required to activate its own transcription. ParAB and FtsZ factors are required for hyphal chromosome segregation and DNA septation, respectively. Three other factors, WhiD, WhiE and σF are required for spore maturation stage. Adapted from (Kaiser& Stoddard, 2011).

1.7 *S. coelicolor* as a model for studying the regulation of secondary metabolisms

S. coelicolor has been used as a model for studying and understanding the regulation of the biosynthesis of secondary metabolism (Hopwood *et al.*, 1995). This is largely because two of the four secondary metabolites it produces under a wide variety of standard laboratory conditions are pigmented: actinorhodin (ACT) and prodigiosin (RED) are blue and red respectively (Okamoto *et al.*, 2003). Their colour has made it relatively easy to identify mutations and growth conditions that affect their production (Hopwood, 1997). The other two secondary metabolites are the calcium-dependent antibiotic (CDA) and methylenomycin (MMY). The genes corresponding to the latter are encoded on the plasmid SCP1 (Kinashi *et al.*, 1987, Kirby & Hopwood, 1977).

Actinorhodin (ACT) is an aromatic polyketide that is red at pH below 8.5 (acidic) and its biosynthesis depends on acetyl CoA as the only carbon precursor (Bruheim *et al.*, 2002). In addition, it has an inhibition activity against Gram-positive bacteria (Xu et al., 2012). It was found that purified γ-ACT had antibiotic activity against Gram-positive bacteria (Nass *et al.*, 2017). ACT gene cluster is used as a model for studying secondary metabolite gene cluster, this cluster consists of nearly 20 genes and four open reading frames (ORFs). It is regulated by ActII-ORF4 which is the pathway-specific transcription regulator that binds to target sites of the *act* promoter (Fernandez-Moreno *et al.*, 1991) (Figure 1.8, panel A). The genes encoding enzymes for the production of individual secondary metabolites are found clustered, often in association with one or more genes that regulate their transcription, as well as genes that confer resistance to the secondary (Zhu *et al.*, 2014).

In brief, the first step in ACT biosynthesis pathway is the condensation of one acetyl-coenzyme unit and seven malonyl-CoA extenders to create a long carbon skeleton by the minimal polyketide synthase (PKS), which is encoded by a gene within *actI* region of the ACT gene cluster (Figure 1.8, panel A). The produced carbon skeleton is subjected to several cyclization steps to form an (S)-DNPA by the products of genes within the region of *actII*I, *actVII*, *actIV*, *actVI-1* and *actVI-3*, respectively and then modified to DHK (5-deoxy-dihydrokalafungin) by *actVI-2*, *actVI-4* and *actVA-6*. In the final step, ACT is produced by dimerization of two DHK molecules by the products of *actVB* and *actVA-5* (Cho *et al.*, 2018) (Figure 1.8, panel B). ACT is mostly intracellular and it is then exported out the cell as a lactone form called γ-actinorhodin by ActA and ActB which are encoded by *actII-ORF2* and *actII-ORF3*, respectively. Both genes are encoded in the same

transcription unit, which is regulated by the transcriptional repressor called ActR encoded by *actII-ORF1* (Tahlan et al., 2007, Yu et al., 2012).

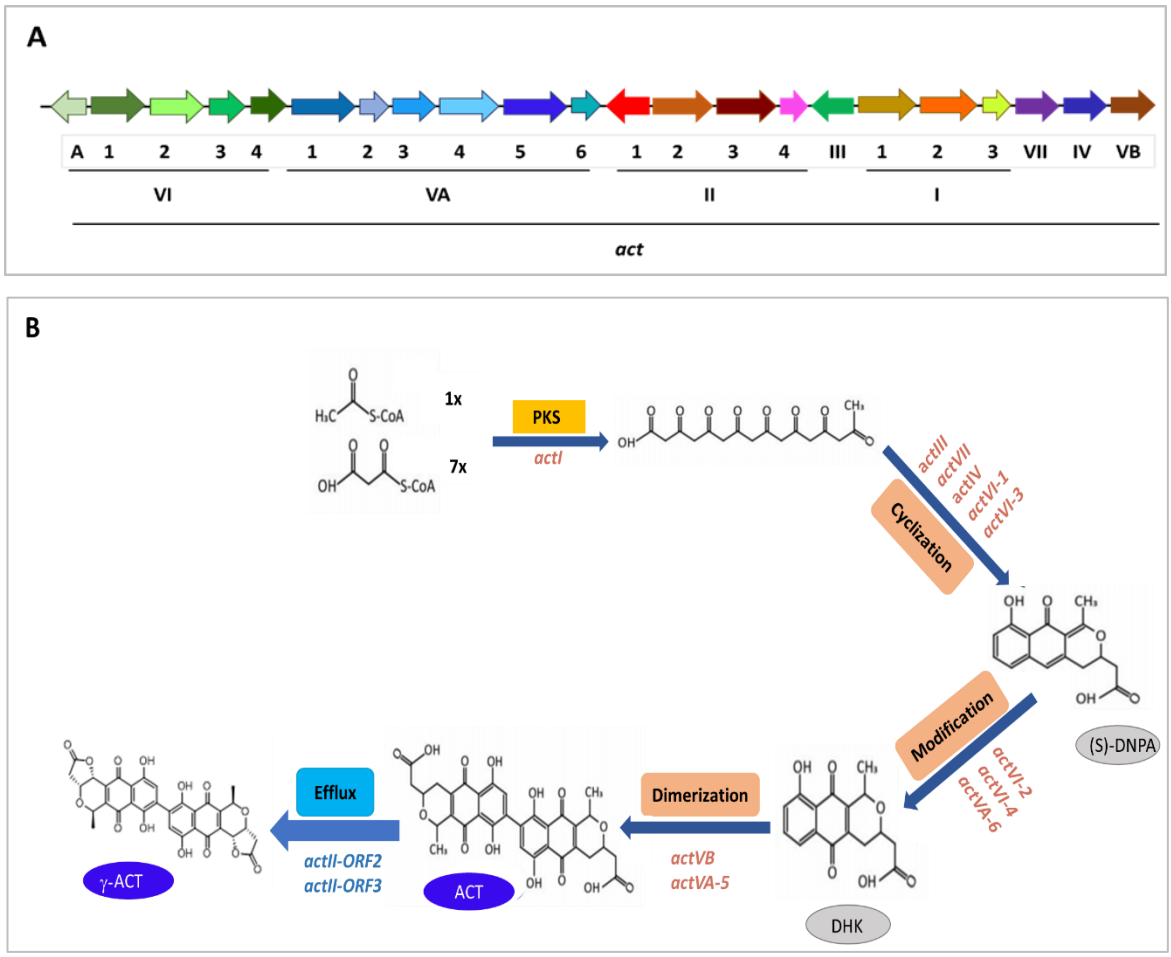

Figure 1.8. Actinorhodin biosynthetic pathway. **(A)** Open reading frame organisation of the 22-kb ACT biosynthetic gene cluster. *actII-ORF4* activator gene is in pink colour while *actR* repressor is in red colour. **(B)** actinorhodin biosynthetic pathway from the condensation of one acetyl-coenzyme A unit and seven malonyl-CoA extender units until actinorhodin production and then export it as γ-actinorhodin. Adapted from (Cho et al., 2018).

The promoter region of *actII-ORF4* is regulated by several transcription factors (Figure 1.9); AtrA which is a member of the TetR family of transcriptional regulators (Uguru *et al.*, 2005) (for more details see Section 1.8), DasR which is a member of the GntR family (Rigali *et al.*, 2004) (for more details see Section 1.7.1.4); AbsA2, which is the response regulator of the AbsA two-component system (TCS) and negatively controls antibiotic synthesis in *S. coelicolor* (Aceti & Champness, 1998, Anderson *et al.*, 2001, McKenzie & Nodwell, 2007); ROK7B7, which is a member of the ROK family and regulates the utilisation of xylose, carbon catabolite repression, and secondary metabolism in *S. coelicolor* (van Wezel & McDowall, 2011, Zhu et al., 2014). In many cases, it has been shown that mutation of the corresponding gene encoding these factors affects the

production of actinorhodin and the transcription factors bind to the promoter of *actII-ORF4 in vitro*. Binding of DasR to the promoter of *actII-ORF4* has also been shown *in vivo* (Rigali *et al.*, 2006, Świątek-Połatyńska *et al.*, 2015).

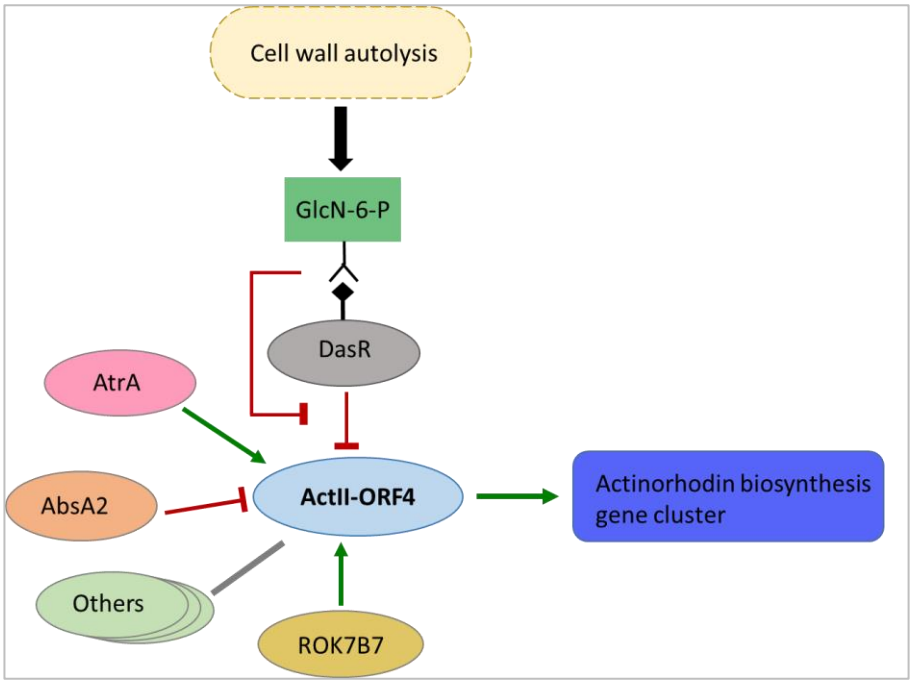

Figure 1.9. Transcriptional factors that bind to the promoter of *actII-ORF4*. A green line ending with an arrow indicates transcriptional activation, while a red rectangle ended line indicates transcriptional repression. A simple line indicates evidence of binding to a promoter region. Adapted from (van Wezel & McDowall, 2011). Under famine conditions, the GlcNAc accumulates as a consequence of peptidoglycan being degraded as part of the wider recycling of the vegetative material to fuel the production of aerial hyphae and spores (Manteca *et al.*, 2006, Rigali *et al.*, 2008). The underlying mechanism is the inactivation of the DNA-binding activity of DasR by GlcN-6-P (Rigali *et al.*, 2006), (see Section 1.7.1.4).

The other pigmented secondary metabolite produced by *S. coelicolor* is undecylprodigiosin (Red). It is a red cell-wall associated compound (Hobbs *et al.*, 1990) and belongs to prodiginine family of tripyrrole red-pigmented compounds possessing antibacterial, antifungal, anticancer immunosuppressant activities (Hobbs *et al.*, 1990, Williamson *et al.*, 2006). Production of undecylprodigiosin in *S. coelicolor* is regulated by the pathway-specific regulator called RedD, which activates the transcription of the final regulator of the RED biosynthetic gene cluster (van Wezel & McDowall, 2011, White & Bibb, 1997). It has been reported that the accumulation of undecylprodigiosin occurred during the stationary phase of growth (Hobbs et al., 1990). Similar to *actII-ORF4*, the promoter region of *redZ* is repressed by AbsA2 and DasR, which proposes that the *redZ* promoter region may respond to the level of GlcNAc and thereby activating undecylprodigiosin production (Rigali *et al.*, 2008), see Section 1.7.1.4. The production

of Red is inhibited by binding the undecylprodigiosin to the RedZ and inhibiting its binding to the target site on the *redD* promoter.

Another secondary metabolite produced by *S. coelicolor* is calcium-dependent antibiotic (CDA). It is a cyclic lipopeptide that requires calcium ions for its antimicrobial activity (Ryding *et al.*, 2002). The production of CDA is regulated by CdaR, which is the pathway-specific regulator. The promoter region of *cdaR* is deactivated by a two- component signal transduction system (AbsA1, AbsA2) and the phosphate response regulator PhoP (Hojati *et al.*, 2002, Ryding *et al.*, 2002, van der Heul *et al.*, 2018). ScbR, which is a transcriptional repressor of the "cryptic" polyketide (Cpk, now named coelimycin) cluster-situated regulator *cpkO* as well as the cAMP receptor protein (CRP), which has a role in the regulation of secondary metabolism and colony development in *S. coelicolor* (Gao et al., 2012, Piette et al., 2005) has been reported to activate *cdaR* (van der Heul et al., 2018).

1.7.1 Our current but incomplete view of the regulation of secondary metabolism

The timing of secondary metabolism production and the quantities of them are affected by the bacterial (p)ppGpp-dependent stringent response, see Section 1.7.1.1, and the growth conditions which affect the uptake and utilisation of numerous nutrients, such as carbon, nitrogen and phosphate (van Wezel & McDowall, 2011). This is in addition to the aforementioned BldA leucyl-tRNA, which is found in some genes required for antibiotic production and morphological differentiation, such as *actII-ORF4*, *redZ*, *adpA* (*bldH*) and *actA*.

1.7.1.1 The stringent response

An important mechanism that enables bacteria to survive sustained periods of nutrient deprivation is the stringent response (Boutte & Crosson, 2013). It is also associated with the production of antibiotics in different *Streptomyces* strains (van Wezel & McDowall, 2011). During nitrogen and amino acid starvation, uncharged tRNAs enter the ribosomal A site resulting in stimulation of ribosome-associated RelA to synthesise a small molecule (p)ppGpp (guanosine tetra-/penta-phosphate), which interacts with RNA polymerase (amongst other targets) and changes its specificity, thereby bringing about the stringent response (Aldridge *et al.*, 2013, Boutte & Crosson, 2013, Traxler *et al.*, 2008). The stringent response is also linked to the aforementioned ribosome-engineering (see Section 1.7.1.2).

1.7.1.2 Ribosome engineering

One of the conventional strategies employed during ribosome engineering is the introduction of mutations in ribosomal components (ribosomal protein, rRNA, or translation factor) that confer resistance to antibiotics that target the ribosome, e.g. streptomycin and kanamycin, in order to select for resistance to the certain drugs (Ochi, 2007, Ochi *et al.*, 2004). As a consequence, these mutations (even in the absence of antibiotic selection) are known to induce the production of at least some antibiotics (Ochi, 2007, Ochi *et al.*, 2004). It has been reported that *S. lividans* was able to produce a large amount of actinorhodin which is an otherwise silent BGC in this strain, after the mutation of 30S ribosomal S12 protein at a site responsible for streptomycin resistance. It also has been shown that introducing the same mutation in *S. coelicolor* led to the overproduction of actinorhodin (Ochi, 2007, Ochi *et al.*, 2004).

1.7.1.3 Quorum sensing and regulation by γ-butyrolactones

Quorum sensing is an extracellular signal transduction system which mediates cell-cell communication to coordinate their behaviours or activities (Du *et al.*, 2011). γ-Butyrolactones, small extracellular signalling molecules known as Microbial hormone-like, play a role in the communication between actinomycetes in the soil and in regulating the production of secondary metabolites (Zhu *et al.*, 2014). The best known example is A-factor (2-isocapryloyl-3R-hydroxymethyl-gamma-butyrolactone) in *S. griseu*s. When A-factor accumulates to a certain level, it induces the production of AdpA (A factor-dependent protein) by binding to ArpA (A-factor receptor protein A), which would otherwise continue to repress transcription from the *adpA* promoter, see Figure 1.10 (Ohnishi et al., 2005). AdpA in *S. griseus* has been shown to control directly the expression of hundreds of genes required for both morphological differentiation and secondary metabolism, acting as a repressor or activator of transcription (Higo et al., 2012, Ohnishi et al., 2004, Onaka et al., 1995). Antibiotic and morphological development in *S. coelicolor*, like *S. griseus*, are dependent on *adpA* (which is synonymous with *bldH*, see Figure 1.6), but unlike *S. griseus,* are not under the control of an A factor-like γ-butyrolactone. Nevertheless, γ-butyrolactones are produced by *S. coelicolor* and appear to moderate the production of actinorhodin and prodigiosin (Chater and Horinouchi, 2003, Nguyen et al., 2003, Takano et al., 2003).

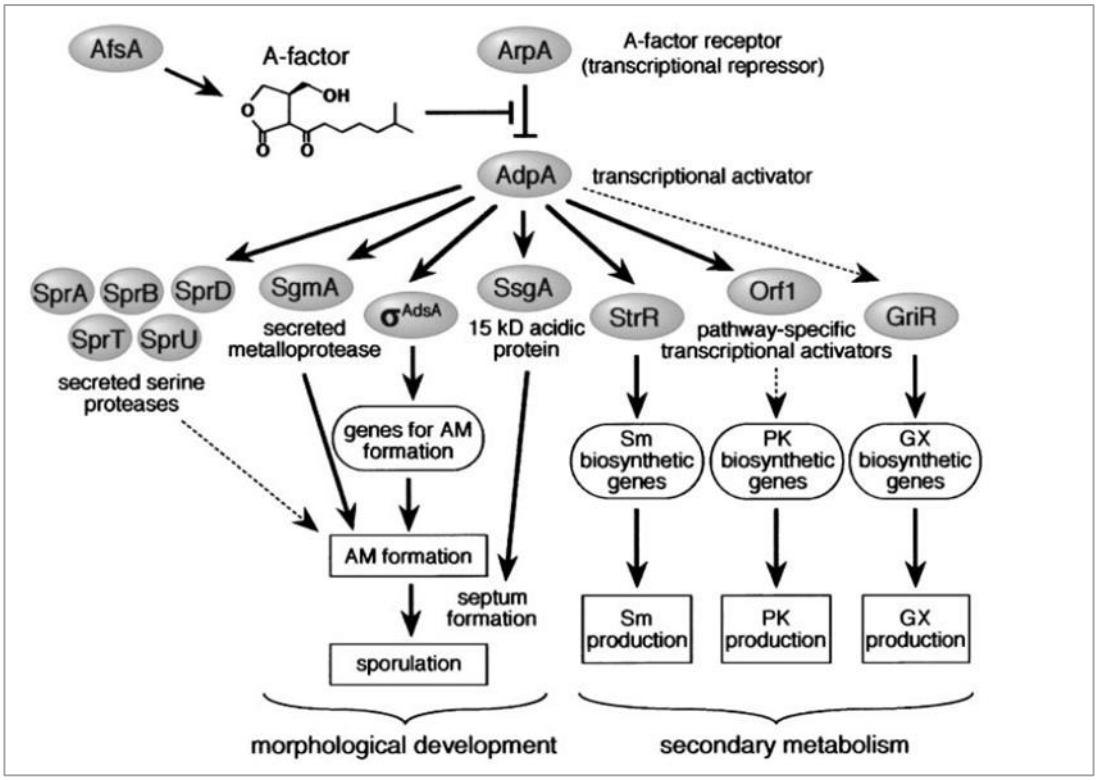

Figure 1.10. The regulatory cascade of A-factor leading to morphological differentiation and secondary metabolism production in *S. griseous*. Taken from (Ohnishi *et al.*, 2005).

1.7.1.4 Regulation by N-acetylglucosamine and the DasR regulon

DasR controls the uptake and metabolism of N-acetylglucosamine (GlcNAc) and the degradation of chitin to N-acetylglucosamine (Rigali et al., 2004). The DasR regulon is induced by glucosamine-6-phosphate (GlcN-6-P; Rigali et al, 2006), an internal intermediate of GlcNAc, allowing mycelia to make maximum use for GlcNAc when it is available. DasR binds to the promoter region *actII-ORF4* and *redZ* which as mentioned earlier encodes the final regulators of the ACT and RED cluster, respectively (van Wezel & McDowall, 2011). The binding site of DasR in the *actII-ORF4* promoter region, as first shown *in vitro* and confirmed *in vivo* by ChIP-seq (Świątek-Połatyńska et al., 2015, Rigali et al., 2006), overlaps that of RNA polymerase. This suggests that DasR represses transcription of *actII-ORF4* in the absence of induction by GlcN-6-P, see Figure 1.9. It is thought that de-repression occurs via the accumulation of GlcNAc as a consequence of peptidoglycan being degraded as part of the wider recycling of the vegetative material to fuel the production of aerial hyphae and spores (Rigali et al., 2008, Manteca et al., 2006). The underlying mechanism is the inactivation of the DNA-binding activity of DasR by GlcN-6-P (Rigali et al., 2006).

1.7.2 Signal transduction and the corresponding molecular systems

Bacterial species use the signal transduction system to adapt to changing environments. Cell detects the signal and transforms it into cellular responses in different mechanisms at a molecular level. Signals are transduced by one and two-component systems and derivatives thereof (Cashin *et al.*, 2006).

The one-component system is the most common signal transduction system in bacteria, there are around 20 families of one-component systems, amongst these is the TetR family of regulators (TFRs) which are widely distributed among bacteria and archaea (Cuthbertson & Nodwell, 2013). In one-component systems, the sensor domain and the DNA-binding domain are located on the same polypeptide. Typically DNA-binding domain is positioned at either N- or C- terminal end of the protein (Ahn *et al.*, 2012, Cuthbertson & Nodwell, 2013, Ulrich *et al.*, 2005). The binding of a small molecule to the sensor domain causes an allosteric change in the conformation of the polypeptide that alter the ability of the reading heads within the DNA-binding domain to engage the cognate sites on DNA. The binding of small molecules can either promote or impede DNA-binding to specific sites depending on the system. The best and well known examples are LacI (Lewis, 2005) and TetR (Meier *et al.*, 1988). There are 153 members of the TetR family in *Streptomyces coelicolor* (Cuthbertson & Nodwell, 2013).

Another important transduction system is the two-component system (TCS), which is abundant in *Streptomyces*, there are around 50 to 100 TCSs found in *Streptomyces* (van der Meij *et al.*, 2017). These systems involve two components, a sensor histidine protein kinase which is regulated by extracellular signal and a response regulatory protein. Once the TCS system activates by an environmental stimuli creating a high energy phosphoryl group, whereby the phosphate group is transferred to a corresponding response regulatory protein, leading to conformational change in the regulatory domain, consequently activation it to respond to the environmental signal (van der Meij *et al.*, 2017, Zschiedrich *et al.*, 2016). An example of a wide-spread if not ubiquitous TCS is PhoRP, which responds to phosphate levels and controls the genes associated with the uptake and assimilation of this inorganic compound and has a role in controlling the production of antibiotics in streptomycetes (van der Meij *et al.*, 2017). Many transduction systems directly or indirectly control the production of secondary metabolites of streptomycetes. For the vast majority, the signals to which they respond have not been identified. The identification of these signals may provide opportunities to elicit the production of secondary metabolites that would otherwise remain cryptic apart from their genomic signature.

1.8 The discovery and subsequent characterisation of AtrA

AtrA, as mentioned above it is a TetR member, is ubiquitous in *Streptomyces* and its function is being studied beyond *S. coelicolor.* Many mutations and growth conditions that affect the production of actinorhodin have been shown to alter the level of *actII-ORF4* mRNA (Aceti & Champness, 1998) suggesting that ultimately their effect is mediated by a change in the transcription of *actII-ORF4*. This prompted a biochemical screen of a *S. coelicolor* extract, which identified an activity that could bind the promoter of *actII-ORF4 in vitro*. Subsequent purification of the activity identified the source as AtrA. Disruption of the corresponding *atrA* gene (SCO4118), which is not associated with any gene cluster for a secondary metabolite (Uguru et al., 2005), reduced the production of actinorhodin, but had no detectable effect on the production of prodigiosin. This indicated that *atrA* has specificity with regard to the biosynthetic clusters it influences (Uguru et al., 2005). Within the streptomycetes, *atrA* (SCO4118) is associated with a divergent gene (SCO4119) encoding NADH dehydrogenase (Ahn et al., 2012), a member of the oxidoreductases. The role of this enzyme in maintaining the redox balance that may link it to actinorhodin, which is an oxidant (Shin et al., 2011). This possibility has yet to be explored.

There are two binding sites for AtrA in the *actII-ORF4* promoter region, centred at −162 and +86 bp relative to the transcriptional start site (Gramajo et al., 1993). Binding to the -162 site has been confirmed *in vivo*, although the identity of the transcription factor was not confirmed (McArthur and Bibb, 2008). More recently, AtrA was found using a biochemical approach to bind to the promoter that directs transcription of the entire cluster for daptomycin (Mao et al., 2015), a cyclic lipopeptide antibiotic produced by *S. roseosporus* (Miao et al., 2005). Disruption of *atrA-sr* produced a *bld* phenotype and completely blocked daptomycin production. In the same study, *atrA-sr* expression was shown to be positively regulated by AdpA, an orthologue of the A-factor receptor (Ohnishi et al., 1999). Thus, in *S. roseosporus* AtrA is a mediator of the aforementioned A-factor signalling pathway (Section 1.7.1.3). Moreover, it was also shown that AtrA-sr binds to its own promoter and autoregulates its own expression. Intriguingly, however, comparison of the binding sites identified in *S. roseosporus* revealed little similarity with those identified in *S. coelicolor*.

In *S. griseus* AtrA is not a mediator of the A-factor regulatory cascade, but can moderate its effects under at least some conditions (Hirano et al., 2008). AtrA-sc binds to the promoter of *strR*, the cluster-situated regulator of streptomycin production, between the binding sites of AdpA (Hirano et al., 2008, Hong et al., 2007). Disruption of AtrA in *S.*

avermitilis led to an increase in the production of avermectin in *S. avermitilis*. However, the underlying mechanism does not appear to involve a direct interaction with the promoter of the corresponding cluster-situated regulator, *aveR* (Chen et al., 2008). Transcriptomics revealed that the disruption of AtrA-sa (also called AveI) affected the expression of the biosynthetic clusters for oligomycin and filipin as well as genes encoding enzymes such as crotonyl-CoA reductase and methylmalonyl-CoA decarboxylase, which are involved in the supply of precursors for avermectin and other antibiotics (Mao et al., 2015). Disruption also altered the expression of several genes involved in protein synthesis and fatty acid metabolism suggesting that AtrA may function as a global regulator of the flux of carbon from primary to secondary metabolism in *S. avermitilis*. This is similar to what has been reported for AtrA in *S. coelicolor* in this work, and adds weight to the notion that the manipulation of AtrA activity merits investigation as a means of improving screens for a new antibiotic.

Evidence is emerging that the DNA-binding activity of AtrA, like many other members of the TetR family (Cuthbertson & Nodwell, 2013), is regulated by the binding of a small molecular weight ligand(s). Collaborators, Bin Hong and colleagues (Peking Union Medical College, China), discovered while investigating the regulation of lidamycin production by *S. globisporus* that the DNA-binding activity of AtrA-gl is inhibited by the binding of heptaene, an unsaturated aliphatic hydrocarbon that is a biosynthetic intermediate of lidamycin (Li *et al.*, 2015b). In addition, they also reported that the activity of AtrA-gl could be inhibited, at least *in vitro*, by actinorhodin. However, it was not shown that the inhibition was specific to AtrA and little information was provided on the properties of the actinorhodin preparation (Li *et al.*, 2015b). Nevertheless, these findings raised the possibility that AtrA from *S. coelicolor* might be responsive to actinorhodin and perhaps other related compounds.

1.9 Broad objective and specific aims of thesis

The broad long-term objective of this work was to investigate the regulation and regulon of *S. coelicolor* AtrA with the intent of not only better understanding the biology of secondary metabolism but evaluating the potential of manipulating AtrA to induce the production of *Streptomyces* natural products that would otherwise have remained undetected.

The specific aims were to:

(i) determine the genomic locations bound by AtrA using a ChIP approach and the extent to which AtrA regulates gene expression using a RNA-seq approach, and by considering the output of both datasets to identify genes that are likely under the direct control of AtrA;

(ii) Analyse the known and predicted functions of AtrA-regulated genes for evidence of higher-level associations in *S. coelicolor* an through the construction of position-weight matrixes, provide tools to predict sites of AtrA binding, in other *Streptomyces* species;

(iii) Report and possibly investigate any unusual features revealed by analysis of the *S. coelicolor* transcriptome or AtrA regulon;

(iv) Extend the analysis of the regulation of the DNA-binding activity of AtrA by extractable small molecules; and

(v) Provide a future perspective on the study of AtrA and findings stemming from its study.

Chapter 2 Materials and Methods

2.1 Bacterial strains

All bacterial strains used in this work are shown in Table 2.1.

Strains	Description	Source/Reference
Streptomyces strains		
M145	SCP1$^-$, SCP2$^-$. Contains a mutation, *sre*-1 gene, (suppression of *relC* effect), that leads to overproduction of actinorhodin.	(Hopwood *et al.*, 1985, Lee *et al.*, 2012, Redenbach *et al.*, 1996)
L645	M145 containing a disrupted *atrA* gene, which encodes a member of the TetR family that binds within the promoter region of *actII*-ORF4.	(Uguru et al., 2005)
M511	M145 containing a disrupted *actII*-ORF4 gene, which encodes the cluster-situated activator of the biosynthetic genes for actinorhodin.	(Floriano & Bibb, 1996)
M1146	M145 derivative in which four gene clusters for well-described secondary metabolites have been deleted; actinorhodin, undecylprodigioson etc. (Δ*act*, Δ*red*, Δ*cpk*, Δ*cda*).	Provided by Dr Ryan Seipke (Gomez-Escribano & Bibb, 2011)
L646	M145 containing a pICLSET-based plasmid pL646 that constitutively expresses *S. coelicolor atrA.*	(Towle, 2007)
L737	L645 containing pAU3-45-based plasmid pAU-*atrA* that encodes *S. coelicolor* AtrA	(Hasan, 2015)
L747	L645 containing a pAU3-45-based plasmid pAU-3x*atrA* that encodes *S. coelicolor* AtrA with the 3 x FLAG tag™ at its N-terminus.	(Hasan, 2015)
E. coli strains		
BL21-Gold (DE3)	*E. coli* B F$^-$ *ompT hsdS*(rB$^-$ mB$^-$) *dcm*$^+$ *tetR gal* λ(DE3) *endA* Hte	Stratagene Corp
XL10-Gold	Tet^r Δ(*mcrA*)183 Δ (*mcrCB-hsdSMR-mrr*)173 *endA1 supE44 thi-1 recA1* gyrA96 *relA1 lac* Hte [F´ *proAB lacI*^{q}*Z Δ M15 Tn10* (Tet^r) Amy Cam^r]	Stratagene Corp
XL1-Blue (MRF')	Δ(*mcrA*)183 Δ(*mcrCB-hsdSMR-mrr*)173 *endA1 supE44 thi-1 recA1 gyrA96 relA1 lac* [F´ *proAB lacI*^{q}*ZΔM15* Tn10 (*Tet*^{r})]	Provided by Dr Ryan Seipke (Agilent)

ET12567 (pUZ8002)	*dam*13::Tn9(*chl*^{R}) *dcm*-6 *hsdM hsdR recF*143 *zjj*-201::Tn10 *galK2 galT22 ara14 lacY1 xyl-5 leuB6 thi-1 tonA31 rpsL136 hisG4 tsx-78 mtl*I *glnV44*, pUZ8002 (*kan*^{R})	Provided by Dr Ryan Seipke (MacNeil *et al.*, 1992)
Top10 (pR9604)	F$^-$ *mcrA* Δ(*mrr*-*hsdRMS*-*mcrBC*) *φ80lacZΔM15 ΔlacX74 recA1 araD139 Δ*(*ara*-*leu*)7697 *galU galK* λ$^-$ *rpsL*(*Str*^{R}) *endA1 nupG*	Provided by Dr Ryan Seipke (Invitrogen)

Table 2.1. Description and sources of bacterial strains.

2.2 Chemical, enzymes and antibiotics

2.2.1 Chemicals

Unless otherwise stated, the chemicals used in this work were purchased from Sigma, Fisher Scientific or Oxoid ™. Soya flour was purchased from Holland and Barrett and casamino acids from Q.BIOgene.

2.2.2 Enzymes

RNaseOUT™ was purchased from Invitrogen, DNase RQ1 and GoTaq® green master mix used in PCR reactions were supplied by Promega, RNase A from Fisher Scientific. Achromopeptidase and alkaline phosphatase were obtained from Sigma, and lactate dehydrogenase from Roche Diagnostics.

2.2.3 Antibiotics

All the antibiotics were used as the following final concentrations after sterilizing the stocks by filtration through a 0.22 µm Millex®GP syringe filter unit: Carbenicillin (CB), 50 µg/mL; apramycin (APR), 50 µg/mL; chloramphenicol (CHL), 25 µg/mL; kanamycin (KAN), 25 µg/mL; and nalidixic acid (NAL), 25 µg/mL.

2.3 Media

Media and solutions were prepared as instructed by the vendor, except where stated otherwised. And they sterilized by autoclaving at 121°C for 20 min. L-proline was sterilised by filtration through a 0.22 µm Millex®GP syringe filter unit.

2.3.1 R5 (Kieser *et al.*, 2000)

The following were added to 1 L of dH_2O and then autoclaved: 103 g sucrose, 0.25 g K_2SO4, 10.12 g $MgCl_2.6H_2O$, 10 g glucose, 0.1 g casamino acids, 2 mL trace elements (1 L made of 4 mg $ZnCl_2$, 200 mg $FeCl_3.6H_2O$, 10 mg $CuCl_2.4H_2O$, 10 mg $MnCl_2.4H_2O$, 10 mg $Na_2B_4O_7.10H_2O$ and 10 mg $(NH_4)_6Mo_7O_{24}.4H_2O$, 5 g yeast extract, 5.73 g TES buffer, and 20 g agar. After autoclaving, the following reagents, which had been autoclaved separately, were added: 10 mL 0.5% (w/v) KH_2PO_4, 4 mL 5 M $CaCl_2.2H_2O$, 15 mL 20% (w/v) L-proline, and 7 mL 1N NaOH.

2.3.2 Mannitol soya flour medium (MSF) (Hobbs et al., 1989)

The following were added to 1 L of tap water: 20 g of each of agar, mannitol and soya flour and autoclaved twice, with gentle shaking after each cycle.

2.3.3 Soft-Agar

The following were added to 1 L dH_2O and then autoclaved: 8 g nutrient broth and 5 g agar.

2.3.4 Tryptone Soya Agar (TSA)

The following were added to 1 L of dH_2O and then autoclaved: 30 g tryptone soya broth and 20 g agar.

2.4 Preparation of *S. coelicolor* spore stocks

New spore stocks of *S. coelicolor* were prepared by scraping the spores from the surface of a well-isolated colony on a TSA plate using a sterile loop and streaking on a SFM plate to produce a fresh well-isolated colony. After incubation for an appropriate time, the spores from a single colony were harvested using a sterile loop and re-suspended in 2 mL of sterilized dH_2O. Aliquots (~ 300 µL) of the suspension was spread over mannitol soya flour medium (MSF) plates with a sterile glass spreader and incubated until the upper surface of the mycelium growing on the agar plate displayed the grey colouration associated with the production of mature spores. The spores were harvested by adding 10 mL of sterilized distilled water to each plate and scraping the medium surface with a sterile cotton swap (Alpha Laboratories Ltd). The combined suspensions were filtered through a plug of sterilized cotton (~5 cm^3) inserted into the barrel of a 20-mL syringe. The filtered spores were centrifuged at 4,700 x *g* for 10 min and the pellet was re-suspended in sterile 25% (v/v) glycerol. The spore suspension was divided into aliquots and stored at -20°C.

2.5 Nucleic acid methods

2.5.1 Extraction of chromosomal DNA from *S. coelicolor* and *E. coli* for use in PCR

A 1/8th volume (3.125 mL) of stop solution (95% [v/v] ethanol; 5% [v/v] phenol) was added to 25 mL of overnight bacterial culture in a 50-mL Falcon™ tube. The mycelial pellet was collected by centrifugation at 5,000 x *g* (Sigma, 11133-rotor) for 10 min and washed with 10 mL sterilized dH_2O and re-harvested. Cell lysis was initiated by re-suspending the mycelial pellet in 10 mL TE buffer (pH 8) containing lysozyme (20 mg/mL) and incubating at 37°C for 60 min. SDS and NaCl were added to final concentrations of 0.5% (w/v) and 150 mM, respectively. The tube was vortexed briefly and placed in a boiling-water bath for 1 min. After cooling in ice, an equal volume of buffer-saturated phenol (pH 8) was added and the tube was vortexed. The cell debris was removed by centrifugation at 13,000 x *g* (Eppendorf centrifuge 5415 R) for 10 min at room temperature. The upper layer was transferred to a new tube and extracted further using an equal volume of phenol (pH 8): chloroform: isoamyl alcohol (25:24:1). The extraction of the upper layer was repeated by using chloroform: isoamyl alcohol (49:1). The aqueous layer was transferred to a fresh Eppendorf tube and the volume measured. To precipitate the nucleic acid, 2.5 volumes of absolute ethanol and NaCl to a final concentration of 150 mM were added and the mixture was incubated at -20°C for 30 min. The precipitate was harvested by centrifugation at 13,000 x *g* for 30 min at 4°C, then the pellet was washed twice with 70% (v/v) ethanol and it re-suspended in nuclease-free water (Sigma) and stored at -20°C.

2.5.2 Extraction of chromosomal DNA from *S. coelicolor* for sequencing

Cells in an overnight culture of 4 mL were pelleted using a microcentrifuge (13,000 x *g*) for 1 min, the mycelial pellet was washed with 1 mL sterilized dH_2O and re-harvested. The pellet was re-suspended in 0.5 mL of 1 x TE buffer (pH 8) containing lysozyme (1 mg/mL) and incubated for 60 min at 37°C. SDS and NaCl were added to final concentrations of 0.5% (w/v) and 150 mM, respectively, and the tube inverted several times to mix the contents. A 0.5 volume of buffer-saturated phenol (pH 8) was added and the contents again mixed by inverting the tube. The emulsion was separated into organic and aqueous layers by centrifugation at 13,000 x *g* (Eppendorf™ centrifuge 5415 R) for 2 min at room temperature. The bulk of the lower organic layer was removed by pipetting and the tube re-centrifugation for 1 min at room temperature. The upper aqueous was transferred to a new tube and extracted further using a 0.5 volume of phenol (pH 8): chloroform: isoamyl alcohol (25:24:1) and the tube was centrifuged at room temperature

for 2 min. The aqueous layer was re-extracted by using chloroform: isoamyl alcohol (49:1). The resulting aqueous phase was transferred to new tube and a 2.5 volume of absolute ethanol was added. The stringy chromosomal DNA was then removed to a fresh 1.5 mL tube, pelleted by brief centrifugation, washed with 200 µL of 70% (v/v) ethanol and air dried. The pellet was then re-suspended in 50 µL of nuclease-free water (Sigma) and treated by adding 2 µL of RNase A (10 mg/mL) and incubating at 37ºC for 30 min. The chromosomal DNA was further purified using SPRI paramagnetic beads (prepared by Kiran Sabharwal, a member of the laboratory). Briefly, an aliquot of 20 µL of the beads was added to 50 µL of DNA sample in an Eppendorf tube, mixed by flicking and the contents incubated on a mixer (Eppendorf Thermomixer) at room temperature for 5 min. After the incubation, the tube was placed onto a magnetic stand (Invitrogen™) and the supernatant was removed by pipetting. The beads were washed twice with 200 µL 70% (v/v) ethanol, air dried. The DNA was eluted by resuspension the washed beads with 20 µL of nuclease-free water (Sigma) and incubation for 2 min at room temperature. The beads were again collected using the magnetic stand and the DNA was transferred to a new Eppendorf tube and stored at -20ºC.

2.5.3 Extraction of RNA from *Streptomyces*

2.5.3.1 Preparation of mycelial patches and RNA isolation

$1x10^5$ spores from M145 and L645 strains were spotted onto R5 plates overlaid with cellophane (Whatman) that had been sterilised by autoclaving and allowed to dry. The plates were incubated at 30°C for 2 d. Immediately after removing plates from the incubator, a 500 µL aliquot of sterile nuclease-free water (Sigma) containing an 1/8 volume of stop solution (95% [v/v] ethanol; 5% [v/v] phenol) was added to the surface of each mycelial patch to inhibit the cell metabolism. The mycelia in each patch was scraped off the cellophane using a sterile blunt-end spatula and placed in 800 µL of sterile nuclease-free water (Sigma) also containing an 1/8 volume of stop solution. The mycelia was harvested by centrifugation at 13,000 x *g* for 1 min (Eppendorf centrifuge 5415 R). The pellets were transferred to Lysing Matrix B tube (MP Biomedicals) containing modified Kirby mix (1% [w/v] SDS, 6% [w/v] sodium-4-aminosalicylate, and 6% [v/v] phenol buffered with 50 mM Tris-HCl [pH 8.3]; Kieser *et al.,* 2000). Lysis was achieved using a benchtop homogenizer (FastPrep®-24 MP Biomedicals, India). Samples were subjected to three cycles of bursts of 50 s at 6.5 M/s with 1 min incubation in ice between each cycle. The resulting lysates were extracted with an equal volume of phenol saturated with 100 mM citrate buffer (pH 4.3), which involved mixing by inverting the tube several times. The phases were separated by centrifugation at 13,000 x *g* for

10 min at room temperature. The aqueous phase was then extracted with an equal volume of phenol (pH 4.3): chloroform: isoamyl alcohol (25:24:1), and then an equal volume of chloroform: isoamyl alcohol (49:1). Total nucleic acid was then precipitated by adding 2.5 volumes of absolute ethanol and NaCl to a final concentration of 150 mM. The samples were incubated for 30 min at -80°C and centrifuged at 13,000 x *g* for 30 min at 4°C. The pellet was washed with 70% (v/v) ethanol, re-suspended in nuclease-free water (Sigma) and stored at -80°C. RNA was isolated from each strain in triplicate under the same growth conditions.

2.5.3.2 DNase I treatment

To obtain RNA samples free of DNA, 100 µg of nucleic acid was incubated with 2 U of DNase RQ1 and 100 U of RNaseOUT^{TM} in 50 µL of 1 x RQ1 DNase buffer at 37°C for 60 min. The reaction mixture was extracted with phenol: chloroform: isoamyl alcohol. To precipitate RNA within the DNA-depleted sample, NaCl was added to a final concentration of 150 mM followed by 2.5 volumes of absolute ethanol and mixing. The mixture was incubated at -80^{o}C for 30 min, and the RNA harvested by centrifugation at 13,000 x *g* for 30 min at 4°C. The pellet was washed twice with 70% (v/v) ethanol, air dried and re-suspended in nuclease-free water (Sigma). To check the integrity of RNA, 500 ng of a sample was run in a 1.2% (w/v) agarose gel containing ethidium bromide (0.5 µg /mL) for 50 min at 10 V cm^{-1}. Nucleic acid in the gel was imaged using a GeneGenius UV transilluminator (Syngene).

2.5.3.3 Quantify the Nucleic Acid Concentration

The concentration of nucleic acid was determined by measuring the absorbance at 260 nm using NanoDropTM 1000 spectrophotometer (Thermo Fisher Scientific).

2.5.3.4 RNA sequencing

RNA-seq was performed at Leeds Clinical Molecular Genetics Centre (St. James' Hospital, University of Leeds) using a Hiseq 3000 (150 bp paired end) platform. Prior to sequencing**,** the RNA samples were enriched for mRNA as part of the service using a Ribo-Zero rRNA Removal Kit (illumina®). Fragmentation and adaptor ligation were done following the protocol in the TrueSeq total RNA kit (illumina®). Output was received in the form of fastq files, which in addition to sequence data and the corresponding identifiers contained quality scores.

2.5.3.5 Differential RNA sequencing

Differential RNA-seq analysis used the open source, web-based Galaxy platform (Goecks *et al.*, 2010). After uploading the fastq files into Galaxy, the sequences were trimmed to remove low quality reads including the adaptor sequence from the ends using Trimmomatic, a flexible trimmer for Illumina sequence data (Bolger *et al.*, 2014). Both reads were input as paired-end (two separate input file), the number of bases to average was 4 and the required average quality required was 20. The trimmed sequences were aligned to the *S. coelicolor* genome (Accession number AL645882.2) using Bowtie2 (Langmead & Salzberg, 2012). These files were input as paired end with the unaligned reads being written (in fastq format) to separate file(s) and the default setting used for analysis. For each annotated gene, the amount of associated transcripts was determined using StringTie (Pertea *et al.*, 2015). The input mapped read in BAM format was specified as reverse strand information. Only reference transcripts were used and the output files for differential expression were DESeq2/edgeR. The average read length was specified as 75. The expression of genes in different biological samples were compared DEseq2 (Love *et al.*, 2014), which estimates the level of deviation from mean values (i.e. variance) as a function of the mean values before testing for differential expression using a model based on the negative binomial distribution.

2.5.4 Standard PCR method

Standard PCR reaction was performed as follows: initial denaturation at 95°C for 5 min, then 30 cycles of denaturation at 95°C for 30 s, annealing at an appropriate temperature (see Table 2.2) for 30 s, followed by extension at 72°C for 1 min/kbp, and a final extension at 72°C for 5 min.

2.5.5 Annealing complementary strands of oligonucleotides

Short double-strand oligonucleotide substrates were generated by annealing two synthetic complementary single-strand oligonucleotides synthesis to each other. Equal volumes of equimolar samples of each complementary oligonucleotides were added to a 1.5 mL microcentrifuge tube, mixed by flicking, and incubated in a heat block at 95°C for 2 min. The tube was then placed on the bench to allow the contents to cool slowly to room temperature over 2 h.

2.5.6 Purification of amplified DNA fragments

Amplicons generated by PCR were first resolved using agarose gel electrophoresis (Sambrook & Russell, 2001) with 1 x TBE buffer as the running buffer. The concentration

of agarose was dependent on the sizes of the expected PCR product, e.g. a small fragments of 80 to 500 bp were resolved using 2% (w/v) agarose, where large fragments of 600 to 800 bp were resolved using 1.2% (w/v) agarose. After gel electrophoresis, slabs of gel containing amplicons of the expected size were removed using a clean blade. The DNA was then extracted from the gel slab using the QIAquick® gel extraction kit, following the manufacturer's instructions (Qiagen). DNA was eluted from spin columns using 50 µL of nuclease-free water (Sigma), and then quantified using NanoDropTM 1000 spectrophotometer. In order to protect fluorescently labelled amplicons from photobleaching (Bernas *et al.*, 2005), samples were stored in foil covered tubes at -20°C.

Name	**Gene substrate**	**Sequence (5'→ 3')**	**Amplicon size (pb)**	**Template**	**Annealing**
actII-4-F*	*actII-ORF4*	TCTCGATGTCGGC CGGTGGATGTGG	395	*S. coelicolor*	55°C
actII-4-R*		FAM-TCGTGCCGCCTGA GGAGCAGCAGC			
actA-F*	*actA* (SCO5083)	CGTGCTCCTCATC GTATGG	102	*S. coelicolor*	58°C
actA-R*		FAM-CGGGTCCTCGACT ATTGG			
tetA-F*	*tetA*	CATTAATTCCTAAT TTTTG	84	XL1-Blue MRF'	45°C
tetA-R*		FAM-CATTTCACTTTTCT CTATC			
Apra-F*	*aac(3)-IV*	TGGGCCACTTGGA CTGAT	800	*S. coelicolor*	60°C
atrA-R*	downstream *atrA*	FAM-CCGCGGTAATAAC GCTCA			

LacO-F	lac operator	GCGAAATTAATACG ACTC ACTATAGGG	88	pET_16b		56°C
lacO-R		FAM-TCTCCTTCTTAAAG TTAAA CAAAATTATTTCTA GAGG				
Kan-F	Neomycin resistance gene	TTGGGTGGAGAGG CTATTCG	267	pWEB		62°C
Kan-R		CTTCCCGCTTCAGT GACAAC				
1842-Tn-F		CGGTGTGCACCTG GAAG	227	SCO1842 mutant	63°C	
1842-Tn-R		CTGGCTGTGGGTG GACA				
6258-Tn-F	Regions adjacent to the point of transposon insertion	TCATCTTCGGCATG ACCAG	199	SCO6258 mutant		
6258-Tn-R		GCCGTAGTTCTTG CTGACG				
6515-Tn-F		AACTGCGCGAGGT AGGTCT	258	SCO6515 mutant	63°C	
6515-Tn-R		GGCCTTCGTCAAG GACTTC				
1390-Tn-F		CTTCCCATGACCA CCGTCT	231	SCO1390 mutant	63°C	
1390-Tn-R		GATGCCGAGATGG GTCAG				
1862-Tn-F		GTCGTCGCTGGTG TACTCG	208	SCO1862	63°C	

1862-Tn-R		CGCCGTCGCTATGTACG		mutant	
4295-Tn-F		TCGTCCGATTGACCTGTTG	250	SCO4295 mutant	63°C
4295-Tn-R		GCGCTGTAGTGGACGAAAA			
7517-Tn-F		ACCCGGAGAACTGGACCT	211	SCO7517 mutant	63°C
7517-Tn-R		CCGATGCCCATCAGTACG			
SCO5529-F	SCO5529 (*leuA2*)	CTACCGGAATGACCG GTTCCACCGT		Complementary oligonucleotides	
SCO5529-R		FAM-ACGGTGGAACCGGTCATTCCGGTAG			

Table 2.2: PCR primers and oligonucleotides used in this thesis. Asterisk indicates primer designed in previous work (Hasan, 2015). All others were designed in this study and supplied by Integrated DNA Technologies (IDT).

2.6 Purified recombinant LacI

2.6.1 Construction of pOPINF-based plasmid encoding oligohistidine-tagged LacI

The LacI coding sequence was amplified by PCR from *E. coli* genomic DNA (see Section, 2.5.1). The forward and reverse primers contained extensions AAGTTCTGTTTCAGGGCCCG and CTGGTCTAGAAAGCT at 5' end, respectively. These sequences were complementary to the ends of linearized pOPINF vector (Berrow *et al.*, 2007), which was generated by incubating circular plasmid with KpnI and HindIII. The linearised plasmid was purified using a QIAquick® PCR purification kit (Qiagen). The amplicon was then inserted into the pOPINF vector using a Gibson assembly kit (NEBuilder® HiFi DNA Assembly Cloning Kit), as recommended by the vendor (New England Biolabs).

2.6.2 Transformation

A 2 µL aliquot of the assembly mix was mixed sequentially with 2 µL of β-mercaptoethanol) and 50 µL of XL10-Gold competent cells (Stratagene Corp) and incubated on ice for 30 min. The cells were incubated at 42°C for 30 s in a metal heat block before immediately returning to ice and incubation for 2 min. A 450-µL aliquot of LB was added to the cells and incubated at 37°C for 1 h with shaking at 225 rpm. Aliquots of 10, 50 and 150 µL were spread onto LB agar plates containing IPTG, X-gal and carbenicillin at final concentrations of 5mM, 50µg/mL and 50µg/mL, respectively. The plates were then incubated at 37°C overnight. Cells from single colonies that were white, which is indicative of transformants containing recombinant pOPINF, were used to inoculate 10 mL of LB broth in a 50 ml Falcon tube and incubated at 37°C overnight. Plasmid was isolated from overnight cultures using a QIAprep® Spin Miniprep kit according to manufacturer's instructions (Qiagen). To confirm the required construction, the isolated plasmids were sequenced by Beckman Coulter Genomics (UK) using universal primers (T7P and T7TERM). The desired construct were then introduced into competent *E. coli* BL21 (DE3) cells as described for XL10-Gold cells.

2.6.3 Overproduction and purification of LacI

Recombinant *E. coli* LacI was overproduced and purified from a culture of *E. coli* BL21 (DE3) cells containing pOPINF-LacI. A 10 mL overnight culture was diluted 1:100 in 400 mL of LB broth containing 50 µg/mL of carbenicillin. The culture was incubated at 37°C and when the OD_{600} reached 0.6, IPTG was added to a final concentration of 5 mM to induce expression of the chromosome-encoded T7 RNA polymerase gene, which in turn induced expression of plasmid-encoded recombinant LacI. Following incubation for a further 3 h, cells were harvested by centrifugation at 4,000 x *g* for 30 min at 4°C (Sorvall RC-5B, SLA-3000 rotor). The pellet was re-suspended in 20 mL of ice-cold lysis buffer (25 mM Tris–HCl [pH 8], 300 mM NaCl, and 20 mM imidazole) and re-centrifuged at 4,000 x *g* for 30 min at 4°C. The pellet was then re-suspended in 10 mL ice-cold lysis buffer containing one tablet of cOmplete™ Mini EDTA-free protease inhibitor cocktail (Roche Diagnostics). The cells were lysed using a pre-cooled cell disruptor (Constant Systems Ltd) with a one head setting at 15,000 psi. Lysate was cleared by ultra-centrifugation at 28,000 x *g* at 4°C for 35 min (Optima™ L-80 XP Beckman Coulter ultracentrifuge), and passed through a 0.45 µm filter (Sartorius stedim) prior to incubating with HisPur™ Nicle-NTA agarose resin (Thermo Scientific). To purify the protein, 400 µL of HisPur™ Nicle-NTA agarose resin was added in a 14 mL Falcon tube and re-

suspended in 5 mL of the lysis buffer and centrifuged at 1000 x *g* for 1 min to sediment the resin. The buffer was removed and the cleared lysate was incubated with the washed resin at 4°C for 1 h on a vertical rotator (Progen Scientific Ltd). The resin was pelleted by centrifugation at 1,000 x *g* rpm for 1 min, and transferred to a Pierce™ centrifuge column (Thermo Fisher Scientific). The resin was washed several times with 5 mL washing buffer (25 mM Tris–HCl [pH 8], 1 M NaCl, and 20 mM imidazole) to remove unbounded protein. Protein bound to the resin via nickel chelation was eluted from the column using 1 mL elusion buffer (25 mM Tris–HCl [pH 8], 300 mM NaCl, 1 M imidazole). The eluate was desalted us a 5-mL PD-10 G25 (GE Healthcare Life Sciences) pre-equilibrated with freshly prepared "dialysis" buffer (20 mM Tris–HCl [pH 7.4], 200 mM KCl, 10 mM EDTA, 3 mM DTT, 5% (v/v) glycerol). Sample was collected from the column and then aliquots of 100 µL were stored at -80°C until required.

2.6.4 Analysis of purified LacI

The eluted protein was analysed by SDS-polyacrylamide gel electrophoresis (PAGE) using a 15% (w/v) polyacrylamide resolving gel (29:1 acrylamide: *bis*-acrylamide; 380 mM Tris-HCl [pH 8.8], 0.1% [w/v] SDS; 0.1% [w/v] APS; 0.1% [v/v] TEMED) in combination with 5% [w/v] stacking gel (29:1 acrylamide: *bis*-acrylamide; 126 mM Tris-HCl pH [6.8], 0.1% [w/v] SDS; 0.1% [w/v] APS; 0.1% [v/v] TEMED). Prior to loading samples, an equal volume of 2 x SDS loading buffer was added and samples were incubated at 99°C for 5 min. Samples were loaded using 200 µL fine pipette tips (Fisher Scientific) and run alongside PageRuler Unstained Protein Ladder (Fermentas). Gel electrophoresis was performed in 1 x Tris-Glycine buffer (25 mM Tris-HCl [pH8.3], 190 mM glycine; 0.1% [w/v] SDS) for 2 h at a constant 12 W. After removing from between glass plates, the gel was stained for 3 h in 20 to 50 mL of Coomassie Blue solution (1 tablet of PhastGEl® Blue R was dissolved in 200 mL dH_2O to which 200 mL of 100% (v/v) methanol and 40 mL of glacial acetic acid were added). The gel was rinsed in tap water to remove excess stain and incubated in destain solution (50% [v/v] methanol, 10% [v/v] glacial acetic acid) for 12 h; destain solution was replaced every 2 h. A GeneGenius UV transilluminator (Syngene) was used to visualize and photograph bands of stained protein under white light.

2.6.5 Protein Quantification

The concentration of LacI was determined by running several dilutions alongside a serial dilution of a sample of bovine serum albumin (BSA) (Sigma) of known concentration

(mg/mL) on an SDS-polyacrylamide gel, as described above, and comparing the intensity of the corresponding bands after staining with Coomassie Blue.

2.7 Chromatin immunoprecipitation (ChIP)

2.7.1 Preparing mycelium and cross linking protein to DNA

In this study, ChIP was performed by using strain L747, which expresses AtrA with a 3 x FLAG tag™ at its N-terminal protein, and strain L737, which also expresses AtrA but an untagged version (see Table 2.1). Using a sterile glass spreader, samples of 5 x 10^5 spores of each strain were spread on R5 plates overlaid with cellophane (2 plates/strain). The plates were incubated at 30^{o}C for 48 h after which the mycelia-covered disks were removed and placed mycelia-face down in 20 mL of a 1% (v/v) formaldehyde solution for 30 min at room temperature to cross-link protein to DNA. The disks were then incubated in 20 mL of 2 M glycine for 5 min to quench the crosslinking reaction. The mycelia were scrapped from the surface of the disks and added to 20 mL of ice-cold phosphate-buffered saline and harvested by centrifugation at 1,100 x *g*, 4^{o}C for 10 min. This wash step was repeated.

2.7.2 Mycelium lysis and chromatin shearing

The harvested mycelia were incubated with 1.5 mL of lysis buffer (10 mM Tris-HCl [pH 8.0], 50 mM NaCl, 10 mg/mL lysozyme, 0.5 mg/mL achromopeptidase, 1 x protease inhibitor (1 tablet of cOmplete Mini EDTA-free protease inhibitor cocktail /10 mL) at 37^{o}C for 30 min. Samples were placed on ice and 1.5 mL of IP Buffer (100mM Tris-HCl [pH 8.0], 250 mM NaCl, 0.5% [v/v] Triton X-100, 0.1% [w/v] SDS, and 1 x protease inhibitor) was added. The samples were sonicated using an Active Motif's EpiShear™ Multi-Sample sonicator combined with a chiller unit (Active Motif. The sonication was done thrice each time for 13 min (run 30s with a 30s rest for each time) with the amplitude set at 30% of maximum. To confirm fragmentation of the DNA, 25 µL from each lysate sample was incubated with 1 µL of RNase A (10 mg/mL) for 30 min at 37^{o}C, extracted with an equal volume of phenol (pH 8): chloroform: isoamyl alcohol (25:24:1) and precipitated using ethanol as described previously. The sample was re-dissolved in 25µL of TE buffer (pH 8) and ~ 1µg of DNA was analysed by electrophoresis using a 2% (w/v) agarose gel. The remainder of the lysates were centrifuged at 16,000 x *g* for 15 min at 4^{o}C and the supernatants transferred into fresh microcentrifuge tubes and placed on ice.

2.7.3 Immunoprecipitation

Anti-FLAG M2® magnetic beads (Sigma) was used to precipitate the desired DNA-protein complexes. An aliquot of 160 µL (40 µL of beads for each sample) was transferred using a tip with a widened opening into a fresh microcentrifuge tube, which was then placed onto magnetic stand to allow removal of the storage buffer by pipetting. The remaining beads were washed 4 times with 500 µL of half-strength IP buffer (50 mM Tris-HCl [pH 8.0], 250 mM NaCl, 0.8% [v/v] Triton X-100, 1 x protease inhibitor), and then re-suspended in 160 µL of half-strength IP buffer. Aliquots of 40 µL of the washed beads were added to each of the cleared lysate and incubated on a vertical rotor (Progen Scientific Ltd) for 14 h at 4^{o}C. The magnetic beads were collected using a magnetic stand and washed thrice with 500 µL of half-strength IP buffer.

2.7.4 Crosslinking reversal, DNA purification and immunoprecipitated DNA sequencing

The crosslinking was reversed by incubating the washed magnetic beads with 100 µL of IP elution Buffer (100 mM Tris-HCl [pH 8.0], 250 mM NaCl, 0.5% [v/v] Triton X-100, 0.1% [w/v] SDS, and 1 x protease inhibitor) at 65^{o}C overnight. The beads were again collected using the corresponding stand and the supernatants transferred to fresh microcentrifuge tubes. An aliquot of 2 µL of proteinase K (10 mg/mL) was added to each and the sample incubated on a 55^{o}C for 90 min. The samples were then extracted with an equal volume of phenol (pH 8): chloroform: isoamyl alcohol (25:24:1) and purified further using a QiaQuick PCR purification column; both steps were as described in previous sections. The DNA was eluted using 30 µL of elution buffer (Qiagen) and stored at -20^{o}C until sent for sequencing.

Samples of DNA from both strains were sent to Leeds Clinical Molecular Genetics Centre (St. James's Hospital, University of Leeds) and were sequenced using a single lane of the NextSeq 75bp single end read platform. As described for the transcriptome analysis (Section 2.4.3.5), the output was received in the form of fastq files.

2.7.5 Analysing ChIP sequencing data

As described for the transcriptome analysis (Section 2.4.3.5), the output was received in the form of fastq files, the sequences trimmed to remove low quality calls from their ends, and aligned to the genome of *S. coelicolor.* The resulting alignment files were converted to bedgraph files using BamCoverage (Ramirez *et al.*, 2014) and uploading into the UCSC Microbial Genome Browser (Chan *et al.*, 2012a, Schneider *et al.*, 2006) to allow the position of peaks relative to other features of the genome to be visualised. The

positions of peaks were assigned by combining manual inspection with automated peaking calling using MACS (Zhang *et al.*, 2008b) as part of a service provided by Omics Ltd (England, UK). The positions of peaks were compared with sites predicted to be bound by AtrA using MEME (Bailey et al., 2009) primed with a selection of binding sites identified by a combination of bioinformatics and *in vitro* binding assays (see (Hasan, 2015)). Where these aligned, the designation provided by MEME was used as an identifier for the peak. The relative positions of peaks relative to transcription units identified by RNA seq (Section 2.4.3.5) were used to classify differentially expressed genes. Where AtrA sites were located a positions consistent with known bacterial forms of regulation of transcription initiation (Lee *et al.*, 2012), the corresponding genes were classified as likely targets of "direct" regulation. All others were classified as likely targets of "indirect" regulation.

2.8 Bioassay methods

2.8.1 Generation of crude preparation of actinorhodin

Fresh spores of M145, L646, M511, M1146 and *S. albus* J1074 (Dr Ryan Seipke, Laboratory stock) were spread on TSA plates and incubated at 28^{o}C for 7 d. The agar was collected and submerged in 2.5 volumes of dH_20 and incubated with shaking (200 rpm) for 1 h at room temperature. The supernatant, which containing diffusible actinorhodin (ACT) was collected and acetic acid added to lower the pH, which resulted in the colour of actinorhodin changing from blue to red. The supernatant was extracted with an equal volume of absolute ethyl acetate (Fisher Scientific) and separated from the aqueous phase by incubation the mixture in a glass separatory funnel for 15 min at room temperature. The ethyl acetate was evaporated using a rotary evaporator (Rotavapor, RE Buchi), and the sample was dried using a parallel evaporator (EZ-2 38 personal evaporator, Genevac). The resulting crude extract was weighed, dissolved in 100% (v/v) methanol to a final concentration of 10 mg/mL, and stored at 4^{o}C.

2.8.2 Antimicrobial activity test

The antimicrobial activity of crude extracts against *S. aureus* (SH 1000) was determined by a disc diffusion according to CLSI methodology (CLSI, 2007). In brief, 3 to 4 colonies of *S. aureus* (SH1000, Dr Alex O'Neill, Laboratory stock) were used to inoculate 10 mL of Mueller Hinton broth in 50 mL Falcon tube and incubated overnight at 37^{o}C with shaking. Bacterial test plates were prepared using a 0.5 McFarland suspension (~ 10^8 CFU/mL), which was spread horizontally from the centre across the surface of a plate of Mueller Hinton agar using a sterile swab.

2.9 Electrophoresis Mobility Shift Assays (EMSA)

Promotor regions of interest were generated by PCR and purified as described in Sections 2.5.4 and 2.5.6. One of the primers used to produce the probes (see Table 2.2) was labelled at the 5' end with 6-FAM™ (fluorescein). The reactions were performed in 1 x TGEK buffer (10 mM Tris-HCl [pH 7], 10% [v/v] glycerol, 0.1 mM EDTA, 50 mM KCl). Each 20 μL of a reaction contained 5 nM of probe and concentrations of protein that are specified elsewhere. Control reactions was prepared by adding all components except protein. The binding reactions were allowed to proceed at room temperature for 20 min before the products were analysed by running in a 4% (w/v) 37.5:1) acrylamide: *bis*-acrylamide gel in 1 x TGED buffer (50 mM Tris-HCl [pH 7], 0.4 M glycine, 2 mM EDTA). Electrophoresis was performed in Bio-Rad Protein II XI tank with a water-cooled central core at 120 V for 40 min in 1 x TGED buffer. The probes were used at concentrations of 5 nM to allow their detection. The final concentrations of protein varied and are specified elsewhere. Control reactions had all the compounds except protein. The protein-DNA complexes were visualized by using Fujifilm FLA-5000 imaging analyser system with an excitation wavelength of 473 nm and a LPB (Y510) filter.

2.10 Enzyme assay

Lactate dehydrogenase (LDH) and alkaline phosphatase (AP) were used to assess the influence of γ-ACT on general enzymatic activity. Enzyme assay was carried out as recommended by a teaching laboratory protocol at Leeds with some modifications. The assay was performed in a 96-well microtiter plate. The activity of γ- ACT against lactate dehydrogenase enzyme was assayed by adding defined concentrations of γ- ACT to each well of a test microtiter plate containing 100 μL of 2.7 mM NADH and 0.1 mM pyruvate in 1xTGEK buffer before adding 1.4 nM of lactate dehydrogenase enzyme, which was empirically determined to be the optimal concentration for this assay. LDH activity was measured in each well over a defined time intervals at 340 nm using a plate reader (FLUOstar OPTIMA). Similarly the activity of γ- ACT against alkaline phosphatase used a microtiter plate with a range of concentrations of γ- ACT in wells across the plate. Again the reaction was 100 μL but contained 30 mM glycine buffer (pH 8), 10 mM $MgCl_2$ and 3 mM of p-nitrophenyl phosphate. The plate was heated to 37°C prior to adding defined concentrations of γ- ACT and then alkaline phosphatase to a final concentration of 54.6 nM. The absorbance at 405 nm was measured immediately over a defined time interval using a plate reader (FLUOstar OPTIMA).

2.11 Ethidium-bromide displacement assay

Ethidium-bromide displacement assay was performed in a 96-well black microplate (Greiner Bio-One). γ- ACT was added at defined concentrations to each well of the plate containing 20 µL of 10% DMSO (v/v), 10mM Tris-HCl (pH 8.0),1 µM of ethidium bromide (Sigma) and 5 µM (base-pairs) of plasmid DNA (pGFP, laboratory stock). After incubation of the reactions at room temperature for 20 min, the fluorescence of ethidium bromide was measured using a plate reader (FLUOstar OPTIMA). The DNA concentration was determined to be the optimal concentration in this assay after measuring the fluorescence of fixed concentration of ethidium bromide (1 µM) in the presence of various concentrations of the plasmid DNA (base-pairs).

2.12 DNA sequestration assay

The maximum absorbance of ethidium bromide in 1 ml dialysis buffer (10% DMSO in 1 x TE buffer (pH 8.0)) was determined to be 500 nm. The dialysis assay was performed in a Slide-A-Lyzer™ MINI Dialysis Device (Thermo Fisher Scientific) placed on top of a 1.5 ml polystyrene semi-micro cuvette (Fisher Scientific) containing 10% (v/v) DMSO, 1 x TE buffer (pH 8.0). Reactions containing ethidium bromide and γ- ACT at a final concentration of 100 µM were set up in microfuge tubes with and without a five-fold excess (base-pairs) of salmon sperm DNA (Invitrogen). Reactions were incubated at room temperature for 20 min before transferring to the dialysis device. Diffusion for each compound was measured every 2 min for 18 min total using a NanoDropTM 1000 spectrophotometer (Thermo Fisher Scientific) at 500 nm.

2.13 Genes knockout methods

2.13.1 Transposon mutagenesis

Mutants were generated using cosmid clones from a *S. coelicolor* transposon mutagenesis library. The cosmids, which contained inserts in which a single identified gene had been disrupted by Tn*5062* (Fernández-Martínez et al., 2011), were ordered from Swansea University. The appropriate cosmids were identified using StrepDB database (http://strepdb.streptomyces.org.uk).

2.13.1.1 Triparental mating

The pR9604 helper plasmid (Jones et al., 2013), which was in *E. coli* TOP10, and cosmid carrying a segment of the *S. coelicolor* with a single gene disrupted by a Tn*5062* transposon, which was in *E. coli* JM109, were transferred into the non-methylating *E.coli* ET12567 strain (MacNeil et al., 1992) via triparental using a widely used method (Jones *et al.*, 2013). Briefly, the three *E.coli* strains were grown overnight at 37^{o}C in 10 mL of

LB containing antibiotics appropriate for each strain: chloramphenicol (25μg/mL) for *E. coli* ET12567 to maintain selection for *dam* mutation, carbenicillin (50 μg/mL) for *E.coli* TOP10 and apramycin (50 μg/mL) for *E. coli* JM109. Aliquots of 100 μL of the overnight cultures of each *E. coli* strain were used to produce separate sub-cultures as above except these were only grown to an OD_{600} of 0.4-0.55. At this point, the cells were pelleted, washed twice with fresh LB to remove antibiotics and re-suspended in 500 μL LB. Aliquots of 20 μL of each suspension were spotted onto the same location on an LB agar plate without antibiotic, the spots was allowed to air dry, and the plates incubated overnight at 37°C. Next day, the resulting growth was streaked on LB plate containing chloramphenicol, carbenicillin and apramycin to select *E.coli* ET12567 that containing both the helper plasmid and cosmid with a single gene disrupted by *Tn*5062.

2.13.1.2 Conjugation

Interspecies conjugation was carried out as described in Kieser *et al*. (2000). A single *E. coli* ET12567 colony containing the desired cosmid was used to inoculate 10 mL of LB containing apramycin (50μg/mL), kanamycin (25μg/mL) and chloramphenicol (25μg/mL). Kanamycin was added to maintain selection for pUZ8002. The overnight culture was diluted 1:100 in fresh LB containing the above selection antibiotics, and grown to an OD_{600} of 0.4. The cell were pelleted, washed twice with LB and re-suspended in 1 mL of LB broth. During the wash steps, $1x10^5$ *S. coelicolor* spores were added to 500 μL 2xYT broth (Sigma) and placed at 50°C for 10 min then allowed to cool. A mixture of 500 μL ''heat -shocked'' spores and 500 μL *E. coli* cells was pelleted and re-suspended in 50 μL of residual liquid. The mixture was then spread over the surface of an SFM plate and incubated for 18 h at 30°C. After 18 h, the plate was overlaid with 1 mL sterilized dH_2O containing 2.5 mg apramycin to select for M145-based transconjugants and 0.5 mg nalidixic acid to kill *E. coli*.

2.13.1.3 Analysis of visible phenotypes

Spores were scraped off the surface of the three well-isolated transconjugants colonies individually using a sterile loop and streaked onto SFM plates containing apramycin (50 μg/mL). After incubation for an appropriate time at 30°C, antibiotic resistance screening was carried out for three well-isolated colonies by streaking spores from the surface of each colony onto TSA containing apramycin (50μg/mL) and TSA containing apramycin (50μg/mL) and kanamycin (25μg/mL) plates. The plates were incubated for an appropriate time and then spore stocks were prepared from each single colony resistance to apramycin and sensitive to kanamycin as described in Section 2.4.

Phenotypes analysis was performed by streaking spores from each mutant onto R5 and TSA plates, and then the plates were incubated at 30^{o}C for 6 days.

Chapter 3 Direct and indirect regulations of AtrA

3.1 Abstract

Bacteria within the soil and related ecosystems are renowned as a rich source of lead compounds for drug development including recently identified and novel activities that may be invaluable in the determined battle against antibiotic resistance. A major factor limiting the screen of bioactive compounds is the elicitation of their production under laboratory conditions, which are deficient in reproducing the complexity of the natural environment and consequently the required signals. Systems that transduce environmental signals are numerous in soil-dwelling bacteria but remarkably their influence on the production of bioactive compounds is largely uncharacterised. AtrA, a member of TetR family of one component signal transducers, has sustained significant interest since being described as activating a notable model, the production of actinorhodin by *Streptomyces coelicolor*. The *Streptomyces* genus has been a particularly valuable source of clinically important antibiotics in addition to other chemotherapeutics. Using a combination of chromatin immunoprecipitation, transcriptomics and bioinformatics, I describe herein for the first time the regulatory network for *S. coelicolor* AtrA, which is found to extend well beyond actinorhodin to other bioactive compounds, key processes including cell wall biosynthesis and morphological development, and central areas of primary metabolism, which provide signals that contribute to the onset of secondary metabolism. Consequently, AtrA may represent a valid target for stimulating the production of bioactive compounds in the *Streptomyces* genus where it is evolutionarily conserved.

3.2 Introduction

Chemotherapeutics derived from *Streptomyces* spp, as part of a structurally highly diverse ‘secondary metabolism’, include anticancer, immunosuppressive, antihelmintic and antifungal as well as antibacterial agents (Colombo *et al.*, 2001, Demain, 2010). The wide range of bioactivities within this secondary metabolism reflects the biotic diversity within the main habitats of streptomycetes, which include soils rich in fungi, nematodes, insects and other bacteria (Tarkka & Hampp, 2008). Whilst some secondary metabolites are likely to be advantageous by sustaining and coordinating the growth and development of the producer (Seipke *et al.*, 2012) many, if not most, have activities that would impede the growth of competing microorganisms(Seipke *et al.*, 2012, van Wezel

& McDowall, 2011). Genomic analysis of an ever increasing number of *Streptomyces* spp has revealed that they all have the capacity to produce secondary metabolites vastly exceeding the number readily detectable by current chemical and biological screens (van Wezel & McDowall, 2011, Wright, 2017). Consequently, there is a drive to develop strategies that elicit the production of secondary metabolites, thereby expanding the opportunity for the discovery of a further generation of chemotherapeutics (Wright, 2017). These include but are not limited to antibiotics, which are much needed given the emergence of widespread resistance (Livermore, 2004). The strategies fall into two broad categories. The first is directed towards specific secondary metabolites, e.g. genetic engineering of specific regulators (Radakovits *et al.*, 2010) or expression of the biosynthetic genes in a heterologous host (Galm & Shen, 2006), and isolates, e.g. co-cultivation (Liu *et al.*, 2017) and ribosome engineering (Ochi *et al.*, 2004), whilst the objective of the second is to elicit the production of a great number of metabolites in the widest range of isolates to enhance screening, e.g. through the addition of small molecules to growth media (Rigali *et al.*, 2008).

Of the several small-molecule elicitors described to date, several are either themselves, or related to, natural signalling molecules that influence transcriptional regulation through their direct interaction with members of families of well-characterised transduction components (Rigali *et al.*, 2006, Takano, 2006), e.g. γ -butyrolactones and glucosamine-6-phosphate, which interact with members of the TetR and GntR families, respectively. *Streptomyces* spp encode a relatively large number of single and multi-component, signal transduction systems reflecting the complexity and dynamic nature of their ecosystems (Shu *et al.*, 2009, Wang *et al.*, 2007a). For the vast majority of these systems, the cognate signal and downstream targets of their regulation are either unknown or only partially characterised. Some of these indefinite systems are known to influence the production of one more secondary metabolite (Shu *et al.*, 2009, Wang *et al.*, 2007a). Thus, screening for new chemotherapeutics could be enhanced by further characterisation of regulatory systems, in particular those that extend to multiple secondary metabolites and are evolutionarily conserved.

The genes encoding enzymes for the production of individual secondary metabolites are found clustered, often in association with one or more genes that regulate their transcription (Zhu *et al.*, 2014). Analysis of the promoter region of *actII-ORF4*, which encodes the single cluster-situated regulator (CSR) of the actinorhodin genes in *S. coelicolor* (Fernandez-Moreno *et al.*, 1991), indicates that it is regulated by several transcription factors (van Wezel & McDowall, 2011). The first of these to be identified was AtrA, which is evolutionarily conserved within the streptomycetes and a member of

the TetR family (Uguru *et al.*, 2005). Subsequent characterisation of AtrA has revealed it represses streptomycin production conditionally in *S. griseus* (Hirano *et al.*, 2008), activates avermectin biosynthesis in *S. avermitilis* (Chen et al., 2008*)*, controls activation of cell-division genes and regulates the sensing and utilisation of N-acetylglucosamine in *S. coelicolor*, is part of the responses linked directly to γ-butyrolactones and phosphate starvation in *S. coelicolor* (van der Heul et al., 2018*)*, and is involved in the regulation of daptomycin production in *S. roseosporus* (Miao *et al.*, 2005) and lidamycin production in *S. globisporus* (Li *et al.*, 2015b) . Combined the above identified AtrA as a target for controlling the production of secondary metabolism. We describe herein the regulatory network extending from *S. coelicolor* AtrA and discuss our findings in relation to previous work and approaches for enhancing the screening of new chemotherapeutics.

3.3 Results

3.3.1 Chromatin immunoprecipitation

To determine the location of the binding sites for AtrA on the *S. coelicolor* chromosome, a ChIP seq-based approach was undertaken that utilised AtrA tagged with a commonly used epitope (Einhauer & Jungbauer, 2001). Initial attempts to pulldown native AtrA using polyclonal antibodies have failed due to substantial cross-reactivity (unpubl. results) with one of more of the 151 homologues in *S. coelicolor* (Hillerich & Westpheling, 2008). Two strains were analysed; both were based on strain L645, in which the chromosomal *atrA* gene is disrupted (Uguru *et al.*, 2005). In previous work, AtrA in strain L737 was untagged, whereas AtrA in strain L747 was tagged at its N-terminus with 3xFLAG® (Hasan, 2015). The tagged and untagged versions of AtrA encoded by a pAU3-45-based plasmid (Bignell *et al.*, 2005). Prior phenotypic analysis had confirmed that this N-terminal tag does not interfere with the ability of plasmid-encoded AtrA to complement the disruption of *atrA* in the chromosome, as judged by the restoration of actinorhodin production (Figure 3.1). Data was collected for three samples of both L737 and L747 grown on R5 medium: two on agar plates and one in liquid broth. The analysis of the plate-grown sample was performed after 2 days of incubation, a point at which the mycelium were red due to the production of undecylprodigiosin and there was not obvious production of the blue, diffusible pigment associated with actinorhodin (Figure 3.2, panel A). The size of the majority of the precipitated fragments ranged from 150 to 400 bp fragments (Figure 3.2, panel B). This information was fed into the MACS analysis (Zhang *et al.*, 2008b), which in combination with manually inspection, has identified 170 peaks (Table S1). The analysis of the liquid-grown sample was performed in collaboration with Bin Hong (Peking Union Medical College, China). L737 and L747 were grown in R5 broth for 2 days, at this point of time, actinorhodin (blue-pigmented) was produced by L747only (Figure 3.2, panel C).

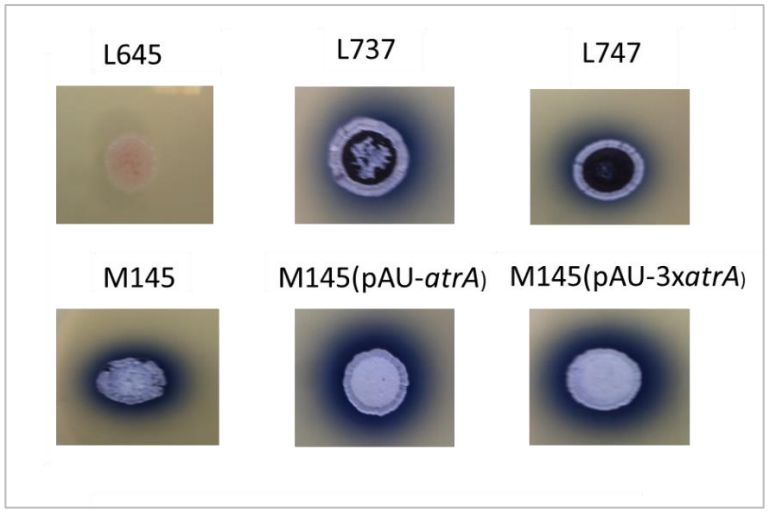

Figure 3.1. Complementation of chromosomal disruption of *atrA* by plasmid-encoded AtrA tagged with 3xFLAG® at its N-terminus. M145 with untagged AtrA (M145 (pAU-*atrA*)) and N- terminally 3 x Flag tagged AtrA (M145 (pAU-3x*atrA*)) were introduced in a previous work (Hasan, 2015). Fixed amounts of transconjugant spores were spotted onto R5 plates and incubated at 30°C.The photographs of the circular patches of each strain were taken after 5 days of incubation.

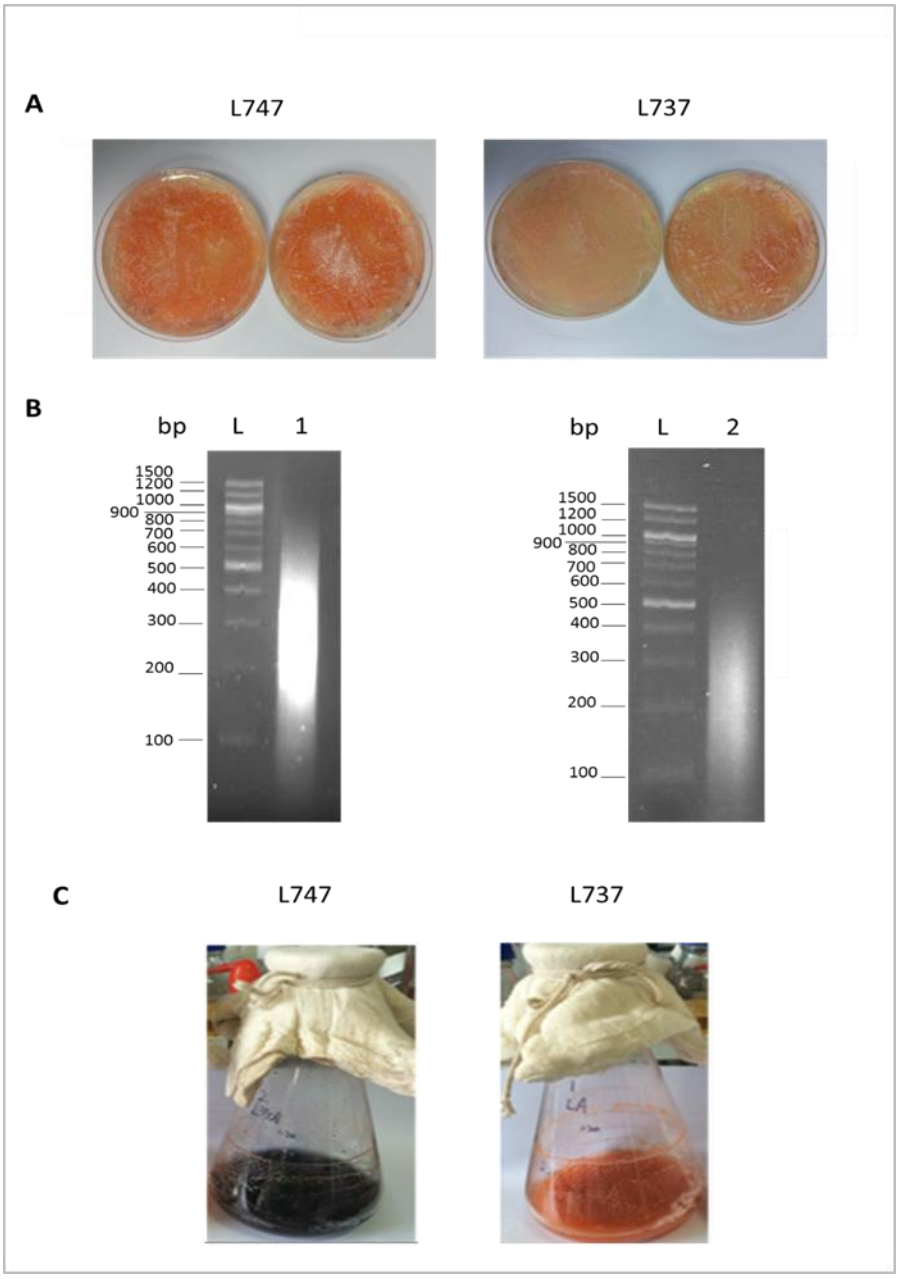

Figure 3.2.**Phenotypes and chromatin fragmentation of L747 and L737 strains**. **Panel A** shows mycelium growth on cellophane-overlaid R5 plates for 48 h. **Panels B** shows the detection of DNA fragmentation after sonication on the agarose gel. Lane 1 and 2 represent genomic DNA sample extracted from plate-grown L747 and L737, respectively. Lane L represents a 100 bp DNA ladder (New England Biolabs). Sizes of the markers in base pair are shown on the left side hand. The samples were analysed on a 2% agarose gel for 30 min using 1X TBE as a running buffer. The images are representative of the two independent replicates. **Panel C** represents the growth of L747 and L737 in R5 both for 48 h as provided by our collaborators in Beijing.

3.3.2 Identification of peaks

To inspect peaks manually, the data for each strain was viewed as three parallel tracks (i.e. Bedgraph files) using the UCSC Microbial Genome Browser (Chan *et al.*, 2012b, Schneider *et al.*, 2006). The vertical viewing range of each track was adjusted individually such that the minimum was set just below the background of reads present along the length of the chromosome. The maximum of each track was set to produce peak profiles of similar overall height in all three tracks (Figure 3.3). The profiles of peaks for samples grown on plates and the sample grown in broth were broadly similar (Figure 3.3) despite the difference in culture method and likely differences in growth parameters, e.g. doubling time. Similarity was not unexpected as, for example, it is well established that members of the TetR family respond to ligands not related to metabolism but other important aspects of bacterial physiology, e.g. antibiotic resistance and cell-cell signalling (Cuthbertson & Nodwell, 2013). It is also possible that AtrA does, like other members of its family, respond to changes in central metabolism, e.g. lipid, amino acid, nitrogen and carbon metabolisms, but that the aspect of metabolism to which AtrA responds is not significantly different between mycelium growth in liquid broth or on the surface of agar plates. The medium was the same and the mycelium in both were growing vegetatively. The mycelium on the agar plates showed no signs of differentiating (Figure 3.2). There are many cases where the activity of repressors are unlikely to be affected by the method of cultures, e.g. LexA repressor, which responds specifically to DNA damage (Irazoki et al., 2016, Janion, 2008).

Therefore, for the purpose of the MACS analysis no distinction was made based on the method of cultivation (Table S1). The tracks were then viewed as overlapping windows of 100,000 bp alongside tracks (i.e. BED files) that depicted the location of peaks predicted using MACS2, as part of a service provided by Omics Ltd, and sequences similar to sites of AtrA binding previously defined biochemically (see below). The sites of AtrA binding were predicted using PREDetector (Hiard *et al.*, 2007), a web tool that utilises a position weight matrix to represent motifs (patterns) found in binding sites. Reassuringly, the summits of the vast majority of the peaks overlapped sites were predicted using PREDetector at a screen resolution of 1,000 bp (data not shown). In order to be identified manually as a site of AtrA binding, distinct peaks had to align in at least two of the three tracks. No weight was given to colocation with sequences identified by PREDetector in assigning sites of AtrA binding. Of the 170 peaks identified by manual inspection, 165 were also identified by MACS2 (Table S1). The coordinates of the remaining five peaks were retrieved manually. There were five instances where doublet peaks were not resolved by the MACS analysis (Table S1). As part of the service

provided by Omics Ltd, the height and width of peaks and their height above background were adjusted such that the majority of the peaks identified manually were also detected by MACS2. The outputs from MACS2, including statistical values, are provided as part of Table S1.

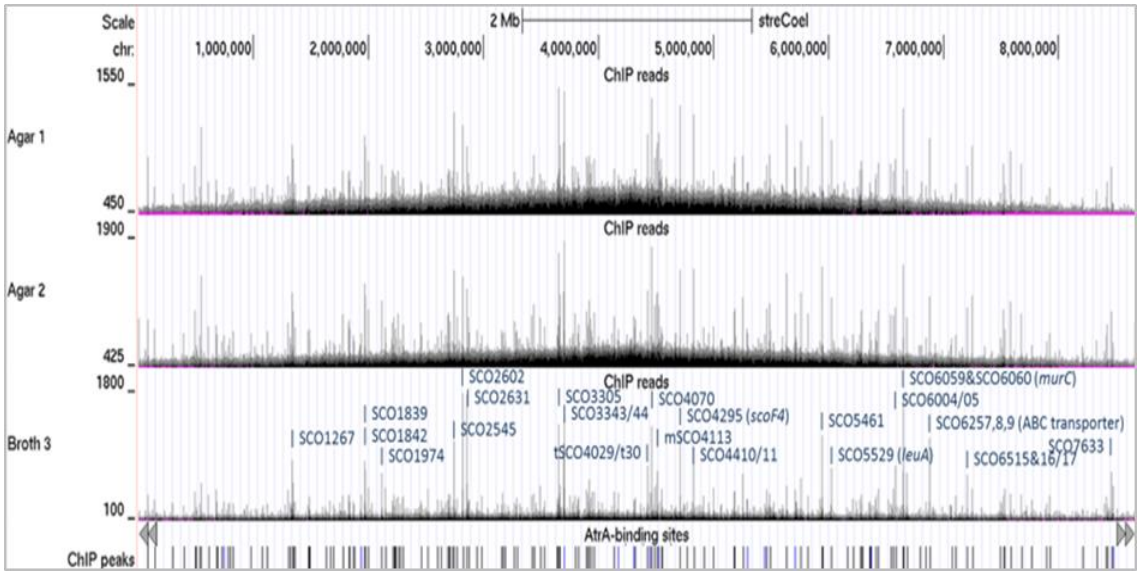

Figure 3.3. Profile of peaks of AtrA binding along the *S. coelicolor* chromosome. The three panels at the top corresponds to the strain L747, which produces AtrA tagged with 3xFLAG® at its N-terminus. Labelling in parentheses identifies the growth conditions. Labelling on the left indicates the peak scales, which have been normalised manually to produce peak profiles of similar overall height, thereby simplifying comparison.

3.3.2.1 Sites of AtrA binding

The sequences of the 170 peaks were analysed using MEME (Multiple Em for Motif Elicitation; (Bailey *et al.*, 2009)), a tool that discovers motifs, i.e. short stretches of similar of identical sequences that are found at a much higher frequency that would be expected to occur by random chance in a group of input sequences. The MEME analysis identified a motif common to 158 of the 170 peaks (Motif 1) and another common to the remaining 12 (Motif 2); both were related to a motif for sequence bound by AtrA as determined earlier (McDowall and others, unpubl. results) using systematic evolution of ligands by exponential enrichment (SELEX; (Tuerk & Gold, 1990)). All three motifs are shown in Figure 3.4. Motif 1 is composed of an indirect repeat of the 6-mer sequence 5′–CGGAAY (where Y is T or C), with the centre of the repeats separated by 11 bp (panel A). The inferred internal palindromic nature of sites represented by Motif 1 and the recognition of sequences separated by one turn of the helix reflects the expected quaternary structure of a member of the TetR family, which tend to form head-to-head dimers (Cuthbertson & Nodwell, 2013, Hillen & Berens, 1994, Meier *et al.*, 1988). The imperfect indirect 6-mer

repeats are separated by 5 bp. However, Motif 1 is 20 not 17 bp in length suggesting, as supported below, a preference for nucleotides distal to the 6-mer repeat found in both halves.

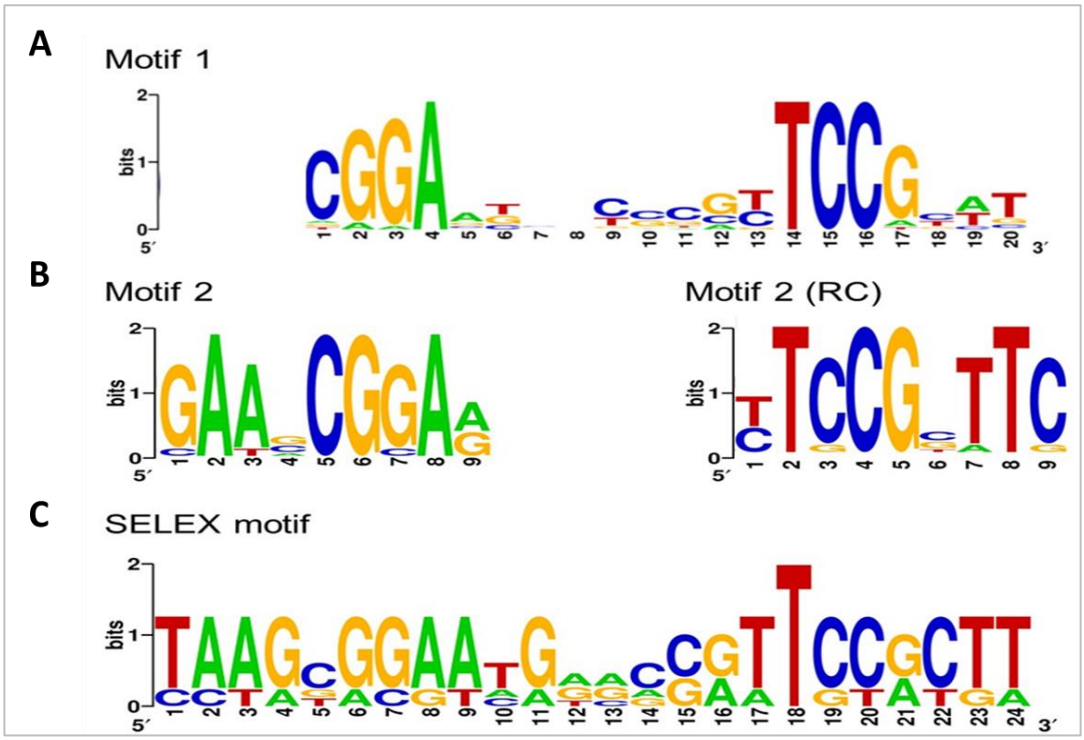

Figure 3.4. Motifs associated with AtrA binding. Each motif was identified using MEME v5.0.5 (Bailey *et al.*, 2009) and the sequences of the contributing sites in a modified "Block" format used as the input for WebLogo v2.8.2 (Crooks *et al.*, 2004). Motif 2 is also shown as the reverse complement (RC) sequence. The overall height of a stack indicates the level of sequence conservation at the corresponding position, while the height of the symbols within each stack indicates the relative frequency of the nucleotides at that position.

Motif 2 (panel B) has a consensus 9-mer sequence 5′–GAAG**CGGAA,** which overlaps five of the 6-mer repeat found in Motif 1 (overlap identified by bold type). Within Motif 2 there is a direct repeat of a 3-mer sequence (identified by underlining) with a separation that would place the repeats on the opposite sides of the helix. Unlike Motif 1, Motif 2 does not infer a palindromic nature that would reflect the quaternary structure of members of the TetR family. The motif for sequences derived by SELEX (panel C) contains elements of both Motif 1 and 2. It contains the imperfect indirect repeat of the 6-mer sequence 5′–CGGAAY (where Y is T or C) found in Motif 1, but each repeat is extended to contain three of the four nucleotides found in the 5′ end of the Motif 2, i.e. 5′–AAG of 5′–GAAG. Given the overlap between the three motifs, it was concluded that sites represented by both Motif 1 and Motif 2 are bound by AtrA, but using different modes (see Discussion). A few sites identified as having Motif 1 were also identified as

having Motif 2 (Table S1). Biochemical analysis indicates that AtrA can bind sites with Motif 2, but with an affinity lower than that of sites containing Motif1 (see Chapter 4).

3.3.3 Expression analysis

In parallel with the ChIP-seq analysis, differential expression analysis was conducted based on the sequencing of RNA isolated from triplicate samples of M145 (the congenic wild-type) and L645 grown on R5 agar plates. The RNA was isolated after 2 days from patches that were red and had started to produce aerial hyphae; at this point, M145 had not started to produce actinorhodin (Figure 3.5, panel A). The RNA was depleted of chromosomal DNA before being sent for analysis to Leeds Clinical Molecular Genetics Centre (St. James' Hospital, University of Leeds). (Figure 3.5, panel B). Analysis of the resulting data, which utilised DEseq2 (Love *et al.*, 2014), a widely used algorithm, identified differential expression for 104 protein-coding genes based on having an adjusted p-value of $\leq$0.05. This number increased by 35 if the adjusted p-value was relaxed to $\leq$0.1, a not uncommon threshold (Martínez-Burgo *et al.*, 2019, Zhao *et al.*, 2018). The adjusted p-values, fold-changes and other output from DEseq2 are provided in Table S2. Of the differentially expressed genes, 33 were found to have a site of AtrA binding as determined by ChIP seq within 300 bp upstream and 50 bp downstream of their annotated start codon or that of the first gene of a multigene transcription unit of which they appeared to be a part. These genes in 27 transcription units were classified as expression-verified targets of direct regulation by AtrA (Table 3.1). The expression of genes in 21 transcription units was increased upon disruption of AtrA indicating that like most members of the TetR family, it tends to function as a repressor of transcription initiation (Cuthbertson & Nodwell, 2013, Ramos *et al.*, 2005).

The expression ratios were converted to log base 2, a transformation that is widely used to compare gene expression between samples as it places increased and decreased gene expression on the linear scale (Berrar *et al*., 2003, Quackenbush, 2002). For example, expression ratios of 2 and 0.5, indicating a two-fold increase and decrease in expression, respectively, become +1 and -1, respectively. Expression ratios of 4 and 0.25, indicating a four-fold increase and decrease in expression, respectively, become +2 and -2, respectively.

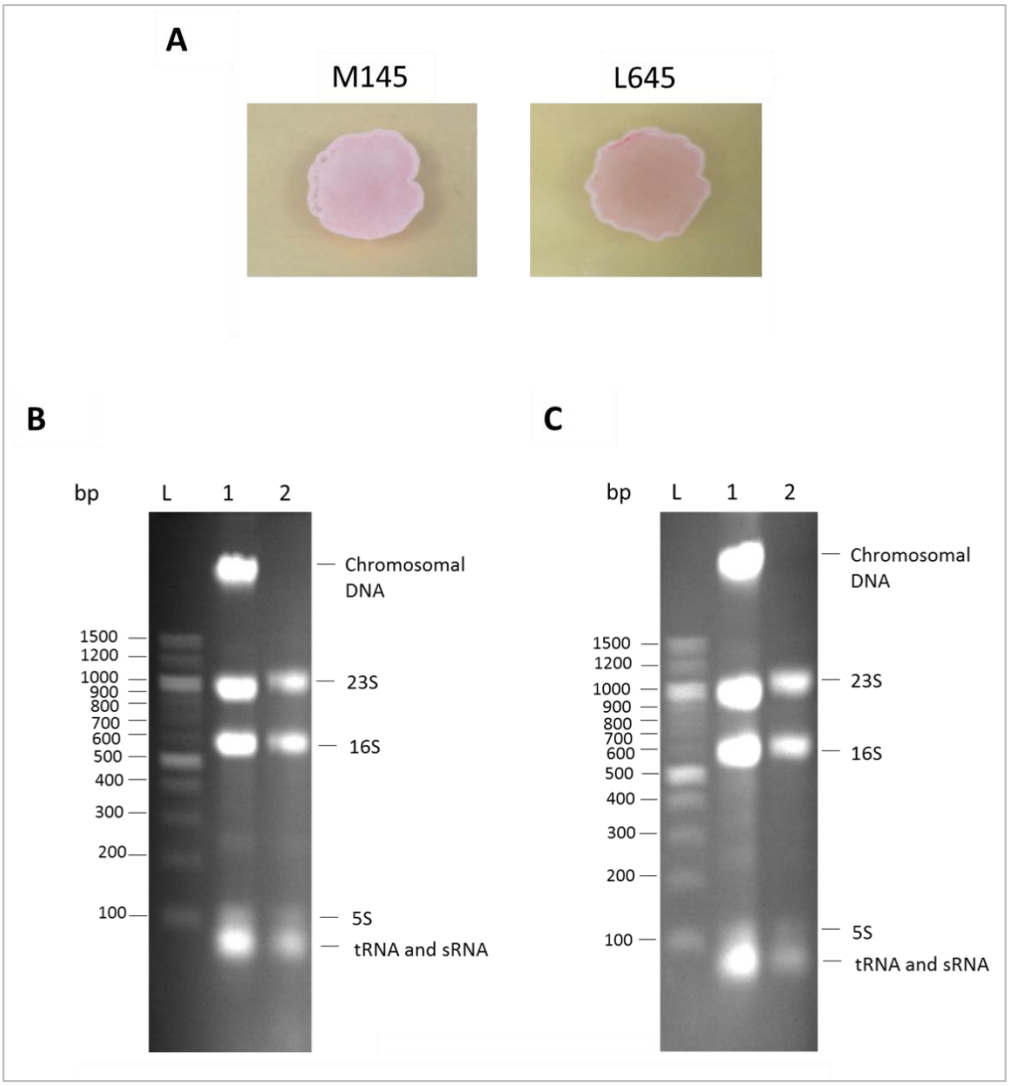

Figure 3.5. The morphology and total RNA analysis of M145 and L645 strains. **Panel A** shows the growth of strains as patches on the cellophane-overlaid R5 plates. **Panel B** and **C** show RNA samples before and after DNase I treatment. Lanes 1 and 2 contain 1 µg of RNA sample from M145 and L645, respectively. Lane L contains a 100 bp DNA ladder (New England Biolabs). Sizes of the markers in base pair are shown on the left side hand. The samples were run on 1.2% agarose gels using 1X TBE as a running buffer.

SCO	Alias	Function	log2(FC)	Adjusted p-value	Motif	Relative position (orfSTART)
Cell wall biogenesis and development						
SCO6059	SCO6059	hypothetical protein	-1.778	0.000	Motif1_1, associated with SCO6059	-65
SCO6060	*murC*	acetylmuramoyl-L-alanine ligase, catalyses first of four steps in synthesis of peptide moiety of peptidoglycan within cytoplasm	-0.613	0.001		
SCO7597	SCO7597	hypothetical protein	-0.966	0.000	Motif1_326, associated with SCO7597	-94
SCO7596	SCO7596	integral membrane transport protein	-0.920	0.004		
SCO7595	*anmK*	anhydro-N-acetylmuramic acid kinase, converts 1,6-anhydro-N-acetylmuramic acid (anhMurNAc), a product of autolysis of peptidoglycan, to N-acetylmuramic acid-6-phosphate (MurNAc-6P) thereby allowing anhMurNAc to be recycled	-0.847	0.000		
SCO0481	*chb3*	chitin-binding protein, part of coelichelin cluster; SCO0482 (chiG), which encodes a chitinase, is likely to be part of regulated transcription unit*	-0.704	0.032	Motif1_130	-175

SCO2907	*nagE2*	sugar PTS; N-acetylglucosamine-specific IIC component	-0.661	0.083	Motif1_1213 and Motif1_219	-214 and -78, respectively
SCO6084	*dnaQ*	DNA polymerase III; epsilon subunit	-1.106	0.000	Motif1_256	-76
SCO6517	*uvrA*	component of the nucleotide-excision DNA repair system	0.583	0.093	Motif1_336	-132
Sugar uptake and utilisation						
SCO1390	*crr*, *ptsA*	sugar phosphotransferase system (PTS); EIIAcrr component	-0.580	0.046	Motif1_35, associated with SCO1390	-90
SCO1391	*pts*I, *ptsP*	sugar PTS; EI, general (non-specific), component	-0.632	0.019		
SCO2907	*nagE2*	sugar PTS; N-acetylglucosamine-specific IIC component	-0.661	0.083	Motif1_1213 and Motif1_219	-214 and -78, respectively
SCO6257	SCO6257	sugar ABC transporter; sugar-binding lipoprotein	-2.262	0.000	Motif1_199, associated with SCO6257	-107
SCO6258	SCO6258	sugar ABC transporter; permease component	-2.333	0.000		
SCO6259	SCO6259	sugar ABC transporter; ATP-binding component	-2.156	0.000		

Amino acid metabolism						
SCO5529	*cimA*, *leuA2*	2-isopropylmalate synthase, catalyses first step of sub-pathway that synthesises L-leucine from an L-valine precursor	-1.114	0.000	Motif1_5	-40
SCO2631	SCO2631	amino acid permease	-1.081	0.001	Motif1_77	-165
SCO4295	*scoF4*	cold shock protein; amino acid transport; long 5′ leader*	0.595	0.084	Motif1_34 and Motif1_93	-360 and -294, respectively
SCO6516	SCO6516	hypothetical protein	-0.886	0.065	Motif1_336, associated with SCO6516	-76
SCO6515	SCO6515	protease	-0.899	0.057		
Secondary metabolism						
SCO1862	SCO1862	integral membrane protein; part of ectoine cluster	1.814	0.000	Motif1_79, associated with SCO1862	-46
SCO1861	SCO1861	hypothetical protein; part of ectoine cluster	0.556	0.002		
SCO1842	SCO1842	hypothetical protein; transposon disruption reduces red production	1.092	0.000	Motif1_218 and Motif2_744	-113 and +80, respectively

SCO0565	SCO0565	polyprenyl synthetase; required for production of isoprenoids,an ancient and diverse class of natural products that includes the sesquiterpene antibiotic albaflavenone; transcribed with upstream SCO0566*, which encodes a probable membrane protein	-0.795	0.001	Motif1_98, associated with SCO0566	-300
SCO2602	SCO2602	hypothetical protein; transposon disruption increases red production	0.753	0.000	Motif1_3	154
Other						
SCO0099	SCO0099	transposase, gene contains TTA codon	-0.457	0.056	Motif1_96	-237
SCO2287	SCO2287	oxidoreductase	-0.631	0.027	Motif1_197	-36
SCO2641	SCO2641	uncharacterized proteins involved in stress response, homologs of TerZ and putative cAMP-binding protein CABP1	0.635	0.079	Motif1_70	-45
SCO3305	SCO3305	putative integral membrane protein	-2.536	0.000	Motif1_16 and Motif1_1213	-32 and -214, respectively
SCO4070	SCO4070	hypothetical protein	-1.419	0.000	Motif1_53	-135
SCO4109	SCO4109	oxidoreductase, probable aldo/keto reductase	-0.778	0.000	Motif1_181	-30
SCO4764	SCO4764	dehydrogenase	-0.583	0.001	Motif1_224	-42
SCO5856	SCO5856	hypothetical protein	-1.186	0.001	Motif1_13	-73

SCO5970	SCO5970	hypothetical protein	-1.655	0.000	Motif1_1051	-166
SCO7517	SCO7517	putative integral membrane protein	-0.660	0.028	Motif1_190	-185

Table 3.1. Expression-verified targets of direct regulation by AtrA. Asterisk indicates gene identified by DEseq analysis using 20-nt bins. See text for further details. The highlights indicate that the genes are part of the same transcriptional unit. Positive and negative values of FC (fold change) mean that the gene expression is higher (activation) and lower (repression) in the presence of AtrA, respectively.

Many of the AtrA-binding sites identified by ChIP were not associated with detectable changes in gene expression upon disruption of *atrA*. This was expected as it is well established that transcription regulation is dynamic and dependent on multiple factors (Calkhoven & Ab, 1996, Martin & Sung, 2018, Ni *et al.*, 2009). For example, the binding of a repressor cannot exert a detectable effect on a promoter that at the time of study would remain inactive due to the binding of another repressor(s) or the absence of a critical activator or the required form of RNA polymerase. It is also possible that AtrA may be only partially active under the conditions analysed as a result of its limited production or inhibition by a small molecule regulator. Genes with binding sites within 350 bp upstream and 100 bp upstream of their start codon, but not associated with a detectable change in gene expression were classified as probable targets of conventional, direct regulation by AtrA. Reassuringly, this group of 88 genes (Table S3), contained a number whose expression has been shown experimentally to be affected by the disruption of *atrA* under different stages or conditions of growth or both, e.g. SCO3925 *(ssgR*) (Kim *et al.*, 2015).

3.3.4 Analysis of non-protein-coding genes

Of the 170 peaks, only 98 were associated with protein-coding genes that were classified above as verified or probable targets of direct regulation by AtrA. Whilst decades of study of the regulation of transcriptional regulation in bacteria have focussed on binding events located a relatively short distance within the start of a gene, ChIP-based approaches are revealing that the majority of bacterial transcription factors also bind to sites far from the start of the nearest gene (Farnham, 2009, Park *et al.*, 2013). The proportion of such binding varies with each transcription factor, but has been observed to be the majority in some cases (e.g. RutR in *E. coli*; (Shimada *et al.*, 2008)). The function of binding sites far from the start of annotated genes is only beginning to be studied. However, suggested functions include the regulation of genes encoding small RNAs (Singh *et al.*, 2014). To investigate whether any of the 72 remaining peaks were associated with altered expression beyond protein-coding genes, 20-nt windows along the chromosome and not annotated genes were used as the units of comparison in further DEseq analysis. This has confirmed the classification of all the expression-verified genes (Table 3.1) and identified altered expression associated with eight genes which were initially identified as probable targets of direct regulation (Table S3). It did not identify altered expression of sRNA genes identified previously, only a few examples of very low levels of transcription have been altered in the vicinity of AtrA-binding sites (data not shown).

The locations of sRNA genes confirmed or identified by the RNA-seq component of this study were recorded (Table 3.2). This analysis was restricted to relatively abundant

sRNAs to avoid the products of pervasive transcription (Lin *et al.*, 2013). Our group has argued that much of the pervasive transcription observed in bacteria is largely a consequence of RNA polymerases initiating transcription from sub-optimal sites at low frequency (Lin *et al.*, 2013). Of the 57 sRNAs that are listed, almost half were associated with attenuated 5′ leaders of mRNAs. Of these several were associated with known riboswitches: Cobalamin (Barrick & Breaker, 2007), Glycine (Khani *et al.*, 2018), FMN (Breaker, 2012). S-adenosyl methionine (class IV) (Poiata *et al.*, 2009) and ATP sensing (Chen *et al.*, 2017). The list also contained the four ubiquitous sRNAs: tmRNA, which is transfer-messenger ribonucleic acid (Shpanchenko *et al.*, 2005), SRP RNA, which is an integral component of the signal recognition particle that delivers the nascent membrane and secretory proteins to their proper site in the membrane (Akopian *et al.*, 2013, Pool, 2005), 6S RNA, which is a small RNA regulator of RNA polymerase (Cavanagh & Wassarman, 2014, Wassarman & Storz, 2000), and the catalytic RNA component of RNase P (Hartmann *et al.*, 2009). Two intermediates of stable RNA processing and 11 antisense RNAs were also identified. No member of the last group has an experimentally confirmed function. The remaining 13 sRNAs were associated with the intergenic regions and also do not have experimentally confirmed functions.

5′ leaders of protein-coding genes	Left	Right	Strand	Size	References
associated with SCO0247, attenuated	236550	236789	fwd	239	This study only
associated with SCO0989, attenuated; Cobalamin riboswitch	1044437	1044626	rvs	189	Rfam (Kalvari et al., 2017)
associated with SCO0991, attenuated; Cobalamin riboswitch	1045926	1046309	fwd	383	Romero et al. (2014), Vockenhuber et al. (2011)
associated with SCO0995, attenuated; Cobalamin riboswitch	1051401	1051583	fwd	182	Rfam (Kalvari et al., 2017)
associated with SCO1378, attenuated; Glycine riboswitch (2 x GcvT elements)	1457604	1457967	rvs	363	Pánek et al. (2008), Rfam (Kalvari et al., 2017)
associated with SCO1423, substantial attenuation or sRNA within intergenic region on same strand as SCO1414 and SCO1423	1519532	1519788	rvs	256	Romero et al. (2014), Moody at al. (2013)
associated with SCO1443, attenuated; FMN riboswitch (RFN element)	1538869	1539444	rvs	575	Rfam (Kalvari et al., 2017)
associated with SCO1554, attenuated	1666456	1666838	rvs	382	This study only
associated with SCO1847, attenuated; Cobalamin riboswitch	1975630	1975888	fwd	258	Rfam (Kalvari et al., 2017)
associated with SCO1928, attenuated	2060189	2060413	fwd	224	This study only
associated with SCO2146, substantial attenuation; class IV S-adenosyl methionine (SAM) riboswitch	2308485	2308789	rvs	304	Swiercz et al. (2008), Rfam (Kalvari et al., 2017), Moody at al. (2013)
associated with SCO2347, attenuated; SraF element	2517342	2517637	rvs	295	Rfam (Kalvari et al., 2017)
associated with SCO3064, attenuated	3356908	3357205	fwd	297	This study only
associated with SCO3097, attenuated; ATP-sensing riboswitch (*ydaO-yuaA* leader)	3392822	3392987	rvs	165	Rfam (Kalvari et al., 2017)
associated with SCO3323, attenuated	3675098	3675329	fwd	231	Vockenhuber et al. (2011)
associated with SCO3972, attenuated	4373878	4374498	fwd	620	This study only
associated with SCO4108, attenuated; ATP-sensing riboswitch (*ydaO-yuaA* leader)	4507166	4507320	fwd	154	Romero et al. (2014), Moody at al. (2013)

associated with SCO4115, attenuated; Streptomyces RNA 4115	4515321	4515494	fwd	173	Romero et al. (2014), Vockenhuber et al. (2011),
associated with SCO4659, attenuated	5088777	5088968	fwd	191	Vockenhuber et al. (2011)
tmRNA	5127282	5127536	fwd	254	Vockenhuber et al. (2011)
associated with SCO5157, substantial attenuation	5604875	5605371	rvs	496	Jeong et al. (2016)
associated with SCO5472, attenuated; Glycine riboswitch (2 x GcvT elements)	5958769	5959106	rvs	337	Rfam (Kalvari et al., 2017)
associated with SCO5610, substantial attenuation	6110270	6110683	rvs	413	This study only
associated with SCO5841,attenuated, and antisense to 5′ end of SCO5842	6394437	6394796	rvs	359	Romero et al. (2014),
associated with SCO5855, attenuated	6412238	6412509	rvs	271	Vockenhuber et al. (2011), Pánek et al. (2008)
associated with SCO6624, substantial attenuation	7347326	7347590	rvs	264	This study only
Long 5' leader of SCO7205 and antisense to SCO7204	8006654	8007401	fwd	747	Jeong et al. (2016)
long antisense RNA (>700 nt)					
antisense to SCO3291 and 3′ half of SCO3290	3639473	3641604	rvs	2131	Moody et al. (2013)
antisense to 5′ half of SCO4567 and SCO4566	4983947	4984793	rvs	846	Jeong et al. (2016), Moody et al. (2013), Vockenhuber et al. (2011)
antisense to 3′ half of SCO6712	7466816	7467612	rvs	796	Jeong et al. (2016)
antisense to 5′ end of SCO6716 and 3′ half of SCO6715	7469796	7470551	rvs	755	This study only
antisense to 5′ half of SCO6762	7517563	7518821	rvs	1258	Jeong et al. (2016), Moody et al. (2013),
antisense to SCO7204 and long 5' leader of SCO7205, attenuated; some sequence similarity to region of cobalamin riboswitch (this work)	8006654	8007401	fwd	747	Jeong et al. (2016)

antisense RNA (<500 nt)					
antisense to 5' end of SCO0627	669652	669953	fwd	301	Jeong et al. (2016), Romero et al. (2014),
antisense to 3′ half of SCO3317 and SCO3318	3669433	3669914	fwd	481	Jeong et al. (2016), Romero et al. (2014), Vockenhuber et al. (2011), Moody et al. (2013)
antisense to SCO3321 and long 5′ leader to SCO3322	3672969	3673312	fwd	343	Jeong et al. (2016)
antisense to 5' end of SCO4933	5367559	5368020	rvs	461	Jeong et al. (2016)
antisense to 3' half of SCO5861	6418705	6419101	rvs	396	This study only
sRNA (undefined)					
associated with 3' end of SCO2025, hypothetical stable intermediate	2170294	2170566	rvs	272	This study only
sRNA within intergenic region, on opposite strand to SCO2100 and SCO2101	2257985	2258213	rvs	228	Jeong et al. (2016), Romero et al. (2014), Swiercz et al. (2008), Moody at al. (2013)
sRNA within intergenic regions of convergent SCO2445 and SCO2446; may encode *Streptomyces* hypothetical protein (accession WP_078653018.1)	2625429	2625648	fwd	219	Jeong et al. (2016), Romero et al. (2014), Moody at al. (2013)
sRNA within intergenic regions of convergent SCO2735 and SCO2736	2982224	2982706	fwd	482	Jeong et al. (2016), Romero et al. (2014), Vockenhuber et al. (2011), Swiercz et al. (2008), Moody at al. (2013)
sRNA within intergenic regions of convergent SCO3076 and SCO3077 or abundant 3' end of SCO3077	3369949	3370222	rvs	273	Jeong et al. (2016), Swiercz et al. (2008)

sRNA within intergenic regions of convergent SCO3928 and SCO3929	4323771	4324454	fwd	683	Jeong et al. (2016), Vockenhuber et al. (2011), Moody at al. (2013)
sRNA within intergenic region, on same strand as SCO4075 and SCO4076; pseudo transfer RNA	4469945	4470136	rvs	191	Pánek et al. (2008)
sRNA within intergenic region, on opposite strand to SCO4388 and SCO4389; Actinobacteria sRNA Ms_IGR-5	4805208	4805789	rvs	581	Jeong et al. (2016), Moody et al. (2013)
sRNA within intergenic region of divergent SCO4688 and SCO4689	5116790	5117050	rvs	260	This study only
sRNA within intergenic region, on same strand as SCO5576 and SCO5577 or possibly greatly attenuated 5' leader of SCO5577; may encode *Streptomyces* hypothetical protein (accession WP_064730026)	6074177	6074626	fwd	449	Jeong et al. (2016)
sRNA within intergenic regions of convergent SCO5675 and SCO5676, may encode protein similar to hypothetical protein FBY48_2244 [*Streptomyces* sp. 4-17] (accession TQK89111)	6176171	6176413	rvs	242	Jeong et al. (2016), Romero et al. (2014), Vockenhuber et al. (2011) , Swiercz et al. (2008), Moody at al. (2013)
sRNA within intergenic region, on opposite strand to SCO5821 and SCO5822; antisense to *Streptomyces* hypothetical protein (accession WP_003973200)	6370296	6370789	rvs	493	Romero et al. (2014), Vockenhuber et al. (2011),
sRNA within intergenic region, on same strand as SCO5916 and SCO5917	6484345	6484924	fwd	579	Jeong et al. (2016), Romero et al. (2014), Moody at al. (2013)
Processing intermediate					
hypothetical stable RNA processing intermediate	3690678	3691139	rvs	461	Pánek et al. (2008), Moody at al. (2013)
hypothetical stable RNA processing intermediate	4530071	4530509	fwd	438	Jeong et al. (2016), Moody at al. (2013)

sRNA defined					
catalytic RNA component of RNase P within intergenic region, on same strand as SCO2293 and SCO2292	2462919	2463260	rvs	341	Romero et al. (2014), Pánek et al. (2008), Rfam (Kalvari et al., 2017)
transfer-messenger RNA within intergenic regions of convergent SCO2965 and SCO2966	3226542	3226936	rvs	394	Romero et al. (2014), Pánek et al. (2008), Rfam (Kalvari et al., 2017)
6S RNA within intergenic regions of convergent SCO3558 and SCO3559	3934693	3934927	fwd	234	Jeong et al. (2016), Romero et al. (2014), Vockenhuber et al. (2011), Pánek et al. (2008), Rfam (Kalvari et al., 2017)
RNA of small signal recognition particle RNA within integenic region, on same strand as SCO4066 and SCO4067	4457035	4457120	fwd	85	Romero et al. (2014), Pánek et al. (2008), Rfam (Kalvari et al., 2017)

Table 3.2. The location of abundant sRNA genes either confirmed or identified by this study. Abundant RNA had reads two standard deviations above the average of the reads from across the chromosome.

3.3.5 Cell wall biogenesis and development

The expression-verified targets identified here (Table 3.1) include two key activities associated with peptidoglycan, a major component of the mycelial wall of *Streptomyces*: UDP-N-acetylmuramoyl-L-alanine ligase (SCO6060, *murC*), which catalyses the first of four steps in the synthesis of the peptide moiety of peptidoglycan within the cytoplasm (Barreteau *et al.*, 2008, Fiuza *et al.*, 2008), and anhydro-N-acetylmuramic acid kinase (SCO7595*, anmK*), which converts 1,6-anhydro-N-acetylmuramic acid (anhMurNAc), a product of autolysis of peptidoglycan, to N-acetylmuramic acid-6-phosphate (MurNAc-6P) thereby allowing anhMurNAc to be recycled (Uehara *et al.*, 2005). The genes for both activities are co-transcribed with genes that co-localised across the streptomycetes (for further details, see Table 3.1). The expression-verified targets also include a protein (SCO0481, *chb3*) that binds chitin, a rich source of N-acetylglucosamine (GlcNAc), a chitinase (SCO0482, *chiG*), and the GlcNAc-specific permease (SCO2907, *nagE2*) of the global phosphotransferase system (PTS, see below). The *nagE2* gene has been shown previously to be regulated by *atrA* (Nothaft *et al.*, 2010). Alternating units of the amino sugars GlcNAc and MurNAc linked by β-1,4-glycosidic bonds form the glycan moiety of peptidoglycan (Sychantha *et al.*, 2018, Vollmer *et al.*, 2008). The link to peptidoglycan is extended through target D-alanyl-D-alanine dipeptidase (SCO1396, *vanX*), which could potentially also be involved in peptidoglycan recycling or remodelling (see below), and through a secreted endopeptidase (SCO6773, *swlC*) shown to be active in remodelling of the cell wall (Haiser *et al.*, 2009). Altered expression upon disruption of *atrA* was detected for the latter, but not the former (Table S3).

Interestingly, AtrA also appears to coordinate the metabolism of the mycelial wall with septation and DNA replication. The ChIP-seq analysis supports previous evidence for direct *atrA*-mediated regulation of SsgR (SCO3925, (Kim *et al.*, 2015)), a known regulator of the morphogene *ssgA*, which controls processes involving remodelling of the cell wall (van Wezel *et al*., 2000) including the hyphal septation that produces spores (Kim *et al.*, 2015, Traag & van Wezel, 2008). During septation, the segregation of chromosomes to produce spores that contain a single chromosome is mediated by FtsK (Wang *et al.*, 2007b). The location of an AtrA-binding site upstream of *ftsK* (SCO5750) indicates that it is also a part of the AtrA regulon. Other probable targets include: DNA topoisomerase I (SCO3543, *topA*), the major enzyme for relaxing negatively supercoiled DNA (Szafran *et al.*, 2016), and a DNA helicase of unknown function (SCO5183). Verified target with links to DNA are the 3′ to 5′ proof-reading ε subunit of DNA polymerase III (SCO6084, *dnaQ*), the primary enzyme involved in DNA replication (McHenry, 1985), and a homologue of UvrA (SCO6517), which is a component of the

nucleotide-excision DNA repair system (Sancar, 1996). In addition to SsgR and FtsK, other probable targets with functions during morphological development include: SigJ (SCO1276), an extracytoplasmic function (ECF) sigma factor (Bobek *et al.*, 2014) linked to the later stages of morphological development (Helmann, 2002) and a nucleotide-binding protein (SCO5968) regulated by the *bldA* morphogene (Li *et al.*, 2007).

3.3.6 Sugar uptake and utilisation

Verified targets include: two active sugar transporters: the IIA^{Crr} phosphotransferase (SCO1390, *crr*, *ptsA*) and EI non-specific component (SCO1391*, ptsI*, *ptsP*) of the global PTS, which has a major role in active uptake of carbohydrates (Tanaka *et al.*, 2008), and the sugar-binding lipoprotein, permease and ATP-binding protein (SCO6257-9) of a member of the ATP-binding cassette (ABC) transporter family (Schneider & Hunke, 1998, Wilkens, 2015). Probable targets include: GlyR (SCO1658), the glycerol-inducible transcriptional regulator of the glycerol operon, which is thought to regulate the major kinase (SCO1660, *glk1*) involved in glycerol uptake and metabolism (Hindle & Smith, 1994); a second glycerol kinase (SCO0509, *glpK2*); and a component of an additional ABC transporter (SCO1707). These findings indicate that the regulation of carbon uptake and utilisation by AtrA extends well beyond the glycan components of peptidoglycan.

3.3.7 Amino acid metabolism

AtrA also regulates the activities associated with amino acid metabolism. Verified targets include: 2-isopropylmalate synthase (SCO5529, *leuA2*), which catalyses the first step of a sub-pathway that synthesises L-leucine from an L-valine precursor (Potter & Baumberg, 1996); an amino acid permease (SCO2631), possibly with specificity towards γ-aminobutyric acid (Hosie *et al.*, 2002); and a cytoplasmic protease (SCO6515, *pfpI*). The probable targets included a decarboxylase (SCO5353, *lysA*), which synthesises L-lysine from diaminopimelate (Bourot *et al.*, 2000). Leucine, isoleucine and valine are all branched chain amino acids that can serve as precursors for various secondary metabolites in *Streptomyces* bacteria including polyketides (Craster *et al.*, 1999, Li *et al.*, 2009). Another probable target is homogentisate 1,2-dioxygenase (SCO1715, *hgd*), which is involved in the catabolism of aromatic rings, more specifically in the breakdown of the amino acids tyrosine and phenylalanine (Pan *et al.*, 2013), which are also important precursors for secondary metabolites (Euverink, 1995) such as pigment compounds and plant hormones (Parthasarathy *et al.*, 2018).

3.3.8 Secondary metabolism

Secondary metabolism is also directly regulated by AtrA beyond the activation of *act*II-ORF4 (van der Heul *et al.*, 2018, van Wezel & McDowall, 2011). Verified targets from this study include: a hypothetical protein and integral membrane protein (SCO1861 and SCO1862, respectively) encoded within the biosynthesis gene cluster for ectoine, a compatible solute that prevents osmotic stresses (Kuhlmann & Bremer, 2002, León *et al.*, 2018); polyprenyl synthetase (SCO0565), which is required for the production of isoprenoids, the most ancient and diverse class of natural products (Kumari *et al.*, 2013, Lange *et al.*, 2000), which includes the sesquiterpene antibiotic albaflavenone (Zhao *et al.*, 2008); and the aforementioned chitin-binding protein (SCO0481, *chb3*) and chitinases (SCO0482, *chiG*), which is encoded within the BGC for coelichelin, a ferric iron siderophore (Barona-Gomez *et al.*, 2006). Probable targets include: a small membrane protein of unknown function (SCO2699) within the BGC for lactonamycin (Zhang *et al.*, 2008a); and a secreted endopeptidase (SCO0752) within the BGC for informatipeptin (Liu *et al.*, 2018). The CSR of the calcium-dependent antibiotic, CdaR (SCO3217), is an example of a gene that contains an AtrA-binding site within the coding region. Whilst no change in *cdaR* expression was detected, the production of many of its downstream targets were affected by *atrA* disruption (Table S2).

3.3.9 Indirect regulation

A high proportion of the expression affected by disruption of *atrA* was not associated with sites of AtrA binding suggesting the underlying regulation is indirect. This finding is unsurprising given the central importance of many of the genes found to be regulated directly by *atrA* under the condition studied (Table 3.1). The 59 genes classified as indirect targets included but were not limited to additional functions associated with transcription and its regulation, peptidoglycan metabolism, amino acid metabolism, membrane transport, and iron homeostasis (Table S2). Scanning of the upstream regulatory regions of these genes did not identify an enriched motif(s) suggesting that the indirect regulation is mediated by multiple factors some of which might act post-transcription initiation (data not shown).

3.4 Discussion

By combining ChIP and RNA seq, it is shown here that AtrA has a direct role in regulating and likely coordinating the expression of genes encoding important functions associated with sugar and amino acid uptake and utilisation, peptidoglycan biosynthesis, morphological development, and secondary metabolism. Moreover, the influence of AtrA over each of these processes is exerted at multiple points. For example, whilst it was already known that AtrA activates the production of the *N*-acetylglucosamine-specific IIC^{GlcNAc} permease (SCO2907, *nagE2*) of the global PTS , the work reported here indicates that it also directly controls the IIA^{Crr} (SCO1390, *ptsA*) and general (non-specific) EI components (SCO1391, *ptsI*), but represses not activates their production (Figure 3. 6). The genes of these components are also associated with DasR binding (Rigali *et al.*, 2006).

During uptake by the PTS, a phosphoryl group is transferred from phosphoenolpyruvate to EI and then the IIA domain of the permease complex via the phosphocarrier Hpr protein (SCO5841). Within the permease, the phosphoryl group moves further to the IIB domain, which eventually phosphorylates the carbon source entering through the IIC transport-channel domain (Nothaft *et al.*, 2010). We speculate that inactivation of AtrA binding, perhaps by binding of small molecule, which is common within the TetR family (Cuthbertson & Nodwell, 2013), may help facilitate the uptake of alternative sugars via the global PTS by increasing the overall level of phosphotransferase activity whilst reducing the level of a component specific to GlcNAc. Reduced uptake of GlcNAc would result in repression of the *nagE2* gene by the global regulator DasR (Rigali *et al.*, 2008), which binds its DNA targets in the absence of itself being bound by GlcNAc-6-P, the immediate product of uptake by the global PTS.

DasR, which is a member of the GntR family conserved in streptomycetes and many other Actinobacteria, does not only control the uptake of GlcNAc but also its metabolism and the degradation of chitin to GlcNAc (Rigali *et al.*, 2006, Rigali *et al.*, 2008) (Figure 3.6). One of the many genes indirectly repressed by AtrA encodes a possible sugar-binding protein (SCO4286) encoded divergent to the transcription unit encoding N-acetylglucosamine kinase (SCO4285; *nagK*) and GlcNAc-6P deacetylase (SCO4284, *nagA*) (Świątek *et al.*, 2012). This gene will be responsive to GlcNAc metabolism via DasR (Świątek *et al.*, 2012). The work reported here also shows the influence of AtrA in relation to sugar metabolism extends beyond the global PTS and GlcNAc metabolism to

multiple steps in the uptake and utilisation of glycerol and other sugar transporters (Table 3.1).

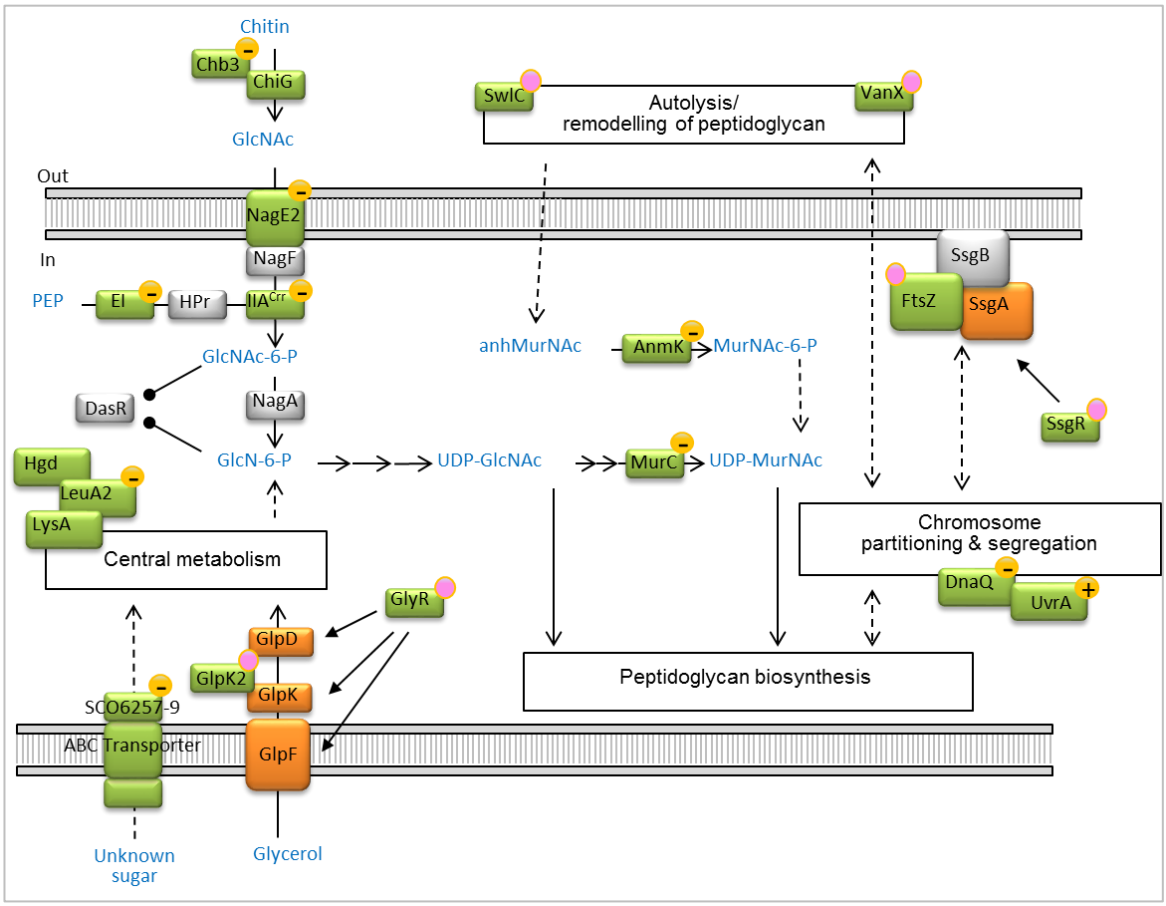

Figure 3.6. Examples of multi-level control of key processes by AtrA. Regulation identified or confirmed in this study for AtrA (Table 3.1) is shown schematically alongside regulation reported to be mediated by DasR (white boxes). The green boxes indicate proteins that appear to be regulated directly by AtrA, whereas the orange boxes indicate proteins regulated by GlyR or SsgR, which appear to be direct targets of AtrA. Yellow circles with plus and minus signs indicate up and down-regulation, respectively. Pink circles indicate probable direct targets of AtrA (there are AtrA binding sites but no detectable change in gene expression under the conditions tested). Open and closed arrows indicate links at the level of metabolism and transcriptional regulation, respectively. Broken lines indicate multi-step connections. The uptake of sugars via the global PTS (top left) requires that transfer of a phosphoryl group from phosphoenolpyruvate to EI and then the IIA domain of the permease complex via the phosphocarrier Hpr protein (Deutscher *et al.*, 2006). Within the permease the phosphoryl group moves further to the IIB subunit, which eventually phosphorylates the carbon source entering through the IIC transport channel (Nothaft *et al.*, 2010). FtsZ, SsgA and SsgB (top right) are shown as a pre-division stage where FtsZ is co-localised and no longer forms spiral-like filaments through the aerial hyphae. At this stage, the chromosomes are uncondensed and increasingly associated with ParB (not shown). Z-rings are then formed, followed by chromosome condensation and segregation and formation of the sporulation septa (Willemse *et al.*, 2011).

The activities of the PTS in *S. coelicolor* are inextricably linked to the onset of antibiotic production and morphogenesis (Nothaft *et al.*, 2010, van der Heul *et al.*, 2018); inactivation of any one of the three general phosphotransferases EI, HPr or IIA^{Crr} blocks the morphological development (Nothaft *et al.*, 2010). This phenotype is independent of the uptake of GlcNAc from the media (Nothaft *et al.*, 2010). Both the link to morphological development and the lack of dependency on GlcNAc are consistent with studies in other bacteria that have revealed the PTS regulates key and often several cellular processes and has a pivotal role in the uptake of multiple sugars (Li *et al.*, 2019). Given the above, the regulation of multiple components of the *S. coelicolor* PTS is one of several means by which AtrA appears to control the transition from vegetative growth to morphological development, which involves extensive septation of aerial hyphae to produce chains of unigenomic spores (Ohnishi *et al.*, 2002). As described above, it also appears to regulate an ECF sigma factor (SigJ, SCO1276) that functions in morphological development and is regulated by DasR (Table S1).

Sporulation is known to be controlled at least in part by proteins related to the product of a gene first identified as a suppressor of a hyper-sporulating *S. griseus* mutant (*ssgA*; (van Wezel *et al.*, 2000)). In *S. coelicolor*, SsgA dynamically controls the localization of its paralogue SsgB, which in turn recruits FtsZ to sites of future septation to initiate sporulation-specific cell division (Willemse *et al.*, 2011). FtsZ is a tubulin-like protein that governs a highly conserved cell-division machine called the divisome that directs the ingrowth of the peptidoglycan cell wall, thereby driving fission of the membrane to form a closed septum (Fenton & Gerdes, 2013). The work reported here not only supports AtrA control of SsgR (SCO3925), a specific transcription factor regulating the production of SsgA (Willemse *et al.*, 2011), but it also indicates that FtsZ (SCO5750), as well as multiple key activities associated with peptidoglycan biosynthesis, are part of the AtrA regulon (Figure 3.6). Thus, AtrA does not only control morphogenic signals derived from the global PTS, but also multiple process that are closely coordinated and central to the actual process of septation. Additional links indicate that the influence of AtrA may also extend to DNA replication, which by analogy with other bacteria (Barry & Bell, 2006, O'Donnell *et al.*, 2013) is likely to be closely entwined with the condensation and segregation of chromosomes in the aerial hyphae of streptomycetes. Depletion of a topoisomerase I (TopA) has been reported to block septation in hyphae (M. Szafran and D. Jakimowicz, unpublished).

The identified role of AtrA in the transition from vegetative growth to morphological development offers an explanation for its co-option into the regulation of several secondary metabolites (Chen *et al.*, 2008, Li *et al.*, 2015b, van der Heul *et al.*, 2018) ,

whose production coincides with this developmental stage and activities may function to minimise the scavenging of nutrients by competing organisms, thereby maximising the yield of spores (van der Heul *et al.*, 2018, van Wezel & McDowall, 2011). For *S. coelicolor*, the influence of AtrA on biosynthetic gene clusters is shown here to extend beyond the reported direct regulation of *actII-ORF4* of the actinorhodin cluster (Uguru *et al.*, 2005). The targets described here are not however other cluster-situated regulators, with the possible exception of CdaR (Table 3.1). Thus, in the context of secondary metabolism, AtrA appears largely to function alongside cluster-situated regulators and their upstream regulators (e.g. DasR) to control the production of secondary metabolites. A widespread requirement for the production of secondary metabolites via increased transcription of CSR genes is induction of the stringent response (Okada & Seyedsayamdost, 2017, van der Heul *et al.*, 2018, van Wezel & McDowall, 2011). The stringent response is evolutionarily conserved and enables bacteria to adjust their metabolism and survive when nutrients become limited (Boutte & Crosson, 2013). Interestingly, AtrA is found here to not only control aspects of the uptake and metabolism of amino sugars, but also certain amino acids (Table 3.1), which are known precursors of secondary metabolites (Craster *et al.*, 1999, Li *et al.*, 2009). Thus, AtrA has extensive control over the uptake and utilisation of major nitrogenous compounds, which may enable streptomycetes to grow and compete efficiently in soil and other environments poor in nitrogen. Additionally, AtrA is part of the “phosphate” regulon (Santos-Beneit, 2015), which regulates the uptake and utilisation of phosphorus, the other major element noted for limiting growth in soil (Aldén *et al.*, 2001). The regulation of AtrA by this and other regulatory systems (van der Heul *et al.*, 2018, van Wezel & McDowall, 2011) attests to its central importance in the growth and development of *Streptomyces*.

It appears that many of what appear to be bona fide binding sites for AtrA (i.e. ChIP peaks with centres aligned to a recognisable motif) are not associated with the promoter regions of known or probable genes. As mention earlier, this has been observed for many other transcription factors, although the frequency varies considerably. It has been suggested that transcription factor binding to what are widely called “intragenic” sites may have no biological function (Mrázek & Karls, 2019), contributing to complexes and higher-order chromosome structures (Woodcock & Ghosh, 2010). Some of which may influence gene expression, provide a reservoir to provide some form of regulatory “buffer” (Corless & Gilbert, 2016), offer a platform for the evolution of new transcriptional networks (Ramani *et al.*, 2016), facilitate levels of gene regulation that are small (and thus difficult to detect) but sufficient to allow their evolutionary conservation (Tanabe *et al.*, 2002) or a combination thereof. In this study a few examples of very low levels of

transcription altered by disruption of AtrA were detected in the vicinity of AtrA-binding sites (data not shown). Only the further study of binding to “intragenic” sites will determine the roles of transcription factors distinct from the regulation to transcription initiation. The finding that all of the binding sites identified by ChIP are associated with at least one of two related motifs (Figures 3.4) which indicates that bioinformatic approaches such as FIMO and PREDetector can be used to predict sites of AtrA binding in other *Streptomyces* species and, when complementary expression data is available, genes regulated directly by AtrA. The motifs can also be used to predict binding sites for AtrA in addition to those that are accessible, and thus detectable by ChIP, under the condition(s) of study. Motifs are present at sites reported previously to be bound by AtrA in the promoter region of *actII-ORF4* (Hasan, 2015, Uguru *et al.*, 2005) but in this study only produced weak ChIP peaks (data not shown).

The identification of two related motifs for the *in vivo* sites suggests the existence of two modes of binding. As indicated above, the presence and spacing of indirect repeats in Motif 1 is typical of interactions between a head-to-head dimer and adjacent major grooves on one side of the double-stranded DNA helix; the identical reading heads, one on each monomer, making a combination of sequence and non-sequence specific contacts and acting cooperatively to mediate the overall interaction. This mode of binding is typified by *E. coli* TetR (L Ramos *et al.*, 2005). Motif 2 is essentially an extension of the sequence found in each half of Motif 1. The lengths of the consensus sequences in both Motif 1 and Motif 2 (6 and 9 nt, respectively) are within the range reported for other members of the TetR family (Yu *et al.*, 2010). Motif 2 may reflect situations where extension of the contact surface with one monomer of an AtrA dimer may reduce the requirement for sequence-specific contacts with the other. Thus, the two modes of binding may simply reflect the extent to which each half contributes to the overall interaction, i.e. Motif 2 represents situations where one half contributes substantially more than the other, and Motif 1 represents everything in between. It will be interesting to determine whether an extended half site is sufficient for AtrA binding *in vitro*.

For the identification of differential expression, our approach of using 20-nt windows rather than annotated genes as the units of comparison provided much richer output. Not only it did provide an indication of the boundary of regulated transcriptional units, but also it appeared to be more sensitive, for reasons that are not yet understood. In our analysis of 20-nt windows, the p-values were not adjusted by plotting as $-\log_{10}$ values. The greater the $-\log_{10}$ value, the greater the confidence that the difference in expression is statistically significant. Oversampling is well-known issue with unadjusted p-values. For example, it can be expected that by sampling over 865 thousand window and setting

a p-value threshold of <0.05, 43 thousand calls (5%) would be false positives. However, in order for a region to be recognised as being differentially expressed in our study, a continuous run of adjacent windows had to have low p-values. The potential power of this approach is shown for a region of the *cda* cluster (Figure 3.7). Whilst only SCO3215 was identified as being differentially expressed by conventional analysis, our approach identified that the expression of all 6 genes of the transcription unit (SCO3215 to SCO3210) were altered by disruption of *atrA*.

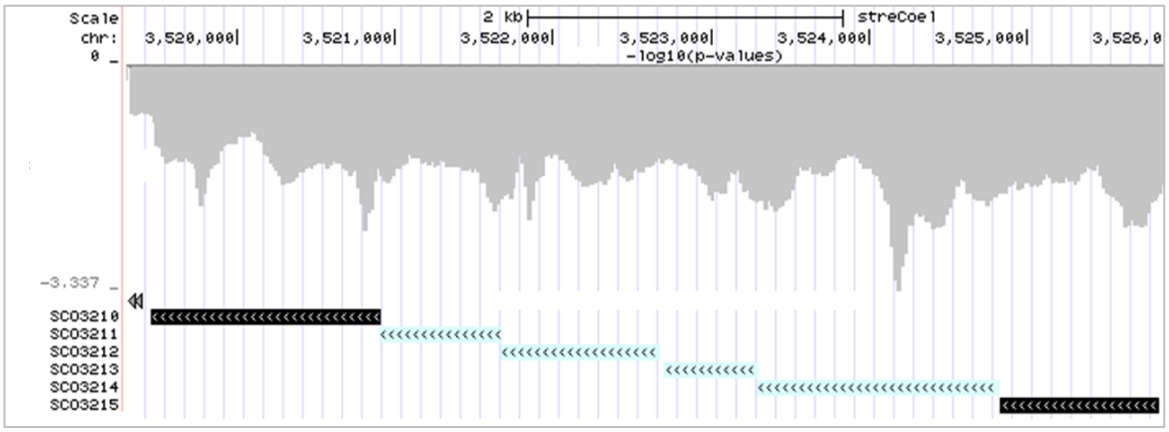

Figure 3.7. Identification of differential expression by using 20-nt windows as the units of comparison in combination with plots of the associated p-values transformed to $-\log_{10}$. A –log10 value of 2 equates to a numerical value of 0.01.

In terms of the potential to enhance the screening of new chemotherapeutics through the manipulation of AtrA, this work has shown that does have multiple links to secondary metabolisms and appears to work largely alongside cluster-situated regulators and their upstream regulators. There are several reports of AtrA directly regulating cluster-situated regulators (van der Heul *et al.*, 2018). This work has also shown multiple new connects to the uptake and metabolism of GlcNac indicating that AtrA also shapes secondary metabolism via DasR, whose manipulation via the addition of a metabolite regulator to the media resulted in the discovery of secondary metabolites that would otherwise have remained cryptic (Rigali *et al.*, 2008). Combined the above is sufficient to suggest that there is merit in investigating the regulation of AtrA activity by small molecules and determining the extent to which disruption of AtrA affect the production of the secondary metabolites by chemical or biological assays.

Chapter 4 Small molecule regulation of *S. coelicolor* AtrA

4.1 Abstract

AtrA has sustained significant interest since being described as activating the production of actinorhodin by *Streptomyces coelicolor*. It is a member of TetR family of one component signal transducers and, as shown in the previous chapter, exerts multi-level control over key activities in cell wall biogenesis and morphological development as well as the uptake and assimilation of sugars and amino acids. A role for AtrA in processes central to the transition from vegetative growth to morphological development offers an explanation for its co-option into the regulation of several secondary metabolites. Here, we exclude actinorhodin as a specific, small molecule regulator of *S. coelicolor* AtrA, but find evidence that actinorhodin and perhaps other small molecules may function as global regulators of transcription. It is speculated that such activity may facilitate silencing of biological processes as part of the developmental pathway leading to spore formation. Approaches to identify specific, small-molecule regulators of transcription are discussed in light of the findings reported herein.

4.2 Introduction

It has been reported that the DNA-binding activity of AtrA, like many other members of the TetR family (Cuthbertson & Nodwell, 2013), is regulated by the binding of a small-molecular-weight ligand(s). Whilst investigating the regulation of lidamycin production by *S. globisporus,* collaborators, Bin Hong and colleagues (Peking Union Medical College, China), discovered that the DNA-binding activity of AtrA-gl is inhibited by the binding of heptaene, an unsaturated aliphatic hydrocarbon that is a biosynthetic intermediate of lidamycin (Li *et al.*, 2015b). In addition, they also reported that the DNA-binding activity of AtrA-gl could be inhibited, at least *in vitro*, by actinorhodin. However, it was not shown that the inhibition was specific to AtrA and little information was provided on the properties of the actinorhodin preparation (Li *et al.*, 2015b). Nevertheless, these findings raised the possibility that AtrA from *S. coelicolor* might be responsive to actinorhodin and perhaps related compounds.

Work in Leeds had already established that there was at least one activity in crude solvent extracts from *S. coelicolor* that could inhibit the DNA-binding activity of AtrA (Hasan, 2015). However, prompted by the work in Beijing, further investigation found an activity that inhibited the DNA-binding activity of AtrA from *S. coelicolor* in an extract from

M1146 (Hasan, 2015), a strain that lacks the entire gene cluster for actinorhodin plus those of undecylprodigiosin, the calcium-dependent antibiotic and the coelimycin (Gomez-Escribano & Bibb, 2011). It has also been reported that the activity in the extract from M1146 was unable to inhibit the DNA-binding activity of TetR from *E. coli* or ActR from *S. coelicolor* suggesting a level of specificity (Hasan, 2015).

This chapter describes the assays used to study the effect of purified γ-actinorhodin and crude extracts of *S. coelicolor* strains on the DNA-binding activity of AtrA. Recent work using the same batch of purified γ-actinorhodin has revealed potent and selective bactericidal activity against key Gram-positive pathogens (Nass *et al.*, 2017). The bactericidal activity of γ-actinorhodin was associated with collapse of the proton motive force and the generation of reactive oxygen species (ROS) (Nass *et al.*, 2017). Contemporaneous studies by others suggest a more complex mode of action for actinorhodin (Mak & Nodwell, 2017). The opportunity was also taken to analyse further the sequence requirements of AtrA binding associated with Motif 2 (see previous chapter).

4.3 Results

4.3.1 Over-production and purification of LacI

Prior to continuing the screening of activities that could disrupt AtrA binding, LacI from *Escherichia coli* was included as a control from outside the TetR family. LacI has been a model for the analysis of bacterial transcriptional regulation since the classical papers of Jacob and Monod (Jacob & Monod, 1959, Jacob & Monod, 1961), and is the archetype of a large family involved in the regulation of central sugar metabolism (Ravcheev *et al.*, 2014). The other controls were *S. coelicolor* ActR, which encodes the regulator of the efflux pump for actinorhodin (Tahlan et al., 2007) and *E. coli* TetR, which controls the expression of the TetA tetracycline resistance determinant (an efflux pump) and is the archetype of the TetR family (Meier et al., 1988). LacI was tagged with oligohistidine at the N-terminus to facilitate purification by immobilised metal affinity purification (Porath *et al.*, 1975) as detailed previously for AtrA, TetR and ActR (Hasan, 2015, Uguru *et al.*, 2005). The integrity of the construct was confirmed by DNA sequencing (data not shown).

LacI was purified as previously described, with minor modification (see Section 2.6.3). SDS-PAGE analysis of the purification of LacI is shown (Figure 4.1). A polypeptide migrated slower than the expected size (38.6 kDa), as do many proteins (Rath & Deber, 2013, Shirai *et al.*, 2008). This polypeptide was clearly induced (cp. lanes 1 and 2), remained in the soluble fraction following lysis of the cells and ultracentrifugation (lane 3), bound to the column with reasonable efficiency (lane 4), remained bound during the wash step (lane 5), was eluted as the major species at higher imidazole concentrations (lanes 6 and 7) and remained soluble during dialysis (lane 8). The purity of LacI was comparable to that of AtrA, TetR and ActR (data not shown).

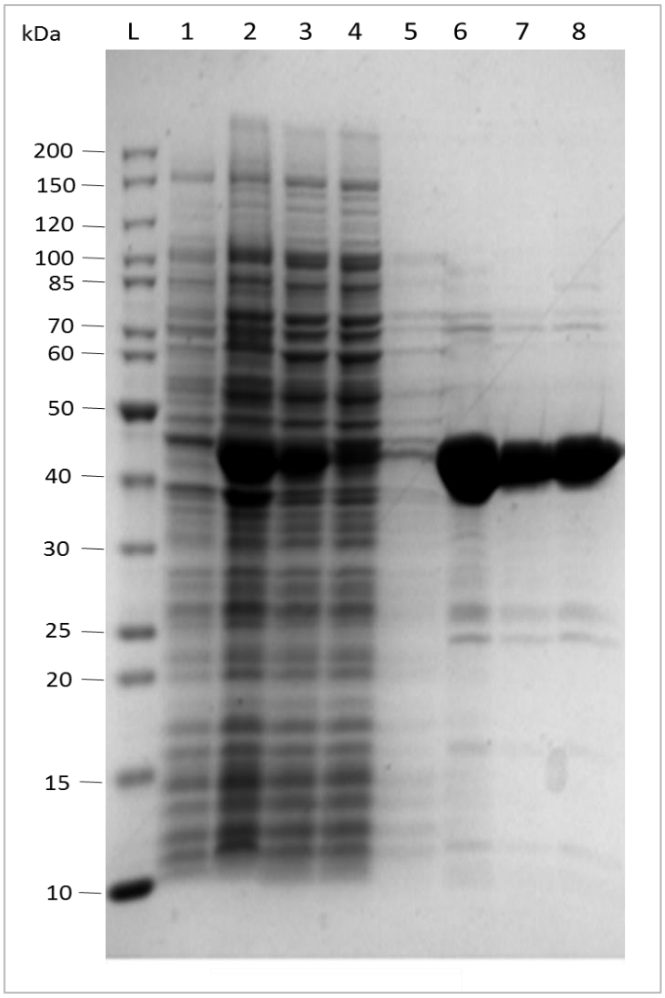

Figure 4.1. SDS-PAGE analysis of the purification of LacI from *E. coli*. Lane 1 and 2 contain samples of cell lysate before and after IPTG induction, respectively. Lane 3 contains a sample of cleared lysate removed after lysis of cells and ultracentrifugation. Lane 4 contains a sample of the flow through from the column. Lane 5 contains a sample from the column wash stage. Lane 6 and 7 contain samples from the first and second elution steps, respectively. Lane 8 shows sample after dialysis of combined the two eluates. The lane labelled M contains PageRuler Unstained Protein Ladder (Fermentas). The sizes of the markers in kDa are shown on the left side hand. The expected size of LacI is 38.6 kDa.

The DNA-binding activity of LacI was confirmed using an EMSA. Increasing concentrations of LacI were incubated with a synthetic double-stranded substrate containing the sequence of the main operator ($lacO_1$) of the *lac* operon (Lewis, 2005) (Figure 4.2). The substrate was synthesised by PCR using a pair of primers, one of which was labelled at its 5′ end with Fluorescein (lane 1). At the lowest protein concentration used (62.5 nM), a single distinct complex was observed (lane 2). This concentration is above the reported dissociation constants (K_D values) for dsDNA fragments containing $lacO_1$ (Forde *et al.*, 2006, Han *et al.*, 2009). At higher concentrations, additional

complexes were formed (lanes 3, 4 and 5). These are likely to be the result of additional non-sequence-specific binding. High-throughput studies of transcription factor binding have challenged the common view that transcription factors are highly sequence specific (Badis *et al.*, 2009). The apparent equilibrium dissociation constant (K_d') of this interaction was estimated of be lower than 62.5 nM as the majority of the substrate appeared to be bound by this concentration (compare levels of unbound substrate in lanes 1 and 2).

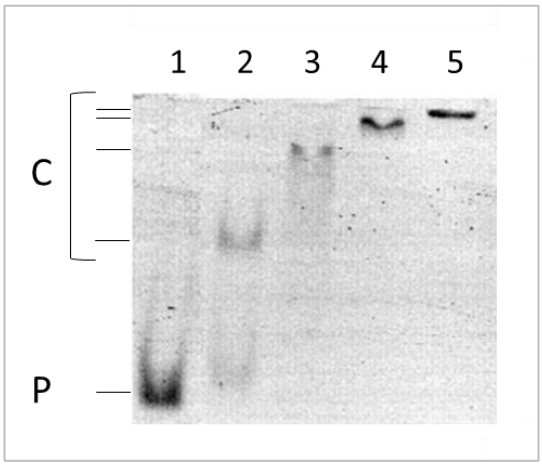

Figure 4.2. Electrophoretic mobility shift assay (EMSA) of *E. coli* LacI protein. The positions of unbound probe (P) and complexes (C) are identified on the left. Lane 1 serves as negative control (containing substrate without protein). Lanes 2 to 5 contains the following concentrations of LacI: 62.5 nM, 250 nM, 1 µM and 4 µM, respectively. Each lane contains 5 nM of *lac* operator. The reactions were run in a 4% (37.5:1) acrylamide: bis-acrylamide gel in 1 x TGED buffer for 40 min at 120 V. The gel was imaged using Fujifilm FLA-5000 imaging analyser system.

4.3.2 Preparation of crude extracts containing actinorhodin

As a step towards to corroborating whether actinorhodin could inhibit the binding of AtrA to cognate sites, small molecules were extracted from strain L646 (Towle, 2007), which over produces actinorhodin as a result of constitutive expression of *actII*-ORF4 from a strong promoter (*ermE**p,(Li *et al.*, 2015a)) and ribosome-binding site (*tuf*, (Krasny *et al.*, 2000). Equivalent extracts from other strains were included as controls: M1146 (Gomez-Escribano & Bibb, 2011), which lacks the clusters for actinorhodin (Act), undecylprodigiosin Red), the calcium-dependent antibiotic (Cda) and the coelimycin; M511 (Floriano & Bibb, 1996), which lacks the *actII*-ORF4 gene; and M145, the congenic wild-type. L646 produces considerable more diffusible, blue-pigment actinorhodin than M145, whilst M1146 and M511 do not produce any detectable blue pigment (data not shown), as reported previously (Hong *et al.*, 2007). Small molecules were extracted from

the mycelia and the supporting agar media, concentrated, dried, weighed and resuspended in small volumes of methanol (see Section 2.8.1). Confirmation that actinorhodin was present in both M145 and L646, but at a higher concentration in the latter, and absent from M1146 and M511 was obtained by assaying for activity that could inhibit the growth of *Staphylococcus aureus* SH1000 (Horsburgh *et al.*, 2002). Samples of extract were spotted onto small sterilised circular filter paper discs (6 mm diameter), air-dried, and placed on the surface of agar plates overlaid with the indicator strain. Discs onto which the solvent and an extract from *Streptomyces albus* J1074 (Dr Ryan Seipke, Laboratory stock, (Chater & Wilde, 1980)) were included as additional controls. Zones of inhibition were only detected for M145 and L646, with the zone being clearly larger for L646 (Figure 4.3).

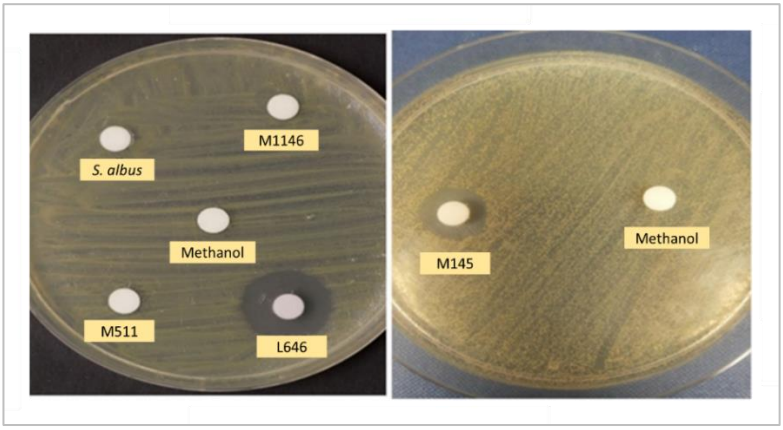

Figure 4.3. Assaying the inhibition of the growth of *S. aureus*. The concentrations of crude extracts were 10mg/ml and the volume of each crude extract added to each disc was 40 µL. Each plate was overlaid with 10 µL of strain SH1000 overnight culture suspended in 5 mL sterilized dH_2O. The plates were photographed after incubating overnight at 37°C. Both plates are from assays conducted at the same time and using the same batch of plates and stock of indicator strain.

Next extracts were analysed for activity that inhibits the binding of AtrA (Figure 4.4). The DNA substrate for the initial assay was a 395-bp fragment containing both of the binding sites in the *actII*-ORF4 promoter region (Hasan, 2015). Preparatory analysis had identified a concentration of AtrA at which the DNA was only partially shifted, i.e. conditions under which inhibition of DNA-binding activity would be readily detected. Inhibition, as determined by an increase in the proportion of DNA in the unbound state, was detected. Moreover, the level of inhibition correlated with the levels of actinorhodin in the crude extracts as determined by the bioassay, e.g. the L646 extract was associated with the largest proportion of unbound DNA. This was the first evidence from Leeds that actinorhodin, or a derivative(s), may inhibit the DNA-binding activity of AtrA from *S. coelicolor*.

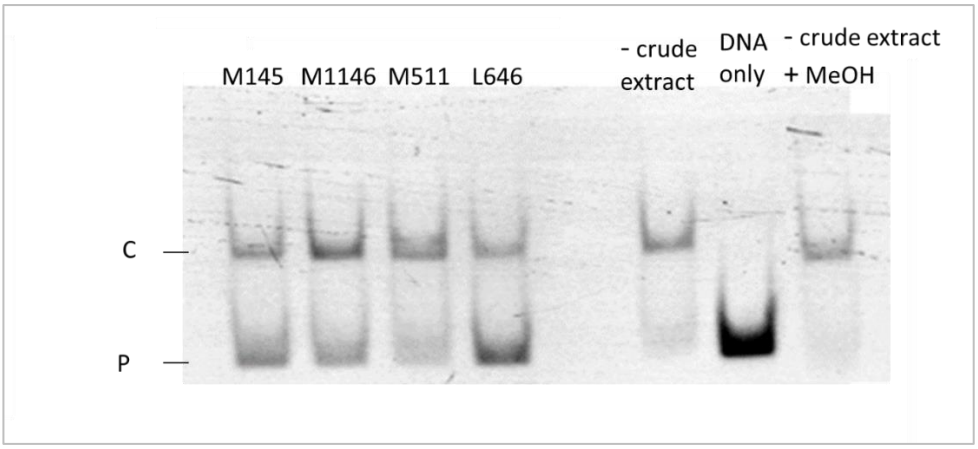

Figure 4.4. Assaying inhibition of the DNA-binding activity of AtrA. The source of the extracts are indicated at the top of the panel. The positions of unbound probe (P) and complexes (C) are identified on the left**.** With the exception of the controls, each reaction contained 5 nM of the substrate (*actII-ORF4* promoter), 62.5 nM of AtrA and 80 ng of crude extract in 0.4 μl of methanol. The components excluded from the control reactions are indicated. The reactions were run in a 4% (37.5:1) acrylamide: bis-acrylamide gel in 1 x TGED buffer for 40 min at 120 V. The gel was imaged using a Fujifilm FLA-5000 imaging analyser system.

4.3.3 Fractionation of crude extracts containing actinorhodin

To investigate further the link with actinorhodin, a crude extract from M145, which at the time was more plentiful, was fractionated using preparative reverse-phase chromatography (Figure 4.5). Sixteen fractions were collected along with the flow through (panel A). These were then dried, weighted and dissolved in methanol. Fractions 11 to 16 were pink in colour, which had been associated previously with crude extracts containing actinorhodin. It appears that the colour of actinorhodin is towards the red-end of the spectrum in methanol, as it is under acidic conditions. The litmus-like properties of actinorhodin are long established (Bystrykh *et al.*, 1996). The pink-pigmented fractions were assayed for activity that inhibits the growth of *S. aureus* and the binding of AtrA to DNA (panels B and C, respectively). The antibiotic activity was detected in the last four fractions, but concentrated in the last three (Fractions 14, 15 and 16). Inhibition of the DNA-binding activity of AtrA was detected in Fractions 12 to 16; however, the highest level of activity was associated with Fraction 16 followed by Fraction 13 and flow through and then Fractions 14 and 15. Fractions 12 to 15 aligned well with distinct peaks with retention of 5.8, 6.3, 6.8 and 7.3 min, respectively (panel A). That pigmentation was associated with multiple peaks was expected as *S. coelicolor* produces a series of closely-related actinorhodin compounds (Bystrykh *et al.*, 1996). These results suggest that whilst there is overlap between antibiotic and AtrA-inhibition activity there is not complete congruence.

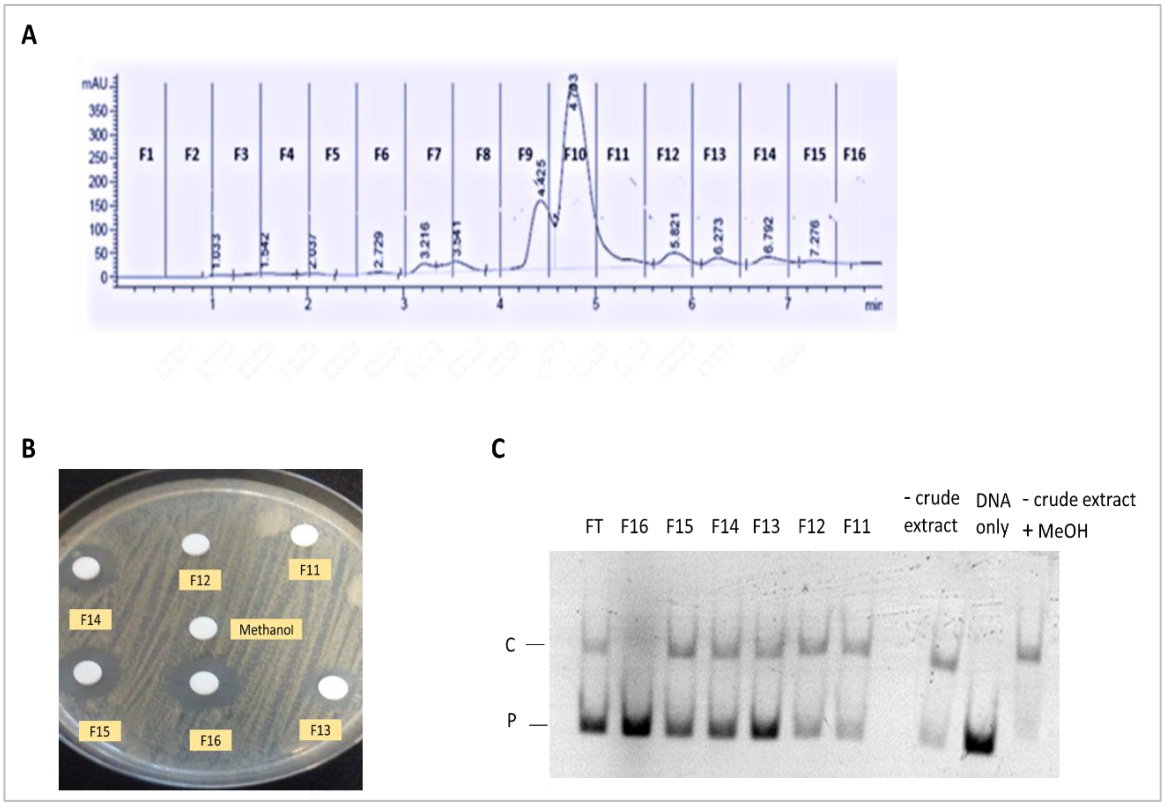

Figure 4.5. Fractionation of crude extract of *S. coelicolor* M145 and the assaying of inhibitory activities. Panel A shows chromatograms for the HPLC fractionation of crude extract of *S. coelicolor* M145. The figure represents a total ion chromatogram (TIC) for crude extract fractionations. Numbers on top of each peak refer to retention time (min) in each fraction. The y-axis displays the sum of the intensities of all ions observed at any point in time. **Panel B** shows the results of the assay for antimicrobial activity. The labelling identified the fractions (F) using the numbering in panel A. **Panel C** shows the results of assaying for activity that inhibits the binding of AtrA. The labelling of the fractions at the top of the panel follows that of panels A and B. FT indicates flow through. The positions of unbound probe (P) and complexes (C) are identified on the left. With the exception of the controls, each reaction contained 5 nM of the substrate (*actII*-ORF4 promoter), 62.5 nM of AtrA and 80 ng of a fraction. The components excluded from the control reactions are indicated. The reactions were run in a 4% (37.5:1) acrylamide: bis-acrylamide gel in 1 x TGED buffer for 40 min at 120 V. The gel was imaged using a Fujifilm FLA-5000 imaging analyser system.

4.3.3.1 Assaying the activities of γ-actinorhodin

In parallel with this study, colleagues in an adjoining group were investigating the antibacterial properties of actinorhodins with a view to evaluating their potential in antibacterial chemotherapy and had elected to work with γ-actinorhodin, the predominant secreted form, to avoid the potential for the analysis to be complicated by a mixture of compounds with different properties, at least potentially (Nass *et al.*, 2017). The identity and purity (>95%) of γ-actinorhodin in their preparation was confirmed by a combination of mass spectrometry, 1-D NMR, 2-D NMR, infrared spectroscopy and analytical HPLC

(Nass *et al.*, 2017). The ability of their preparation of γ-actinorhodin species to inhibit AtrA binding was assayed (Figure 4.6). At this stage in the analysis of actinorhodin, the binding of LacI to its cognate operator was included as a control. Preparatory work had established the concentration of LacI that produced a partial shift. The assays, which involved adding increasing concentrations of γ-actinorhodin to the binding reaction, revealed that at concentrations that inhibited the DNA-binding activity of AtrA (10 and 100μM, panel A), also inhibited the DNA-binding activity of LacI, which as indicated above is an unrelated transcription factor (panel B). Purified γ-actinorhodin was also able to inhibit the DNA-binding activities of *E. coli* TetR and *S. coelicolor* ActR (panels C and D, respectively). The latter is reported to be specifically regulated by metabolites from the actinorhodin biosynthetic pathway (Tahlan *et al.*, 2007). Interestingly, the level of inhibition of the DNA-binding activity of ActR was less than that of AtrA and LacI, but similar to that of TetR (as judged by the reduced proportion in the complex that is labelled). Inhibition of the DNA-binding activity of ActR and TetR was only clear at the highest concentration of γ-actinorhodin (100 μM, panels C and D). The faster migrating complex for TetR at the highest concentration of γ-actinorhodin was unexpected. Its possible identity is not obvious. Taken together, the above results suggest that γ-actinorhodin is a non-specific inhibitor of multiple transcription factors. It appears not to be specific regulator of ActR. The solvent in which the γ-actinorhodin was dissolved did not inhibit any of the four DNA-protein interactions.

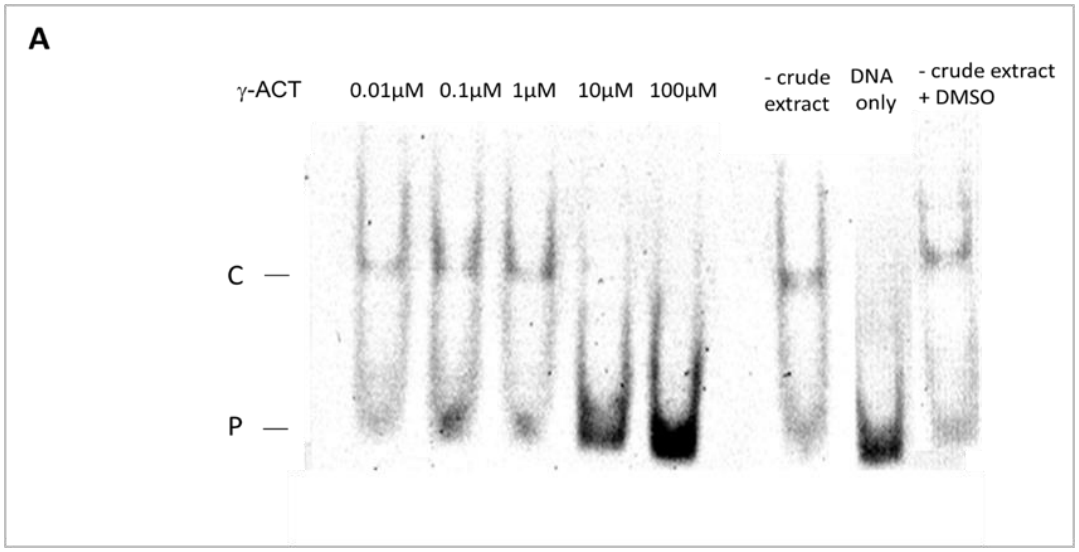

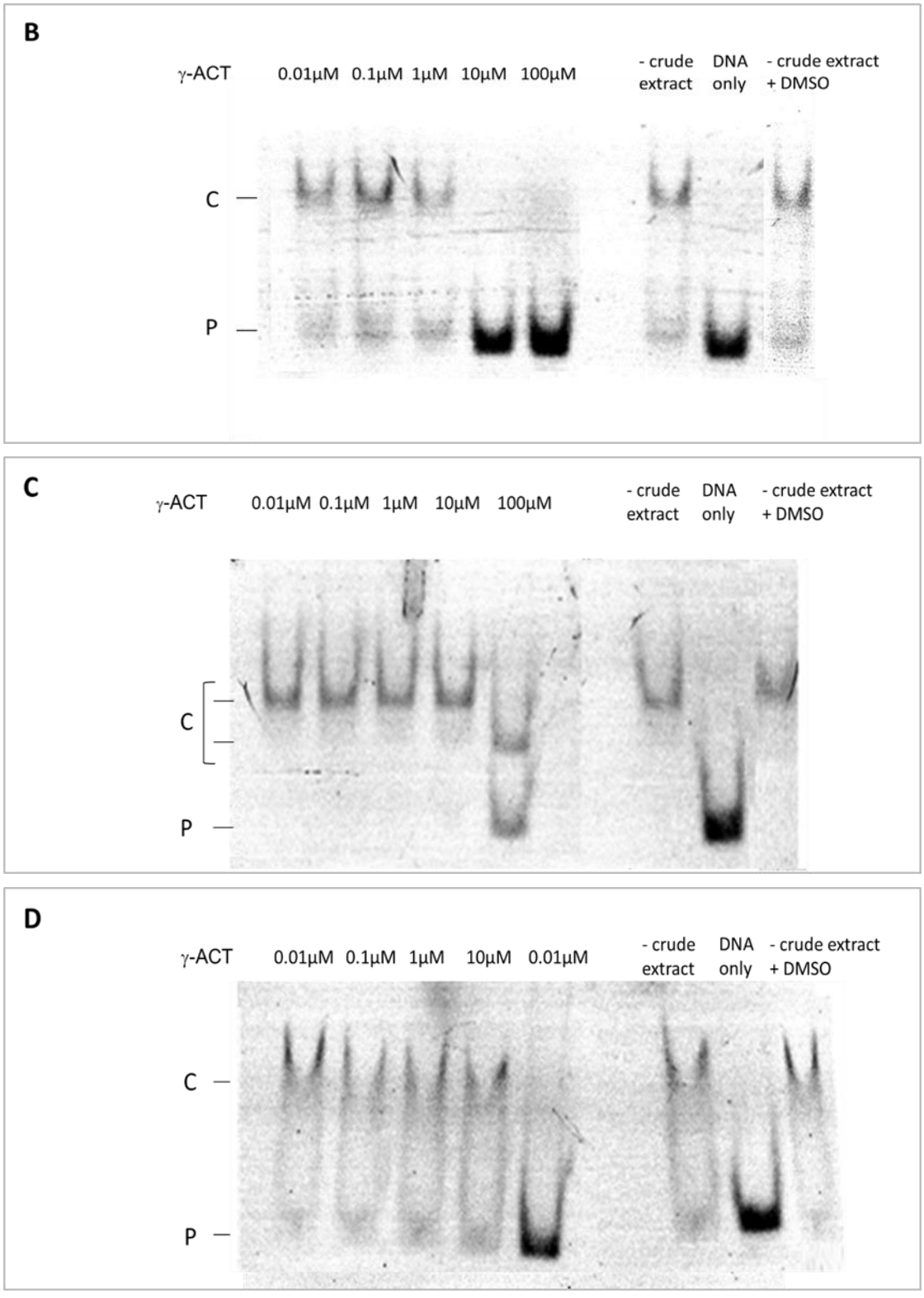

Figure 4.6. The effect of γ-actinorhodin on the DNA binding activities of transcription factors. **Panels A**, **B**, **C** and **D** represent the ability of γ-actinorhodin to inhibit the binding of AtrA to *actII*-ORF4 promoter, ActR to the promoter region of *actA* (Caballero *et al.*, 1991), which encodes the efflux pump for actinorhodin (Fernandez-Moreno *et al.*, 1991), the binding of *E.coli* TetR to the promoter region of *tetA* (Meier *et al.*, 1988), which encodes the efflux pump for tetracycline (Hillen & Berens, 1994) and the binding of *E.coli* LacI to the *lac* operator (Fuerst *et al.*, 1989), respectively. The

positions of unbound probe (P) and complexes (C) are identified on the left of each panel. With the exception of the controls, each reaction contained 5 nM of a specific substrate, 62.5 µM of the protein and γ-actinorhodin at a concentration indicated at the top of the panel. The components excluded from the control reactions are indicated. Conditions are as Figure 4.2.

4.3.3.1.1 The activity of γ-actinorhodin against alkaline phosphatase and lactate dehydrogenase

To investigate whether γ-actinorhodin inhibits DNA-protein interactions by somehow denaturing the protein component, different amounts of γ-actinorhodin were added to well established, time-course assays for alkaline phosphatase and lactate dehydrogenase. Comparison of the initial rates of the reactions did not provide any indication of concentration-dependent inhibition (Figure 4.7). A remaining possible was that γ-actinorhodin may interact directly with DNA. Polyketide-related compounds that interact with DNA have been descibed, e.g. daunorubicin and charteusin (Belloc *et al.*, 1992). The possible interaction of γ-actinorhodin with DNA was investigated using two assays: DNA sequestration and ethidium-bromide displacement (Banerjee et al., 2013). Ethidium bromide was used in the DNA sequestration assay, as the positive control.

In the first of the two assays, the rate at which ethidium bromide was able to diffuse through a dialysis membrane into fresh buffer was measured. Ethidium bromide that diffused into the fresh buffer was detected by measuring absorbance at 500 nM. Preparatory analysis had established that 500 nM was the λ_{Max} for ethidium bromide in the dialysis buffer (10% DMSO in 1 X TE buffer). This value agrees well with those that have been published (Martz, 1971). The rate of dialysis of ethidium bromide was measured in the presence and absence of sufficient DNA to present a five-fold excess of base-pairs (Figure 4.8). In the presence of DNA, the rate of dialysis of ethidium bromide was reduced by ~7-fold, consistent with its well-established ability to intercalate into DNA, which was unable to pass through the dialysis membrane. When the assay was repeated for γ-actinorhodin, it was found that γ-actinorhodin on its own diffuses slowly possibly because it interacts with the membrane. In the presence of DNA, no significant difference in the rate of diffusion of γ-actinorhodin was observed, but the sensitivity of the assay was diminished by the slow rate of diffusion.

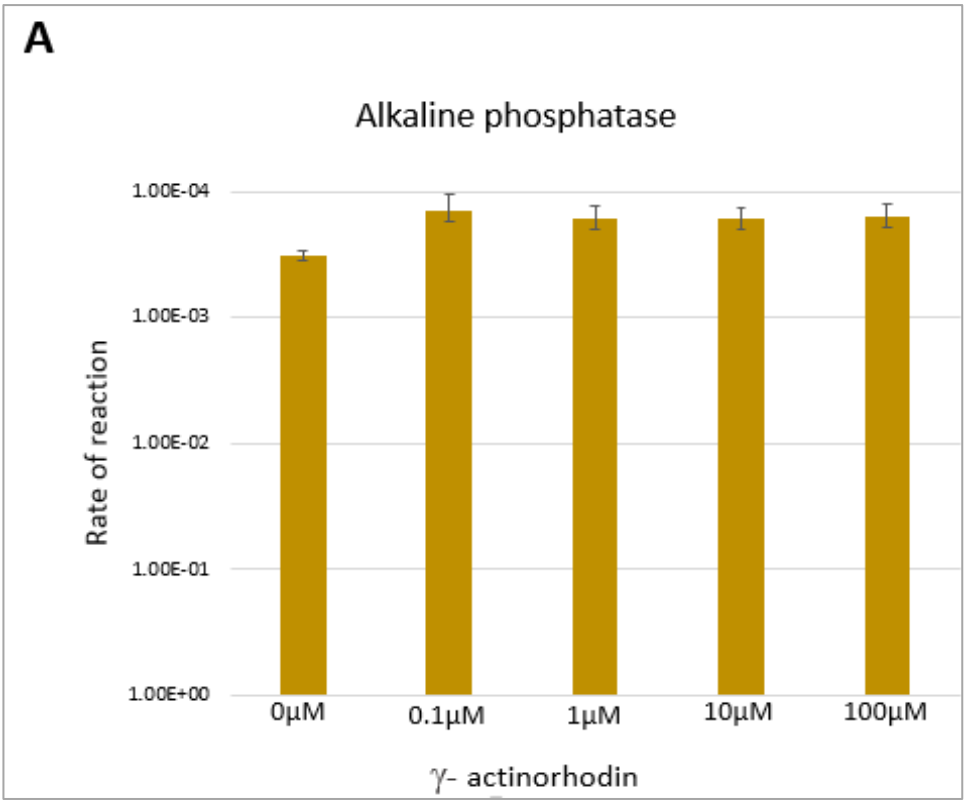

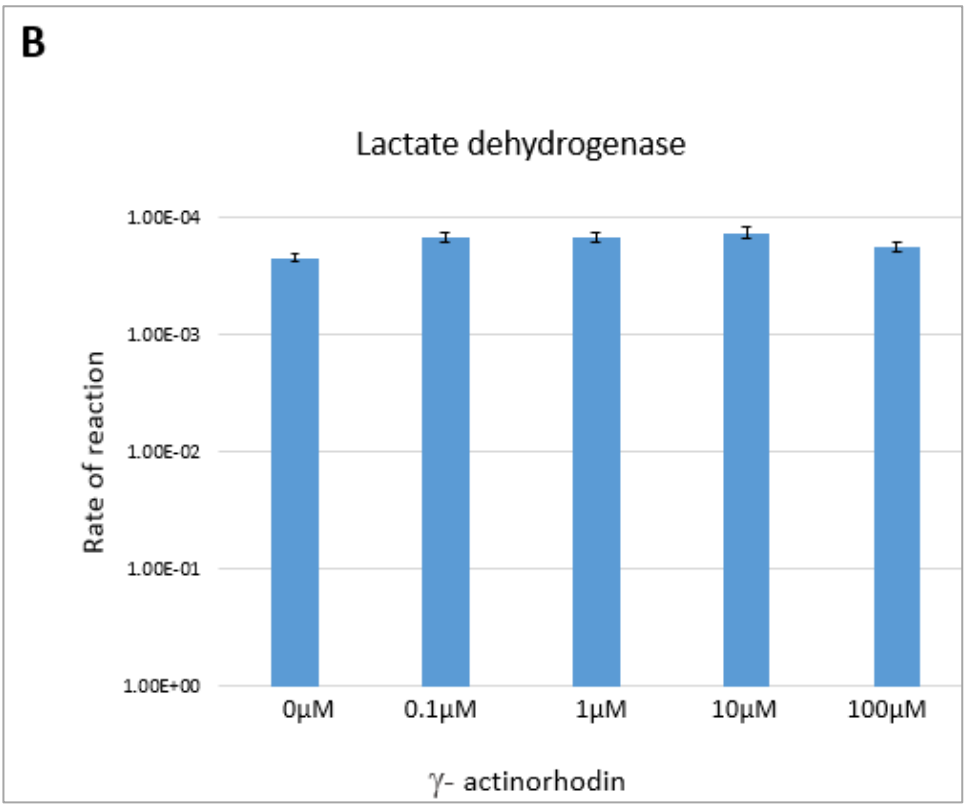

Figure 4.7. **The effect of γ-actinorhodin on enzymatic activities. Panel A** and **B** are histograms showing the initial rates of the reactions for alkaline phosphatase (54.6 nM) and lactate dehydrogenase (1.4 nM), respectively**.** The corresponding substrates were p-nitrophenyl phosphate and pyruvate, respectively**.** The concentrations of γ-actinorhodin in the reactions are indicated at the bottom of the vertical bars. For further

details of the assay conditions, see Materials and Methods, Section 2.10. The Y axis has a log scale. The rates of the reactions are in arbitrary units.

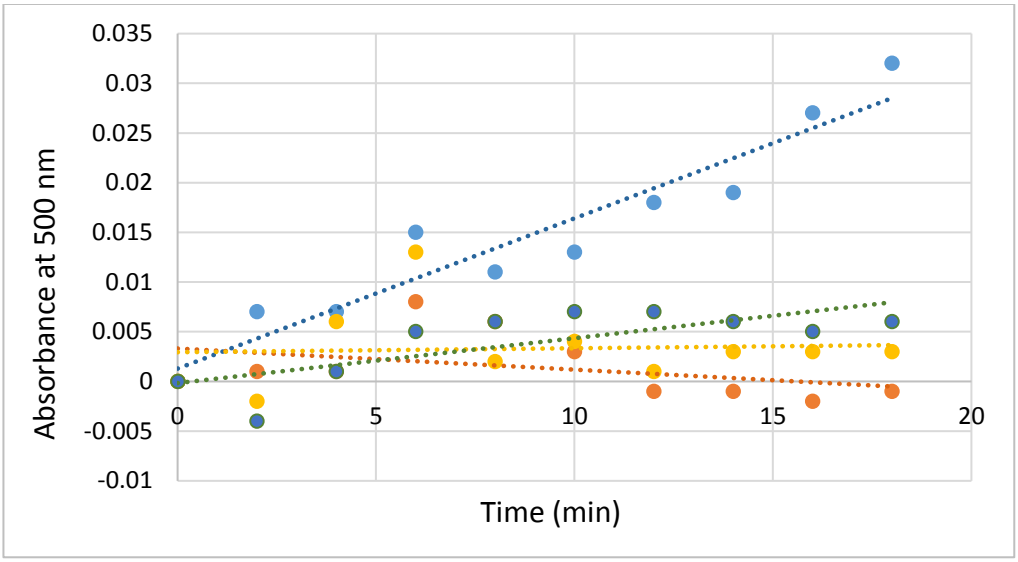

Figure 4.8. Assaying rates of dialysis in the presence and absence of DNA. The absorbance of the diffused ethidium bromide and γ-actinorhodin through the dialysis membrane was measured every 2 minutes in the presence and absence of a five-fold excess of base-pairs of DNA, individually. Blue circles represent the absorbance of the diffused ethidium bromide only (100 μM). Green circles represent the absorbance of diffused of ethidium bromide after adding 500 μM of base-pairs (15 mM base-pairs salmon sperm DNA (Invitrogen)). Orange circles represent the absorbance of the diffused γ-actinorhodin. Yellow circles represent the absorbance of the diffused γ-actinorhodin in the presence of 500 μM base-pairs. The dialysis buffer contained 10% DMSO in 1 x TE buffer (pH 8.0).

In the second of the assays, the fluorescence of ethidium bromide in the presence of plasmid DNA and increasing amounts of γ-actinorhodin was measured (Figure 4.9). The fluorescence of ethidium bromide is substantial higher when intercalated in the hydrophobic environment of stacked base-pairs as water is an effective quencher of fluorescence from ethidium bromide (Heller & Greenstock, 1994, Olmsted & Kearns, 1977). Prior to assaying the effect of adding increasing amount of γ-actinorhodin, the fluorescence of a fixed concentration of ethidium bromide in the absence and presence of increasing amounts of plasmid DNA was measured (panel A). As expected, the fluorescence of ethidium bromide increased in the presence of plasmid DNA. In a five-fold excess (base pairs vs ethidium bromide), the fluorescence was 2-fold higher than in the absence of plasmid, i.e. the majority of the fluorescence was attributable to intercalated ethidium bromide. The fluorescence began to plateau over the concentration range used, consistent with the system becoming saturated (i.e. the amount of ethidium

bromide that could be intercalated was reaching the maximum). Reactions containing a five-fold excess of DNA (base-pairs) were then used to determine the effects of γ-actinorhodin (panel B). A higher fold excess would have reduced the level of potential competition between ethidium bromide and γ-actinorhodin by presenting additional sites for intercalation. The fluorescent of ethidium bromide decreased with the addition of increasing concentrations of γ-actinorhodin (panel B). This result is consistent with γ-actinorhodin interacting with DNA and competing with ethidium bromide. Encouraged by this result, an attempt was made to study the potential interaction of γ-actinorhodin with DNA using NMR in collaboration with the NMR Laboratory at Leeds (https://www.astbury.leeds.ac.uk/ABSL/NMR/people/people.php). Whilst spectra were recorded for the DNA substrate (1D and 2D NOESY and TOCSY), and changes were observed with the titration of γ-actinorhodin, the results were inconclusive as the possibility that the changes were due to DMSO was not eliminated (Arnout Kalverda, pers. comm). The removal of DMSO by dialysis resulted in the precipitation of the majority of the γ-actinorhodin (Arnout Kalverda, pers. comm).

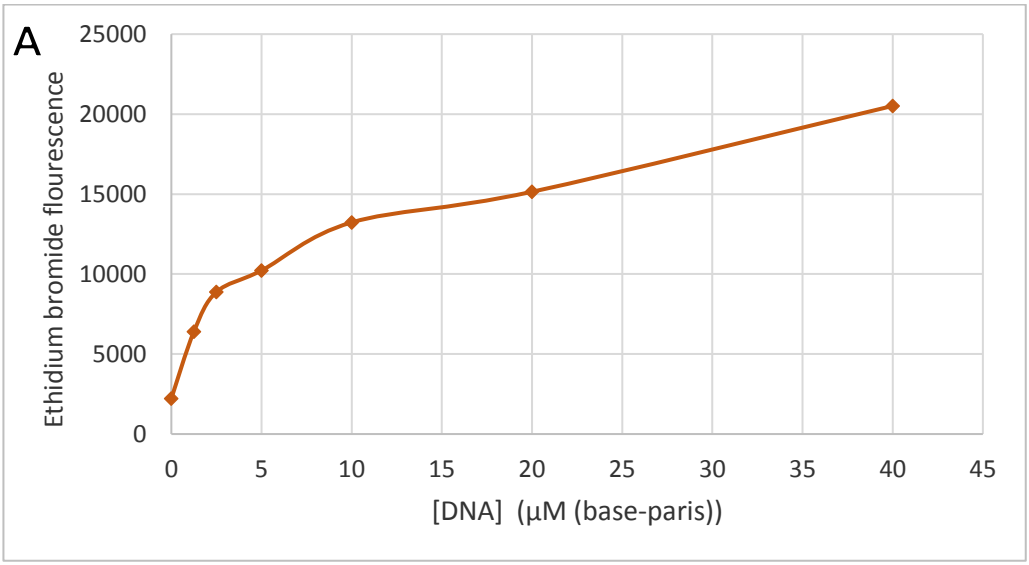

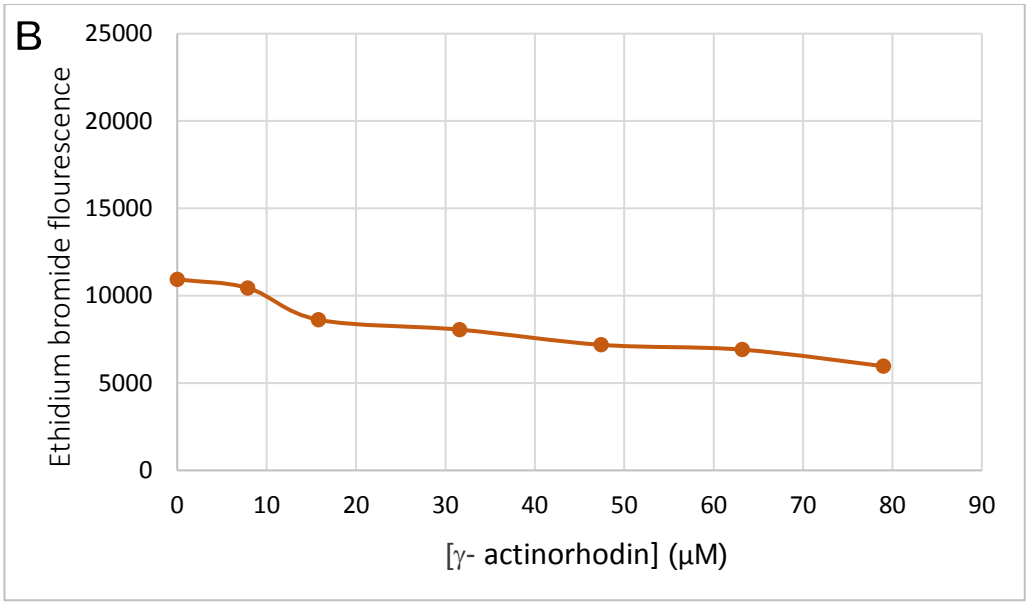

Figure 4.9. Assaying the fluorescence of DNA-associated ethidium bromide in the presence of increasing amounts of γ-actinorhodin. **Panel A** represents the fluorescence of ethidium bromide (1μM) in the presence of the increasing amount of DNA (base-pairs). **Panel B** shows the fluorescence of ethidium bromide with 5μM (base-pairs) of DNA and increasing concentrations of γ-actinorhodin. The assay buffer contained 10% (v/v) DMSO and 10mM Tris-HCL (pH 8.0).

4.3.3.2 Further analysis of the crude extract from M1146

Having established that γ-actinorhodin (Figure 4.6) is not specific for AtrA, analysis was continued of the extract from strain M1146 (Figure 4.10), which lacks the entire gene cluster for actinorhodin plus those of undecylprodigiosin, the calcium-dependent antibiotic and the coelimycin (Gomez-Escribano & Bibb, 2011). The concentration of crude extract was increased and LacI, ActR and TetR were included as controls. Whilst the proportion of the unbound DNA did appear to increase slightly in a concentration dependent manner for AtrA (panel A), this appeared to be also true for LacI (Panel B), TetR (Panel C) and ActR (Panel D). Thus, the potential inhibitory activity was deemed not to be specific, and the crude extract was not analysed further. At the highest concentration of extract, there was some evidence for a TetR-derived complex migrating faster that the complex identified in the absence of extract, which is consistent with the earlier result (Figure 4.6, panel C).

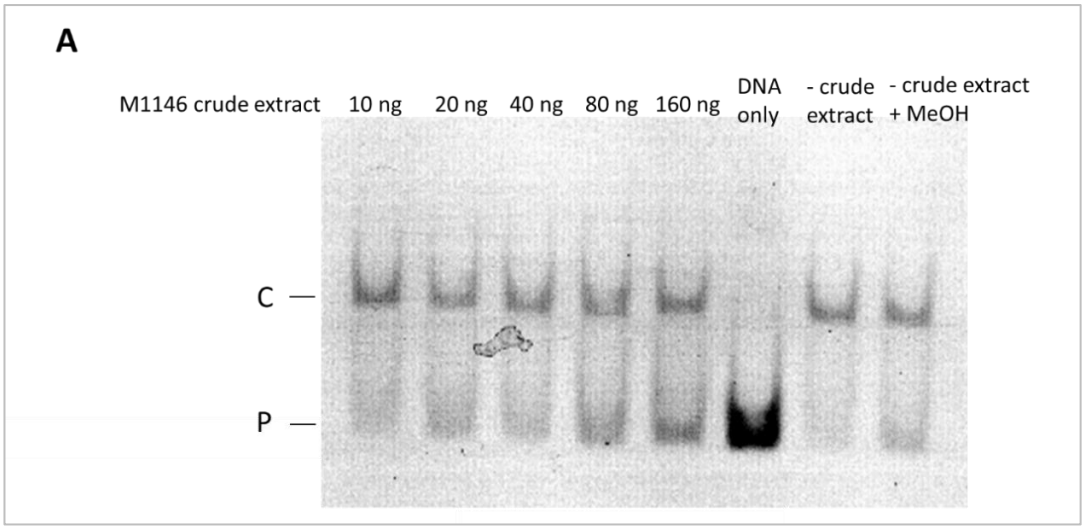
A
M1146 crude extract
10 ng
20 ng
40 ng
80 ng
160 ng
DNA only
- crude extract
- crude extract + MeOH
C
P

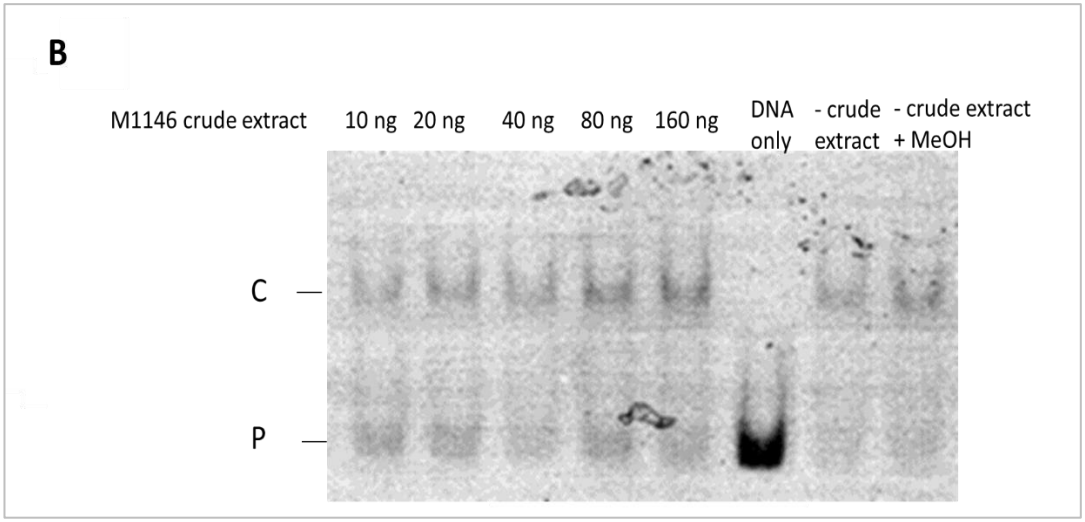
B
M1146 crude extract
10 ng
20 ng
40 ng
80 ng
160 ng
DNA only
- crude extract
- crude extract + MeOH
C
P

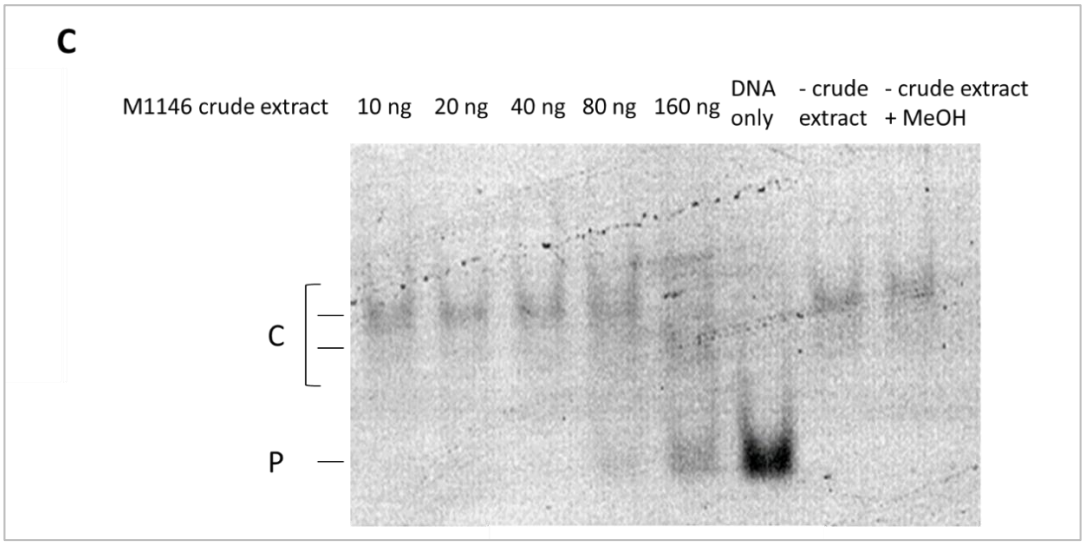
C
M1146 crude extract
10 ng
20 ng
40 ng
80 ng
160 ng
DNA only
- crude extract
- crude extract + MeOH
C
P

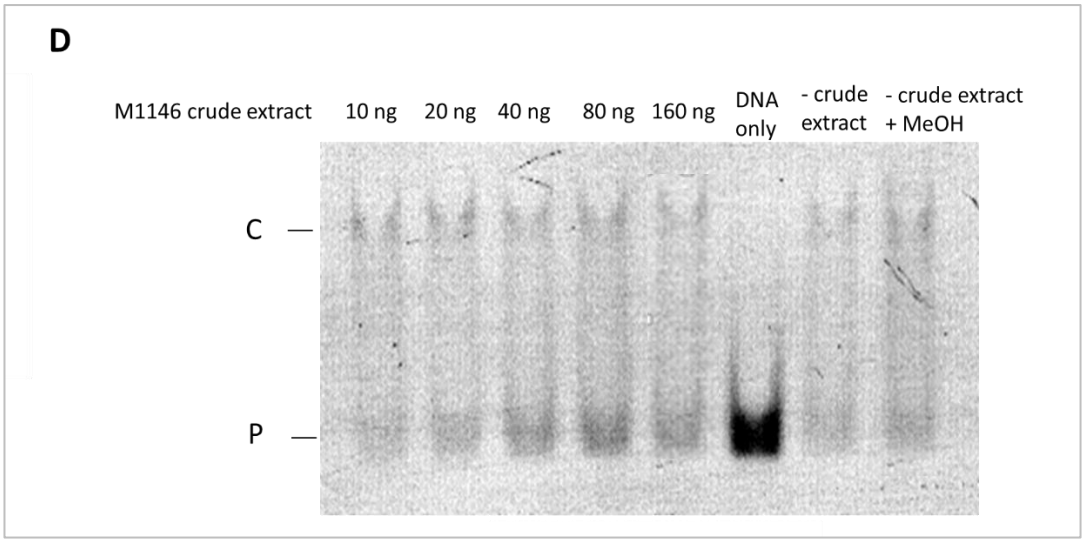

Figure 4.10. The effect of crude extract from M1146 on the binding activities of TetR family regulator and LacI. Panels A, B, C and D represent the interaction of M1146 crude extract with AtrA, LacI, TetR and ActR, respectively. The labelling on the left of the panel identifies unbound and bound DNA. With the exception of the controls, each reaction contained 5 nM of a specific substrate, 62.5 µM of the protein and M1146 crude extract at a concentration as indicated at the top of the panel. The components excluded from the control reactions are indicated. Conditions are as Figure 4.2.

Whilst conducting gel-shift assays to screen for inhibitors of the DNA-binding activity of AtrA, the binding of AtrA to Motif 2 were analysed. EMSAs were used to quantify AtrA binding to sites contain Motif2 (Figure 4.11). The incubation of AtrA with double- or single-stranded *lac*O_1, which lacks sequence recognisably similar to Motif1 or Motif2, produced a shift when the concentration of AtrA reached 500 nM (lane 8, panels A and B). The resulting complex(es) did not appear to enter the well. In contrast, incubation of AtrA with a double-stranded substrate containing an extended Motif1 derived by SELEX (see Chapter 3) produced a distinct complex at 7 nM, the lowest possible concentration that could shift a significant proportion of the 5 nM substrate (lane 2, panel C). Incubation of AtrA with one half of the extended Motif1 did not produce a significant shift until the AtrA concentration reached 500 nM, the concentration at which non-sequence-specific binding is observed (lane 8, panel D). This is consistent with the notion that high-affinity binding of AtrA requires the simultaneous recognition of both halves of a Motif1 site by what is likely a head-to-head dimer of AtrA (see Discussion, Chapter 3). The substrate was designed such that sequence-specific recognition of the half-site (which was placed at the centre of the substrate) could not be accompanied by non-sequence-specific recognition via the other head of the dimer as the length of the substrate was designed to be insufficient. Incubation of a Motif 2-containing site associated with peak 84 (#33),

and two associated with peak 95 (#42 and #43) produced for each a distinct complex with 250 nM AtrA (lane 7, panels E, F and G), a concentration just below the point at which AtrA binds non-specifically (lane 8, panels A and B).

Incubation with sites containing multiple copies of Motif 2 resulted in shifting occurring at lower concentrations of AtrA. A site associated with peak 78, which has three copies of Motif2 (#118, #119 and #275), started to shift at 125 nM (lane 6, panel H), whilst a site associated with peak 170, which has seven copies of Motif2 (#240 to #246), appeared to start to shift at 62.5 nM (lane 5, panel I). The apparent correlation between the number of copies of Motif 2 in a site and the affinity of the interaction with AtrA suggest cooperative binding. It is possible that dimers of AtrA bound side by side can interact, thereby stabilising their association with DNA. An amplicon containing the promoter region of *actII*-ORF4, which contains two well-separated Motif 1 sites and was the first target to be identified for AtrA (Uguru *et al.*, 2005), was predominantly bound at the first site at 31.25 nM, with evidence of binding to both (slower migration of upper boundary of band) at 62.5 nM (lanes 4 and 5, respectively, panel J). The formation of a second complex at 62.5 nM was confirmed by repeating the assay with a 4% polyacrylamide gel (data not shown). The affinity of AtrA for the first site it binds in the *actII*-ORF4 promoter is within the middle of the range measured for numerous Motif1 sites (McDowall, pers. comm.). Nevertheless, it is higher than all the sites analysed here than the three sites that contain single copy of Motif 2. Sites containing multiple copies of juxtapositioned Motif2 are the exception. The above shows that AtrA can bind sites with Motif 2, but in general the affinities of these interactions are lower than those for sites with Motif 1.

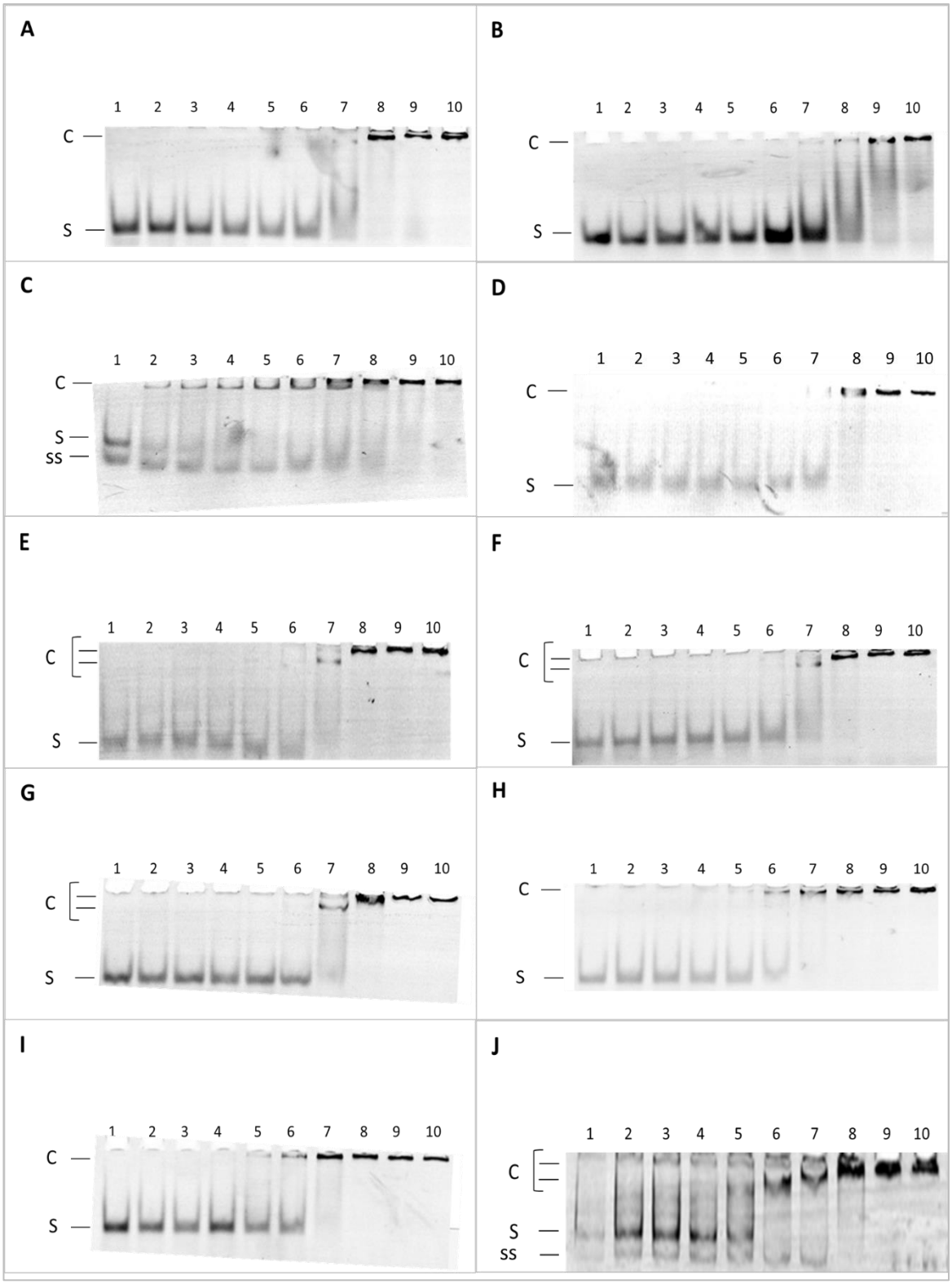

Figure 4.11. Experimental analysis of AtrA binding to sites containing Motif 2. Panel A and B contain negative controls: double-stranded and single-stranded *lac*O_1. Panel C contains a positive control: a sequence derived by SELEX that contains Motif 1. Panel D contains a half-site of the sequence derived by SELEX. Panel E contains a site with a single copy of Motif2 from peak 84, whilst panels F and G contain two similar sites from peak 95. Panels H and I contain sites with multiple copies of Motif 2 from peaks 78 and 170, respectively. Panel K contains the promoter region of *actII-ORF4*. Labelling on

the left of each panel indicates the position of substrate (S), which is double stranded except in the case of one of the *lac*O_1 controls, and complex resolved within the gel (C). Any single-stranded DNA resulting from incomplete hybridisation during the production of the substrate is indicated (ss). All of the substrates were labelled with Fluorescein and used at a concentration of 5 nM. Lanes labelled 1 to 13 contain 0, 7.5, 15.6, 32.1, 62.5, 125, 250, 500, 1000, 2000 nM AtrA. The reactions were run in a 10% (37.5:1) acrylamide: *bis*-acrylamide gel in 1 x TGED buffer for 40 min at 120 V. The gel was imaged using Fujifilm FLA-5000 imaging analyser system. These assays in this figure were carried out by a master student, Nicola Mtetwa, under my supervision.

4.4 Discussion

Work described in this chapter has shown that as reported previously (Hasan, 2015) the DNA-binding activity of AtrA is inhibited by preparations of actinorhodin (Figures 4.6, Panel A). However, the inhibition is not specific to AtrA (Figures 4.6, Panel B, Panel C and panel D) and might be mediated by the intercalation of actinorhodin into DNA (Figures 4.9, Panel B). It is well established that the intercalation of small molecules into DNA can hinder the binding of many different classes of DNA-binding protein (Bhaduri *et al.*, 2018, Sheng *et al.*, 2013). The intercalation of small molecules between stacked bases perturbs the structure and mechanical properties of DNA (Lerman, 1961, Neto & Lapis, 2009). To accommodate such intercalators, the DNA unwinds slightly resulting in lengthening of linear DNA. Intercalators typically, but not necessarily, have planar polyaromatic rings and cationic (positively charged) groups (Sheng et al., 2013; Snyder et al., 2005). Polyaromatic rings but not cationic groups are found in actinorhodin. The main driving force for intercalation is thought to be π interactions, with significant contributions from van der Waals, which is an electrical interaction (attraction) between molecules that are very close to each other (Tkatchenko & Scheffler, 2009) and hydrophobic interactions (Chaires, 1997, Gago, 1998), which is the attraction of hydrophobic molecules in water to minimize their contact with water molecules (Meyer *et al.*, 2006). It would be interesting to predict the energetics of binding of a γ-actinorhodin-DNA complex using specialised docking tools such as Intercalate (Soni *et al.*, 2017).

To investigate further the mode of inhibition of γ-actinorhodin, the DNA Intercalation assay is suggested (Mitchenall *et al.*, 2018). As already mentioned, compounds that are able to intercalate into DNA (or bind in the groove) can lead to unwinding of the DNA. However, if the substrate is circular and covalently closed the linking number (i.e. the number of times a strand of DNA winds around the axis of the double helix) is fixed. Thus, intercalation into covalently closed circular DNA substrates causes coiling of the axis around which the DNA binds (i.e. supercoiling). If such supercoiled DNA is incubated with a topoisomerase the supercoiling is removed by reducing the linking number. On removal of the intercalator (e.g. by butanol extraction), the DNA will rewind, which will cause supercoiling, but opposite to that caused by the original intercalation. This “negative” supercoiling can be detected by gel electrophoresis as supercoiled plasmids run faster through agarose (De Mattos *et al.*, 2004). A positive outcome requires that the topoisomerase is not inhibited by the intercalator.

Several secondary metabolites from *Streptomyces* species have been reported to intercalate into DNA (Tenconi *et al.*, 2018). They include actinomycins and anthracyclines (Sobell, 1985). Much of the interest in intercalating agents stems from their potential as leads for the development of new anti-cancer drugs (Wang *et al.*, 2016b). Actinomycin D (dactinomycin) is already used clinically to treat a range of cancers (Karimi Goftar *et al.*, 2014, Koba & Konopa, 2005). Like Actinomycin D, γ-actinorhodin lacks a positive charge. It has been suggested for Actinomycin D that a high dipole moment (a large difference in the distribution of positive and negative charges), as a result of a non-symmetrical distribution of polar substituents, is compensatory (Gallego et al, 1997). Polar carboxyl and hydroxyl groups are present in γ-actinorhodin (Figure 4.12). It would be interesting to investigate if γ-actinorhodin has anti-cancer in addition to its antibacterial activity. Studies of the antibacterial activity of actinorhodin did not identify DNA as the target (Nass *et al.*, 2017).

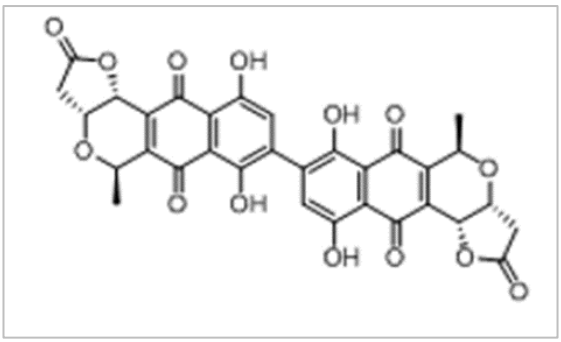

Figure 4.12. Chemical structure of γ-actinorhodin. Taken from (Nass *et al.*, 2017)**.**

The actinorhodin cluster in *S. coelicolor* contains an efflux pump that is required for the export of γ-actinorhodin. This is consistent with the notion that γ-actinorhodin thwarts the growth of competing micro-organisms, a function of external to the producer. However, it is speculated that the production of γ-actinorhodin, and possibly all DNA intercalators, will dampen transcription and replication within the vegetative mycelium and that this might have functional significance in the shifting of activity and resources to the aerial hyphae for the production of spores. To our knowledge such a function has not been proposed previously for DNA intercalators. However, there is precedent for the production of quiescent cellular states (Rittershaus *et al.*, 2013). Quiescence has been reported to be important in the production and maintenance of biofilms and subpopulations of growing cells (Archer *et al.*, 2011, Rittershaus *et al.*, 2013). The latter is believed to be part of a "gaming" strategy to ensure that at least some cells within a population are prepared for a downturn in the growth conditions (Davis & Isberg, 2016, Vulin *et al.*, 2018). Quiescence has been associated with persister cells that survive

antibiotic treatment (Rittershaus *et al.*, 2013). The best-described mediators of quiescence are toxin-antitoxin systems (Amitai *et al.*, 2009, Gerdes & Maisonneuve, 2012, Yamaguchi & Inouye, 2011). It would be interesting to measure and compare the global levels of transcription in the presence and absence of actinorhodin production. Several methods for measuring global transcription have been described (Uddin *et al.*, 1984) One of the most recent is compatible with confocal microscope and can be used to provide spatial and well as quantitative information (Jao & Salic, 2008).

The possibility that actinorhodin may function as a non-specific inhibitor of DNA-binding activity was not considered by a previous study (Li *et al.*, 2015b). Whilst it was shown that a preparation of actinorhodin could inhibit the DNA-binding activity of AtrA from *S. globisporus*, TetR and ActR controls used to show that inhibition by heptaene was specific to AtrA-gl were not included in the study of the inhibitory effects of actinorhodin (Li *et al.*, 2015b). Therefore, the results of DNA-binding assays presented here for AtrA from *S. coelicolor* are not inconsistent with those published for AtrA-gl. The study of AtrA-gl also showed by SPR that a component of a preparation of actinorhodin could bind to immobilised AtrA-gl. It was implied that this result supported specific inhibition of AtrA-gl by actinorhodin. However, the identity of the ligand that bound AtrA-gl was not confirmed neither was the specificity of the ligand for the AtrA-gl. Thus, there is no result from the previous analysis of AtrA-gl that contradicts results reported herein. The possibility that heptaene regulates the activity of AtrA from *S. coelicolor* should be investigated given that it is now the only link to specific regulation of AtrA.

A preparation of actinorhodin has also been studied in relation of ActR, the TetR-family that represses production of ActA, an efflux pump within the BGC for actinorhodin (Tahlan *et al.*, 2007). As for the study of AtrA-gl, extracts of actinorhodin were shown to inhibit the DNA-binding activity of ActR; however, controls to show that inhibition was specific to ActR were not included (Tahlan *et al.*, 2007). However, subsequent studies, revealed the crystal structures bound to both actinorhodin and (*S*)-DNPA (4-dihydro-9-hydroxy-1-methyl-10-oxo-3-H-naphtho-[2,3-c]-pyran-3-(S)-acetic acid), a tricyclic biosynthetic precursors (Willems *et al.*, 2008). The latter was found to inhibit DNA-binding by ActR at lower concentrations than actinorhodin (Tahlan *et al.*, 2007). This was interpreted as evidence that intermediates may serve as the most biologically significant triggers of ActA production, a conclusion supported by the study of further ligands (Tahlan *et al.*, 2008). This and the proposed DNA-intercalating properties of γ-actinorhodin are not mutually exclusive. On reflection, it would have been interesting to have included ActR (as well as TetR and LacI) when screening fractions of the crude extract of actinorhodin (Figure 4.5). Their inclusion may allow the identification of

fractions specific for ActR. It would also have been interesting to have determined the elution time of purified γ-actinorhodin. It is formally possible that the fraction of the crude extract that inhibited the binding of AtrA is not γ-actinorhodin, i.e. an intermediate may also be able to intercalate DNA.

Chapter 5 Phenotypic characterization of a selection of AtrA target genes

5.1 Abstract

A high-throughput, transposon-based mutagenesis process was previously developed to allow functional characterisation of the *S. coelicolor* genome, thereby allowing more light to be shed on the intricate and complex biology and chemistry of a model for a commercially and clinically valuable group of bacteria. This process was applied here to provide a panel of mutants to determine better the role of members of the AtrA regulon with known or inferred functions. Unfortunately, the transposon was not inserted into the expected insertion sites so not all the AtrA target genes were disrupted. The disruption of one gene from central metabolism was found to accelerate the production of actinorhodin and morphological development. This finding supports a model in which AtrA influences secondary metabolism beyond the regulation of targets within biosynthetic gene clusters. The next steps required in the characterisation of the mutagenized genes are described.

5.2 Introduction

Work described earlier in this thesis revealed for the first time that AtrA has a role in regulating and likely coordinating the expression of genes encoding important functions associated with sugar and amino acid uptake and utilisation, peptidoglycan biosynthesis, morphological development, and secondary metabolism (Chapter 3). However, the regulon of AtrA also extends to genes of unknown function and our understanding of the regulon's attributes could be refined where the specificity of some of the member genes is currently not known, e.g. the specific sugar(s) imported by the products of genes annotated as encoding components of a sugar transporter, or the specific role of gene annotated as encoding a membrane protein.

Approaches to establish the functions and interactions of genes and their products are increasingly genome wide and where they are genome wide are described as functional genomics (Gray *et al.*, 2015). This growing, but already well-established field incorporates information from the gene-by-gene approaches of classic molecular biology with high-throughput mutagenesis studies and the measurement and comparison of the transcriptome, proteome and interactomes under different stages of development, conditions of growth and in different genetic backgrounds. The methodologies for functional genomics are constantly evolving and tend to be universal, i.e. not specific to

an individual organism or group (Segata & Huttenhower, 2011). The area where there is arguable most specialisation is the systematic mutagenesis of the genome; this can vary significantly between different organism(s) of study. In recent years, CRISPR/Cas9 has been used widely increasingly (Zhang *et al.*, 2018). Prior to the development of CRISPR/Cas9, a comprehensive platform was established for the systematic mutagenesis of the *S. coelicolor* genome (Bishop *et al.*, 2004). The ordered cosmid library that formed the basis of the sequencing of the *S. coelicolor* genome has been mutagenised *in vitro* using transposons (Tn*5062*) and returned to *E. coli* where the sites of transposon insertions were identified and the corresponding clones stored in a central repository and catalogued in StrepDB (http://strepdb.streptomyces.org.uk). These clones can be ordered and transferred by intergeneric conjugation into *Streptomyces*, where the appropriate gene replacement can be selected. This approach has been reported to yield gene replacements in upward of 90% of cases (Bishop *et al.*, 2004) and has been used widely in several genetic backgrounds (Muñoz-López & García-Pérez, 2010). Although CRISPR/Cas9-based editing is being successfully applied to the *Streptomyces* (Cobb et al., 2015) initial studies not described here indicated it required significant optimisation; therefore, progress in establishing and characterising a library of mutants of the AtrA regulon is described here using transposon-disrupted cosmids. The REDIRECT system, which allows Recombineering (recombination-mediated genetic engineering), was also considered (Munnoch *et al.*, 2016). Although this system can introduce in-frame deletion with only small “scars” (i.e. heterologous DNA), which should avoid the risk of mutations being “polar” (*i.e.* affecting the expression of downstream genes, often those that are co-transcribed; (Zipser, 1969)), it would have required greater resource and time to produce mutants. With the transposon-approach the mutant constructs have already been generated.

5.3 Result

5.3.1 Analysis of the mutant phenotypes and confirmation of the disruption of the genes

The genes selected for mutagenesis are listed alongside the corresponding transposon-disrupted cosmid clones (Table 5.1). For further details of the functions of these genes, see Table 3.1. The process for the generation of gene replacements is shown schematically (Figure 5.1). Briefly, the corresponding transposon-disrupted cosmids (based on pWEB a derivative of SuperCOS-1) were first transferred to *E. coli* ET12567 by triparental mating. In each mating, the parental strains were JM109 (Yanisch-Perron *et al.*, 1985) containing the transposon-disrupted cosmid, TOP10 (Invitrogen) containing the driver plasmid pR9604 (Jones *et al.*, 2013), which mediates the intergeneric conjugation, and ET12567 (MacNeil *et al.*, 1992), the planned recipient of the cosmid and driver plasmid. The use of a methylation-deficient *E. coli* host such as ET12567 in intergeneric conjugation circumvents the potent methyl-specific restriction system of *S. coelicolor* and other species (MacNeil *et al.*, 1992). The desired progeny of the triparental mating were selected using chloramphenicol, which specifically selects ET12567, apramycin, which specifically selects the transposon insertion and carbenicillin, which selects pR9604. However, the carbenicillin selection was not unique to pR9604 as carbenicillin resistance is also conferred by the cosmid. Both JM109 contain transposon-disrupted cosmid and TOP10 containing pR9604 grew on plates containing carbenicillin (data not shown). Despite the carbenicillin selection not be exclusive to pR9604, ET12567 strains were selected that could transfer transposon-disrupted cosmid into *S. coelicolor*.

Gene	Name of cosmid carrying Tn*5062* insertion
SCO0072	J11.1.B08_J11-1_062_2007-04-23.seq
SCO0091*	J11.1.D01_J11-1_009_2007-04-23.seq
SCO0481	2B02.1.D09_2BO2-1rpt-240409_073_2009-04-24.seq
SCO1390	1A8A.2.E09
SCO1391	1A8A.1.A01
SCO1842	SCI8.2.D12_04091007HG.seq
SCO1861	I39.2.F06
SCO1862	I39.2.D04
SCO2191*	5F7.1.D05_SF-5F7-1_041_2007-02-22.seq

SCO2287	C30.1.B06_SF-C30-1_046_2006-11-21.seq
SCO2602	SCC88.1.G04_01121319E8.seq
SCO2631	SC8E4A.2.C11_04032106XF.seq
SCO3305	E68.1.D11_E68-1_089_2007-04-23.seq
SCO4070	D25.2.H07
SCO4295	D95A.2.C03
SCO5529	1C2.2.E04
SCO5856	9B10.1.D12_9B10_090_2008-08-07.seq
SCO6059	SC9B1.2.G04_04022115N8.seq
SCO6060	SC9B1.1.C04_04021916LX.seq
SCO6084	7F04.1.a09.EZR1.seq
SCO6257	AH10.2.D11_AH10-2_089_2008-08-07.seq
SCO6258	AH10.2.C06_AH10-2_044_2008-08-07.seq
SCO6259	AH10.1.D07_AH10-1_057_2008-08-07.seq
SCO6515	SC1E6.2.G07_0404280022.seq
SCO6516	SC1E6.2.H12_0404280843.seq
SCO7517	4C01.2.f08.EZR1.seq
SCO7595	7H9.2.A03
SCO7596	7H9.2.D07

Table 5.1: Cosmids library used in transposon mutagenesis. Asterisks indicate transposon insertion sites are outside the protein-coding region.

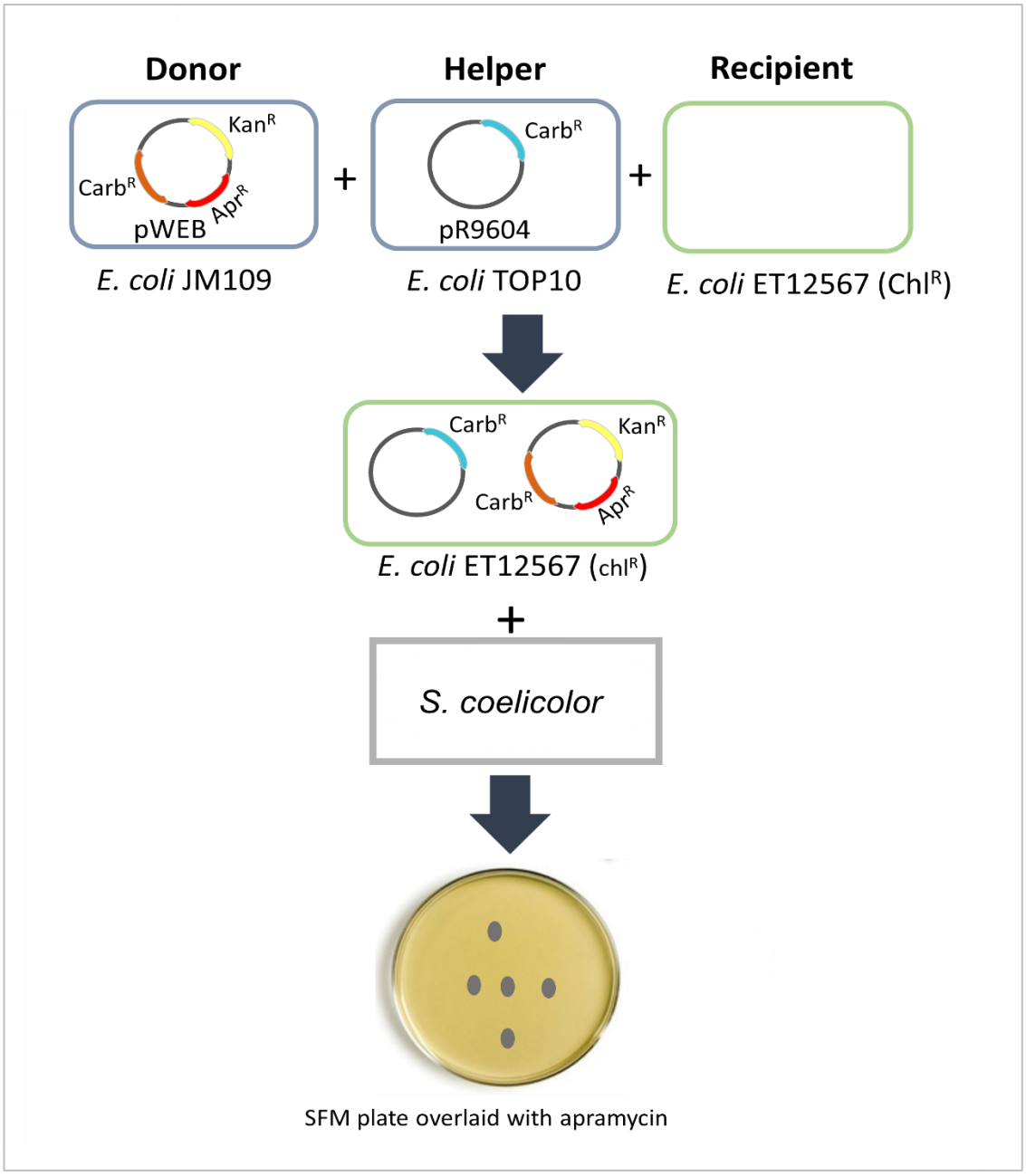

Figure 5.1. Schematic representation of the triparental mating procedure and the introducing of the pWEB to *S. coelicolor*.

Transconjugants were selected on the basis of resistance to apramycin and then multiple isolates were tested for sensitivity to kanamycin for each cross. For the majority of the different crosses (19 out of 28), at least three isolates were obtained that were kanamycin sensitive, although this is required for some crosses in the screening of multiple batches of transconjugants. For a few crosses (2 out of 28), screening of original transconjugants only produced two isolates that were kanamycin sensitive (Table 5.2). This was deemed sufficient for preliminary characterisation of their phenotypes. The remaining crosses (7 of 28) did not produce transconjugants that were kanamycin sensitive from the original

plates. For these, spores from a single transconjugant of each cross were streaked out onto a fresh plate containing apramycin and then colonies of the second generation screened for kanamycin sensitivity as described above. The screening of multiple batches eventually led to the identification of at least three kanamycin sensitive isolates for some of the remaining crosses. For four crosses (corresponding to SCO0091, SCO0072, SCO7595 and SCO2287), no kanamycin-sensitive isolates were obtained. It was noted whether kanamycin-sensitive transconjugants were obtained from the original plates or the second generation (Table 5.2). Spores from colonies identified as being kanamycin-sensitive were streak onto agar plates and a single well-isolated colony was chosen from which to prepared spore stocks. This passaging was done to ensure the stocks were from a pure, unigenomic source. In total 70 spore stocks of strains with the antibiotic profile (Kan^S, Apr^R) that is indicative of successful gene replacement were generated for 24 different crosses.

A qualitative assessment of the production of pigmented antibiotics (ACT and RED) was conducted by streaking mutants and the M145 parent onto TSA and R5 (Table 5.2). The majority of the mutants displayed the same phenotypes; however, these phenotypes were different from M145. For the purpose of classifying the mutants, the phenotype of the majority of the mutants was used as the baseline. It was considered possible that the spore inoculum for M145, which was prepared separately from the others, was in some way different or the presence of the disrupting transposon affected the phenotype. Regarding the former possibility, there have been several anecdotal reports of observing phenotypes being dependent on the preparation of spores (McDowall and Seipke, pers. comm.). It has even been suggested that there might be epigenetic control of *Streptomyces* phenotypes (Dijkhuizen *et al.*, 2008). More recently, a case has been made for stochastic germination as a beneficial strategy in uncertain environments. Stochastic variation has been observed and reported to be affected by spore density and chemicals released from spores (Xu & Vetsigian, 2017).

Gene replacement	TSA			R5		
	1	2	3	1	2	3
SCO0481	Pale, no ACT	Red, no ACT	Red, no ACT	Pale blue	Pale blue	Pale blue
SCO1390	Pale, no ACT	Red, no ACT	Red, no ACT	Pale blue	Pale blue	Pale blue
SCO1391	Red, no ACT	Red, no ACT	Red, no ACT	Pale blue	Pale blue	Pale blue
SCO1842[#]	Pale blue	Pale blue	Pale blue	Dark blue	Dark blue	Dark blue
SCO1861	Red, no ACT	Red, no ACT	Red, no ACT	Pale blue	Pale blue	Pale blue
SCO1862	Red, no ACT	Red, no ACT	Red, no ACT	Pale blue	Pale blue	Pale blue
SCO2191	Red, no ACT	Red, no ACT	Red, no ACT	Pale blue	Pale blue	Pale blue
SCO2631	Red, no ACT	Red, no ACT	Red, no ACT	Pale blue	Pale blue	Pale blue
SCO3305	Red, no ACT	Red, no ACT	Red, no ACT	Pale blue	Pale blue	Pale blue
SCO4070	Red, no ACT	Red, no ACT	Red, no ACT	Pale blue	Pale blue	Pale blue
SCO5529	Red, no ACT	Red, no ACT	Red, no ACT	Pale blue	Pale blue	Red, no ACT
SCO5856	Red, no ACT	Pale, not ACT	Red, no ACT	Pale blue	Red, no ACT	Red, no ACT
SCO6059	Red, no ACT	Red, no ACT	Red, no ACT	Pale blue	Pale blue	Pale blue
SCO6060	Red, no ACT	Red, no ACT	Red, no ACT	Pale blue	Pale blue	Pale blue

SCO6084	Red, no ACT	Red, no ACT	Red, no ACT	Pale blue	Pale blue	Pale blue
SCO6257	Red, no ACT	Red, no ACT	Red, no ACT	Pale blue	Pale blue	Pale blue
SCO6258#	Dark blue	Dark blue	Dark blue	Dark blue	Dark blue	Dark blue
SCO6259	Red, no ACT	Red, no ACT	Red, no ACT	Pale blue	Pale blue	Pale blue
SCO6515	Red, no ACT	Pale, no ACT	Red, no ACT	Red, no ACT	Red, no ACT	Pale blue
SCO6516	Red, no ACT	Red, no ACT	Red, no ACT	Pale blue	Pale blue	Pale blue
SCO7596#	Red, no ACT	Red, no ACT	Red, no ACT	Pale blue	Pale blue	Pale blue
SCO2602*	Pale blue	Pale blue		Dark blue	Dark blue	
SCO4295*	Red, no ACT	Red, no ACT		Dark blue	Dark blue	
SCO7517	Red, no ACT	Red, no ACT	Red, no ACT	Pale blue	Pale blue	Pale blue
M145	Pale blue			Pale blue		

Table 5.2. Phenotypes of the mutants on TSA and R5 media. The phenotypes of the mutants and the production of actinorhodin (ACT) were checked after incubation the strains for 6 days at 30^{o}C and using M145 as a control. The growth media is indicated at the top of the table. Numbering at the top indicates the original spore stocks for each mutant. An asterisk (*) indicates that only two spore stocks were generated from single colonies sensitive to kanamycin, whilst the number symbol (#) indicates mutants derived after passaging transconjugants that were kanamycin resistant, i.e. the product of cosmid integration.

On TSA plates, the majority of the mutants produced undecylprodigiosin, as indicated by the red colour of the patches, but did not produce actinorhodin, as indicated by the lack of blue pigment in the surrounding media. However, there were exceptions: three out of three mutants corresponding to SCO1842, two out of two mutants corresponding to SCO2602 and three out of three mutants corresponding to SCO6258 did produce detectable amounts of diffusible blue pigment, i.e. actinorhodin. The level of actinorhodin production was noticeably higher for the SCO6258 mutants. No changes were detected for SCO6257 and SCO6259 which have products that are likely to interact physically and functionally with the product of SCO6258 (see Table 3.1, for further details of function). For five genes, one of the three isolates produced patches with a pale colour, indicating impairment of undecylprodigiosin production: SCO481, SCO1390, SCO5856 and SCO6515. PCR-based analysis of the genotypes of a selection of mutants is described below.

On R5 plates, the majority of the mutants produced actinorhodin, with the mutants that produced detectable amounts of actinorhodin when others did not on TSA plates (SCO1842, SCO2602 and SCO6258) producing noticeably higher levels of actinorhodin. For another gene, SCO4295, two of two mutants also produced noticeable higher levels of actinorhodin. On R5 the mutants of this gene did not produce detectable actinorhodin unlike the mutants of SCO1842, SCO2602 and SCO6258. Thus, the mutants of four genes appear to increase actinorhodin production when grown on R5, TSA or both. For two genes, SCO5856 and SCO6515, two of the three corresponding mutants did not produce detectable levels of actinorhodin when grown on R5 plates. The phenotypes on TSA and R5 plates of the mutants of the genes highlighted are shown in Figure 5.2. The mutants of all the genes that appeared increase actinorhodin production were also grown on SFM plates, but streaked out rather than spotted to produce a single patch. This revealed that mutants corresponding to SCO6258 not only produced higher levels of actinorhodin relative to other mutants and M145, but sporulated earlier (Figure 5.3).

As a step towards confirming that the mutants contained the expected gene replacement, primers were designed to target regions adjacent to the point of transposon insertion for all of the genes that appeared to have an altered phenotype when mutated (see Table 2.2). All of the mutants had the antibiotic-resistance profile indicative of gene replacements (see above). The results of the PCR analysis are shown in Figure 5.4. For genes with mutants displaying the same phenotype, only one isolate was analysed, whilst for those displaying different phenotypes, one of each type was analysed (see Table 5.1). Amplicons of the expected size were produced using genomic DNA from M145, which lacks transposon-mutagenized genes. For the mutants of SCO6258, and

SCO1842 and one of the two mutants associated with SCO6515 amplicons corresponding to the insertion site were not produced. These results are consistent with replacement of the targeted gene. The mutant of SCO6515 that appears to have the expected gene replacement appears to be impaired in the production of actinorhodin. For all the others, amplicons of the expected size were produced suggesting that the target had not be replaced contrary to the antibiotic resistance profile of the mutants.

To confirm that the cosmid has not integrated and been maintained, primers were designed to amplify a segment of the neomycin gene (see Table 2.2) in the cosmid that confers kanamycin resistance. Whilst an amplicon of the expected size was produced readily using a kanamycin-resistant transconjugant, amplicons of the expected size were not produced for any of the mutants (Figure 5.5). This was supportive of the cosmid not being maintained in the mutants. However, this needed to be reconciled with the clear PCR evidence (Figure 5.4) that not all sites expected to contain transposon insertions were undisrupted. It seemed unlikely that the spore stocks were not derived from pure culture and were contaminated with cells containing integrated cosmid as the transconjugants had been passaged on agar plates before preparing spore stocks and the PCR analysis of cultures derived from these stocks did not reveal evidence of the cosmid-associated neomycin gene. One explanation is that genes have been replaced but not at the targeted sites because cosmids have been switched during the mutagenesis process. To investigate an attempt was made to sequence the genomes of a selection of mutants using Oxford Nanopore technology but failed for technical reason that is now known.

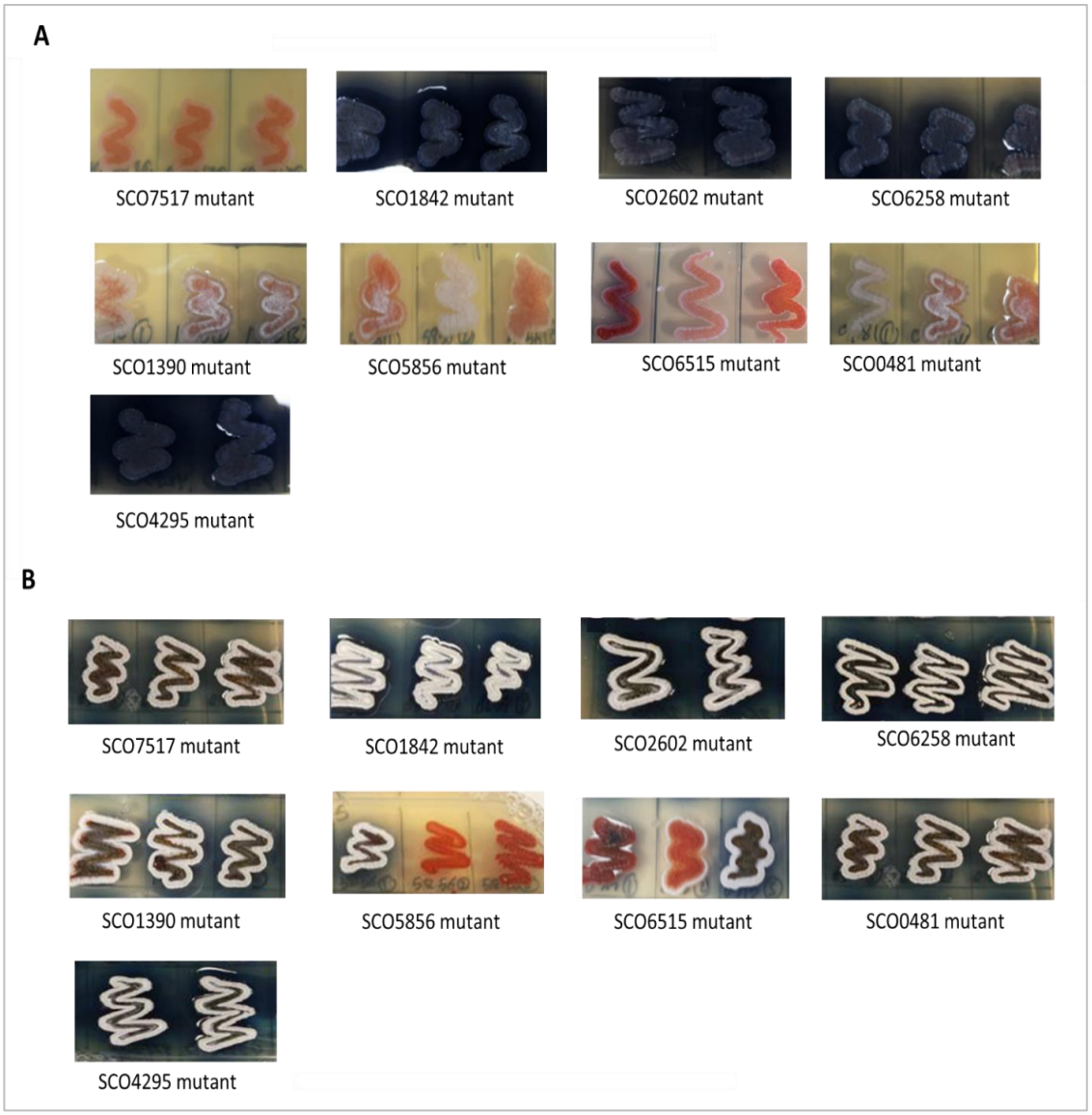

Figure 5.2. Phenotypes of the mutants on TSA and R5 plates. The phenotypes of the mutants were screened by streaking spores on the surface of TSA and R5 plates. **Panel A** represents the phenotypes of the mutants on TSA plate. **Panel B** represents the phenotypes of the mutants on R5 plate**.** The photographs were taken after incubation the plates for 6 days at 30ºC. The results for three independent isolates of transconjugants corresponding to SCO7517 are representative of the results obtained for the majority of the mutants.

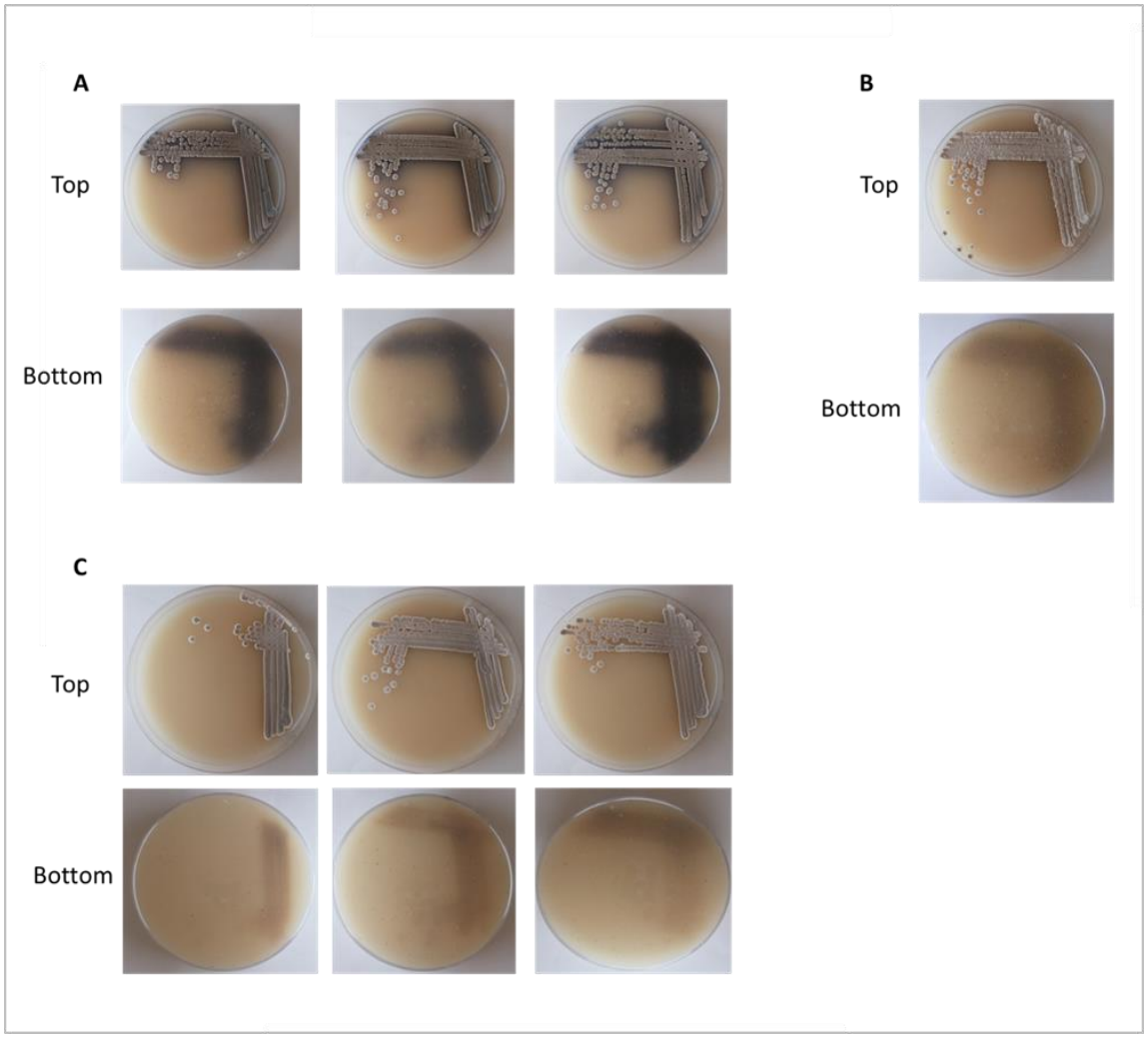

Figure 5.3. The phenotype of some mutants on SFM plate. For each mutant, the spores were streaked from three spore stocks on the surface of SFM plate individually and the plates were photographed (the top and the bottom parts of the plate) after incubation for 4 days at 30^{o}C. **Panel A** represents the phenotype of SCO6258 mutant. The blue pigment in the plate corresponds to actinorhodin. **Panel B** shows the phenotype of M145. **Panel C** is a representative photograph to show the phenotypes of three independent isolates for the following mutants; SCO1842, SCO6258, SCO2602, SCO4295 and SCO6515.

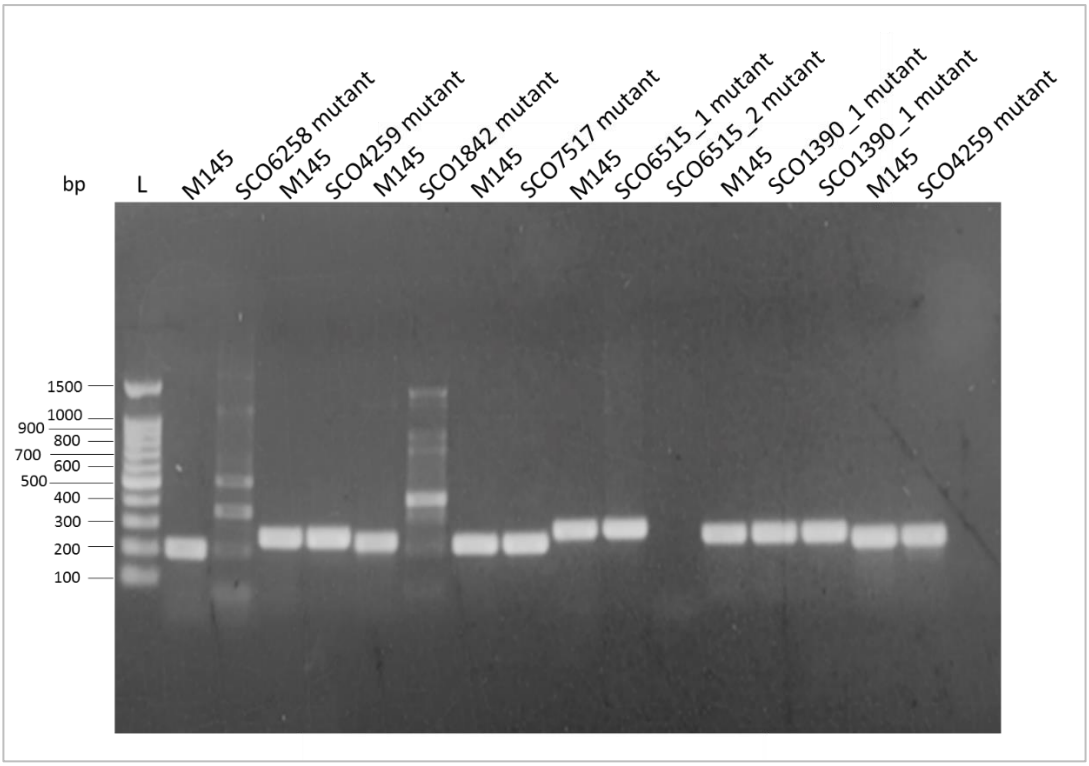

Figure 5.4. PCR analysis of transposon insertion within the genes using mutants genomic DNA and M145 genomic DNA as templates. The labelling at the top indicates the strains**.** Lane L contains a 100 bp DNA ladder (Promega). Sizes of the markers in base pair are shown on the left side hand. The samples were run on 1.2% agarose gels using 1 x TBE as a running buffer.

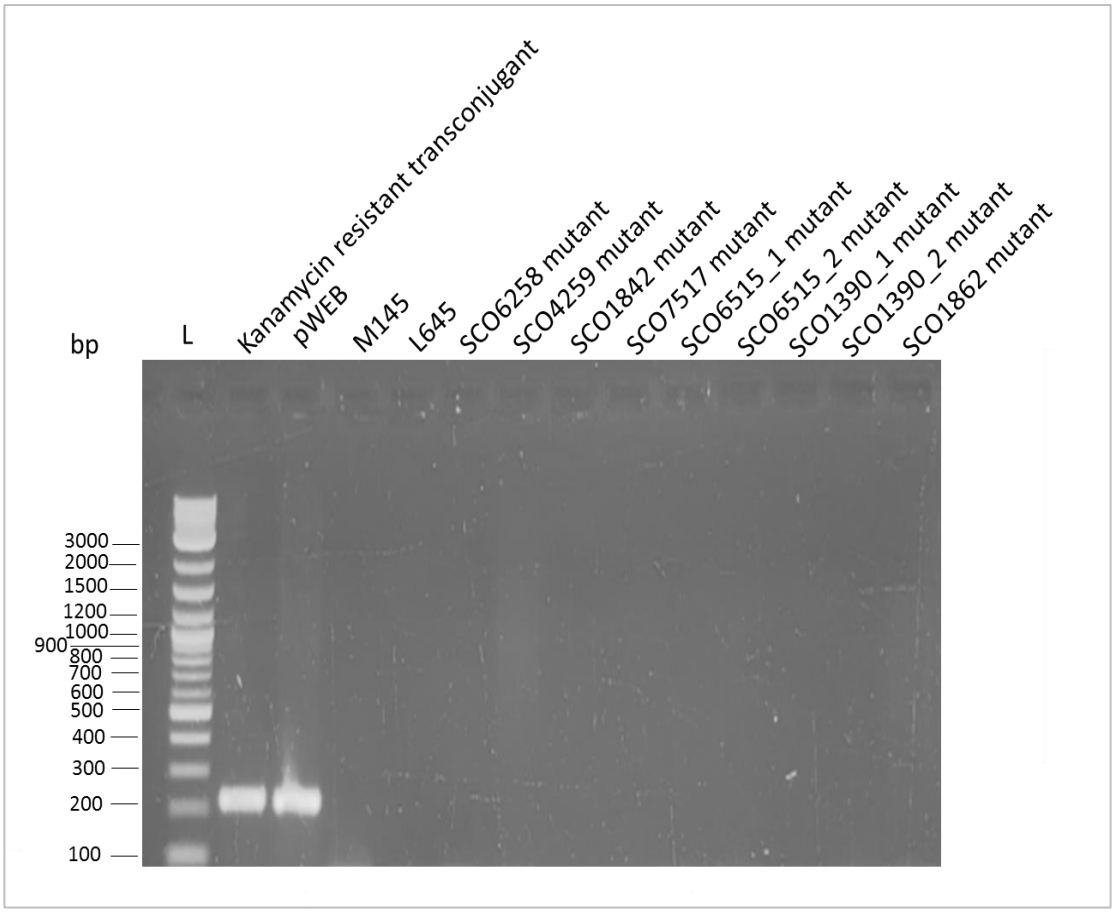

Figure 5.5. Confirmation the arising of mutants by double cross over gene replacement using PCR. Primers designed to tag the kanamycin resistance genes carried on the pWEB. The labelling at the top indicates the strains. pWEB was used as positive control. Lane L contains a 1 kb Plus DNA Ladder (New England BioLabs). Sizes of the markers in base pair are shown on the left side hand. The samples were run on 1.2% agarose gels using 1X TBE as a running buffer. The expected size of the amplicon for the neomycin resistance gene (*neo*) was 267 bp.

5.4 Discussion

This chapter was successful in providing a platform, albeit incomplete, for exploring further the function of genes within the AtrA regulon and their interconnection. Although the genotype of the mutants has yet to be confirmed by sequencing, the initial indication is promising, with three genes being identified as having functions that when disrupted, had an influence on the production of actinorhodin and perhaps secondary metabolites that are not pigmented. The replacement of SCO6258 and SCO1842 with transposon-disrupted alleles increased the production of actinorhodin whilst replacement of SCO6515 reduced production (Figure 5.2). The mutation of SCO6515 also appeared to hasten the onset of sporulation under at least one growth condition (Figure 5.2). Two other set of mutations also appear to increase the production of actinorhodin, but the locations of the gene disruptions were not confirmed by PCR analysis (Figure 5.4). Although incomplete, this work has revealed that AtrA can influence actinorhodin production beyond its influence on ActII-ORF4, the associated cluster-situated regulator, and the DasR regulon.

The putative function of SCO6515 is proteolysis. It would be interesting to assay this mutant for protease activity. A simple assay in which powdered milk, which has a high-protein content, is added to agar plates has been developed and used widely for proteases, or at least those that are secreted (Lewis *et al.*, 2003). However, the product of SCO6515 may be a homologue of PfpI from *Pseudomonas aeruginosa* in which case it is likely to be intracellular (Fernández *et al.*, 2012). PfpI has been reported to provide general stress protection (Fernández *et al.*, 2012). This aspect of possible function could be investigated by assaying viability following exposure to UV irradiation, thermal stress etc. SCO1842 is a hypothetical protein of unknown function. Thus, there is no obvious path for investigating further the relationship of this gene with actinorhodin production. In contrast, it is highly probable that SCO6258 is the permease of a three component ABC active transport system for unknown sugar(s). The other two components are a sugar-binding lipoprotein (product of SCO6257) and the ATP-binding protein (product of SCO6258). Interestingly, mutants that are hoped to correspond to these genes did not have obvious alteration of actinorhodin production. Thus, the effect of disrupting SCO6258 may not be simply a consequence of disrupting the uptake of a sugar(s). It would nevertheless be interesting to investigate the growth of SCO6258 mutants on a range of sugars as the source of carbon and energy.

Clearly the next step is to confirm and in some cases determine the genotypes of the mutants generated as part of this work. It is proposed that the Oxford Nanopore platform

is again used with a fresh cell as the pores in cell that used previously were inactive due to reusing it more than one time. Instead of performing whole genome sequencing an approach, CRISPR/Cas9 could be used (Stevens *et al.*, 2019). This would involve designing guide RNAs that would direct cleavage by the Cas9 nuclease within the transposon sequence. Sequencing adapters thus would be primarily ligated adjacent to the transposon insertion, sequencing reads would thus contain a portion of transposon sequence followed by the gene that contains the insertion. Base-called data could be sorted for strands that contain the transposon sequence.

RUBRIC (Edwards *et al.*, 2019) could also be employed together with CRISPR/Cas9 mediated sequencing or as an alternative. RUBRIC enables real-time base calling along with sequence selectivity, which would for strands containing the transposon sequence be selectively sequenced. As the above approach would lead to enrichment of transposon-containing sequences in the strands that were sequenced.

Chapter 6 Concluding remarks and future work

This thesis has been successful in revealing for the first time that AtrA exerts direct and often multi-level control over genes encoding important functions associated with sugar and amino acid uptake and utilisation, peptidoglycan biosynthesis, morphological development, and secondary metabolism (Chapter 3). It has also provided evidence that γ-actinorhodin is able to block DNA-protein interactions non-specifically probably by intercalating into DNA (Chapter 4) and provided a collection of mutants whose continued study should be invaluable in refining our understanding of the role of AtrA in coordinating and controlling secondary metabolism (Chapter 5). Within each results chapter, the significance of the findings has been discussed and suggestions for progressing the study of AtrA have been described. Consequently, in this final chapter consideration is given to the wider challenge of producing the next generation of antibiotics given the emerging global crisis (Buckland, 2017).

At the start of this project, it was hoped that the cognate, small molecular regulator of the DNA-binding activity of AtrA could be identified, with a view to assessing whether it had value in eliciting the production of secondary metabolites that would otherwise be cryptic under standard laboratory conditions. As mentioned in the Introduction, species of *Streptomyces* and their close relatives still have potential as sources of new antibiotics given their genetic capacity for secondary metabolism vastly exceeds that detected under standard growth conditions (Wright, 2017, Zhang, 2007). The value of this so called “cryptic” secondary metabolism is widely acknowledged, as evidenced for example by the considerable number of studies aimed at its activation via the addition of small molecules and genetic engineering (Moore *et al.*, 2012, Rigali *et al.*, 2008, Wang *et al.*, 2009a). Locally, its value prompted the creation of the panel of *Streptomyces coelicolor* strains in which the promoters of key biosynthetic genes in all of the BGCs have been individually fused to the *gusA* reporter gene to allow their expression to be readily determined. This panel is already being used to screen for small molecules and growth conditions that stimulate secondary metabolism (O’Neill and Seipke, pers. comm.). As suggested earlier (Chapter 4), this panel could be expanded to include fusions to *atrA* and a selection of its targets, thereby providing another route to the eventual identification of the small molecular regulator of the DNA-binding activity of AtrA.

Since this study commenced, the interest in the soil as a source of new antibiotics has continued to grow, but importantly with a focus on screening the activities of previously

uncultivatable bacteria. There has been considerable early success, which includes the discovery of teixobactin, a new class of antibiotic that kills drug resistant Gram-positive pathogens by binding to precursors of the cell wall (Ling *et al.*, 2015). The discovery of teixobactin was facilitated by using isolation chips (iChip), which allowed small molecular compounds to permeate from soil into isolation chambers, thereby facilitating the growth of captured bacteria cells (Lodhi *et al.*, 2018, Nichols *et al.*, 2010). The producer of teixobactin is *Elftheria terrae*, a previously undescribed β-proteobacterium. The iChip technology is believed to have a produced a collection of >64,000 previously uncultivatable microbes from which another lead antibacterial compound Novo29 has been isolated. Both teixobactin and novo29 are being developed commercially by NovoBiotic Pharmaceuticals (taken from press releases, https://www.novobiotic.com/news (accessed: 15 August 2019)).

The importance of soil components in facilitating laboratory culture is reinforced further by a recent study that has shown the addition of a mix of low-molecular-weight substances (LMWS), extracted from soil using a simple organic solvent, allows the growth on agar plates of a plethora of previously uncultured bacteria (Nguyen *et al.*, 2018). The addition of LMWS extracted from soil and other environments where bacteria compete for growth may hold great potential to allow the bioscreening of previously uncultured bacteria, with or without the use of isolation chambers. The soil has also been the source of the recently discovered malacidins, calcium-dependent antibiotics with activity against multidrug-resistant, Gram-positive pathogens (Hover *et al.*, 2018). The discovery pipeline that produced malacidins was culture-independent and based on the bioinformatic analysis and heterologous expression of BGCs captured on DNA extracted from environmental samples. Discovery pipelines are also being updated by screening for compounds active against ESKAPE and other contemporary pathogens of clinical importance (Devasahayam *et al.*, 2010).

Whilst the former “Golden Era” of antibiotic discovery focussed largely on the genus *Streptomyces*, the new era will almost certainly focus on the activities of previously uncultivatable bacteria. It can be anticipated that genera other than *Streptomyces* will have structurally diverse ‘secondary metabolisms’ that will include compounds with anti-cancer, immunosuppressive, anti-helminthic and anti-fungal as well as anti-bacterial activity (Zhang, 2007). This assumes that the primary function of many, if not most, of the products of *Streptomyces* secondary metabolism is to impede the growth of competing microorganisms. Moreover, as competition for nutrients is common to all microbial soil dwellers, it can be anticipated that many other bacterial species from this environment will produce compounds of potential clinical value.

It seems timely to investigate systematically, the conditions that would facilitate the growth of previously uncultivable bacteria. The aforementioned work that showed LMWS from soil can facilitate the growth of an increased diversity of bacteria (Nguyen *et al.*, 2018) used a simple mixture of 80% methanol/20% water showed that this mixture was much more effective as a solvent than water or aqueous buffers (Nguyen *et al.*, 2018). However, as the active LMWS have yet to be identified other solvents may be more effective. Indeed, extending the range of solvents and determining their effectiveness at extracted LMWS that increase the diversity of cultivatable bacteria, would allow comparisons that could provide a platform for identifying the specific LMWS that facilitate the growth of an increased diversity of soil bacteria. Extraction could be extended to solvents that have already been used in soil studies and are relatively non-toxic, e.g. 85% ethanol /10% water/5% 1-pentanol and 50% ethyl acetate/40% acetone/10% water (Silva *et al.*, 2005). The techniques described in this thesis to extract secondary metabolites and characterise preparations of γ-actinorhodin could be used to study LMWS extracted from soil.

In terms of a starting media for comparing the effects of LMWS, the use of R2A is suggested (Pham & Kim, 2016). This medium is routinely used to isolate soil bacteria (Pulschen *et al.*, 2017) and is commercially available in powdered form. It is further suggested that attention will focus on any extract that facilitates the growth of the greatest number of previously uncultivated isolates. The diversity of bacteria can be assessed readily by 16S rRNA profiling (Peterson *et al.*, 2019) in conjunction with the EzTaxon database (Chun *et al.*, 2007). This would be done in parallel with the screening of isolates for novel antibacterial activity that for example prevent the growth of meticillin-resistant *Staphylococcus aureus*. The genomes of isolates of interest, based on novel taxonomy and bioactivity profiles, would be sequenced and BGCs located and analysed to predict the properties of the corresponding product using well-established bioinformatics tools such as antiSMASH (Blin *et al.*, 2019).

Candidate BGCs for antibacterial compound(s) would be mutagenized using CRISPR/Cas9 technology, which is now used routinely in Leeds, and their products identified by co-metabolic profiling with the WT strain using ultra-high-pressure liquid chromatography coupled with high resolution/high accuracy Orbitrap® mass spectrometry (UHPLC-HRMS) (Cheng *et al.*, 2017, Wang *et al.*, 2012). In the event that strains are genetically intractable, BGCs of interest could be cloned using transformation-associated recombination in yeast (Kouprina & Larionov, 2016) and expressed in a genome-minimised heterologous hosts originating from *S. coelicolor* and *S. albus* (Zaburannyi *et al.*, 2014, Komatsu *et al.*, 2010). UHPLC-MS should provide accurate

mass information and enable the generation of possible molecular formulae for metabolites in the extract that would be used to query the SciFinder Chemical Database (Gabrielson, 2018) to determine if there is novel chemistry in the extract. The MS2 profile enable further dereplication using Global Natural Products Social Molecular Networking (Wang *et al.*, 2016a). Crude extracts possessing novel chemistry would be fractionated using preparative HPLC and fractions bioassayed to identify those with activity. This procedure would be repeated and refined until a minimum number of compounds are present in bioactive extracts. A medium-scale fermentation and purification would be performed to produce enough pure material for NMR analysis and structure determination, which would be significantly aided by the aforementioned bioinformatics analyses.

The *Streptomyces* should not be forgotten and may yet yield new leads for antibiotics. As part of the above, it is suggested that the substantial collection of *Streptomyces spp*. held in Leeds and the laboratories of collaborators are spotted onto R2A and tryptone soya broth (TSB) plates with and without the addition of LMWS extracts. The plates would then be overlaid with indicator strains, e.g. *S. aureus* SH1000 (Horsburgh *et al.*, 2002), to determine whether LMWS extracts can stimulate the production of otherwise cryptic anti-bacterial activities. This approach has been used previously to identify small molecule elicitors of secondary metabolism (Wang *et al.*, 2013a). It would also be interesting to screen for LMWS that stimulate the expression of *gusA* in the aforementioned reporter library.

The outcomes of the work described above would be a methodology for activating secondary metabolism in soil bacteria and a list of ‘hits’ or organisms that produce lead compound(s) for future chemical characterisation.

Supplementary tables

		Peaks					Motifs		
Manually verified	**MACS**	**Start**	**End**	**Length (nt)**	**-log10 (p-value)**	**-log10 (q-value)**	**Name**	**Start**	**Stop**
Peak 1	MACS 1	82160	82803	644	421.9	419.2	Motif1_96_(15.4)	82463	82482
Peak 2	MACS 2	138810	139374	565	396.6	393.9	Motif1_135_(15.1)	139097	139116
Peak 3	MACS 3	299200	299640	441	160.4	158.1	Motif1_226_(14.2)	299372	299391
Peak 4	MACS 4	394005	394580	576	232.4	230.1	Motif1_209_(14.3)	394269	394288
Peak 5	MACS 5	491112	491763	652	799.2	796.2	Motif1_118_(15.2)	491422	491441
Peak 6	MACS 6	501336	501706	371	60.3	58.4	Motif1_130_(15.2)	501513	501532
Peak 7	MANID 7	533510	533883	373	n.d.	n.d.	Motif1_43_(16.3)	533667	533686
Peak 8	MACS 8	543876	544487	612	1445.0	1441.7	Motif1_231_(14.2)	544178	544197
Peak 9	MACS 9	609200	609788	589	366.1	363.5	Motif1_98_(15.4094)	609476	609495
Peak 10	MACS 10	677098	677533	436	214.2	211.8	Motif1_120_(15.2)	677290	677309
Peak 11	MACS 11	684623	684990	368	168.3	166.0	Motif1_370_(13.4)	684812	684831
Peak 12	MANID 12	724183	724601	418	n.d.	n.d.	Motif1_605_(12.5)	724408	724427
Peak 13	MANID 13	743613	744125	512	n.d.	n.d.	Motif2_316_(15.0)	743828	743836
Peak 14	MACS 14	778462	778879	418	57.0	55.0	Motif1_537_(12.8)	778663	778682
							Motif2_253_(15.8)	778675	778683
Peak 15	MACS 15	795967	796372	406	94.5	92.4	Motif1_116_(15.3)	796173	796192
Peak 16	MACS 16	823778	824245	468	139.2	137.0	Motif1_82_(15.6)	824009	824028
Peak 17	MACS 17	977061	977636	576	98.8	96.7	Motif1_322_(13.6)	977338	977357
Peak 18	MACS 18	1077306	1077823	518	93.8	91.7	Motif1_391_(13.3)	1077549	1077568
Peak 19	MACS 19	1118885	1119489	605	298.7	296.2	Motif1_264_(14.0)	1119168	1119187
Peak 20	MACS 20	1300162	1300785	624	538.4	535.6	Motif1_18_(17.6)	1300479	1300498
Peak 21	MACS 21	1321709	1322265	557	187.8	185.5	Motif1_45_(16.302)	1321982	1322001
Peak 22	MACS 22	1338276	1338891	616	2055.8	2052.1	Motif1_36_(16.5772)	1338537	1338556
Peak 23	MACS 23	1344860	1345481	622	505.9	503.1	Motif1_42_(16.3691)	1345123	1345142
Peak 24	MACS 24	1346313	1346961	649	778.9	775.9	Motif1_7_(18.8859)	1346641	1346660
Peak 25	MACS 25	1359205	1359785	581	375.5	372.9	Motif1_2190_(10.3624)	1359518	1359537

Peak 26	MACS 26	1473903	1474538	636	166.2	164.0	Motif1_35_(16.6644)	1474190	1474209
Peak 27	MACS 27	1483420	1484397	978	348.3	345.7	Motif2_327_(15)	1483743	1483751
Peak 28	MANID 28	1483617	1484409	792	n.d.	n.d.	Motif1_660_(12.3826)	1484091	1484110
Peak 29	MACS 29	1489901	1490690	790	102.9	100.8	Motif1_493_(12.9329)	1490521	1490540
Peak 30	MACS 30	1630628	1631225	598	109.1	107.0	Motif1_198_(14.4564)	1630923	1630942
Peak 31	MACS 31	1666648	1667275	628	219.5	217.2	Motif1_353_(13.4899)	1666943	1666962
							Motif2_432_(14.6)	1666960	1666968
Peak 32	MACS 32	1695468	1696139	672	118.5	116.4	Motif2_433_(14.6)	1695727	1695735
							Motif1_235_(14.1342)	1695782	1695801
Peak 33	MACS 33	1776233	1776847	615	625.8	622.9	Motif1_132_(15.1208)	1776517	1776536
Peak 34	MACS 34	1828293	1828941	649	551.8	549.0	Motif1_214_(14.2349)	1828646	1828665
Peak 35	MACS 35	1835342	1836009	668	288.5	286.1	Motif1_285_(13.8389)	1835683	1835702
Peak 36	MACS 36	1866484	1867851	1368	188.2	185.9	Motif1_260_(14)	1867541	1867560
Peak 37	MACS 37	1877014	1877530	517	83.1	81.1	Motif1_230_(14.1611)	1877212	1877231
Peak 38	MACS 38	1935195	1936011	817	362.8	360.2	Motif2_330_(15)	1935428	1935436
							Motif2_780_(12.3)	1935546	1935554
Peak 39	MACS 39/40	1967229	1968143	915	2101.1	2097.4	Motif1_4_(19.5436)	1967579	1967598
Peak 40	MACS 39/40	1967229	1968143	915	2101.1	2097.4	Motif1_10_(18.0067)	1967854	1967873
Peak 41	MACS 41	1970917	1971707	791	1227.4	1224.1	Motif1_218_(14.2215)	1971338	1971357
							Motif2_744_(12.6)	1971537	1971545
Peak 42	MACS 42	1996558	1997488	931	706.7	703.7	Motif1_79_(15.6711)	1996869	1996888
Peak 43	MACS 43	2112913	2113630	718	1238.0	1234.8	Motif1_41_(16.4027)	2113244	2113263
Peak 44	MACS 44	2148528	2149148	621	510.4	507.6	Motif1_153_(14.953)	2148857	2148876
Peak 45	MACS 45	2211229	2211881	653	429.6	426.9	Motif1_29_(16.9396)	2211541	2211560
Peak 46	MACS 46	2223399	2224065	667	442.7	440.1	Motif1_953_(11.7919)	2223750	2223769
Peak 47	MACS 47	2232338	2232904	567	252.7	250.3	Motif1_1420_(11.1544)	2232572	2232591
Peak 48	MACS 48	2237888	2238665	778	253.2	250.8	Motif1_477_(12.9799)	2238333	2238352
Peak 49	MACS 49	2258327	2260055	1729	614.7	611.8	Motif1_176_(14.7383)	2259723	2259742
Peak 50	MACS 50	2275009	2275577	569	175.6	173.4	Motif2_787_(12.3)	2275287	2275295
							Motif1_886_(11.906)	2275288	2275307
Peak 51	MACS 51	2300644	2301476	833	399.0	396.4	Motif1_507_(12.8591)	2301145	2301164
Peak 52	MACS 52	2457584	2458243	660	235.9	233.5	Motif1_197_(14.4966)	2457907	2457926

Peak 53	MACS 53	2458489	2458959	471	100.7	98.7	Motif1_50_(16.2081)	2458815	2458834
Peak 54	MACS 54	2514310	2515065	756	360.2	357.6	Motif1_373_(13.3826)	2514816	2514835
Peak 55	MACS 55	2601482	2602372	891	277.4	274.9	Motif1_734_(12.2282)	2601873	2601892
							Motif2_674_(13.1)	2601885	2601893
Peak 56	MACS 56	2634234	2635014	781	338.2	335.6	Motif1_227_(14.1745)	2634643	2634662
Peak 57	MACS 57	2689483	2690105	623	454.0	451.3	Motif1_267_(13.9732)	2689784	2689803
Peak 58	MACS 58	2698335	2699293	959	528.6	525.8	Motif1_63_(15.9329)	2698632	2698651
Peak 59	MACS 59	2706079	2706966	888	506.5	503.7	Motif1_258_(14.0067)	2706686	2706705
Peak 60	MACS 60	2728257	2728916	660	89.9	87.9	Motif1_458_(13.047)	2728620	2728639
Peak 61	MACS 61	2742744	2743872	1129	2215.9	2212.2	Motif1_69_(15.8725)	2743410	2743429
Peak 62	MACS 62	2769282	2769885	604	552.1	549.3	Motif1_304_(13.698)	2769610	2769629
Peak 63	MACS 63	2821718	2823397	1680	3165.7	3161.5	Motif1_3_(19.7584)	2822567	2822586
Peak 64	MACS 64	2856352	2858175	1824	3185.4	3181.1	Motif1_77_(15.7181)	2857124	2857143
Peak 65	MACS 65	2871215	2872275	1061	440.8	438.1	Motif1_70_(15.8322)	2871925	2871944
Peak 66	MACS 66	2873871	2874531	661	288.2	285.8	Motif1_21_(17.5436)	2874205	2874224
Peak 67	MACS 67	2942293	2943254	962	317.9	315.4	Motif1_1060_(11.6309)	2942937	2942956
Peak 68	MACS 68	2984326	2985907	1582	328.4	325.9	Motif1_957_(11.7919)	2985560	2985579
Peak 69	MACS 69	3158848	3159739	892	206.5	204.1	Motif1_219_(14.2215)	3159140	3159159
Peak 70	MACS 70	3167338	3168406	1069	266.9	264.5	Motif1_330_(13.5906)	3168090	3168109
Peak 71	MACS 71	3186329	3187629	1301	248.6	246.2	Motif1_498_(12.8993)	3186912	3186931
Peak 72	MACS 72	3270636	3271303	668	351.5	348.9	Motif1_382_(13.3557)	3270982	3271001
Peak 73	MACS 73	3291861	3292557	697	338.0	335.4	Motif1_471_(13.0201)	3292195	3292214
Peak 74	MACS 74	3420738	3421809	1072	466.4	463.7	Motif1_465_(13.0268)	3421439	3421458
Peak 75	MACS 75	3439323	3440784	1462	519.1	516.3	Motif1_160_(14.8792)	3439834	3439853
Peak 76	MACS 76	3495265	3496009	745	559.7	556.9	Motif1_40_(16.4631)	3495842	3495861
Peak 77	MACS 77	3529588	3530370	783	236.1	233.7	Motif1_60_(15.9664)	3530006	3530025
Peak 78	MACS 78	3641348	3642291	944	191.0	188.7	Motif1_2583_(10.0872)	3641619	3641755
							Motif2_275_(15.8)	3641680	3641688
							Motif2_118_(16.6)	3641692	3641700
							Motif2_119_(16.6)	3641698	3641706
Peak 79	MACS 79	3644193	3646283	2091	254.2	251.8	Motif1_649_(12.4094)	3645569	3645588
Peak 80	MACS 80/81	3653137	3657141	4005	2812.4	2808.4	Motif1_1213_(11.4161)	3655846	3655865

Peak 81	MACS 80/81	3653137	3657141	4005	2812.4	2808.4	Motif1_16_(17.698)	3656028	3656047
Peak 82	MACS 82	3662422	3664678	2257	1052.7	1049.5	Motif1_66_(15.9195)	3663504	3663523
Peak 83	MACS 83/84	3700267	3701492	1226	3964.9	3959.6	Motif1_37_(16.5101)	3700602	3700621
Peak 84	MACS 83/84	3700267	3701492	1226	3964.9	3959.6	Motif2_33_(16.6)	3700900	3700908
Peak 85	MACS 85	3796174	3798709	2536	700.3	697.3	Motif1_255_(14.0201)	3796636	3796655
Peak 86	MACS 86	3825115	3825652	538	385.3	382.7	Motif1_99_(15.4094)	3825330	3825349
Peak 87	MACS 87	3826134	3826744	611	481.2	478.5	Motif1_100_(15.4094)	3826432	3826451
Peak 88	MACS 88	3893545	3895254	1710	671.7	668.8	Motif1_56_(16.0604)	3894250	3894269
Peak 89	MACS 89	3906286	3907522	1237	370.7	368.1	Motif1_101_(15.4094)	3907228	3907247
Peak 90	MACS 90/91	3914103	3919645	5543	1066.3	1063.1	Motif1_901_(11.8859)	3916633	3916652
Peak 91	MACS 90/91	3914103	3919645	5543	1066.3	1063.1	Motif1_986_(11.7517)	3918096	3918115
Peak 92	MACS 92	3933906	3935403	1498	305.4	302.9	Motif1_2584_(10.0872)	3934596	3934752
Peak 93	MACS 93	3960583	3962556	1974	702.8	699.9	Motif1_1684_(10.8456)	3962081	3962100
							Motif2_121_(16.6)	3962096	3962104
Peak 94	MACS 94	4134868	4137368	2501	471.7	469.0	Motif2_41_(16.6)	4135130	4135138
							Motif1_355_(13.4832)	4135131	4135150
Peak 95	MACS 95	4172633	4173918	1286	436.5	433.8	Motif2_42_(16.6)	4172948	4172956
							Motif2_43_(16.6)	4173239	4173247
Peak 96	MACS 96	4305988	4307195	1208	396.4	393.8	Motif2_557_(14.2)	4306765	4306773
Peak 97	MACS 97	4317469	4319383	1915	407.9	405.2	Motif1_11_(17.9933)	4318355	4318374
Peak 98	MACS 98	4423555	4426934	3380	2048.3	2044.6	Motif1_58_(16.0403)	4426075	4426094
Peak 99	MACS 99	4450075	4451484	1410	365.4	362.8	Motif2_280_(15.8)	4450779	4450787
Peak 100	MACS 100	4461774	4464455	2682	3446.4	3442.0	Motif1_53_(16.1879)	4463212	4463231
Peak 101	MACS 101	4486470	4488435	1966	878.3	875.2	Motif1_85_(15.5369)	4487654	4487673
Peak 102	MACS 102	4505896	4509275	3380	948.0	944.9	Motif1_181_(14.7047)	4508474	4508493
Peak 103	MACS 103	4512528	4513502	975	1422.0	1418.7	Motif1_30_(16.9396)	4512876	4512895
Peak 104	MACS 104	4523455	4526066	2612	105.4	103.3	Motif2_1402_(9.1)	4524742	4524750
Peak 105	MACS 105	4544640	4545217	578	306.6	304.1	Motif1_1150_(11.4966)	4544972	4544991
Peak 106	MACS 106	4552674	4553370	697	232.5	230.1	Motif1_1136_(11.5302)	4553017	4553036
Peak 107	MACS 107/8	4709444	4711060	1617	2757.3	2753.4	Motif1_34_(16.6913)	4710213	4710232
Peak 108	MACS 107/8	4709444	4711060	1617	2757.3	2753.4	Motif1_93_(15.4295)	4710279	4710298
Peak 109	MACS 109	4771786	4772593	808	236.5	234.1	Motif1_1107_(11.5638)	4772100	4772119

							Motif2_282_(15.8)	4772112	4772120
Peak 110	MACS 110	4827783	4829065	1283	1773.2	1769.7	Motif1_278_(13.8658)	4828220	4828239
							Motif2_182_(16.2)	4828235	4828243
Peak 111	MACS 111	4915438	4916374	937	280.3	277.9	Motif2_183_(16.2)	4915916	4915924
							Motif1_164_(14.8322)	4915917	4915936
Peak 112	MACS 112	4998644	5000261	1618	661.2	658.3	Motif1_398_(13.2685)	4999587	4999606
Peak 113	MACS 113	5176531	5178008	1478	561.3	558.5	Motif1_224_(14.1946)	5177233	5177252
Peak 114	MACS 114	5183914	5184569	656	487.6	484.8	Motif1_317_(13.651)	5184248	5184267
Peak 115	MACS 115	5255166	5255846	681	1087.3	1084.2	Motif1_22_(17.5101)	5255476	5255495
Peak 116	MACS 116	5291258	5292260	1003	429.4	426.7	Motif1_83_(15.557)	5291864	5291883
Peak 117	MACS 117	5294468	5295761	1294	422.9	420.2	Motif2_225_(15.8)	5295499	5295507
Peak 118	MACS 118	5443744	5444384	641	209.9	207.5	Motif2_380_(15)	5444066	5444074
Peak 119	MACS 119	5462192	5462786	595	568.6	565.7	Motif1_168_(14.7987)	5462472	5462491
Peak 120	MACS 120	5488720	5489896	1177	512.5	509.7	Motif1_678_(12.349)	5489527	5489546
Peak 121	MACS 121	5493953	5494650	698	161.6	159.3	Motif1_1070_(11.6242)	5494276	5494295
Peak 122	MACS 122	5633761	5635011	1251	1208.4	1205.1	Motif1_6_(19.0805)	5634510	5634529
Peak 123	MACS 123	5709082	5709823	742	684.8	681.9	Motif2_451_(14.6)	5709393	5709401
Peak 124	MACS 124	5757897	5759529	1633	1544.4	1541.0	Motif1_54_(16.1745)	5759202	5759221
Peak 125	MACS 125	5819954	5820609	656	510.4	507.7	Motif1_329_(13.604)	5820281	5820300
Peak 126	MACS 126	5941905	5942599	695	88.4	86.3	Motif1_684_(12.3423)	5942217	5942236
							Motif2_57_(16.6)	5942405	5942413
Peak 127	MACS 127/8	5947270	5948451	1182	2325.2	2321.4	Motif1_46_(16.2953)	5947592	5947611
Peak 128	MACS 127/8	5947270	5948451	1182	2325.2	2321.4	Motif1_20_(17.5638)	5948041	5948060
Peak 129	MACS 129	6023082	6024231	1150	1399.3	1396.0	Motif1_5_(19.5235)	6023618	6023637
Peak 130	MACS 130	6165051	6165601	551	80.2	78.1	Motif1_286_(13.8255)	6165340	6165359
Peak 131	MACS 131	6213379	6214002	624	233.7	231.3	Motif1_591_(12.5973)	6213814	6213833
Peak 132	MACS 132	6275560	6275950	391	45.2	43.4	Motif1_236_(14.1208)	6275736	6275755
Peak 133	MACS 133	6285668	6286372	705	452.4	449.7	Motif1_123_(15.2013)	6286033	6286052
Peak 134	MACS 134	6292118	6292744	627	265.8	263.4	Motif1_24_(17.4027)	6292401	6292420
Peak 135	MACS 135	6356744	6357227	484	212.2	209.9	Motif1_265_(13.9933)	6357101	6357120
Peak 136	MACS 136	6361038	6361698	661	153.0	150.8	Motif1_39_(16.4698)	6361364	6361383
Peak 137	MACS 137	6371460	6372087	628	140.4	138.2	Motif2_139_(16.6)	6371768	6371776

Peak 138	MACS 138	6412043	6413006	964	292.2	289.7	Motif1_13_(17.8456)	6412646	6412665
Peak 139	MACS 139	6413626	6414159	534	134.4	132.2	Motif1_81_(15.6242)	6413913	6413932
Peak 140	MACS 140	6431089	6431683	595	598.8	595.9	Motif1_48_(16.2349)	6431352	6431371
Peak 141	MACS 141	6539433	6540063	631	202.4	200.0	Motif1_238_(14.1007)	6539746	6539765
Peak 142	MACS 142	6541049	6541646	598	400.6	397.9	Motif1_1051_(11.651)	6541330	6541349
Peak 143	MACS 143	6562968	6563651	684	633.5	630.6	Motif1_14_(17.8255)	6563295	6563314
Peak 144	MACS 144	6583578	6584207	630	1522.4	1519.0	Motif1_203_(14.3826)	6583901	6583920
Peak 145	MACS 145	6647187	6648150	964	652.8	649.9	Motif1_279_(13.8658)	6647747	6647766
							Motif2_606_(14.2)	6647753	6647761
Peak 146	MACS 146	6648398	6649184	787	898.7	895.7	Motif1_397_(13.2752)	6648701	6648720
Peak 147	MACS 147	6650865	6652123	1259	4073.0	4067.0	Motif1_1_(20.5772)	6651540	6651559
Peak 148	MACS 148	6682029	6683017	989	1243.8	1240.6	Motif1_256_(14.0134)	6682658	6682677
Peak 149	MACS 149	6797989	6798503	515	120.3	118.2	Motif1_1022_(11.7047)	6798246	6798265
Peak 150	MACS 150	6847478	6848086	609	316.9	314.4	Motif1_143_(15.047)	6847794	6847813
Peak 151	MACS 151	6878858	6879506	649	2054.5	2050.9	Motif1_199_(14.4497)	6879179	6879198
Peak 152	MACS 152	7071428	7071920	493	167.3	165.0	Motif1_210_(14.2617)	7071670	7071689
Peak 153	MACS 153	7104723	7105340	618	379.8	377.1	Motif1_38_(16.4966)	7105027	7105046
Peak 154	MACS 154	7205835	7206637	803	1083.4	1080.3	Motif1_336_(13.5772)	7206290	7206309
Peak 155	MACS 155	7250507	7251254	748	964.7	961.6	Motif1_28_(16.9866)	7250927	7250946
Peak 156	MACS 156	7493641	7494212	572	212.0	209.7	Motif1_597_(12.5705)	7493924	7493943
Peak 157	MACS 157	7523409	7524004	596	555.7	552.9	Motif1_25_(17.3557)	7523700	7523719
Peak 158	MACS 158	7530789	7531412	624	597.7	594.8	Motif1_12_(17.9396)	7531061	7531080
Peak 159	MACS 159	7585900	7586519	620	777.4	774.4	Motif1_315_(13.651)	7586194	7586213
Peak 160	MACS 160	7676204	7676712	509	349.5	346.9	Motif1_97_(15.4094)	7676495	7676514
Peak 161	MACS 161	7767472	7768167	696	249.2	246.8	Motif1_49_(16.2215)	7767912	7767931
Peak 162	MACS 162	7897944	7898398	455	104.7	102.6	Motif1_44_(16.3289)	7898222	7898241
Peak 163	MACS 163	7923623	7924227	605	422.5	419.9	Motif1_1437_(11.1342)	7923864	7923883
Peak 164	MACS 164	7923623	7924227	605	422.5	419.9	Motif1_243_(14.094)	7924015	7924034
Peak 165	MANID 165	8209685	8209946	261	n.d.	n.d.	Motif1_529_(12.7987)	8209786	8209805
Peak 166	MACS 166	8331835	8332216	382	74.8	72.8	Motif1_190_(14.5973)	8332022	8332041
Peak 167	MACS 167	8417074	8417502	429	170.9	168.6	Motif1_157_(14.9329)	8417273	8417292
Peak 168	MACS 168	8424726	8425224	499	247.6	245.2	Motif1_326_(13.6107)	8424961	8424980

Peak 169	MACS 169	8462507	8463143	637	1209.0	1205.8	Motif1_51_(16.2013)	8462820	8462839
Peak 170	MACS 170	8475689	8476293	605	450.3	447.6	Motif2_240_(15.8)	8475922	8475930
							Motif2_241_(15.8)	8475928	8475936
							Motif2_242_(15.8)	8475934	8475942
							Motif2_243_(15.8)	8475940	8475948
							Motif2_244_(15.8)	8475958	8475966
							Motif2_245_(15.8)	8475964	8475972
							Motif2_246_(15.8)	8475970	8475978

Table S1. Sites of AtrA binding along the *S. coelicolor* chromosome. MANID indicates manually identified peak**.**

SCO	Base mean	log2(FC)	StdErr	Wald-Stats	p-value	Adjusted p-value
SCO0004	3697	0.43	0.13	3.41	6.5E-04	5.0E-02 *
SCO0071	281	1.43	0.25	5.76	8.6E-09	1.7E-06
SCO0072	17789	1.59	0.27	5.96	2.6E-09	5.8E-07
SCO0099	1591	-0.46	0.14	-3.36	7.7E-04	5.6E-02
SCO0295	287	0.94	0.20	4.78	1.7E-06	2.7E-04
SCO0481	194	-0.70	0.20	-3.55	3.8E-04	3.2E-02
SCO0565	579	-0.79	0.18	-4.48	7.3E-06	9.7E-04
SCO0764	31912	0.42	0.13	3.22	1.3E-03	7.9E-02 *
SCO0873	66	0.91	0.27	3.41	6.6E-04	5.0E-02
SCO0874	525	1.93	0.20	9.53	1.6E-21	6.1E-19
SCO0875	212	2.36	0.20	11.70	1.2E-31	5.8E-29
SCO0941	57	0.83	0.26	3.19	1.4E-03	8.6E-02 *
SCO0978	4953	0.49	0.15	3.25	1.2E-03	7.5E-02 *
SCO1173	2648	0.46	0.14	3.35	8.0E-04	5.7E-02 *
SCO1390	9727	-0.58	0.17	-3.43	6.0E-04	4.6E-02
SCO1391	30488	-0.63	0.17	-3.73	1.9E-04	1.9E-02
SCO1471	924	0.57	0.17	3.31	9.5E-04	6.5E-02 *
SCO1481	2937	-0.69	0.19	-3.63	2.8E-04	2.5E-02
SCO1482	3534	-0.88	0.18	-4.84	1.3E-06	2.2E-04
SCO1483	30333	-0.83	0.17	-4.90	9.5E-07	1.6E-04
SCO1557	2889	-0.67	0.16	-4.17	3.1E-05	3.5E-03
SCO1558	1230	-0.63	0.17	-3.66	2.5E-04	2.4E-02
SCO1570	1965	0.87	0.24	3.63	2.8E-04	2.5E-02
SCO1580	1458	0.84	0.24	3.49	4.8E-04	3.9E-02
SCO1693	91	0.79	0.24	3.28	1.0E-03	6.9E-02 *
SCO1694	828	0.65	0.16	4.02	5.8E-05	6.2E-03 *
SCO1766	1419	0.85	0.24	3.55	3.9E-04	3.2E-02
SCO1767	1846	0.65	0.19	3.36	7.7E-04	5.6E-02
SCO1800	69173	0.81	0.26	3.18	1.5E-03	8.8E-02
SCO1842	2957	1.09	0.19	5.90	3.7E-09	8.0E-07

SCO1861	5135	0.56	0.13	4.32	1.6E-05	1.9E-03	*
SCO1862	2511	1.81	0.17	10.79	4.0E-27	1.7E-24	
SCO2113	719	-0.64	0.17	-3.68	2.3E-04	2.2E-02	
SCO2210	1600	-0.79	0.23	-3.39	6.9E-04	5.2E-02	
SCO2287	2013	-0.63	0.17	-3.61	3.0E-04	2.7E-02	
SCO2336	1149	-0.73	0.21	-3.44	5.8E-04	4.5E-02	
SCO2511	194	1.78	0.25	7.05	1.7E-12	5.1E-10	
SCO2602	10455	0.75	0.16	4.79	1.7E-06	2.7E-04	
SCO2631	756	-1.08	0.24	-4.58	4.7E-06	6.4E-04	
SCO2632	700	0.62	0.19	3.25	1.1E-03	7.5E-02	*
SCO2641	10120	0.64	0.20	3.23	1.3E-03	7.9E-02	
SCO2704	239	0.64	0.17	3.74	1.9E-04	1.8E-02	*
SCO2819	10507	-0.68	0.12	-5.80	6.5E-09	1.4E-06	
SCO2864	573	1.37	0.27	5.10	3.5E-07	6.3E-05	
SCO2885	1945	-1.46	0.17	-8.43	3.5E-17	1.1E-14	
SCO2907	2075	-0.66	0.21	-3.21	1.4E-03	8.3E-02	
SCO2977	3577	0.43	0.13	3.36	7.8E-04	5.6E-02	*
SCO3097	45029	-0.74	0.23	-3.26	1.1E-03	7.4E-02	
SCO3174	3303	-0.67	0.11	-6.00	2.0E-09	4.6E-07	
SCO3215	41562	0.69	0.22	3.14	1.7E-03	9.8E-02	
SCO3227	46771	0.57	0.18	3.15	1.6E-03	9.3E-02	
SCO3228	32470	0.70	0.19	3.65	2.7E-04	2.4E-02	
SCO3229	86845	0.62	0.15	4.00	6.3E-05	6.7E-03	
SCO3230	632937	0.56	0.16	3.60	3.2E-04	2.8E-02	
SCO3231	339830	0.57	0.18	3.16	1.6E-03	9.1E-02	
SCO3232	224488	0.59	0.17	3.46	5.5E-04	4.3E-02	
SCO3233	58460	0.53	0.16	3.25	1.2E-03	7.5E-02	
SCO3305	4641	-2.54	0.15	-16.73	7.5E-63	8.5E-60	
SCO3521	1147	-0.77	0.19	-3.96	7.4E-05	7.6E-03	
SCO3546	10928	-0.56	0.14	-4.14	3.4E-05	3.8E-03	
SCO3655	4712	0.79	0.24	3.32	8.9E-04	6.2E-02	
SCO3991	5053	1.21	0.21	5.91	3.5E-09	7.7E-07	

SCO3999	7544	1.00	0.24	4.26	2.1E-05	2.4E-03
SCO4061	480	0.69	0.18	3.75	1.7E-04	1.7E-02
SCO4063	3724	1.26	0.19	6.62	3.7E-11	1.0E-08
SCO4064	140	1.04	0.26	3.98	7.0E-05	7.3E-03
SCO4070	43420	-1.42	0.17	-8.49	2.1E-17	7.2E-15
SCO4109	7572	-0.78	0.14	-5.70	1.2E-08	2.4E-06
SCO4117	23506	-1.94	0.14	-14.24	5.5E-46	3.4E-43
SCO4118	6355	4.52	0.14	31.92	1.3E-223	1.1E-219
SCO4173	4931	1.21	0.20	6.11	1.0E-09	2.4E-07
SCO4174	1608	3.82	0.26	14.93	2.2E-50	1.7E-47
SCO4175	1749	3.99	0.24	16.34	5.1E-60	5.1E-57
SCO4201	15129	-0.77	0.14	-5.57	2.5E-08	4.7E-06
SCO4214	43191	-4.59	0.21	-22.20	3.6E-109	1.4E-105
SCO4215	14145	-1.81	0.19	-9.71	2.7E-22	1.1E-19
SCO4261	127905	-0.46	0.11	-4.36	1.3E-05	1.6E-03
SCO4266	879	-1.08	0.23	-4.71	2.5E-06	3.7E-04
SCO4267	1301	-1.95	0.24	-8.10	5.4E-16	1.7E-13
SCO4286	9843	-0.57	0.16	-3.48	4.9E-04	3.9E-02
SCO4295	123869	0.59	0.19	3.20	1.4E-03	8.4E-02
SCO4370	719	0.62	0.19	3.23	1.2E-03	7.9E-02 *
SCO4673	6023	0.41	0.11	3.55	3.9E-04	3.2E-02 *
SCO4677	19439	0.99	0.18	5.48	4.1E-08	7.7E-06
SCO4764	2676	-0.58	0.13	-4.55	5.4E-06	7.2E-04
SCO4771	31216	-0.33	0.10	-3.22	1.3E-03	7.9E-02 *
SCO4836	299	0.77	0.19	4.08	4.5E-05	4.9E-03 *
SCO4937	168	-1.26	0.27	-4.69	2.7E-06	3.9E-04
SCO5161	16796	-0.39	0.12	-3.31	9.2E-04	6.4E-02
SCO5358	25724	-0.71	0.20	-3.53	4.2E-04	3.4E-02
SCO5529	7163	-1.11	0.23	-4.76	1.9E-06	3.0E-04
SCO5630	5754	1.51	0.19	7.92	2.4E-15	7.4E-13
SCO5632	20667	-0.67	0.18	-3.74	1.9E-04	1.8E-02
SCO5638	3474	-3.95	0.18	-21.85	8.6E-106	2.3E-102

SCO5639	1941	-3.33	0.24	-13.93	4.3E-44	2.4E-41	
SCO5640	1480	-3.84	0.20	-19.37	1.4E-83	2.8E-80	
SCO5710	25309	0.76	0.16	4.65	3.4E-06	4.7E-04	
SCO5840	2219	-0.69	0.18	-3.76	1.7E-04	1.7E-02	
SCO5856	33845	-1.19	0.27	-4.47	7.7E-06	1.0E-03	
SCO5970	9475	-1.66	0.19	-8.72	2.9E-18	1.0E-15	
SCO6018	5607	-2.91	0.16	-18.78	1.1E-78	1.5E-75	
SCO6059	9308	-1.78	0.16	-11.04	2.6E-28	1.1E-25	
SCO6060	15495	-0.61	0.14	-4.47	7.9E-06	1.0E-03	
SCO6074	1892	0.93	0.25	3.68	2.3E-04	2.2E-02	
SCO6084	9069	-1.11	0.20	-5.67	1.4E-08	2.8E-06	
SCO6086	811	-0.98	0.22	-4.39	1.2E-05	1.5E-03	
SCO6088	1488	-1.19	0.19	-6.38	1.8E-10	4.6E-08	
SCO6197	36569	0.80	0.24	3.26	1.1E-03	7.3E-02	
SCO6198	55792	1.12	0.26	4.37	1.2E-05	1.5E-03	
SCO6199	26017	1.31	0.19	6.85	7.2E-12	2.0E-09	
SCO6237	1864	4.30	0.22	19.13	1.4E-81	2.2E-78	
SCO6238	3379	2.50	0.17	14.32	1.8E-46	1.3E-43	
SCO6257	4258	-2.26	0.17	-13.04	7.3E-39	3.6E-36	
SCO6258	1805	-2.33	0.17	-13.85	1.3E-43	6.6E-41	
SCO6259	1107	-2.16	0.14	-15.19	4.1E-52	3.7E-49	
SCO6382	21100	-0.65	0.20	-3.29	1.0E-03	6.7E-02	
SCO6393	6619	1.19	0.19	6.17	6.9E-10	1.7E-07	
SCO6394	2854	1.06	0.22	4.74	2.2E-06	3.3E-04	
SCO6396	4521	1.26	0.19	6.52	6.9E-11	1.8E-08	
SCO6481	797	-0.56	0.17	-3.36	7.8E-04	5.6E-02	
SCO6515	2316	-0.89	0.27	-3.30	9.6E-04	6.5E-02	
SCO6516	1506	-0.90	0.27	-3.35	8.1E-04	5.7E-02	
SCO6517	6547	0.58	0.18	3.15	1.6E-03	9.3E-02	
SCO6828	2320	-3.00	0.21	-14.25	4.4E-46	2.9E-43	
SCO7036	4387	0.93	0.22	4.19	2.8E-05	3.2E-03	
SCO7309	1326	-0.50	0.14	-3.61	3.1E-04	2.7E-02	*

SCO7314	2279	-0.84	0.27	-3.14	1.7E-03	9.6E-02	
SCO7316	1250	-0.86	0.27	-3.19	1.4E-03	8.6E-02	
SCO7432	2160	0.68	0.18	3.66	2.6E-04	2.4E-02	
SCO7437	329	0.64	0.18	3.49	4.8E-04	3.9E-02	*
SCO7514	293	0.84	0.20	4.29	1.8E-05	2.1E-03	
SCO7515	153	1.02	0.21	4.94	8.0E-07	1.4E-04	
SCO7517	1954	-0.66	0.18	-3.59	3.3E-04	2.8E-02	
SCO7588	1399	1.02	0.22	4.65	3.2E-06	4.6E-04	
SCO7595	1277	-0.85	0.18	-4.75	2.0E-06	3.1E-04	
SCO7596	1250	-0.92	0.22	-4.14	3.5E-05	3.8E-03	
SCO7597	1494	-0.97	0.19	-5.07	3.9E-07	6.9E-05	
SCO7644	1143	0.43	0.13	3.18	1.5E-03	8.8E-02	*
SCO7843	3787	0.47	0.14	3.38	7.4E-04	5.5E-02	*

Table S2. Genes with expression altered by disruption of the *atrA* gene. Asterisk indicates the alteration in the gene expression is not confirmed by DE analysis of 20-nt windows.

SCO	Strand	Start	End	Name	Start	Stop	Middle	Relative position (orfSTART)
SCO0098	-	82441	81601	Motif1_96_(15.4094)	82463	82482	82473	-32
SCO0500	-	533773	533533	Motif1_43_(16.3289)	533667	533686	533677	96
SCO0509	+	544193	545717	Motif1_231_(14.1544)	544178	544197	544188	-5
SCO0566	-	609186	608901	Motif1_98_(15.4094)	609476	609495	609486	-300 *
SCO0567	+	609516	610356	Motif1_98_(15.4094)	609476	609495	609486	-30
SCO0636	+	677226	678861	Motif1_120_(15.2349)	677290	677309	677300	74
SCO0752	-	796002	794688	Motif1_116_(15.2617)	796173	796192	796183	-181
SCO0929	-	977265	976452	Motif1_322_(13.6242)	977338	977357	977348	-83
SCO1022	+	1077500	1078328	Motif1_391_(13.2953)	1077549	1077568	1077559	59
SCO1060	-	1119111	1117869	Motif1_264_(13.9933)	1119168	1119187	1119178	-67
SCO1226	-	1300331	1297130	Motif1_18_(17.5772)	1300479	1300498	1300489	-158
SCO1276	+	1346692	1347289	Motif1_7_(18.8859)	1346641	1346660	1346651	-41
SCO1287	-	1359243	1358280	Motif1_2190_(10.3624)	1359518	1359537	1359528	-285
SCO1396	-	1483572	1482747	Motif2_327_(15)	1483743	1483751	1483747	-175
SCO1397	+	1483775	1484795	Motif2_327_(15)	1483743	1483751	1483747	-28
SCO1657	-	1776333	1772820	Motif1_132_(15.1208)	1776517	1776536	1776527	-194
SCO1658	+	1776736	1777501	Motif1_132_(15.1208)	1776517	1776536	1776527	-209
SCO1707	-	1828488	1827150	Motif1_214_(14.2349)	1828646	1828665	1828656	-168
SCO1714	-	1835573	1835003	Motif1_285_(13.8389)	1835683	1835702	1835693	-120
SCO1715	+	1835783	1837109	Motif1_285_(13.8389)	1835683	1835702	1835693	-90
SCO1755	-	1877167	1876318	Motif1_230_(14.1611)	1877212	1877231	1877222	-55
SCO1839	-	1967457	1967235	Motif1_4_(19.5436)	1967579	1967598	1967589	-132
SCO1973	-	2113110	2112315	Motif1_41_(16.4027)	2113244	2113263	2113254	-144
SCO2071	-	2223637	2222050	Motif1_953_(11.7919)	2223750	2223769	2223760	-123
SCO2286	-	2457821	2456144	Motif1_197_(14.4966)	2457907	2457926	2457917	-96
SCO2496	+	2690015	2690456	Motif1_267_(13.9732)	2689784	2689803	2689794	-221
SCO2508	+	2706800	2707220	Motif1_258_(14.0067)	2706686	2706705	2706696	-104
SCO2530	+	2728655	2728922	Motif1_458_(13.047)	2728620	2728639	2728630	-25
SCO2545	+	2743632	2744982	Motif1_69_(15.8725)	2743410	2743429	2743420	-212
SCO2566	-	2769481	2768599	Motif1_304_(13.698)	2769610	2769629	2769620	-139
SCO2630	-	2857072	2856328	Motif1_77_(15.7181)	2857124	2857143	2857134	-62

SCO2699	+	2943091	2943364	Motif1_1060_(11.6309)	2942937	2942956	2942947	-144
SCO2918	+	3168247	3168835	Motif1_330_(13.5906)	3168090	3168109	3168100	-147
SCO3016	+	3292316	3293012	Motif1_471_(13.0201)	3292195	3292214	3292205	-111
SCO3119	-	3421340	3420020	Motif1_465_(13.0268)	3421439	3421458	3421449	-109
SCO3138	-	3439685	3438623	Motif1_160_(14.8792)	3439834	3439853	3439844	-159
SCO3139	+	3439884	3441573	Motif1_160_(14.8792)	3439834	3439853	3439844	-40 *
SCO3189	+	3496078	3496558	Motif1_40_(16.4631)	3495842	3495861	3495852	-226
SCO3312	+	3663565	3663976	Motif1_66_(15.9195)	3663504	3663523	3663514	-51
SCO3344	+	3700570	3702733	Motif1_37_(16.5101)	3700602	3700621	3700612	42
SCO3466	+	3825370	3826210	Motif1_99_(15.4094)	3825330	3825349	3825340	-30 *
SCO3467	+	3826472	3827312	Motif1_100_(15.4094)	3826432	3826451	3826442	-30 *
SCO3527	+	3894466	3894697	Motif1_56_(16.0604)	3894250	3894269	3894260	-206
SCO3539	+	3907268	3908108	Motif1_101_(15.4094)	3907228	3907247	3907238	-30 *
SCO3543	-	3917885	3915026	Motif1_986_(11.7517)	3918096	3918115	3918106	-221
SCO3583	+	3962278	3963043	Motif1_1684_(10.8456)	3962081	3962100	3962091	-187
				Motif2_121_(16.6)	3962096	3962104	3962100	-178
SCO3761	-	4134996	4134483	Motif2_41_(16.6)	4135130	4135138	4135134	-138
				Motif1_355_(13.4832)	4135131	4135150	4135141	-145
SCO3794	-	4172662	4171888	Motif2_42_(16.6)	4172948	4172956	4172952	-290
SCO3911	+	4306856	4308332	Motif2_557_(14.2)	4306765	4306773	4306769	-87
SCO3925	+	4318647	4319373	Motif1_11_(17.9933)	4318355	4318374	4318365	-282
SCO4059	+	4451074	4451410	Motif2_280_(15.8)	4450779	4450787	4450783	-291
SCO4119	+	4524820	4526149	Motif2_1402_(9.1)	4524742	4524750	4524746	-74
SCO4409	-	4827958	4827364	Motif1_278_(13.8658)	4828220	4828239	4828230	-272
SCO4410	+	4828286	4828667	Motif1_278_(13.8658)	4828220	4828239	4828230	-56
SCO4409	-	4827958	4827364	Motif2_182_(16.2)	4828235	4828243	4828239	-281
SCO4410	+	4828286	4828667	Motif2_182_(16.2)	4828235	4828243	4828239	-47
SCO4497	+	4915936	4916236	Motif2_183_(16.2)	4915916	4915924	4915920	-16
				Motif1_164_(14.8322)	4915917	4915936	4915927	-9
SCO4578	-	4999690	4999465	Motif1_398_(13.2685)	4999587	4999606	4999597	93
SCO4772	+	5184448	5185669	Motif1_317_(13.651)	5184248	5184267	5184258	-190
SCO4826	+	5255657	5257154	Motif1_22_(17.5101)	5255476	5255495	5255486	-171
SCO4863	+	5291931	5292354	Motif1_83_(15.557)	5291864	5291883	5291874	-57

SCO5049	-	5489422	5488831	Motif1_678_(12.349)	5489527	5489546	5489537	-115
SCO5050	+	5489639	5490971	Motif1_678_(12.349)	5489527	5489546	5489537	-102
SCO5183	+	5634640	5638120	Motif1_6_(19.0805)	5634510	5634529	5634520	-120
SCO5248	-	5709316	5708737	Motif2_451_(14.6)	5709393	5709401	5709397	-81
SCO5249	+	5709623	5711030	Motif2_451_(14.6)	5709393	5709401	5709397	-226
SCO5357	+	5820662	5822053	Motif1_329_(13.604)	5820281	5820300	5820290	-372
SCO5461	+	5948079	5948694	Motif1_20_(17.5638)	5948041	5948060	5948051	-28
SCO5750	+	6286096	6288886	Motif1_123_(15.2013)	6286033	6286052	6286043	-53
SCO5754	+	6292410	6292956	Motif1_24_(17.4027)	6292401	6292420	6292411	1
SCO5813	+	6357218	6357857	Motif1_265_(13.9933)	6357101	6357120	6357111	-107
SCO5816	+	6361398	6363003	Motif1_39_(16.4698)	6361364	6361383	6361374	-24
SCO5968	+	6539765	6540974	Motif1_238_(14.1007)	6539746	6539765	6539756	-9
SCO5987	-	6563093	6562883	Motif1_14_(17.8255)	6563295	6563314	6563305	-212
SCO5988	+	6563334	6563778	Motif1_14_(17.8255)	6563295	6563314	6563305	-29 *
SCO6054	-	6647781	6646290	Motif1_279_(13.8658)	6647747	6647766	6647757	24
				Motif2_606_(14.2)	6647753	6647761	6647757	24
SCO6055	-	6648371	6647789	Motif1_397_(13.2752)	6648701	6648720	6648711	-340
SCO6552	-	7250677	7248850	Motif1_28_(16.9866)	7250927	7250946	7250937	-260
SCO6739	+	7493868	7495605	Motif1_597_(12.5705)	7493924	7493943	7493934	66
SCO6773	+	7531178	7532117	Motif1_12_(17.9396)	7531061	7531080	7531071	-107 *
SCO6822	+	7586409	7587975	Motif1_315_(13.651)	7586194	7586213	7586204	-205
SCO6910	-	7676473	7675633	Motif1_97_(15.4094)	7676495	7676514	7676505	-32
SCO7108	-	7898264	7897517	Motif1_44_(16.3289)	7898222	7898241	7898232	32
SCO7132	+	7923954	7924674	Motif1_1437_(11.1342)	7923864	7923883	7923874	-80
				Motif1_243_(14.094)	7924015	7924034	7924025	71
SCO7590	-	8416959	8415438	Motif1_157_(14.9329)	8417273	8417292	8417283	-324 *
SCO7598	+	8424897	8425014	Motif1_326_(13.6107)	8424961	8424980	8424971	74
SCO7599	+	8425072	8426008	Motif1_326_(13.6107)	8424961	8424980	8424971	-101

SCO7648	-	8475881	8475215	Motif2_240_(15.8)	8475922	8475930	8475926	-45
				Motif2_241_(15.8)	8475928	8475936	8475932	-51
				Motif2_242_(15.8)	8475934	8475942	8475938	-57
				Motif2_243_(15.8)	8475940	8475948	8475944	-63
				Motif2_244_(15.8)	8475958	8475966	8475962	-81
				Motif2_245_(15.8)	8475964	8475972	8475968	-87
				Motif2_246_(15.8)	8475970	8475978	8475974	-93

Table S3. Possible targets of conventional regulation. Asterisk indicates gene with altered expression identified by DESeq analysis of 20-nt bins.

List of References

Abdelmohsen, U.R., T. Grkovic, S. Balasubramanian, M.S. Kamel, R.J. Quinn & U. Hentschel, (2015) Elicitation of secondary metabolism in actinomycetes. *Biotechnol Adv* **33**: 798-811.

Abraham, E.P., E. Chain, C.M. Fletcher, A.D. Gardner, N.G. Heatley, M.A. Jennings & H.W. Florey, (1941) Further observations on penicillin. *The Lancet* **238**: 177-189.

Aceti, D.J. & W.C. Champness, (1998) Transcriptional regulation of *Streptomyces coelicolor* pathway-specific antibiotic regulators by the *absA* and *absB* loci. *J Bacteriol* **180**: 3100-3106.

Adedeji, W.A., (2016) The treasure called antibiotics. *Ann Ib Postgrad Med* **14**: 56-57.

Ahmed, S., A. Craney, S.M. Pimentel-Elardo & J.R. Nodwell, (2013) A synthetic, species-specific activator of secondary metabolism and sporulation in *Streptomyces coelicolor. ChemBioChem* **14**: 83-91.

Ahn, S.K., L. Cuthbertson & J.R. Nodwell, (2012) Genome context as a predictive tool for identifying regulatory targets of the TetR family transcriptional regulators. *PloS one* **7**: e50562.

Akopian, D., K. Shen, X. Zhang & S.O. Shan, (2013) Signal recognition particle: an essential protein-targeting machine. *Annu Rev Biochem* **82**: 693-721.

Alanis, A.J., (2005) Resistance to antibiotics: are we in the post-antibiotic era? *Arch Med Res* **36**: 697-705.

Aldén, L., F. Demoling & E. Bååth, (2001) Rapid Method of Determining Factors Limiting Bacterial Growth in Soil. *Applied and Environmental Microbiology* **67**: 1830-1838.

Aldred, K.J., R.J. Kerns & N. Osheroff, (2014) Mechanism of quinolone action and resistance. *Biochemistry* **53**: 1565-1574.

Aldridge, M., P. Facey, L. Francis, S. Bayliss, R. Del Sol & P. Dyson, (2013) A novel bifunctional histone protein in *Streptomyces*: a candidate for structural coupling between DNA conformation and transcription during development and stress? *Nucleic Acids Res* **41**: 4813-4824.

Alksne, L.E. & P.M. Dunman, (2008) Target-Based Antimicrobial Drug Discovery. In: Bacterial Pathogenesis: Methods and Protocols. F.R. DeLeo & M. Otto (eds). Totowa, NJ: Humana Press, pp. 271-283.

Amitai, S., I. Kolodkin-Gal, M. Hananya-Meltabashi, A. Sacher & H. Engelberg-Kulka, (2009) *Escherichia coli* MazF leads to the simultaneous selective synthesis of both "death proteins" and "survival proteins". *PLoS Genet* **5**: e1000390.

Anderson, T.B., P. Brian & W.C. Champness, (2001) Genetic and transcriptional analysis of absA, an antibiotic gene cluster-linked two-component system that regulates multiple antibiotics in *Streptomyces coelicolor*. *Mol Microbiol* **39**: 553-566.

Archer, N.K., M.J. Mazaitis, J.W. Costerton, J.G. Leid, M.E. Powers & M.E. Shirtliff, (2011) *Staphylococcus aureus* biofilms: properties, regulation, and roles in human disease. *Virulence* **2**: 445-459.

Armstrong, G.L., L.A. Conn & R.W. Pinner, (1999) Trends in Infectious Disease Mortality in the United States During the 20th Century. *JAMA* **281**: 61-66.

Ashkenazi, S., (2013) Beginning and possibly the end of the antibiotic era. *J Paediatr Child Health* **49**: E179-182.

Bachmann, B.O., S.G. Van Lanen & R.H. Baltz, (2014) Microbial genome mining for accelerated natural products discovery: is a renaissance in the making? *J Ind Microbiol Biotechnol* **41**: 175-184.

Badis, G., M.F. Berger, A.A. Philippakis, S. Talukder, A.R. Gehrke, S.A. Jaeger, E.T. Chan, G. Metzler, A. Vedenko, X. Chen, H. Kuznetsov, C.F. Wang, D. Coburn,

D.E. Newburger, Q. Morris, T.R. Hughes & M.L. Bulyk, (2009) Diversity and complexity in DNA recognition by transcription factors. *Science* **324**: 1720-1723.
Bailey, T.L., M. Boden, F.A. Buske, M. Frith, C.E. Grant, L. Clementi, J. Ren, W.W. Li & W.S. Noble, (2009) MEME SUITE: tools for motif discovery and searching. *Nucleic Acids Res* **37**: W202-208.
Baker, D.D., M. Chu, U. Oza & V. Rajgarhia, (2007) The value of natural products to future pharmaceutical discovery. *Natural Product Reports* **24**: 1225-1244.
Bangert, M., L. Bricio-Moreno, S. Gore, G. Rajam, E.W. Ades, S.B. Gordon & A. Kadioglu, (2012) P4-mediated antibody therapy in an acute model of invasive pneumococcal disease. *J Infect Dis* **205**: 1399-1407.
Barona-Gomez, F., S. Lautru, F.X. Francou, P. Leblond, J.L. Pernodet & G.L. Challis, (2006) Multiple biosynthetic and uptake systems mediate siderophore-dependent iron acquisition in *Streptomyces coelicolor* A3(2) and *Streptomyces ambofaciens* ATCC 23877. *Microbiology* **152**: 3355-3366.
Barreteau, H., A. Kovač, A. Boniface, M. Sova, S. Gobec & D. Blanot, (2008) Cytoplasmic steps of peptidoglycan biosynthesis. *FEMS Microbiology Reviews* **32**: 168-207.
Barrick, J.E. & R.R. Breaker, (2007) The distributions, mechanisms, and structures of metabolite-binding riboswitches. *Genome biology* **8**: R239.
Barry, E.R. & S.D. Bell, (2006) DNA Replication in the Archaea. *Microbiology and Molecular Biology Reviews* **70**: 876-887.
Bastos, R.G., S. Borsuk, F.K. Seixas & O.A. Dellagostin, (2009) Recombinant *Mycobacterium bovis* BCG. *Vaccine* **27**: 6495-6503.
Belloc, F., F. Lacombe, P. Dumain, F. Lopez, P. Bernard, M.R. Boisseau & J. Reifers, (1992) Intercalation of anthracyclines into living cell DNA analyzed by flow cytometry. *Cytometry* **13**: 880-885.
Bernas, T., B.P. Rajwa, E.K. Asem & J.P. Robinson, (2005) *Loss of image quality in photobleaching during microscopic imaging of fluorescent probes bound to chromatin,* p. 1-9, 9. SPIE.
Berrar, D.P., W. Dubitzky & M. Granzow, (2003) A practical approach to microarray data analysis. *Springer,*pp.15-19
Berrow, N.S., D. Alderton, S. Sainsbury, J. Nettleship, R. Assenberg, N. Rahman, D.I. Stuart & R.J. Owens, (2007) A versatile ligation-independent cloning method suitable for high-throughput expression screening applications. *Nucleic Acids Res* **35**: e45.
Bhaduri, S., N. Ranjan & D.P. Arya, (2018) An overview of recent advances in duplex DNA recognition by small molecules. *Beilstein journal of organic chemistry* **14**: 1051-1086.
Bignell, D.R., K. Tahlan, K.R. Colvin, S.E. Jensen & B.K. Leskiw, (2005) Expression of *ccaR*, encoding the positive activator of cephamycin C and clavulanic acid production in *Streptomyces clavuligerus*, is dependent on *bldG*. *Antimicrob Agents Chemother* **49**: 1529-1541.
Binda, E., F. Marinelli & G.L. Marcone, (2014) Old and New Glycopeptide Antibiotics: Action and Resistance. *Antibiotics (Basel)* **3**: 572-594.
Bishop, A., S. Fielding, P. Dyson & P. Herron, (2004) Systematic insertional mutagenesis of a *streptomycete* genome: a link between osmoadaptation and antibiotic production. *Genome Res* **14**: 893-900.
Blin, K., S. Shaw, K. Steinke, R. Villebro, N. Ziemert, S.Y. Lee, M.H. Medema & T. Weber, (2019) antiSMASH 5.0: updates to the secondary metabolite genome mining pipeline. *Nucleic Acids Research* **47**: W81-W87.
Bobek, J., E. Strakova, A. Zikova & J. Vohradsky, (2014) Changes in activity of metabolic and regulatory pathways during germination of *S. coelicolor*. *BMC Genomics* **15**: 1173.
Bolger, A.M., M. Lohse & B. Usadel, (2014) Trimmomatic: a flexible trimmer for Illumina sequence data. *Bioinformatics (Oxford, England)* **30**: 2114-2120.

Bourot, S., O. Sire, A. Trautwetter, T. Touzé, L.F. Wu, C. Blanco & T. Bernard, (2000) Glycine Betaine-assisted Protein Folding in a lysAMutant of *Escherichia coli*. *Journal of Biological Chemistry* **275**: 1050-1056.

Boutte, C.C. & S. Crosson, (2013) Bacterial lifestyle shapes stringent response activation. *Trends Microbiol* **21**: 174-180.

Breaker, R.R., (2012) Riboswitches and the RNA world. *Cold Spring Harbor perspectives in biology* **4**: a003566.

Bruheim, P., H. Sletta, M.J. Bibb, J. White & D.W. Levine, (2002) High-yield actinorhodin production in fed-batch culture by a *Streptomyces lividans* strain overexpressing the pathway-specific activator gene *actII-ORF4. J Ind Microbiol Biotechnol* **28**: 103-111.

Buckland, D., (2017) Antimicrobial resistance and the race to find new antibiotics. **28**: 12-15.

Bystrykh, L.V., M.A. Fernandez-Moreno, J.K. Herrema, F. Malpartida, D.A. Hopwood & L. Dijkhuizen, (1996) Production of actinorhodin-related "blue pigments" by *Streptomyces coelicolo*r A3(2). *J Bacteriol* **178**: 2238-2244.

Caballero, J.L., F. Malpartida & D.A. Hopwood, (1991) Transcriptional organization and regulation of an antibiotic export complex in the producing *Streptomyces* culture. *Molecular and General Genetics MGG* **228**: 372-380.

Calkhoven, C.F. & G. Ab, (1996) Multiple steps in the regulation of transcription-factor level and activity. *Biochem J* **317 (Pt 2)**: 329-342.

Carnero, A., (2006) High throughput screening in drug discovery. *Clinical and Translational Oncology* **8**: 482-490.

Cars, O., L.D. Hogberg, M. Murray, O. Nordberg, S. Sivaraman, C.S. Lundborg, A.D. So & G. Tomson, (2008) Meeting the challenge of antibiotic resistance. *Bmj* **337**: a1438.

Cashin, P., L. Goldsack, D. Hall & R. O'Toole, (2006) Contrasting signal transduction mechanisms in bacterial and eukaryotic gene transcription. *FEMS Microbiol Lett* **261**: 155-164.

Cavanagh, A.T. & K.M. Wassarman, (2014) 6S RNA, a global regulator of transcription in *Escherichia coli*, *Bacillus subtilis*, and beyond. *Annu Rev Microbiol* **68**: 45-60.

Chaires, J.B., (1997) Energetics of drug-DNA interactions. *Biopolymers* **44**: 201-215.

Champness, W.C., (1988) New loci required for *Streptomyces coelicolor* morphological and physiological differentiation. *J Bacteriol* **170**: 1168-1174.

Chan, P.P., A.D. Holmes, A.M. Smith, D. Tran & T.M. Lowe, (2012a) The UCSC Archaeal Genome Browser: 2012 update. *Nucleic Acids Res* **40**: D646-652.

Chan, Y.H., M.M. Fan, C.M. Fok, Z.L. Lok, M. Ni, C.F. Sin, K.K. Wong, S.M. Wong, R. Yeung, T.T. Yeung, W.C. Chow, T.H. Lam & C.M. Schooling, (2012b) Antibiotics nonadherence and knowledge in a community with the world's leading prevalence of antibiotics resistance: implications for public health intervention. *Am J Infect Control* **40**: 113-117.

Chater, K.F. & S. Horinouchi, (2003) Signalling early developmental events in two highly diverged *Streptomyces* species. *Mol Microbiol* **48**: 9-15.

Chater, K.F. & L.C. Wilde, (1980) *Streptomyces albus* G mutants defective in the SalGI restriction-modification system. *J Gen Microbiol* **116**: 323-334.

Chen, L., Y.H. Lu, J. Chen, W.W. Zhang, D. Shu, Z.J. Qin, S. Yang & W.H. Jiang, (2008) Characterization of a negative regulator AveI for avermectin biosynthesis in *Streptomyces avermitilis* NRRL8165. *Applied Microbiology and Biotechnology* **80**: 277-286.

Chen, Y., H. Zhou, M. Wang & T. Tan, (2017) Control of ATP concentration in *Escherichia coli* using an ATP-sensing riboswitch for enhanced S-adenosylmethionine production. *RSC Advances* **7**: 22409-22414.

Cheng, Q., L. Shou, C. Chen, S. Shi & M. Zhou, (2017) Application of ultra-high-performance liquid chromatography coupled with LTQ-Orbitrap mass spectrometry for identification, confirmation and quantitation of illegal adulterated

weight-loss drugs in plant dietary supplements. *J Chromatogr B Analyt Technol Biomed Life Sci* **1064**: 92-99.
Cho, S., J. Shin & B.K. Cho, (2018) Applications of CRISPR/Cas System to Bacterial Metabolic Engineering. *Int J Mol Sci* **19**.
Chopra, I. & M. Roberts, (2001) Tetracycline antibiotics: mode of action, applications, molecular biology, and epidemiology of bacterial resistance. *Microbiol Mol Biol Rev* **65**: 232-260 ; second page, table of contents.
Chun, J., J.-H. Lee, Y. Jung, M. Kim, S. Kim, B.K. Kim & Y.-W. Lim, (2007) EzTaxon: a web-based tool for the identification of prokaryotes based on 16S ribosomal RNA gene sequences. *International journal of systematic and evolutionary microbiology* **57**: 2259-2261.
Claessen, D., W. de Jong, L. Dijkhuizen & H.A. Wosten, (2006) Regulation of *Streptomyce*s development: reach for the sky! *Trends Microbiol* **14**: 313-319.
Clatworthy, A.E., E. Pierson & D.T. Hung, (2007) Targeting virulence: a new paradigm for antimicrobial therapy. *Nature Chemical Biology* **3**: 541.
CLSI, (2007) Performance standards for antimicrobial susceptibility testing; seventeenth informational supplement. *CLSI document M100-S17, Clinical and laboratory standards institute, Wayne*.
Coates, A.R. & Y. Hu, (2007) Novel approaches to developing new antibiotics for bacterial infections. *Br J Pharmacol* **152**: 1147-1154.
Cobb, R.E., Y. Wang & H. Zhao, (2015) High-efficiency multiplex genome editing of *Streptomyces* species using an engineered CRISPR/Cas system. *ACS Synth Biol* **4**: 723-728.
Colombo, V., M. Fernandez-de-Heredia & F. Malpartida, (2001) A polyketide biosynthetic gene cluster from *Streptomyces* antibioticus includes a LysR-type transcriptional regulator. *Microbiology* **147**: 3083-3092.
Corless, S. & N. Gilbert, (2016) Effects of DNA supercoiling on chromatin architecture. **8**: 51-64.
Cox, G., A. Sieron, A.M. King, G. De Pascale, A.C. Pawlowski, K. Koteva & G.D. Wright, (2017) A Common Platform for Antibiotic Dereplication and Adjuvant Discovery. *Cell Chemical Biology* **24**: 98-109.
Cox, G., G.S. Thompson, H.T. Jenkins, F. Peske, A. Savelsbergh, M.V. Rodnina, W. Wintermeyer, S.W. Homans, T.A. Edwards & A.J. O'Neill, (2012) Ribosome clearance by FusB-type proteins mediates resistance to the antibiotic fusidic acid. *Proc Natl Acad Sci U S A* **109**: 2102-2107.
Craney, A., C. Ozimok, S.M. Pimentel-Elardo, A. Capretta & J.R. Nodwell, (2012) Chemical perturbation of secondary metabolism demonstrates important links to primary metabolism. *Chemistry & biology* **19**: 1020-1027.
Craster, H.L., C.A. Potter & S. Baumberg, (1999) End-product control of expression of branched-chain amino acid biosynthesis genes in *Streptomyces coelicolor* A3(2): paradoxical relationships between DNA sequence and regulatory phenotype. *Microbiology* **145 (Pt 9)**: 2375-2384.
Crooks, G.E., G. Hon, J.M. Chandonia & S.E. Brenner, (2004) WebLogo: a sequence logo generator. *Genome Res* **14**: 1188-1190.
Cuthbertson, L. & J.R. Nodwell, (2013) The TetR family of regulators. *Microbiol Mol Biol Rev* **77**: 440-475.
Czaplewski, L., R. Bax, M. Clokie, M. Dawson, H. Fairhead, V.A. Fischetti, S. Foster, B.F. Gilmore, R.E. Hancock, D. Harper, I.R. Henderson, K. Hilpert, B.V. Jones, A. Kadioglu, D. Knowles, S. Olafsdottir, D. Payne, S. Projan, S. Shaunak, J. Silverman, C.M. Thomas, T.J. Trust, P. Warn & J.H. Rex, (2016) Alternatives to antibiotics-a pipeline portfolio review. *Lancet Infect Dis* **16**: 239-251.
Darken, M.A., H. Berenson, R.J. Shirk & N.O. Sjolander, (1960) Production of tetracycline by *Streptomyces aureofaciens* in synthetic media. *Appl Microbiol* **8**: 46-51.

David, B., J.-L. Wolfender & D.A. Dias, (2015) The pharmaceutical industry and natural products: historical status and new trends. *Phytochemistry Reviews* **14**: 299-315.
Davies, J. & D. Davies, (2010) Origins and evolution of antibiotic resistance. *Microbiol Mol Biol Rev* **74**: 417-433.
Davis, K.M. & R.R. Isberg, (2016) Defining heterogeneity within bacterial populations via single cell approaches. *Bioessays* **38**: 782-790.
De Mattos, J.C., F.J. Dantas, A. Caldeira-de-Araujo & M.O. Moraes, (2004) Agarose gel electrophoresis system in the classroom: Detection of DNA strand breaks through the alteration of plasmid topology. *Biochem Mol Biol Educ* **32**: 254-257.
Decker, M.D. & K.M. Edwards, (2000) Acellular pertussis vaccines. *Pediatric Clinics of North America* **47**: 309-335.
Delogu, G., M. Sali & G. Fadda, (2013) The biology of *Mycobacterium tuberculosis* infection. *Mediterr J Hematol Infect Dis* **5**: e2013070.
Demain, A.L., (2010) Induction of microbial secondary metabolism. *International Microbiology* **1**: 259-264.
Den Hengst, C.D., N.T. Tran, M.J. Bibb, G. Chandra, B.K. Leskiw & M.J. Buttner, (2010) Genes essential for morphological development and antibiotic production in *Streptomyces coelicolor* are targets of BldD during vegetative growth. *Mol Microbiol* **78**: 361-379.
Deutscher, J., C. Francke & P.W. Postma, (2006) How phosphotransferase system-related protein phosphorylation regulates carbohydrate metabolism in bacteria. *Microbiol Mol Biol Rev* **70**: 939-1031.
Devasahayam, G., W.M. Scheld & P.S. Hoffman, (2010) Newer antibacterial drugs for a new century. *Expert Opin Investig Drugs* **19**: 215-234.
Dijkhuizen, L., M. Goodfellow, P.A. Hoskisson & I. Sutcliffe, (2008) Actinomycetologists: a vibrant and strong scientific community. Papers from the 14th International Symposium on the Biology of Actinomycetes. *Antonie van Leeuwenhoek* **94**: 1-2.
Donhofer, A., S. Franckenberg, S. Wickles, O. Berninghausen, R. Beckmann & D.N. Wilson, (2012) Structural basis for TetM-mediated tetracycline resistance. *Proc Natl Acad Sci U S A* **109**: 16900-16905.
Du, Y.-L., X.-L. Shen, P. Yu, L.-Q. Bai & Y.-Q. Li, (2011) Gamma-Butyrolactone regulatory system of *Streptomyces chattanoogensis* links nutrient utilization, metabolism, and development. *Applied and Environmental Microbiology* **77**: 8415-8426.
Edwards, H.S., R. Krishnakumar, A. Sinha, S.W. Bird, K.D. Patel & M.S. Bartsch, (2019) Real-Time Selective Sequencing with RUBRIC: Read Until with Basecall and Reference-Informed Criteria. *Scientific Reports* **9**: 1-11.
Einhauer, A. & A. Jungbauer, (2001) The FLAG peptide, a versatile fusion tag for the purification of recombinant proteins. *J Biochem Biophys Methods* **49**: 455-465.
Elliot, M.A., M.J. Bibb, M.J. Buttner & B.K. Leskiw, (2001) BldD is a direct regulator of key developmental genes in *Streptomyces coelicolor* A3(2). *Mol Microbiol* **40**: 257-269.
Es'haghi, Z., (2011) Photodiode array detection in clinical applications; quantitative analyte assay advantages, limitations and disadvantages. In: Photodiodes-Communications, Bio-Sensings, Measurements and High-Energy Physics. IntechOpen, pp. 25.
Etebu, E. & I. Arikekpar, (2016) Antibiotics: Classification and mechanisms of action with emphasis on molecular perspectives. *International Journal of Applied Microbiology and Biotechnology Research* **4**: 90-101.
Euverink, G.J.W., (1995) Biosynthesis of phenylalanine and tyrosine in the methylotrophic actinomycete Amycolatopsis methanolica. In.: Rijksuniversiteit Groningen, pp.160.
Farnham, P.J., (2009) Insights from genomic profiling of transcription factors. *Nat Rev Genet* **10**: 605-616.

Fenton, A.K. & K. Gerdes, (2013) Direct interaction of FtsZ and MreB is required for septum synthesis and cell division in *Escherichia coli*. *Embo j* **32**: 1953-1965.
Fernandez-Moreno, M.A., J.L. Caballero, D.A. Hopwood & F. Malpartida, (1991) The *act* cluster contains regulatory and antibiotic export genes, direct targets for translational control by the bldA tRNA gene of *Streptomyces*. *Cell* **66**: 769-780.
Fernández, L., E.B. Breidenstein, D. Song & R.E. Hancock, (2012) Role of intracellular proteases in the antibiotic resistance, motility, and biofilm formation of *Pseudomonas aeruginosa*. *Antimicrob Agents Chemother* **56**: 1128-1132.
Fernández, L. & R.E.W. Hancock, (2012) Adaptive and Mutational Resistance: Role of Porins and Efflux Pumps in Drug Resistance. *Clinical Microbiology Reviews* **25**: 661-681.
Ferreira, L.G., R.N. Dos Santos, G. Oliva & A.D. Andricopulo, (2015) Molecular docking and structure-based drug design strategies. *Molecules* **20**: 13384-13421.
Finch, R.G., D. Greenwood, R.J. Whitley & S.R. Norrby, (2010) Antibiotic and Chemotherapy. *Elsevier Health Sciences*: pp 1-9.
Fischbach, M.A. & C.T. Walsh, (2009) Antibiotics for Emerging Pathogens. *Science* **325**: 1089-1093.
Fischetti, V.A., (2018) Development of Phage Lysins as Novel Therapeutics: A Historical Perspective. *Viruses* **10**.
Fiuza, M., M.J. Canova, D. Patin, M. Letek, I. Zanella-Cléon, M. Becchi, L.M. Mateos, D. Mengin-Lecreulx, V. Molle & J.A. Gil, (2008) The MurC ligase essential for peptidoglycan biosynthesis is regulated by the serine/threonine protein kinase PknA in *Corynebacterium glutamicum*. *J Biol Chem* **283**: 36553-36563.
Flärdh, K. & M.J. Buttner, (2009) *Streptomyces* morphogenetics: dissecting differentiation in a filamentous bacterium. *Nature Reviews Microbiology* **7**: 36-49.
Fleming, A., (1919) The action of chemical and physiological antiseptics in a septic wound. *BJS* **7**: 99-129.
Fleming, A.G., (1929) Responsibilities and Opportunities of the Private Practitioner in Preventive Medicine. *Can Med Assoc J* **20**: 11-13.
Floriano, B. & M. Bibb, (1996) *afsR* is a pleiotropic but conditionally required regulatory gene for antibiotic production in *Streptomyces coelicolor* A3(2). *Mol Microbiol* **21**: 385-396.
Forde, G.M., S. Ghose, N.K. Slater, A.V. Hine, R.A. Darby & A.G. Hitchcock, (2006) LacO-LacI interaction in affinity adsorption of plasmid DNA. *Biotechnol Bioeng* **95**: 67-75.
Franzen, C., (2008) Syphilis in composers and musicians—Mozart, Beethoven, Paganini, Schubert, Schumann, Smetana. *European Journal of Clinical Microbiology & Infectious Diseases* **27**: 1151-1157.
Fuerst, T.R., M.P. Fernandez & B. Moss, (1989) Transfer of the inducible lac repressor/operator system from *Escherichia coli* to a vaccinia virus expression vector. *Proc Natl Acad Sci U S A* **86**: 2549-2553.
Furfaro, L.L., M.S. Payne & B.J. Chang, (2018) Bacteriophage Therapy: Clinical Trials and Regulatory Hurdles. *Frontiers in Cellular and Infection Microbiology* **8**.
Fyfe, C., T.H. Grossman, K. Kerstein & J. Sutcliffe, (2016) Resistance to Macrolide Antibiotics in Public Health Pathogens. *Cold Spring Harb Perspect Med* **6**.
Gabrielson, S.W., (2018) SciFinder. *Journal of the Medical Library Association : JMLA* **106**: 588-590.
Gago, F., (1998) Stacking interactions and intercalative DNA binding. *Methods* **14**: 277-292.
Galm, U. & B. Shen, (2006) Expression of biosynthetic gene clusters in heterologous hosts for natural product production and combinatorial biosynthesis. *Expert Opin Drug Discov* **1**: 409-437.
Gaynes, R., (2017) The Discovery of Penicillin—New Insights After More Than 75 Years of Clinical Use. *Emerging Infectious Diseases* **23(5):849–853**.

Gerdes, K. & E. Maisonneuve, (2012) Bacterial persistence and toxin-antitoxin loci. *Annu Rev Microbiol* **66**: 103-123.

Goecks, J., A. Nekrutenko & J. Taylor, (2010) Galaxy: a comprehensive approach for supporting accessible, reproducible, and transparent computational research in the life sciences. *Genome Biol* **11**: R86.

Gomez-Escribano, J.P. & M.J. Bibb, (2011) Engineering *Streptomyces coelicolor* for heterologous expression of secondary metabolite gene clusters. *Microb Biotechnol* **4**: 207-215.

Gould, K., (2016) Antibiotics: from prehistory to the present day. *Journal of Antimicrobial Chemotherapy* **71**: 572-575.

Gray, A.N., B.M. Koo, A.L. Shiver, J.M. Peters, H. Osadnik & C.A. Gross, (2015) High-throughput bacterial functional genomics in the sequencing era. *Curr Opin Microbiol* **27**: 86-95.

Gross, M., (2013) Antibiotics in crisis. *Current Biology* **23**: R1063-R1065.

Haiser, H.J., M.R. Yousef & M.A. Elliot, (2009) Cell Wall Hydrolases Affect Germination, Vegetative Growth, and Sporulation in *Streptomyces coelicolor*. *Journal of Bacteriology* **191**: 6501-6512.

Halabalaki, M., K. Vougogiannopoulou, E. Mikros & A.L. Skaltsounis, (2014) Recent advances and new strategies in the NMR-based identification of natural products. *Current Opinion in Biotechnology* **25**: 1-7.

Han, Y., S. Gras & G.M. Forde, (2009) Binding properties of peptidic affinity ligands for plasmid DNA capture and detection. *AIChE Journal* **55**: 505-515.

Harro, J.M., B.M. Peters, G.A. O'May, N. Archer, P. Kerns, R. Prabhakara & M.E. Shirtliff, (2010) Vaccine development in *Staphylococcus aureus*: taking the biofilm phenotype into consideration. *Pathogens and Disease* **59**: 306-323.

Hartmann, R.K., M. Goessringer, B. Spaeth, S. Fischer & A. Marchfelder, (2009) The making of tRNAs and more–RNase P and tRNase Z. *Progress in molecular biology and translational science* **85**: 319-368.

Hasan, A., (2015) Specific and global networks of gene regulation in *streptomyces coelicolor*. In: School of Molecular and Cellular Biology. Leeds: Leeds University, pp. 146.

Hasani, A., A. Kariminik & K. Issazadeh, (2014) Streptomycetes: characteristics and their antimicrobial activities. *Int J Adv Biol Biomed Res* **2**: 63-75.

Hassoun, A., P.K. Linden & B. Friedman, (2017) Incidence, prevalence, and management of MRSA bacteremia across patient populations-a review of recent developments in MRSA management and treatment. *Crit Care* **21**: 211.

Hawkey, P.M., (2003) Mechanisms of quinolone action and microbial response. *J Antimicrob Chemother* **51 Suppl 1**: 29-35.

Heller, D.P. & C.L. Greenstock, (1994) Fluorescence lifetime analysis of DNA intercalated ethidium bromide and quenching by free dye. *Biophys Chem* **50**: 305-312.

Helmann, J.D., (2002) The extracytoplasmic function (ECF) sigma factors. *Adv Microb Physiol* **46**: 47-110.

Heras, B., M.J. Scanlon & J.L. Martin, (2015) Targeting virulence not viability in the search for future antibacterials. *Br J Clin Pharmacol* **79**: 208-215.

Hernandez, V., T. Crépin, A. Palencia, S. Cusack, T. Akama, S.J. Baker, W. Bu, L. Feng, Y.R. Freund, L. Liu, M. Meewan, M. Mohan, W. Mao, F.L. Rock, H. Sexton, A. Sheoran, Y. Zhang, Y.-K. Zhang, Y. Zhou, J.A. Nieman, M.R. Anugula, E.M. Keramane, K. Savariraj, D.S. Reddy, R. Sharma, R. Subedi, R. Singh, A. O'Leary, N.L. Simon, P.L. De Marsh, S. Mushtaq, M. Warner, D.M. Livermore, M.R.K. Alley & J.J. Plattner, (2013) Discovery of a Novel Class of Boron-Based Antibacterials with Activity against Gram-Negative Bacteria. *Antimicrobial Agents and Chemotherapy* **57**: 1394-1403.

Hiard, S., R. Maree, S. Colson, P.A. Hoskisson, F. Titgemeyer, G.P. van Wezel, B. Joris, L. Wehenkel & S. Rigali, (2007) PREDetector: a new tool to identify regulatory elements in bacterial genomes. *Biochem Biophys Res Commun* **357**: 861-864.

Hillen, W. & C. Berens, (1994) Mechanisms underlying expression of Tn10 encoded tetracycline resistance. *Annu Rev Microbiol* **48**: 345-369.

Hillerich, B. & J. Westpheling, (2008) A new TetR family transcriptional regulator required for morphogenesis in *Streptomyces coelicolor*. *J Bacteriol* **190**: 61-67.

Hirano, S., K. Tanaka, Y. Ohnishi & S. Horinouchi, (2008) Conditionally positive effect of the TetR-family transcriptional regulator AtrA on streptomycin production by *Streptomyces griseus*. *Microbiology-Sgm* **154**: 905-914.

Hobbs, G., C. M. Frazer, D. C. J. Gardner, F. Flett & S. G. Oliver, (1990) Pigmented antibiotic production by *Streptomyces coelicolor A3(2): Kinetics and the influence of nutrients,* p. 2291-2296.

Hojati, Z., C. Milne, B. Harvey, L. Gordon, M. Borg, F. Flett, B. Wilkinson, P.J. Sidebottom, B.A. Rudd, M.A. Hayes, C.P. Smith & J. Micklefield, (2002) Structure, biosynthetic origin, and engineered biosynthesis of calcium-dependent antibiotics from *Streptomyces* coelicolor. *Chem Biol* **9**: 1175-1187.

Hong, B., S. Phornphisutthimas, E. Tilley, S. Baumberg & K.J. McDowall, (2007) *Streptomycin* production by *Streptomyces griseus* can be modulated by a mechanism not associated with change in the adpA component of the A-factor cascade. *Biotechnol Lett* **29**: 57-64.

Hopwood, D.A., (1997) Genetic contributions to understanding polyketide synthases. *Chem Rev* **97**: 2465-2498.

Hopwood, D.A., M.J. Bibb, K.E. Chater, T. Kieser, C.J. Bruton, H.M. Kieser, D.J. Lydiate, C.P. Smith, J.M. Ward & H. Schrempf, (1985) Genetic Manipulation of *Streptomyces* : A Laboratory Manual. *The John Innes Foundation Norwich.*

Hopwood, D.A., K.F. Chater & M.J. Bibb, (1995) Genetics of antibiotic production in *Streptomyces coelicolor* A3(2), a model streptomycete. *Biotechnology* **28**: 65-102.

Horsburgh, M.J., J.L. Aish, I.J. White, L. Shaw, J.K. Lithgow & S.J. Foster, (2002) sigmaB modulates virulence determinant expression and stress resistance: characterization of a functional rsbU strain derived from *Staphylococcus aureus* 8325-4. *J Bacteriol* **184**: 5457-5467.

Hosie, A.H., D. Allaway, C.S. Galloway, H.A. Dunsby & P.S. Poole, (2002) Rhizobium leguminosarum has a second general amino acid permease with unusually broad substrate specificity and high similarity to branched-chain amino acid transporters (Bra/LIV) of the ABC family. *J Bacteriol* **184**: 4071-4080.

Hover, B.M., S.-H. Kim, M. Katz, Z. Charlop-Powers, J.G. Owen, M.A. Ternei, J. Maniko, A.B. Estrela, H. Molina, S. Park, D.S. Perlin & S.F. Brady, (2018) Culture-independent discovery of the malacidins as calcium-dependent antibiotics with activity against multidrug-resistant Gram-positive pathogens. *Nature Microbiology* **3**: 415-422.

Hubert, J., J.-M. Nuzillard & J.-H. Renault, (2017) Dereplication strategies in natural product research: How many tools and methodologies behind the same concept? *Phytochemistry Reviews* **16**: 55-95.

Hughes, D. & A. Karlén, (2014) Discovery and preclinical development of new antibiotics. *Ups J Med Sci* **119**: 162-169.

Hurdle, J.G., A.J. O'Neill & I. Chopra, (2005) Prospects for Aminoacyl-tRNA Synthetase Inhibitors as New Antimicrobial Agents. *Antimicrobial Agents and Chemotherapy* **49**: 4821-4833.

Ibba, M. & D. Soll, (2000) Aminoacyl-tRNA synthesis*. Annual review of biochemistry* **69**: 617-650.

Irazoki, O., A. Mayola, S. Campoy & J. Barbé, (2016) SOS system induction inhibits the assembly of chemoreceptor signaling clusters in Salmonella enterica. *PloS one* 11: e0146685.

Jacob, F. & J. Monod, (1959) Genes of structure and genes of regulation in the biosynthesis of proteins. *C R Hebd Seances Acad Sci* **249**: 1282-1284.
Jacob, F. & J. Monod, (1961) Genetic regulatory mechanisms in the synthesis of proteins. *Journal of Molecular Biology* **3**: 318-356.
Janion, C., (2008) Inducible SOS response system of DNA repair and mutagenesis in *Escherichia coli*. *International journal of biological sciences* **4**: 338.
Jao, C.Y. & A. Salic, (2008) Exploring RNA transcription and turnover *in vivo* by using click chemistry. *Proceedings of the National Academy of Sciences* **105**: 15779-15784.
Jones, A.C., B. Gust, A. Kulik, L. Heide, M.J. Buttner & M.J. Bibb, (2013) Phage p1-derived artificial chromosomes facilitate heterologous expression of the FK506 gene cluster. *PLoS One* **8**: e69319.
Karageorgis, G., M. Dow, A. Aimon, S. Warriner & A. Nelson, (2015) Activity-Directed Synthesis with Intermolecular Reactions: Development of a Fragment into a Range of Androgen Receptor Agonists. *Angewandte Chemie International Edition* **54**: 13538-13544.
Karimi Goftar, M., N. Moradi Kor & Z. Moradi Kor, (2014) DNA Intercalators and Using Them as Anticancer Drugs. *International Journal of Advanced Biological and Biomedical Research* **2**: 811-822.
Kawai, K., G. Wang, S. Okamoto & K. Ochi, (2007) The rare earth, scandium, causes antibiotic overproduction in *Streptomyces* spp. *FEMS Microbiol Lett* **274**: 311-315.
Khani, A., N. Popp, B. Kreikemeyer & N. Patenge, (2018) A Glycine Riboswitch in *Streptococcus pyogenes* Controls Expression of a Sodium:Alanine Symporter Family Protein Gene. *Front Microbiol* **9**: 200.
Kieser, T., M.J. Bibb, M.J. Buttner, K.F. Chater & D.A. Hopwood, (2000) Practical *Streptomyces* Genetics*,* p. 613. The John Innes Foundation, Norwich.
Kim, S.H., B.A. Traag, A.H. Hasan, K.J. McDowall, B.-G. Kim & G.P. van Wezel, (2015) Transcriptional analysis of the cell division-related *ssg* genes in *Streptomyces coelicolor* reveals direct control of *ssgR* by AtrA. *Antonie van Leeuwenhoek* **108**: 201-213.
Kinashi, H., M. Shimaji & A. Sakai, (1987) Giant linear plasmids in *Streptomyces* which code for antibiotic biosynthesis genes. *Nature* **328**: 454-456.
Kirby, R. & D.A. Hopwood, (1977) Genetic determination of methylenomycin synthesis by the SCP1 plasmid of *Streptomyces coelicolor* A3(2). *J Gen Microbiol* **98**: 239-252.
Klein, E., D.L. Smith & R. Laxminarayan, (2007) Hospitalizations and deaths caused by methicillin-resistant *Staphylococcus aureus*, United States, 1999-2005. *Emerg Infect Dis* **13**: 1840-1846.
Koba, M. & J. Konopa, (2005) Actinomycin D and its mechanisms of action. *Postepy Hig Med Dosw (Online)* **59**: 290-298.
Komatsu, M., T. Uchiyama, S. Ōmura, D.E. Cane & H. Ikeda, (2010) Genome-minimized *Streptomyces* host for the heterologous expression of secondary metabolism. *Proceedings of the National Academy of Sciences* **107**: 2646-2651.
Kouprina, N. & V. Larionov, (2016) Transformation-associated recombination (TAR) cloning for genomics studies and synthetic biology. *Chromosoma* **125**: 621-632.
Krasny, L., T. Vacik, V. Fucik & J. Jonak, (2000) Cloning and characterization of the *str* operon and elongation factor Tu expression in *Bacillus stearothermophilus*. *J Bacteriol* **182**: 6114-6122.
Krause, K.M., A.W. Serio, T.R. Kane & L.E. Connolly, (2016) Aminoglycosides: an overview. *Cold Spring Harbor perspectives in medicine* **6**: a027029.
Kuhlmann, A.U. & E. Bremer, (2002) Osmotically regulated synthesis of the compatible solute ectoine in *Bacillus pasteuri*i and related *Bacillus* spp. *Appl Environ Microbiol* **68**: 772-783.

Kumari, S., P. Priya, G. Misra & G. Yadav, (2013) Structural and biochemical perspectives in plant isoprenoid biosynthesis. *Phytochemistry Reviews* **12**.
Kunin, V., A. Copeland, A. Lapidus, K. Mavromatis & P. Hugenholtz, (2008) A bioinformatician's guide to metagenomics. *Microbiol Mol Biol Rev* **72**: 557-578, Table of Contents.
L Ramos, J., M. Martínez-Bueno, A. J Molina-Henares, W. Teran, K. Watanabe, X. Zhang, M.-T. Gallegos, R. Brennan & R. Tobes, (2005) The TetR Family of Transcriptional Repressors. *Microbiology and molecular biology reviews : MMBR* **69**: 326-356.
Lange, B.M., T. Rujan, W. Martin & R. Croteau, (2000) Isoprenoid biosynthesis: the evolution of two ancient and distinct pathways across genomes. *Proc Natl Acad Sci U S A* **97**: 13172-13177.
Langmead, B. & S.L. Salzberg, (2012) Fast gapped-read alignment with Bowtie 2. *Nature methods* **9**: 357-359.
Lawlor, E.J., H.A. Baylis & K.F. Chater, (1987) Pleiotropic morphological and antibiotic deficiencies result from mutations in a gene encoding a tRNA-like product in *Streptomyces coelicolor* A3(2). *Genes Dev* **1**: 1305-1310.
Lee, D.J., S.D. Minchin & S.J. Busby, (2012) Activating transcription in bacteria. *Annual review of microbiology* **66**: 125-152.
Leggett, J.E., (2017) Aminoglycosides. In: Infectious Diseases (Fourth Edition). J. Cohen, W.G. Powderly & S.M. Opal (eds). Elsevier, pp. 1233-1238.e1231.
León, M.J., T. Hoffmann, C. Sánchez-Porro, J. Heider, A. Ventosa & E. Bremer, (2018) Compatible solute synthesis and import by the moderate halophile *spiribacter salinus*: Physiology and Genomics. *Frontiers in Microbiology* **9**.
Lerman, L.S., (1961) Structural considerations in the interaction of DNA and acridines. *Journal of Molecular Biology* **3**: 18-IN14.
Levine, D.P., (2006) Vancomycin: a history. *Clin Infect Dis* **42 Suppl 1**: S5-12.
Lewis, K., (2013) Platforms for antibiotic discovery. *Nat Rev Drug Discov* **12**: 371-387.
Lewis, L., R.M. Daniel & T. Coolbear, (2003) Detection and impact of protease and lipase activities in milk and milk powders. *International Dairy Journal* **13**: 255-275.
Lewis, M., (2005) The lac repressor. *C R Biol* **328**: 521-548.
Li, S., J. Wang, X. Li, S. Yin, W. Wang & K. Yang, (2015a) Genome-wide identification and evaluation of constitutive promoters in *streptomycetes*. *Microb Cell Fact* **14**: 172.
Li, W., G.C. Atkinson, N.S. Thakor, U. Allas, C.C. Lu, K.Y. Chan, T. Tenson, K. Schulten, K.S. Wilson, V. Hauryliuk & J. Frank, (2013) Mechanism of tetracycline resistance by ribosomal protection protein Tet(O). *Nat Commun* **4**: 1477.
Li, W., J. Wu, W. Tao, C. Zhao, Y. Wang, X. He, G. Chandra, X. Zhou, Z. Deng, K.F. Chater & M. Tao, (2007) A genetic and bioinformatic analysis of *Streptomyces coelicolor* genes containing TTA codons, possible targets for regulation by a developmentally significant tRNA. *FEMS Microbiology Letters* **266**: 20-28.
Li, X., T. Yu, Q. He, K.J. McDowall, B. Jiang, Z. Jiang, L. Wu, G. Li, Q. Li, S. Wang, Y. Shi, L. Wang & B. Hong, (2015b) Binding of a biosynthetic intermediate to AtrA modulates the production of lidamycin by *Streptomyces globisporus*. *Molecular Microbiology* **96**: 1257-1271.
Li, Z., Z. Xiang, J. Zeng, Y. Li & J. Li, (2019) A GntR Family Transcription Factor in *Streptococcus mutans* Regulates Biofilm Formation and Expression of Multiple Sugar Transporter Genes. *Frontiers in Microbiology* **9**.
Li, Z.L., Y.H. Wang, J. Chu, Y.P. Zhuang & S.L. Zhang, (2009) Effect of branched-chain amino acids, valine, isoleucine and leucine on the biosythesis of bitespiramycin 4"-O-acylspiramycins. *Braz J Microbiol* **40**: 734-746.
Lin, Y.-f., D.R. A, S. Guan, L. Mamanova & K.J. McDowall, (2013) A combination of improved differential and global RNA-seq reveals pervasive transcription initiation and events in all stages of the life-cycle of functional RNAs in

Propionibacterium acnes, a major contributor to wide-spread human disease. *BMC Genomics* **14**: 620.
Ling, L.L., T. Schneider, A.J. Peoples, A.L. Spoering, I. Engels, B.P. Conlon, A. Mueller, T.F. Schäberle, D.E. Hughes & S. Epstein, (2015) A new antibiotic kills pathogens without detectable resistance. *Nature* **517**: 455.
Lipsitch, M. & G.R. Siber, (2016) How Can Vaccines Contribute to Solving the Antimicrobial Resistance Problem? *MBio* **7**.
Liu, S., H. Dai, C. Heering, C. Janiak, W. Lin, Z. Liu & P. Proksch, (2017) Inducing new secondary metabolites through co-cultivation of the fungus Pestalotiopsis sp. with the bacterium Bacillus subtilis. *Tetrahedron Letters* **58**: 257-261.
Liu, W., F. Sun & Y. Hu, (2018) Genome Mining-Mediated Discovery of a New Avermipeptin Analogue in *Streptomyces actuosus* ATCC 25421. **7**: 558-561.
Livermore, D.M., (2004) The need for new antibiotics. *Clin Microbiol Infect* **10 Suppl 4**: 1-9.
Lodhi, A.F., Y. Zhang, M. Adil & Y. Deng, (2018) Antibiotic discovery: combining isolation chip (iChip) technology and co-culture technique. *Applied Microbiology and Biotechnology* **102**: 7333-7341.
Love, M.I., W. Huber & S. Anders, (2014) Moderated estimation of fold change and dispersion for RNA-seq data with DESeq2. *Genome Biol* **15**: 550.
MacNeil, D.J., K.M. Gewain, C.L. Ruby, G. Dezeny, P.H. Gibbons & T. MacNeil, (1992) Analysis of *Streptomyces avermitilis* genes required for avermectin biosynthesis utilizing a novel integration vector. *Gene* **111**: 61-68.
Mak, S. & J.R. Nodwell, (2017) Actinorhodin is a redox-active antibiotic with a complex mode of action against Gram-positive cells. **106**: 597-613.
Manteca, A., U. Mäder, B.A. Connolly & J. Sanchez, (2006) A proteomic analysis of *Streptomyces coelicolor* programmed cell death. *Proteomics* **6**: 6008-6022.
Marsh, I., (2002) Easing the chemistry bottleneck: careers in high-throughput chemistry. *Nature Reviews Drug Discovery* **1**: 925-925.
Martin, E.W. & M.H. Sung, (2018) Challenges of Decoding Transcription Factor Dynamics in Terms of Gene Regulation. *Cells* **7**.
Martínez-Burgo, Y., J. Santos-Aberturas, A. Rodríguez-García, E.G. Barreales, J.R. Tormo, A.W. Truman, F. Reyes, J.F. Aparicio & P. Liras, (2019) Activation of Secondary Metabolite Gene Clusters in *Streptomyces clavuligerus* by the PimM Regulator of *Streptomyces* natalensis. *Front Microbiol* **10**: 580.
Martz, W.W., (1971) The interaction of ethidium bromide with nucleic acids. In.: Loyola University, pp. 241.
McHenry, C.S., (1985) DNA polymerase III holoenzyme of *Escherichia coli*: Components and function of a true replicative complex. *Molecular and Cellular Biochemistry* **66**: 71-85.
McKenzie, N.L. & J.R. Nodwell, (2007) Phosphorylated AbsA2 negatively regulates antibiotic production in *Streptomyces coelicolor* through interactions with pathway-specific regulatory gene promoters. *J Bacteriol* **189**: 5284-5292.
Meier, I., L.V. Wray & W. Hillen, (1988) Differential regulation of the Tn10-encoded tetracycline resistance genes tetA and tetR by the tandem tet operators O1 and O2. *Embo j* **7**: 567-572.
Meyer, E.E., K.J. Rosenberg & J. Israelachvili, (2006) Recent progress in understanding hydrophobic interactions. *Proceedings of the National Academy of Sciences* **103**: 15739-15746.
Miao, V., M.F. Coeffet-Legal, P. Brian, R. Brost, J. Penn, A. Whiting, S. Martin, R. Ford, I. Parr, M. Bouchard, C.J. Silva, S.K. Wrigley & R.H. Baltz, (2005) Daptomycin biosynthesis in *Streptomyces roseosporus*: cloning and analysis of the gene cluster and revision of peptide stereochemistry. *Microbiology* **151**: 1507-1523.
Mingeot-Leclercq, M.P., Y. Glupczynski & P.M. Tulkens, (1999) Aminoglycosides: activity and resistance. *Antimicrob Agents Chemother* **43**: 727-737.

Mitchenall, L.A., R.E. Hipkin, M.M. Piperakis, N.P. Burton & A. Maxwell, (2018) A rapid high-resolution method for resolving DNA topoisomers. *BMC research notes* **11**: 37.

Moore, J.M., E. Bradshaw, R.F. Seipke, M.I. Hutchings & M. McArthur, (2012) Use and discovery of chemical elicitors that stimulate biosynthetic gene clusters in *Streptomyces* bacteria. In: Methods in enzymology. Elsevier, pp. 367-385.

Mrázek, J. & A.C. Karls, (2019) In silico simulations of occurrence of transcription factor binding sites in bacterial genomes. *BMC Evol Biol* **19**: 67.

Munita, J.M. & C.A. Arias, (2016) Mechanisms of Antibiotic Resistance. *Microbiol Spectr* **4**.

Munnoch, J.T., D.A. Widdick, G. Chandra, I.C. Sutcliffe, T. Palmer & M.I. Hutchings, (2016) Cosmid based mutagenesis causes genetic instability in *Streptomyces coelicolor*, as shown by targeting of the lipoprotein signal peptidase gene. *Scientific Reports* **6**: 29495.

Muñoz-López, M. & J.L. García-Pérez, (2010) DNA transposons: nature and applications in genomics. *Curr Genomics* **11**: 115-128.

Nass, N.M., S. Farooque, C. Hind, M.E. Wand, C.P. Randall, J.M. Sutton, R.F. Seipke, C.M. Rayner & A.J. O'Neill, (2017) Revisiting unexploited antibiotics in search of new antibacterial drug candidates: the case of γ-actinorhodin. *Scientific Reports* **7**: 17419.

Neto, B.A. & A.A. Lapis, (2009) Recent developments in the chemistry of deoxyribonucleic acid (DNA) intercalators: principles, design, synthesis, applications and trends. *Molecules* **14**: 1725-1746.

Nguyen, T.M., C. Seo, M. Ji, M.-J. Paik, S.-W. Myung & J. Kim, (2018) Effective soil extraction method for cultivating previously uncultured soil bacteria. *Applied and Environmental Microbiology* **84**: e01145-01118.

Ni, L., C. Bruce, C. Hart, J. Leigh-Bell, D. Gelperin, L. Umansky, M.B. Gerstein & M. Snyder, (2009) Dynamic and complex transcription factor binding during an inducible response in yeast. *Genes Dev* **23**: 1351-1363.

Nichols, D., N. Cahoon, E.M. Trakhtenberg, L. Pham, A. Mehta, A. Belanger, T. Kanigan, K. Lewis & S.S. Epstein, (2010) Use of Ichip for High-Throughput in situ cultivation of "uncultivable" microbial species. *Applied and Environmental Microbiology* **76**: 2445-2450.

Nielsen, K., M. Månsson, C. Rank, J. Frisvad & T.O. Larsen, (2011) Dereplication of microbial natural products by LC-DAD-TOFMS. **74**: 2338-2348.

Nodwell, J.R., K. McGovern & R. Losick, (1996) An oligopeptide permease responsible for the import of an extracellular signal governing aerial mycelium formation in *Streptomyces coelicolor*. *Molecular Microbiology* **22**: 881-893.

Nothaft, H., S. Rigali, B. Boomsma, M. Swiatek, K.J. McDowall, G.P. Van Wezel & F. Titgemeyer, (2010) The permease gene *nagE2* is the key to N-acetylglucosamine sensing and utilization in *Streptomyces coelicolor* and is subject to multi-level control. *Mol Microbiol* **75**: 1133-1144.

O'Donnell, M., L. Langston & B. Stillman, (2013) Principles and concepts of DNA replication in bacteria, archaea, and eukarya. *Cold Spring Harb Perspect Biol* **5**.

O'Neill, A.J. & I. Chopra, (2006) Molecular basis of fusB-mediated resistance to fusidic acid in Staphylococcus aureus. *Mol Microbiol* **59**: 664-676.

O'Neill, J., (2016) Vaccines and alternative approaches: Reducing our dependence on antimicrobials. *Proceedings on review of antimicrobial resistance (tackling drug-resistant infections globally)*: 1-29.

Ochi, K., (2007) From microbial differentiation to ribosome engineering. *Bioscience Biotechnology and Biochemistry* **71**: 1373-1386.

Ochi, K., S. Okamoto, Y. Tozawa, T. Inaoka, T. Hosaka, J. Xu & K. Kurosawa, (2004) Ribosome Engineering and Secondary Metabolite Production. *Advances in applied microbiology* **56**: 155-184.

Ohnishi, Y., J.-W. Seo & S. Horinouchi, (2002) Deprogrammed sporulation in *Streptomyces*. *FEMS Microbiology Letters* **216**: 1-7.

Ohnishi, Y., H. Yamazaki, J.Y. Kato, A. Tomono & S. Horinouchi, (2005) AdpA, a central transcriptional regulator in the A-factor regulatory cascade that leads to morphological development and secondary metabolism in *Streptomyces griseus*. *Biosci Biotechnol Biochem* **69**: 431-439.

Okada, B.K. & M.R. Seyedsayamdost, (2017) Antibiotic dialogues: induction of silent biosynthetic gene clusters by exogenous small molecules. *FEMS Microbiol Rev* **41**: 19-33.

Okamoto, S., A. Lezhava, T. Hosaka, Y. Okamoto-Hosoya & K. Ochi, (2003) Enhanced expression of S-adenosylmethionine synthetase causes overproduction of actinorhodin in *Streptomyces coelicolor* A3 (2). *Journal of bacteriology* **185**: 601-609.

Olmsted, J., 3rd & D.R. Kearns, (1977) Mechanism of ethidium bromide fluorescence enhancement on binding to nucleic acids. *Biochemistry* **16**: 3647-3654.

Osada, H., (2016) Chemical and biological studies of reveromycin A. *The Journal Of Antibiotics* **69**: 723.

Pan, Y.H., Y. Zhang, J. Cui, Y. Liu, B.M. McAllan, C.C. Liao & S. Zhang, (2013) Adaptation of phenylalanine and tyrosine catabolic pathway to hibernation in bats. *PLoS One* **8**: e62039.

Park, D.M., M.S. Akhtar, A.Z. Ansari, R. Landick & P.J. Kiley, (2013) The bacterial response regulator ArcA uses a diverse binding site architecture to regulate carbon oxidation globally. *PLoS Genet* **9**: e1003839.

Parthasarathy, A., P.J. Cross, R.C.J. Dobson, L.E. Adams, M.A. Savka & A.O. Hudson, (2018) A Three-Ring Circus: Metabolism of the Three Proteogenic Aromatic Amino Acids and Their Role in the Health of Plants and Animals. *Frontiers in Molecular Biosciences* **5**.

Pertea, M., G.M. Pertea, C.M. Antonescu, T.C. Chang, J.T. Mendell & S.L. Salzberg, (2015) StringTie enables improved reconstruction of a transcriptome from RNA-seq reads. **33**: 290-295.

Peterson, C.T., V. Sharma, S.N. Iablokov, L. Albayrak, K. Khanipov, S. Uchitel, D. Chopra, P.J. Mills, Y. Fofanov, D.A. Rodionov & S.N. Peterson, (2019) 16S rRNA gene profiling and genome reconstruction reveal community metabolic interactions and prebiotic potential of medicinal herbs used in neurodegenerative disease and as nootropics. *PLoS One* **14**: e0213869.

Peterson, L.R., (2008) Currently available antimicrobial agents and their potential for use as monotherapy. *Clin Microbiol Infect* **14 Suppl 6**: 30-45.

Pham, V. & J. Kim, (2016) Improvement for Isolation of Soil Bacteria by Using Common Culture Media. *Journal of Pure and Applied Microbiology* **10**.

Pillai, S.K., R. Moellering & G.M. Eliopoulos, (2005) Antimicrobial combinations. *Antibiotics in laboratory medicine* **5**: 365-440.

Pires, D.P., S. Cleto, S. Sillankorva, J. Azeredo & T.K. Lu, (2016) Genetically Engineered Phages: a Review of Advances over the Last Decade. *Microbiology and Molecular Biology Reviews* **80**: 523-543.

Poiata, E., M.M. Meyer, T.D. Ames & R.R. Breaker, (2009) A variant riboswitch aptamer class for S-adenosylmethionine common in marine bacteria. *Rna* **15**: 2046-2056.

Pool, M.R., (2005) Signal recognition particles in chloroplasts, bacteria, yeast and mammals (review). *Mol Membr Biol* **22**: 3-15.

Porath, J., J.A.N. Carlsson, I. Olsson & G. Belfrage, (1975) Metal chelate affinity chromatography, a new approach to protein fractionation. *Nature* **258**: 598-599.

Potter, C.A. & S. Baumberg, (1996) End-product control of enzymes of branched-chain amino acid biosynthesis in *Streptomyces coelicolor*. *Microbiology* **142 (Pt 8)**: 1945-1952.

Principi, N. & S. Esposito, (2016) Prevention of Community-Acquired Pneumonia with Available Pneumococcal Vaccines. *Int J Mol Sci* **18**.

Pulschen, A.A., A.G. Bendia, A.D. Fricker, V.H. Pellizari, D. Galante & F. Rodrigues, (2017) Isolation of Uncultured Bacteria from Antarctica Using Long Incubation Periods and Low Nutritional Media. **8**.

Pye, C.R., M.J. Bertin, R.S. Lokey, W.H. Gerwick & R.G. Linington, (2017) Retrospective analysis of natural products provides insights for future discovery trends. *Proceedings of the National Academy of Sciences*: 201614680.

Quackenbush, J., (2002) Microarray data normalization and transformation. *Nature genetics* **32**: 496-501

Radakovits, R., R.E. Jinkerson, A. Darzins & M.C. Posewitz, (2010) Genetic Engineering of Algae for Enhanced Biofuel Production. *Eukaryotic Cell* **9**: 486-501.

Ramani, V., J. Shendure & Z. Duan, (2016) Understanding Spatial Genome Organization: Methods and Insights. *Genomics Proteomics Bioinformatics* **14**: 7-20.

Ramirez, F., F. Dundar, S. Diehl, B.A. Gruning & T. Manke, (2014) deepTools: a flexible platform for exploring deep-sequencing data. *Nucleic acids research* **42**: W187-191.

Ramos, J.L., M. Martínez-Bueno, A.J. Molina-Henares, W. Terán, K. Watanabe, X. Zhang, M.T. Gallegos, R. Brennan & R. Tobes, (2005) The TetR family of transcriptional repressors. *Microbiol Mol Biol Rev* **69**: 326-356.

Randall, C.P., D. Rasina, A. Jirgensons & A.J. O'Neill, (2016) Targeting Multiple Aminoacyl-tRNA Synthetases Overcomes the Resistance Liabilities Associated with Antibacterial Inhibitors Acting on a Single Such Enzyme. *Antimicrobial Agents and Chemotherapy* **60**: 6359-6361.

Rath, A. & C.M. Deber, (2013) Correction factors for membrane protein molecular weight readouts on sodium dodecyl sulfate-polyacrylamide gel electrophoresis. *Anal Biochem* **434**: 67-72.

Ravcheev, D.A., M.S. Khoroshkin, O.N. Laikova, O.V. Tsoy, N.V. Sernova, S.A. Petrova, A.B. Rakhmaninova, P.S. Novichkov, M.S. Gelfand & D.A. Rodionov, (2014) Comparative genomics and evolution of regulons of the LacI-family transcription factors. *Frontiers in microbiology* **5**: 294-294.

Redenbach, M., H.M. Kieser, D. Denapaite, A. Eichner, J. Cullum, H. Kinashi & D.A. Hopwood, (1996) A set of ordered cosmids and a detailed genetic and physical map for the 8 Mb *Streptomyces coelicolor* A3(2) chromosome. *Mol Microbiol* **21**: 77-96.

Rice, L.B., (2008) Federal Funding for the Study of Antimicrobial Resistance in Nosocomial Pathogens: No ESKAPE. *The Journal of Infectious Diseases* **197**: 1079-1081.

Rigali, S., H. Nothaft, E.E. Noens, M. Schlicht, S. Colson, M. Muller, B. Joris, H.K. Koerten, D.A. Hopwood, F. Titgemeyer & G.P. van Wezel, (2006) The sugar phosphotransferase system of *Streptomyces* coelicolor is regulated by the GntR-family regulator DasR and links N-acetylglucosamine metabolism to the control of development. *Mol Microbiol* **61**: 1237-1251.

Rigali, S., M. Schlicht, P. Hoskisson, H. Nothaft, M. Merzbacher, B. Joris & F. Titgemeyer, (2004) Extending the classification of bacterial transcription factors beyond the helix–turn–helix motif as an alternative approach to discover new cis/trans relationships. *Nucleic acids research* **32**: 3418-3426.

Rigali, S., F. Titgemeyer, S. Barends, S. Mulder, A.W. Thomae, D.A. Hopwood & G.P. van Wezel, (2008) Feast or famine: the global regulator DasR links nutrient stress to antibiotic production by *Streptomyces*. *EMBO Rep* **9**: 670-675.

Rittershaus, E.S., S.H. Baek & C.M. Sassetti, (2013) The normalcy of dormancy: common themes in microbial quiescence. *Cell Host Microbe* **13**: 643-651.

Ryding, N.J., T.B. Anderson & W.C. Champness, (2002) Regulation of the *Streptomyces coelicolor* calcium-dependent antibiotic by *absA*, encoding a cluster-linked two-component system. *Journal of Bacteriology* **184**: 794-805.

Saga, T. & K. Yamaguchi, (2009) History of antimicrobial agents and resistant. *JMAJ* **52***:* 103-108.
Sambrook, J. & D.W. Russell, (2001) Molecular cloning: A laboratory manual. Cold Spring Harbor Laboratories, New York.
Sancar, A., (1996) DNA Excision Repair. *Annual Review of Biochemistry* **65**: 43-81.
Santos-Beneit, F., (2015) The Pho regulon: a huge regulatory network in bacteria. *Frontiers in Microbiology* **6**.
Schneider, E. & S. Hunke, (1998) ATP-binding-cassette (ABC) transport systems: Functional and structural aspects of the ATP-hydrolyzing subunits/domains. *FEMS Microbiology Reviews* **22**: 1-20.
Schneider, K.L., K.S. Pollard, R. Baertsch, A. Pohl & T.M. Lowe, (2006) The UCSC Archaeal Genome Browser. *Nucleic Acids Res* **34**: D407-410.
Seah, C., D.C. Alexander, L. Louie, A. Simor, D.E. Low, J. Longtin & R.G. Melano, (2012) MupB, a New high-level mupirocin resistance mechanism in *Staphylococcus aureus*. *Antimicrobial Agents and Chemotherapy* **56**: 1916-1920.
Segata, N. & C. Huttenhower, (2011) Toward an efficient method of identifying core genes for evolutionary and functional microbial phylogenies. *PLoS One* **6**: e24704.
Seipke, R.F., M. Kaltenpoth & M.I. Hutchings, (2012) *Streptomyces* as symbionts: an emerging and widespread theme? *FEMS Microbiology Reviews* **36**: 862-876.
Sheng, J., J. Gan & Z. Huang, (2013) Structure-based DNA-targeting strategies with small molecule ligands for drug discovery. *Medicinal research reviews* **33**: 1119-1173.
Shimada, T., A. Ishihama, S.J. Busby & D.C. Grainger, (2008) The *Escherichia coli* RutR transcription factor binds at targets within genes as well as intergenic regions. *Nucleic Acids Res* **36**: 3950-3955.
Shirai, A., A. Matsuyama, Y. Yashiroda, A. Hashimoto, Y. Kawamura, R. Arai, Y. Komatsu, S. Horinouchi & M. Yoshida, (2008) Global analysis of gel mobility of proteins and its use in target identification. *J Biol Chem* **283**: 10745-10752.
Shpanchenko, O.V., M.I. Zvereva, P.V. Ivanov, E.Y. Bugaeva, A.S. Rozov, A.A. Bogdanov, M. Kalkum, L.A. Isaksson, K.H. Nierhaus & O.A. Dontsova, (2005) Stepping transfer messenger RNA through the ribosome. *J Biol Chem* **280**: 18368-18374.
Shu, D., L. Chen, W. Wang, Z. Yu, C. Ren, W. Zhang, S. Yang, Y. Lu & W. Jiang, (2009) *afsQ1*-Q2-sigQ is a pleiotropic but conditionally required signal transduction system for both secondary metabolism and morphological development in *Streptomyces coelicolor*. *Appl Microbiol Biotechnol* **81**: 1149-1160.
Silva, A., C. Delerue-Matos & A. Fiúza, (2005) Use of solvent extraction to remediate soils contaminated with hydrocarbons. *Journal of Hazardous Materials* **124**: 224-229.
Singh, D.P., B. Saudemont, G. Guglielmi, O. Arnaiz, J.F. Gout, M. Prajer, A. Potekhin, E. Przybos, A. Aubusson-Fleury, S. Bhullar, K. Bouhouche, M. Lhuillier-Akakpo, V. Tanty, C. Blugeon, A. Alberti, K. Labadie, J.M. Aury, L. Sperling, S. Duharcourt & E. Meyer, (2014) Genome-defence small RNAs exapted for epigenetic mating-type inheritance. *Nature* **509**: 447-452.
Skinner, R., E. Cundliffe & F.J. Schmidt, (1983) Site of action of a ribosomal RNA methylase responsible for resistance to erythromycin and other antibiotics. *J Biol Chem* **258**: 12702-12706.
Sobell, H.M., (1985) Actinomycin and DNA transcription. *Proceedings of the National Academy of Sciences of the United States of America* **82**: 5328-5331.
Soni, A., P. Khurana, T. Singh & B. Jayaram, (2017) A DNA intercalation methodology for an efficient prediction of ligand binding pose and energetics. *Bioinformatics* **33**: 1488-1496.
Spyrou, M., M. Keller, R. Tukhbatova, E. Nelson, A. Andrades Valtueña, D. Walker, A. Alterauge, N. Carty, H. Fetz, M. Gourvennec, R. Hartle, M. Henderson, K. von

Heyking, S. Kacki, E. L. Knox, C. Later, J. Peters, J. Schreiber, D. Castex & J. Krause, (2018) A phylogeography of the second plague pandemic revealed through the analysis of historical *Y. pestis* genomes. *BioRxiv* **1**:481242

Stevens, R.C., J.L. Steele, W.R. Glover, J.F. Sanchez-Garcia, S.D. Simpson, D. O'Rourke, J.S. Ramsdell, M.D. MacManes, W.K. Thomas & A.P. Shuber, (2019) A novel CRISPR/Cas9 associated technology for sequence-specific nucleic acid enrichment. *PloS one* **14**: e0215441.

Sutherland, R., R.J. Boon, K.E. Griffin, P.J. Masters, B. Slocombe & A.R. White, (1985) Antibacterial activity of mupirocin (pseudomonic acid), a new antibiotic for topical use. *Antimicrob Agents Chemother* **27**: 495-498.

Świątek-Połatyńska, M.A., G. Bucca, E. Laing, J. Gubbens, F. Titgemeyer, C.P. Smith, S. Rigali & G.P. van Wezel, (2015) Genome-wide analysis of *in vivo* binding of the master regulator DasR in *Streptomyces coelicolor* identifies novel non-canonical targets. *PloS one* **10**: e0122479.

Świątek, M.A., E. Tenconi, S. Rigali & G.P. van Wezel, (2012) Functional analysis of the N-acetylglucosamine metabolic genes of *Streptomyces coelicolor* and role in control of development and antibiotic production. *J Bacteriol* **194**: 1136-1144.

Swinney, D.C., (2013) Phenotypic vs. Target-Based Drug Discovery for First-in-Class Medicines. *Clinical Pharmacology & Therapeutics* **93**: 299-301.

Sychantha, D., A.S. Brott, C.S. Jones & A.J. Clarke, (2018) Mechanistic Pathways for Peptidoglycan O-Acetylation and De-O-Acetylation. *Front Microbiol* **9**: 2332.

Szafran, M.J., M. Gongerowska, P. Gutkowski, J. Zakrzewska-Czerwinska & D. Jakimowicz, (2016) The Coordinated Positive Regulation of Topoisomerase Genes Maintains Topological Homeostasis in *Streptomyces coelicolor*. *J Bacteriol* **198**: 3016-3028.

Szymański, P., M. Markowicz & E. Mikiciuk-Olasik, (2012) Adaptation of high-throughput screening in drug discovery-toxicological screening tests. *Int J Mol Sci* **13**: 427-452.

Tagliabue, A. & R. Rappuoli, (2018) Changing Priorities in Vaccinology: Antibiotic Resistance Moving to the Top. *Front Immunol* **9**: 1068.

Tahlan, K., S.K. Ahn, A. Sing, T.D. Bodnaruk, A.R. Willems, A.R. Davidson & J.R. Nodwell, (2007) Initiation of actinorhodin export in *Streptomyces coelicolor*. *Mol Microbiol* **63**: 951-961.

Tahlan, K., Z. Yu, Y. Xu, A.R. Davidson & J.R. Nodwell, (2008) Ligand Recognition by ActR, a TetR-Like Regulator of Actinorhodin Export. *Journal of Molecular Biology* **383**: 753-761.

Takano, E., (2006) γ-Butyrolactones: *Streptomyces* signalling molecules regulating antibiotic production and differentiation. *Current opinion in microbiology* **9**: 287-294.

Tanabe, H., S. Müller, M. Neusser, J. von Hase, E. Calcagno, M. Cremer, I. Solovei, C. Cremer & T. Cremer, (2002) Evolutionary conservation of chromosome territory arrangements in cell nuclei from higher primates. *Proceedings of the National Academy of Sciences* **99**: 4424-4429.

Tanaka, Y., N. Okai, H. Teramoto, M. Inui & H. Yukawa, (2008) Regulation of the expression of phosphoenolpyruvate: carbohydrate phosphotransferase system (PTS) genes in Corynebacterium glutamicum R. *Microbiology* **154**: 264-274.

Tarkka, M. & R. Hampp, (2008) Secondary Metabolites of Soil Streptomycetes in Biotic Interactions. In., pp. 107-126.

Tawfike, A., C. Viegelmann & R. Edrada-Ebel, (2013) Metabolomics and Dereplication Strategies in Natural Products. *Methods in molecular biology (Clifton, N.J.)* **1055**: 227-244.

Taylor, L.H., S.M. Latham & M.E. Woolhouse, (2001) Risk factors for human disease emergence. *Philos Trans R Soc Lond B Biol Sci* **356**: 983-989.

Tenconi, E., M.F. Traxler, C. Hoebreck, G.P. van Wezel & S. Rigali, (2018) Production of Prodiginines Is Part of a Programmed Cell Death Process in *Streptomyces coelicolor*. *Frontiers in microbiology* **9**: 1742-1742.

Thomas, T., J. Gilbert & F. Meyer, (2012) Metagenomics - a guide from sampling to data analysis. *Microb Inform Exp* **2**: 3.

Tkatchenko, A. & M. Scheffler, (2009) Accurate Molecular Van Der Waals Interactions from Ground-State Electron Density and Free-Atom Reference Data. *Physical Review Letters* **102**: 073005.

Towle, J.E., (2007) AtrA-mediated transcriptional regulation in *Streptomyces* secondary metabolite production and development. In.: University of Leeds, pp. 208.

Traag, B.A. & G.P. van Wezel, (2008) The SsgA-like proteins in actinomycetes: small proteins up to a big task. *Antonie van Leeuwenhoek* **94**: 85-97.

Traxler, M.F., S.M. Summers, H.T. Nguyen, V.M. Zacharia, G.A. Hightower, J.T. Smith & T. Conway, (2008) The global, ppGpp-mediated stringent response to amino acid starvation in *Escherichia coli*. *Mol Microbiol* **68**: 1128-1148.

Trotter, C.L., J. McVernon, M.E. Ramsay, C.G. Whitney, E.K. Mulholland, D. Goldblatt, J. Hombach & M.P. Kieny, (2008) Optimising the use of conjugate vaccines to prevent disease caused by *Haemophilus influenzae* type b, *Neisseria meningitidis* and *Streptococcus pneumoniae*. *Vaccine* **26**: 4434-4445.

Tuerk, C. & L. Gold, (1990) Systematic evolution of ligands by exponential enrichment: RNA ligands to bacteriophage T4 DNA polymerase. *Science* **249**: 505-510.

Uddin, M., G.G. Altmann & C.P. Leblond, (1984) Radioautographic visualization of differences in the pattern of [3H]uridine and [3H]orotic acid incorporation into the RNA of migrating columnar cells in the rat small intestine. *J Cell Biol* **98**: 1619-1629.

Uehara, T., K. Suefuji, N. Valbuena, B. Meehan, M. Donegan & J.T. Park, (2005) Recycling of the anhydro-N-acetylmuramic acid derived from cell wall murein involves a two-step conversion to N-acetylglucosamine-phosphate. *J Bacteriol* **187**: 3643-3649.

Uguru, G.C., K.E. Stephens, J.A. Stead, J.E. Towle, S. Baumberg & K.J. McDowall, (2005) Transcriptional activation of the pathway-specific regulator of the actinorhodin biosynthetic genes in *Streptomyces coelicolor*. *Mol Microbiol* **58**: 131-150.

Ulrich, L.E., E.V. Koonin & I.B. Zhulin, (2005) One-component systems dominate signal transduction in prokaryotes. *Trends in Microbiology* **13**: 52-56.

Vadekeetil, A., H. Saini, S. Chhibber & K. Harjai, (2016) Exploiting the antivirulence efficacy of an ajoene-ciprofloxacin combination against *Pseudomonas aeruginosa* biofilm associated murine acute pyelonephritis. *Biofouling* **32**: 371-382.

van der Heul, H.U., B.L. Bilyk, K.J. McDowall, R.F. Seipke & G.P. van Wezel, (2018) Regulation of antibiotic production in Actinobacteria: new perspectives from the post-genomic era. *Nat Prod Rep* **35**: 575-604.

van der Lee, T.A.J. & M.H. Medema, (2016) Computational strategies for genome-based natural product discovery and engineering in fungi. *Fungal Genet Biol* **89**: 29-36.

van der Meij, A., G.P. van Wezel, M.I. Hutchings & S.F. Worsley, (2017) Chemical ecology of antibiotic production by actinomycetes. *FEMS Microbiology Reviews* **41**: 392-416.

van Wezel, G.P. & K.J. McDowall, (2011) The regulation of the secondary metabolism of *Streptomyces*: new links and experimental advances. *Nat Prod Rep* **28**: 1311-1333.

van Wezel, G.P., J. van der Meulen, S. Kawamoto, R.G. Luiten, H.K. Koerten & B. Kraal, (2000) *ssgA* is essential for sporulation of *Streptomyces coelicolor* A3(2) and affects hyphal development by stimulating septum formation. *J Bacteriol* **182**: 5653-5662.

Ventola, C.L., (2015) The antibiotic resistance crisis. part 1: causes and threats. *P t* **40**: 277-283.
Vollmer, W., B. Joris, P. Charlier & S. Foster, (2008) Bacterial peptidoglycan (murein) hydrolases. *FEMS Microbiology Reviews* **32**: 259-286.
Vulin, C., N. Leimer, M. Huemer, M. Ackermann & A.S. Zinkernagel, (2018) Prolonged bacterial lag time results in small colony variants that represent a sub-population of persisters. *Nature Communications* **9**: 4074.
Wahdan, M.H., J.E. Sippel, I.A. Mikhail, A.E. Rahka, E.S. Anderson, H.A. Sparks & B. Cvjetanovic, (1975) Controlled field trial of a typhoid vaccine prepared with a nonmotile mutant of Salmonella typhi Ty2. *Bull World Health Organ* **52**: 69-73.
Walsh, C., (2013) Antibiotics: actions, origins, resistance. *ASM Press*, Washington, DC.
Wang, C., H. Ge, H. Dong, C. Zhu, Y. Li, J. Zheng & P. Cen, (2007a) A novel pair of two-component signal transduction system ecrE1/ecrE2 regulating antibiotic biosynthesis in *Streptomyces coelicolor*. *Biologia* **62**: 511-516.
Wang, C.M., F.L. Zhao, L. Zhang, X.Y. Chai & Q.G. Meng, (2017) Synthesis and Antibacterial Evaluation of a Series of 11,12-Cyclic Carbonate Azithromycin-3-O-descladinosyl-3-O-carbamoyl Glycosyl Derivatives. *Molecules* **22**.
Wang, D., J. Yuan, S. Gu, Q.J.A.M. Shi & Biotechnology, (2013a) Influence of fungal elicitors on biosynthesis of natamycin by *Streptomyces natalensis* HW-2. **97**: 5527-5534.
Wang, H.H., F.J. Isaacs, P.A. Carr, Z.Z. Sun, G. Xu, C.R. Forest & G.M. Church, (2009a) Programming cells by multiplex genome engineering and accelerated evolution. *Nature* **460**: 894-898.
Wang, J., W. Chow, D. Leung & J. Chang, (2012) Application of Ultrahigh-Performance Liquid Chromatography and Electrospray Ionization Quadrupole Orbitrap High-Resolution Mass Spectrometry for Determination of 166 Pesticides in Fruits and Vegetables. *Journal of Agricultural and Food Chemistry* **60**: 12088-12104.
Wang, L., Y. Yu, X. He, X. Zhou, Z. Deng, K.F. Chater & M. Tao, (2007b) Role of an FtsK-like protein in genetic stability in *Streptomyces coelicolor* A3(2). *J Bacteriol* **189**: 2310-2318.
Wang, M., J.J. Carver, V.V. Phelan, L.M. Sanchez, N. Garg, Y. Peng, D.D. Nguyen, J. Watrous, C.A. Kapono, T. Luzzatto-Knaan, C. Porto, A. Bouslimani, A.V. Melnik, M.J. Meehan, W.-T. Liu, M. Crüsemann, P.D. Boudreau, E. Esquenazi, M. Sandoval-Calderón, R.D. Kersten, L.A. Pace, R.A. Quinn, K.R. Duncan, C.-C. Hsu, D.J. Floros, R.G. Gavilan, K. Kleigrewe, T. Northen, R.J. Dutton, D. Parrot, E.E. Carlson, B. Aigle, C.F. Michelsen, L. Jelsbak, C. Sohlenkamp, P. Pevzner, A. Edlund, J. McLean, J. Piel, B.T. Murphy, L. Gerwick, C.-C. Liaw, Y.-L. Yang, H.-U. Humpf, M. Maansson, R.A. Keyzers, A.C. Sims, A.R. Johnson, A.M. Sidebottom, B.E. Sedio, A. Klitgaard, C.B. Larson, C.A.B. P, D. Torres-Mendoza, D.J. Gonzalez, D.B. Silva, L.M. Marques, D.P. Demarque, E. Pociute, E.C. O'Neill, E. Briand, E.J.N. Helfrich, E.A. Granatosky, E. Glukhov, F. Ryffel, H. Houson, H. Mohimani, J.J. Kharbush, Y. Zeng, J.A. Vorholt, K.L. Kurita, P. Charusanti, K.L. McPhail, K.F. Nielsen, L. Vuong, M. Elfeki, M.F. Traxler, N. Engene, N. Koyama, O.B. Vining, R. Baric, R.R. Silva, S.J. Mascuch, S. Tomasi, S. Jenkins, V. Macherla, T. Hoffman, V. Agarwal, P.G. Williams, J. Dai, R. Neupane, J. Gurr, A.M.C. Rodríguez, A. Lamsa, C. Zhang, K. Dorrestein, B.M. Duggan, J. Almaliti, P.-M. Allard, P. Phapale*, et al.*, (2016a) Sharing and community curation of mass spectrometry data with Global Natural Products Social Molecular Networking. *Nature biotechnology* **34**: 828-837.
Wang, M., Y. Yu, C. Liang, A. Lu & G. Zhang, (2016b) Recent Advances in Developing Small Molecules Targeting Nucleic Acid. *Int J Mol Sci* **17**.
Wang, R., Y. Mast, J. Wang, W. Zhang, G. Zhao, W. Wohlleben, Y. Lu & W. Jiang, (2013b) Identification of two-component system AfsQ1/Q2 regulon and its cross-regulation with GlnR in *Streptomyces coelicolor*. *Mol Microbiol* **87**: 30-48.

Wang, Y., J. Xiao, T.O. Suzek, J. Zhang, J. Wang & S.H. Bryant, (2009b) PubChem: a public information system for analyzing bioactivities of small molecules. *Nucleic Acids Res.* **37**: W623-633.
Ward, A.C. & N.E. Allenby, (2018) Genome mining for the search and discovery of bioactive compounds: the *Streptomyces* paradigm. *FEMS Microbiol. Lett.* **365**.
Wassarman, K.M. & G. Storz, (2000) 6S RNA Regulates *E. coli* RNA Polymerase Activity. *Cell* **101**: 613-623.
Weisblum, B., (1995) Erythromycin resistance by ribosome modification. *Antimicrob Agents Chemother* **39**: 577-585.
Wetzel, S., R.S. Bon, K. Kumar & H. Waldmann, (2011) Biology-Oriented Synthesis. *Angewandte Chemie International Edition* **50**: 10800-10826.
White, J. & M. Bibb, (1997) *bldA* dependence of undecylprodigiosin production in *Streptomyces coelicolor* A3(2) involves a pathway-specific regulatory cascade. *J Bacteriol* **179**: 627-633.
WHO, (2015) Global Action Plan on Antimicrobial Resistance. WHO, Geneva, Switzerland.
Wilkens, S., (2015) Structure and mechanism of ABC transporters. *F1000Prime Rep* **7**: 14.
Willems, A.R., K. Tahlan, T. Taguchi, K. Zhang, Z.Z. Lee, K. Ichinose, M.S. Junop & J.R. Nodwell, (2008) Crystal structures of the *Streptomyces coelicolor* TetR-like protein ActR alone and in complex with actinorhodin or the actinorhodin biosynthetic precursor (S)-DNPA. *J Mol Biol* **376**: 1377-1387.
Willemse, J., J.W. Borst, E. de Waal, T. Bisseling & G.P. van Wezel, (2011) Positive control of cell division: FtsZ is recruited by SsgB during sporulation of *Streptomyces*. *Genes Dev* **25**: 89-99.
Williamson, N.R., P.C. Fineran, F.J. Leeper & G.P. Salmond, (2006) The biosynthesis and regulation of bacterial prodiginines. *Nature reviews. Microbiology* **4**: 887-899.
Woodcock, C.L. & R.P. Ghosh, (2010) Chromatin higher-order structure and dynamics. *Cold Spring Harb Perspect Biol* **2**: a000596.
Woodford, N., (2010) Chapter 20 - Glycopeptides. In: Antibiotic and Chemotherapy (Ninth Edition). R.G. Finch, D. Greenwood, S.R. Norrby & R.J. Whitley (eds). London: W.B. Saunders, pp. 265-271.
Wright, G.D., (2014) Something old, something new: revisiting natural products in antibiotic drug discovery. *Can J Microbiol* **60**: 147-154.
Wright, G.D., (2017) Opportunities for natural products in 21(st) century antibiotic discovery. *Nat Prod Rep* **34**: 694-701.
Xu, Y. & K. Vetsigian, (2017) Phenotypic variability and community interactions of germinating *Streptomyces* spores. *Sci Rep* **7**: 699.
Yamaguchi, Y. & M. Inouye, (2011) Regulation of growth and death in *Escherichia coli* by toxin–antitoxin systems. *Nature Reviews Microbiology* **9**: 779-790.
Yanisch-Perron, C., J. Vieira & J. Messing, (1985) Improved M13 phage cloning vectors and host strains: nucleotide sequences of the M13mp18 and pUC19 vectors. *Gene* **33**: 103-119.
Yu, Z., S.E. Reichheld, A. Savchenko, J. Parkinson & A.R. Davidson, (2010) A Comprehensive Analysis of Structural and Sequence Conservation in the TetR Family Transcriptional Regulators. *Journal of Molecular Biology* **400**: 847-864.
Yu, Z., H. Zhu, F. Dang, W. Zhang, Z. Qin, S. Yang, H. Tan, Y. Lu & W. Jiang, (2012) Differential regulation of antibiotic biosynthesis by DraR-K, a novel two-component system in *Streptomyces coelicolor*. *Mol Microbiol* **85**: 535-556.
Zaburannyi, N., M. Rabyk, B. Ostash, V. Fedorenko & A. Luzhetskyy, (2014) Insights into naturally minimised *Streptomyces* albus J1074 genome. *BMC Genomics* **15**: 97.
Zhang, J., W. Zhou, X. Wang & L. Wang, (2018) The CRISPR-Cas9 system: a promising tool for discovering potential approaches to overcome drug resistance in cancer. *RSC advances* **8**: 33464-33472.

Zhang, X., L.B. Alemany, H.-P. Fiedler, M. Goodfellow & R.J. Parry, (2008a) Biosynthetic investigations of lactonamycin and lactonamycin Z: cloning of the biosynthetic gene clusters and discovery of an unusual starter unit. *Antimicrobial Agents and Chemotherapy* **52**: 574-585.

Zhang, Y., (2007) Mechanisms of antibiotic resistance in the microbial world. *Baltimore, USA*.

Zhang, Y., T. Liu, C.A. Meyer, J. Eeckhoute, D.S. Johnson, B.E. Bernstein, C. Nusbaum, R.M. Myers, M. Brown, W. Li & X.S. Liu, (2008b) Model-based analysis of ChIP-Seq (MACS). *Genome Biol* **9**: R137.

Zhao, B., A. Erwin & B. Xue, (2018) How many differentially expressed genes: A perspective from the comparison of genotypic and phenotypic distances. *Genomics* **110**: 67-73.

Zhao, B., X. Lin, L. Lei, D.C. Lamb, S.L. Kelly, M.R. Waterman & D.E. Cane, (2008) Biosynthesis of the sesquiterpene antibiotic albaflavenone in *Streptomyces coelicolor* A3(2). *J Biol Chem* **283**: 8183-8189.

Zhu, H., S.K. Sandiford & G.P. van Wezel, (2014) Triggers and cues that activate antibiotic production by actinomycetes. *Journal of industrial microbiology & biotechnology* **41**: 371-386.

Ziemert, N., M. Alanjary & T. Weber, (2016) The evolution of genome mining in microbes–a review. *Natural product reports* **33**: 988-1005.

Zipser, D., (1969) Polar Mutations and Operon Function. *Nature* **221**: 21-25.

Zschiedrich, C.P., V. Keidel & H. Szurmant, (2016) Molecular mechanisms of two-component signal transduction. *J Mol Biol* **428**: 3752-3775.